Application of Endurance Time Method in Structural Optimization of the Dampers for Seismic Design of Concrete Structures

Hamed Amouzegar, Hossein Tajmir Riahi and Maryam Daei
Department of Civil Engineering, University of Isfahan, Isfahan, Iran

Summary

Optimization techniques play an important role in structural design. These methods help a designer to find the best solutions in order to maximize benefits derivation from the available resources. Additionally, to mitigate damage resulting from seismic hazard, an alternative design approach is to introduce seismic isolation systems or supplemental energy dissipation which can distribute energy dissipation within a structure when subjected to seismic ground motions. The optimization design of structure by using damper, including the optimization of damper characteristics and its position in structure, is an accurate function since mentioned parameters have fundamental effect on the structural energy absorption. The main goal of this paper is the evaluation of concrete moment-resisting frames strengthened using dampers by Incremental Dynamic Analysis (IDA) and Endurance Time (ET) analysis. ET analysis is a new dynamic pushover procedure in which structures are subjected to gradually intensifying acceleration functions and their performances are assessed based on their responses. This has been performed using OpenSees software. In order to model deteriorating connections, frames are modeled using concentrated plastic hinges. Therefore the material model with stiffness degradation and strength deterioration characteristic is considered in this study. To perform incremental dynamic analysis a set of ground motion accelerograms is selected from the database of the records used in FEMA 695. In this paper special attention is given to the results accuracy assessment and application of ET analysis in estimating structural optimization by using damper. It is clearly observed that structural responses resulted from endurance time analysis are compatible with those obtained from Incremental Dynamic analysis (IDA). Optimization results of dampers characteristics and their positions in the structures obtained by ET analysis are the same as the results of IDA in most cases. Also it is shown that ET analysis can clearly identify the structure with a better performance even in the case study of structures with a relatively complicated nonlinear behavior.

KEYWORDS: Damper Devices, Structural Optimization, Endurance Time Method, Incremental Dynamic Analysis, Concrete Structures.

ISSN 2285-2735, Pages 9 - 24

1. INTRODUCTION

Analytical and experimental studies show that by using dampers in structures the structural damping is increased notably and damages to the structures due to strong earthquakes can be reduced significantly. Optimum design of structures with damper, including optimization of dampers' parameters and optimization of dampers' location in the structure, is a major task, because rational parameters and proper location of dampers will lead to most effective energy dissipation [1].

Endurance time method is basically a dynamic pushover method that tries to predict seismic response of structures by analyzing their performance when subjected to predesigned intensifying acceleration functions [2]. If ET acceleration functions can assemble the major characteristics of real ground motions with different intensities, they can provide a good estimate of the real response of the structures to be used in performance based engineering [1]. Therefore this method can be used to check the performance of different systems and find the one with the best performance. In this research, half of provisions of ASCE/SEI 41-06 [3] have been considered for setting design objectives and acceptance criteria, the Basic safety earthquake 1 (BSE-1) and Basic safety earthquake 2 (BSE-2).
On earthquake intensities, BSE-2 hazard level represents the most intensive probable earthquake having the probability of exceedance of 2% in 50 years or return period of 2475 years and BSE-1 hazard level has the probability of exceedance of 10% in 50 years or return period of 474 years. These hazard levels are defined as acceleration response spectra or acceleration time-histories which are scaled according to corresponding 5% damped design spectrum ASCE-07 [4].
In this paper it is tried to find the optimum arrangement of viscous dampers in Reinforced Concrete (RC) Special Moment Frame (SMF) to reach the expected performance by using ET method as the analysis tool along with the genetic algorithm as the optimization tool.
The frames with nonlinear behavior and controlled design drift in initial design are modeled using OPENSEES [5]. Using genetic algorithm, the arrangement of dampers along the altitude of structure is assigned such that the structure satisfies the half of two allowable code performances in the two levels of BSE-1 and BSE-2 at the least sum of required damping coefficients. In this paper the acceleration functions using in ET method have a matched response spectrum with the 5% damped design spectrum ASCE-07. For evaluating ET method the results are compared with the results of incremental dynamic analysis [6] with spectrum matched records.

2. ET ACCELERATION FUNCTIONS AND SPECTRUM MATCHED RECORDS

A major factor in the success of the endurance time method is in the availability of suitable intensifying excitation functions. Previous studies show that usable intensifying excitations (i.e. acceleration functions in this study) can actually be designed [7]. Acceleration functions are designed in such a way that each window from zero to time t produces a response spectrum that is proportional to the template spectrum with proportionality factor that is linearly increasing with time and equal to unity at particular time called t_{Target}. To achieve this goal, the target acceleration response of ET acceleration function can be defined as in Eq (1):

$$S_{aT}(T,t) = \frac{t}{t_{Target}} S_{aC}(T) \quad (1)$$

Where $S_{aT}(T,t)$ is the target acceleration response spectrum at time t and period of vibration T. $S_{aC}(T)$ is the template acceleration response spectrum. Acceleration functions used in this study (ETA40g or series g) have been optimized in such a way that, the response spectrum of SDOF system with 5% damping for the window from zero to 10 (t_{Target}) seconds of ETA40g is fit to design spectral acceleration ASCE-07 (2005) code for soil type C with Ss=1.5, S1=0.6, Fa=1.0, Fv=1.3 and TL=8. The response of SDOF system to the acceleration function series ETA40g with a window from zero to any other time have a linear relation with ASCE-07 spectrum. For example for time 5 sec or 15 sec the spectrum will be equal to 0.5 or 1.5 times to ASCE-07 spectrum.

Optimization of these acceleration functions is for 200 periods in 0 to 5 seconds plus 20 points from period = 6 to period = 50 seconds. The whole time of these acceleration functions is 40.96 seconds. Figure 1 shows one of these acceleration functions.

Seven near fault ground motions (series OGM) were selected from the series of fourteen near-field pulse records subset listed in FEMA P695 [8]. The specifications of the ground motions of this set are shown in Table 1. The records have been spectrum matched to the same design earthquake spectrum ASEC-07 that acceleration functions ETA40g are optimized to fit. The spectrum matching procedure is applied in time domain using wavelet method. The wavelet used in this study is reverse impulse presented by Abrahamson (1992).

After using impulse reverse wavelet for prevention of non-zero displacement and velocity at the end of the time series a linearly base line correction has been applied to the spectrum matched results. This procedure has the advantage that the shape and frequency content of time series after spectrum matching are almost the same before [9].

Figure. 2. shows the arias intensity, fourier amplitude and acceleration time history of record DZC befor and after of spectrum matching. Figure. 3. shows the mean

response acceleration of acceleration functions ETA40g at t = 10 and 15 seconds, OGM set with scale factor 1 and 1.5 and spectrum matched set (GM) with scale factor 1 and 1.5. The obtained coefficients for GM set and ET acceleration functions proportionate with the performance levels are shown in Table 2 .

Table 1. Description of the GM set of ground motions used in this study.

Date	Name	Magnitude (Ms)	Station Name	PGA (g)	Component (degree)	Epicentral (km)	Abbreviation
1999	Duzce, Turkey	7.1	Duzce	0.52	270	1.6	DZC
1992	Erzican, Turkey	6.7	Erzincan	0.49	N-S	9	ERZ
1979	Imperial Valley-06	6.5	El Centro Array #6	0.44	230	27.5	H-E
1999	Kocaeli, Turkey	7.5	Izmit	0.22	90	5.3	IZT
1992	Landers	7.3	Lucerne	0.79	0	44	LCN
1992	Cape Mendocino	7	Petrolia	0.63	90	4.5	PET
1994	Northridge-01	6.7	Rinaldi Receiving Sta	0.87	228	10.9	RRS

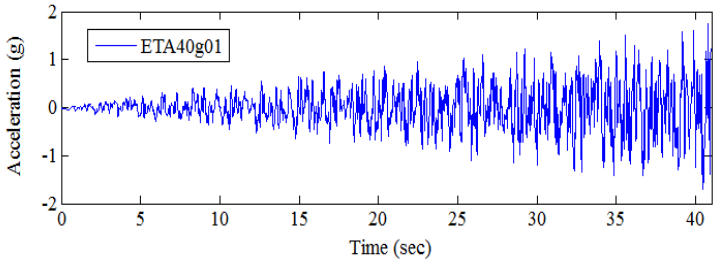

Figure 1. Acceleration Function ETA40g01

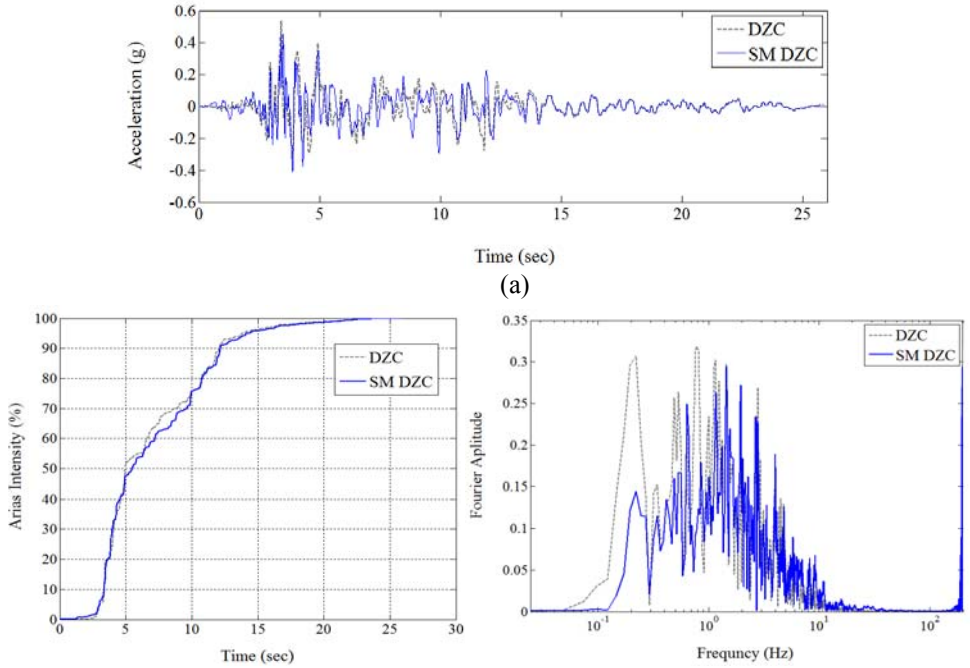

Figure 2. a) apparent shape, b) Arias intensity and c) Fourier amplitude of record DZC before and after spectrum matching.

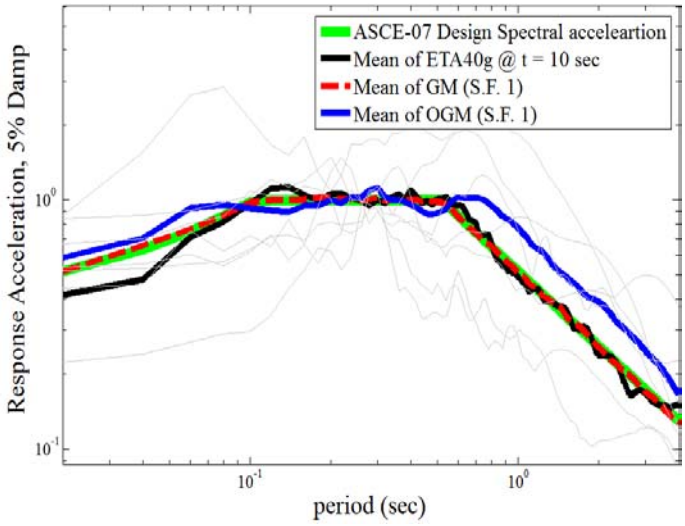

(a)

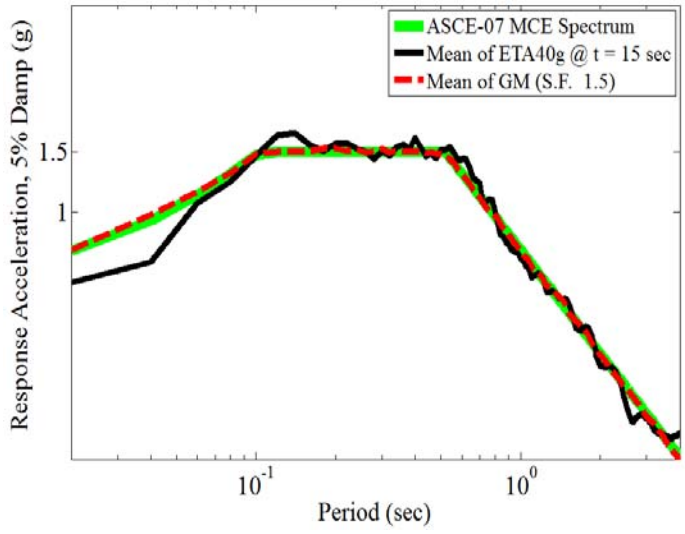

(b)

Figure 3. Response spectrum acceleration a) of ETA40g at time 10 sec, GM and OGM sets with scale factor 1 b) of ETA40g at time 15 sec, GM set with scale factor 1.5.

Table 2. Scale factors for GM1 and ET time in 3 hazard levels.

Performance levels	Scale factor	ET time (sec)	Maximum interstory drift ratio (MIDR)
BSE-1 (Basic safety earthquake 1) ASCE-07 design earthquake (L.S.)	1.00	10	1.25 % (1/2 * 2.5 %)
BSE-2 (Basic safety earthquake 2) ASCE-07 maximum considered earthquake (C.P.)	1.50	15	2.5 % (1/2 * 5 %)

3. STRUCTURAL MODELS AND VISCOUS DAMPERS

In this study three Reinforced Concrete Special Moment Frame (RC-SMF) with two, four and eight story and three bays are considered. The generic frames are adopted from the models developed by Haselton (2011) [10]. These frames are designed according to ASCE7-02 and ACI318-02. The geometry and specifications of four story model is depicted in Figure 4 and The specifications of frames are shown in Table 3. Height of story one in all frames is 15 feet and the height of the all other stories is 13 feet. Length of each bay is 20 feet. For the two story, Column size concrete strength are designed to satisfy joint shear requirements, specifically the column widths were increased to increase column area. Beams strength were

controlled by force demand, but four beams had additional reinforcement added to keep the same rho ratio between the floors. Column strengths are controlled by strong-column weak-beam (SCWB) except two exterior lower columns that were controlled by flexural demands and two upper story exterior columns controlled by minimum the reinforcement requirement. Beam stirrups were controlled by the minimum requirement. The column stirrups were controlled by confinement requirement. For the four and eight story, Initial member sizes (beam depths, column dimensions) were determined mostly by joint shear and minimum size requirements, in addition to column-beam compatibility considerations. The depth of the grade beams was increased to help alleviate joint shear concerns. Beam strengths were controlled by force demands, particularly lateral forces. Fourth floor beam strength was increased slightly to help reduce SCWB ratio at affected joints. Column strengths were determined by strong-column weak-beam (SCWB) ratios except in the first story, where flexural demands controlled. Concrete strength was increased to 7.0 ksi for four story and was stepped up to 6.0 ksi for eight story in the lower columns to help meet joint shear requirements. Beam stirrups were controlled by shear capacity design. The column stirrups were controlled by both the shear capacity design and the confinement requirements. The frames are modeled in OPENSEES (2011). A primary frame and Grade Beam at the basement has been considered in all frames. The joints were defined as joint shear panel zones. Modeling Flexural Behavior of Reinforced Concrete Beam-Column Elements is shown in figure 5.

Viscous dampers are widely used in mechanical systems. The force induced in viscous damper depends on velocity; therefore, the maximum damper force in an earthquake is always $\pi/2$ out of phase with respect to displacement, and the maximum speed occurs at the time that the displacement is zero. This is an advantage for these kinds of dampers because when the structure endures great internal forces due to displacements created by earthquakes, they induce least extra forces on the structure. To model viscous dampers as bracing, viscous material available in OPENSEES is used. The induced stress in this material is acquired from this equation:

$$\sigma = C_0 |\dot{\epsilon}|^{\alpha} sign(\dot{\epsilon}) \tag{2}$$

Where σ represents the induced stress in the material, $\dot{\epsilon}$ strain rate, C_0 damping ratio and α damping exponent.

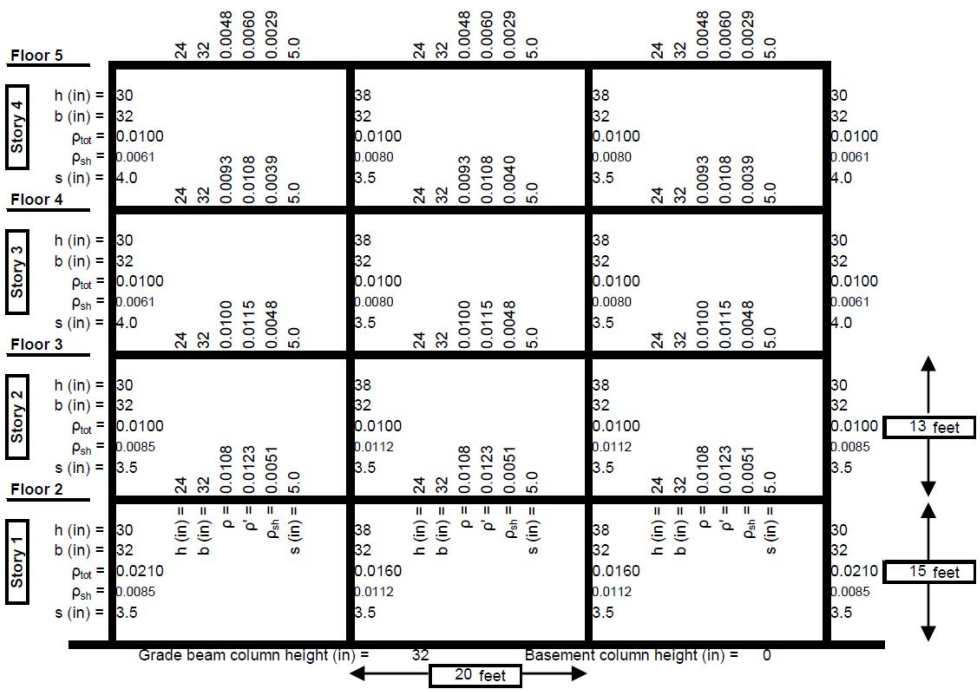

Design base shear = 0.092g, 386 k ***f'c*** beams = 5ksi ***f'c*** cols, upper = 5ksi
f'c cols, lower = 7ksi, ***fy*** rebar, nom = 60ksi

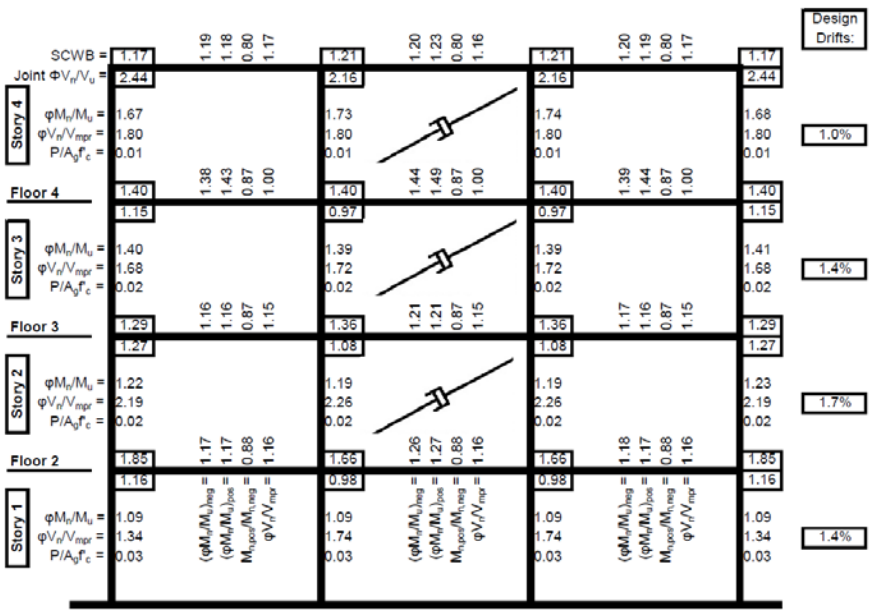

Figure 4. Schematics of four story frame under investigation.

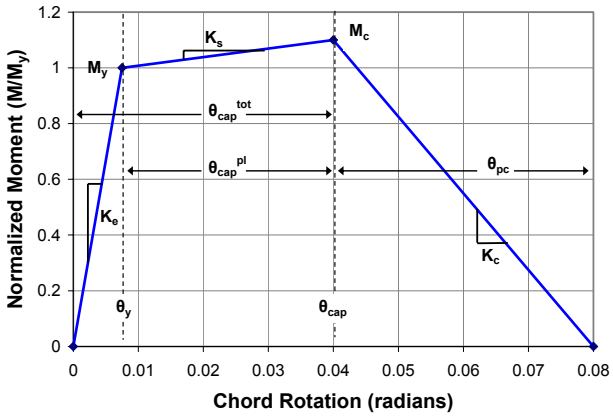

Figure 5. Modeling Flexural Behavior of Reinforced Concrete Beam-Column Elements

Table 3. Specification of the frames.

ID Number	No. of stories	Fundamental Period (sec)	Strength/Stiffness Distribution Over height	Foundation Fixity Assumed in Design
2064	2	0.66	A*	GB**
1003	4	1.12	A	GB
1011	8	1.71	A	GB

* Expected practitioner design; strength and stiffness stepped over height as would be done in common design practice.

** "Grade Beam" - this considers the rotational stiffness of the grade beam and any basement columns.

4. ANALYSIS AND OPTIMIZATION PROCEDURE

The problem is going to find optimized damper coefficients in each story so that the MIDR of the frame in two level of ASCE-07 satisfy the limit levels of half of ASCE41-06 (MIDR = 1.25 % for design earthquake and MIDR = 2.5 % for maximum considered earthquake (MCE)). At first step some value should be assigned to the dampers and in the next step OPENSEES is running and then it's got to be check that MIDR has satisfied the limit levels or not. So this problem needs an optimization procedure. It seems that the genetic algorithm is a good optimization procedure for this problem. In genetic algorithm a primary population is randomly generated then after generation the fitness function will be check. The good population will be remain with a cross over rate and remain are killed. After that a new population will be generated from the good ones. For prevention of stick answer in a local space, the algorithm is doing a mutation. In this specific problem the fitness function is defined sum of damping coefficients in all stories. Before checking fitness function the constraint (MIDR should have an acceptable difference with the Limits) should be controlled. If primary population satisfy the

constraint the algorithm can go on, if not the population should change. Because of negligible changes in MIDR under primary population, the algorithm may never converge, so the first population should be potential for the solution. The convergences criteria may be defined algorithm halts after a specified number of iteration or converge in damping coefficient. After generation organisms (coefficient), the structure is analyzed under ETA40g. Then ET curve corresponding to MIDR is drown. MIDR correspond to time 10 sec is equivalent to MIDR for design earthquake (Life Safety (LS)), and at time 15 sec is equivalent to MCE (Collapse Prevention (CP)). After checking both MIDR of LS and CP levels with limit levels, if feasible solution is obtained then genetic algorithm tries to find optimal solution. Else new population of organisms should be reproduced.

5. ANALYSIS AND OPTIMIZATION RESULTS

5.1. ET acceleration functions and ground motions

The response spectrum of seven records and ETA40g are exactly match to the ASCE-07 spectrum (target spectrum). So any scale factor multiplied by the records produce a spectrum that is scale factor times to target spectrum. The performance criterion for BSE-1 level is considered to be LS (1.25% MIDR) and for BSE-2 level is considered to be CP. So for controlling MIDR at BSE-1 level, the scale factor is 1 and for controlling BSE-2 (2.5% MIDR) level the scale factor is 1.5 respectively. In the endurance time method particularly for ETA40g the dynamic analysis is going to the last time of the acceleration function that is here 40.96. Then the ET curve is drown correspond to MIDR. MIDR at time 10 sec should be compared with BSE-1 level and at time 15 sec should be compared with BSE-2 level.

5.2. ET analysis and optimization

In this research, according to the code, the design objectives ‘p’ and ‘k’ are assigned as the rehabilitation objectives. Therefore, the structure should satisfy the CP performance level in BSE-2 hazard level and LS level in BSE-1 hazard level. This would be the basic safety objective or BSO. According to ASCE41-06, the allowable transient interstory drift ratio is 5 % for the CP level or 2.5 % for those structures that without damper satisfy the limits levels and 2.5 % for the LS level. In this paper because the frames satisfied the limits so they are considered relatively 1.25 % and 2.5 % for BSE-1 and BSE-2. By drawing the performance curve similar to the curve in Figure. 6 and comparing with the allowable limits of the code, the vulnerability of each structure can be distinguished [11]. In this stage using the genetic algorithm with the purpose of reaching the acceptable

performance stated in the code, which is equivalent to make the performance curve (ET curve) below the allowable limit of the code presented in Figure. 8 to Figure. 10, the required damping for each structure is evaluated (Figure. 7). For example, for the eight frame, the required damping in the first and sixth stories is more than the other stories and the second and fifth stories have least influence on controlling MIDR rather than other stories.

The performance curves of the structures before and after the rehabilitation are compared in Figure. 8 to Figure. 10. As shown, the performance curve of the structure after rehabilitation (damper installation) is quite close to allowable limit of the code and the smoothed curve has contacted it at a point, this indicates the optimal use of structure capacity.

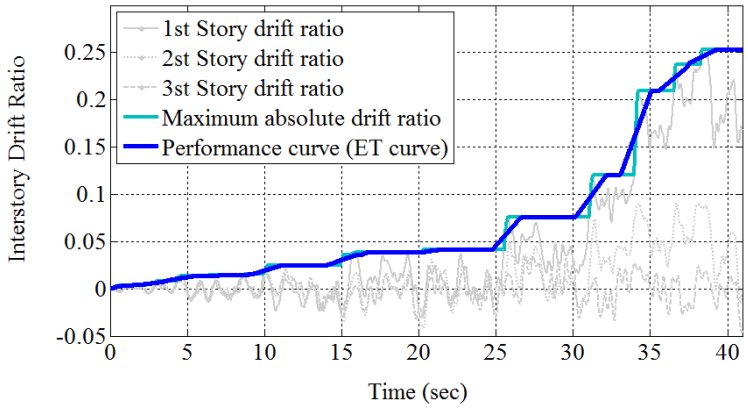

Figure 6. Generating performance curve (ET curve) for FM03B1RGW based on interstory drift ratio.

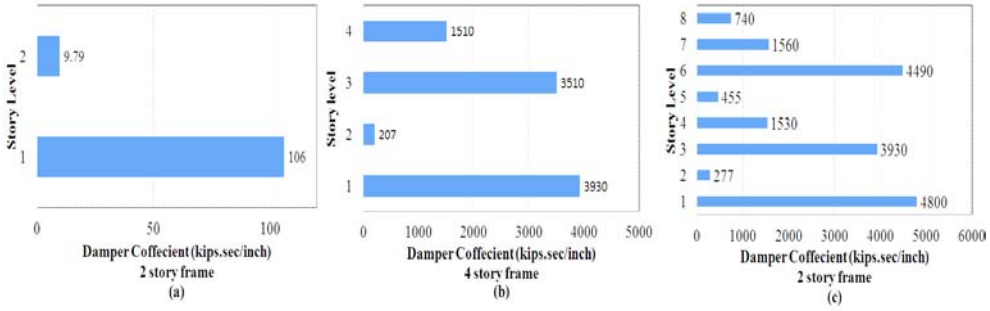

Figure 7. Optimum damper distribution for (a) 2 story frame (b) 4 story frame (c) 8 story frame.

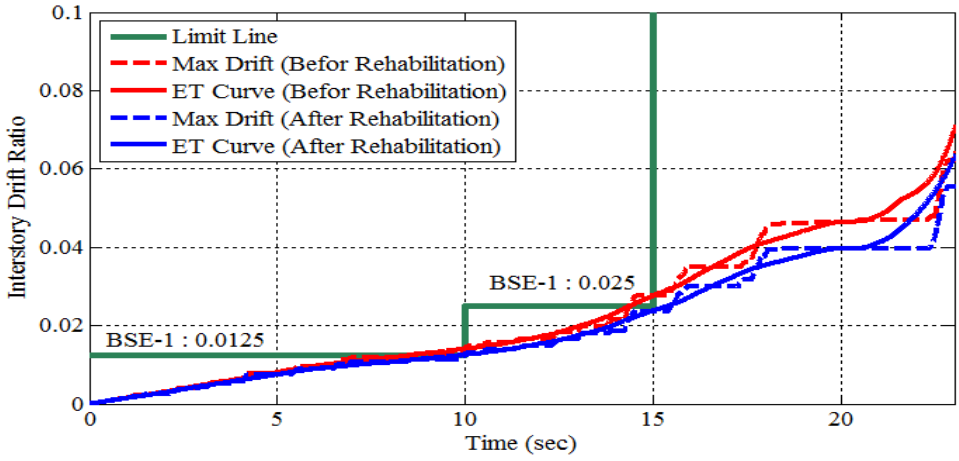

Figure 8. Prformance curve (ET curve) for 2 story frame before and after rehabilitation.

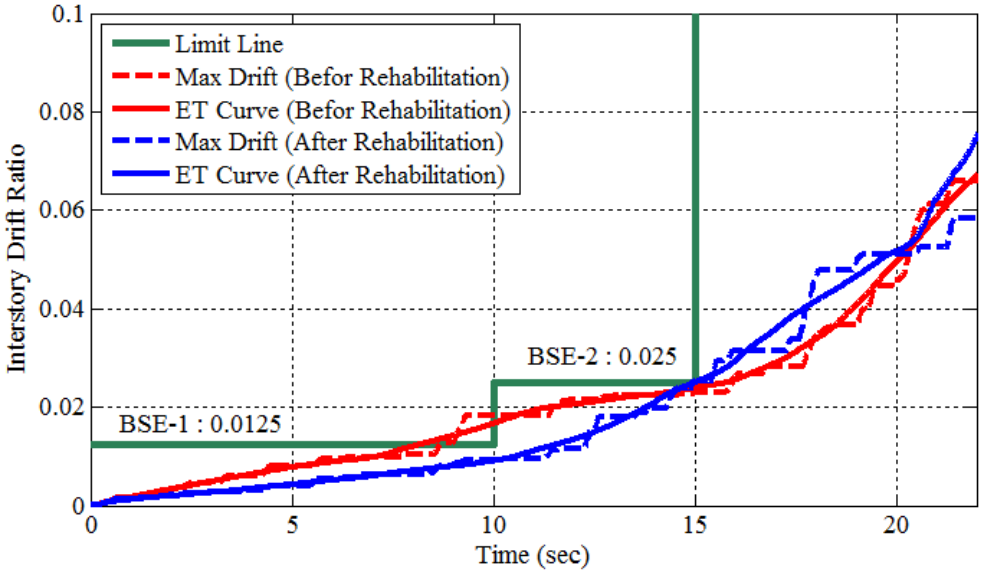

Figure 9. Prformance curve (ET curve) for 4 story frame before and after rehabilitation.

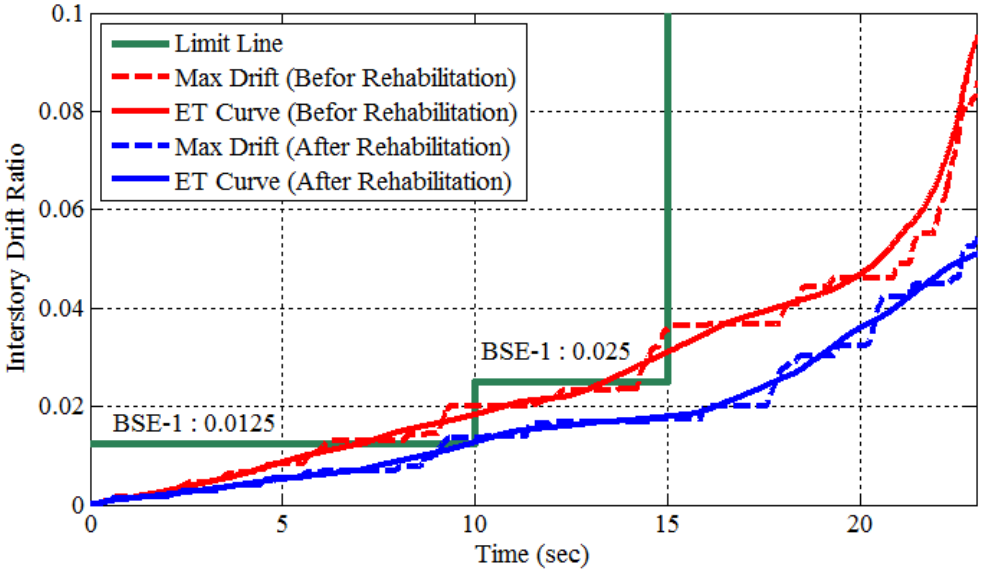

Figure 10. Prformance curve (ET curve) for 8 story frame before and after rehabilitation.

5.3. Verification and comparative study

In order to investigate the structure behavior under earthquake records and to compare them with the ET method estimation, the average response of the structure to seven earthquake records and also the response of the structure to the ET acceleration function before and after the rehabilitation in the frames are compared in Figure. 11 to Figure. 13.

As figures show there is a good compatibility between the resullts of two method, especially in 4 and 8 story frames. In 4 and 8 story frames, It can be seen that ET analyses properly estimate the response of the structure under GM set of ground motions in both hazard levels. The structure’s behavior after rehabilitation is also acceptable according to time-history analyses of the considered limits. In two story frames, although the interstory drift ratio line is over the limit line but almost it’s difference between ET result and limit line is neglible. In four story frame, at the BSE-1 hazard level MIDR (the second story) considerably reduced in two method and after rehabilitation it has a acceptance amount whereas there is no difference between MIDR (second story) before and after rehabilitation the BSE-2 hazard level.

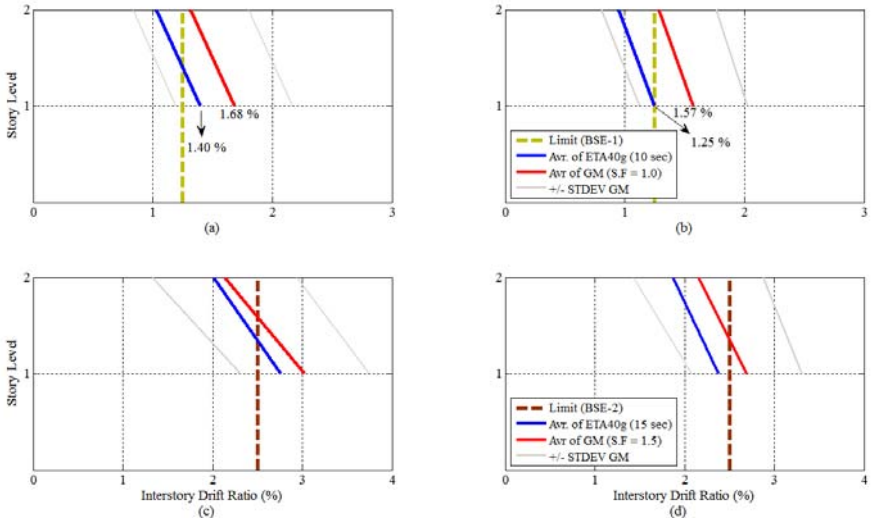

Figure 11. Average interstory drift ratios of 2 story frame under GM set of ground motions and ET estimation a) before rehabilitation in BSE-1 b) after rehabilitation in BSE-1 c) before rehabilitation in BSE-2 d) after rehabilitation in BSE-2

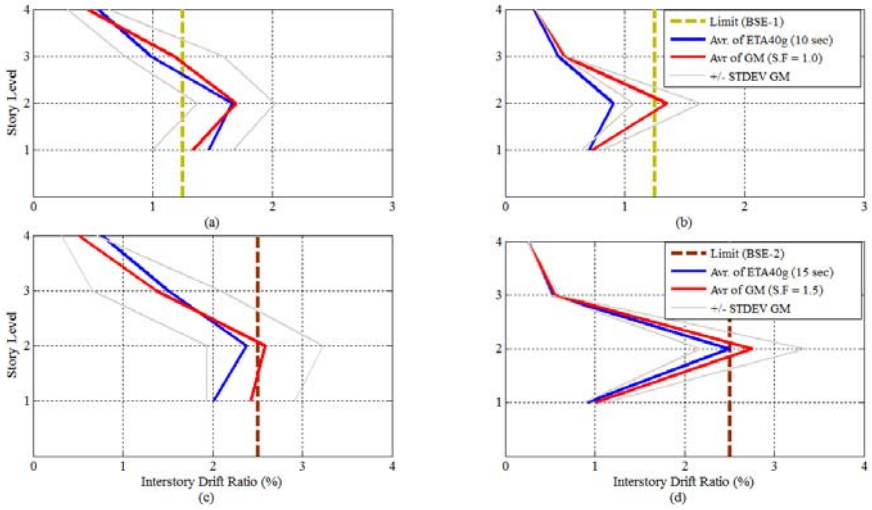

Figure 12. Average interstory drift ratios of 4 story frame under GM set of ground motions and ET estimation a) before rehabilitation in BSE-1 b) after rehabilitation in BSE-1 c) before rehabilitation in BSE-2 d) after rehabilitation in BSE-2

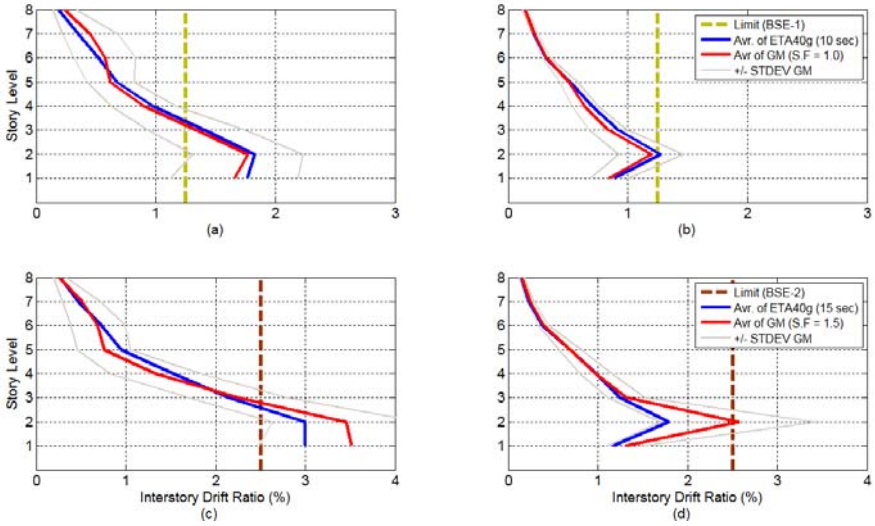

Figure 13. Average interstory drift ratios of 8 story frame under GM set of ground motions and ET estimation a) before rehabilitation in BSE-1 b) after rehabilitation in BSE-1 c) before rehabilitation in BSE-2 d) after rehabilitation in BSE-2

6. CONCLUSIONS

ET method can be considered an effective procedure in performance based optimum design of structures hugely reducing the required computational effort. This reduction of the number of required time-history analyses is accompanied by some loss of accuracy, suggesting classical procedures to be used for final verification of the design. Thus, the ET method can play a role in making the response-history analysis performance based seismic optimization a practical design alternative. Results show that ET analysis with acceleration functions series g has a good compatibility with IDA analysis with spectrum matched records on Reinforced Concrete (RC) Special Moment Frame (SMF) with and without dampers. By waiving the negligible difference between the results of two method it is be reasonable to use acceleration functions and ET method in optimization instead of IDA with with more much time for analyzing. Although yet this is not clear that which records and how many should be used for in IDA analyzing.

Acknowledgements

The authors would like to thank University of Isfahan for their support on this research.

References

1. Estekanchi, H. E., Riahi, H. T. and Vafai, A., Application of Endurance Time Method in Seismic Assessment of Steel Frames, *Engineering Structures*, 33:9, 2535-2546, 2011.
2. Riahi, H. T. and Estekanchi, H., E.Seismic Assessment of Steel Frames with Endurance Time Method, *Journal of Constructional Steel Research*, 66:6, 780-792, 2010.
3. ASCE/SEI 41-06, ASCE standard,Seismic rehabilitation of existing buildings, American Society of Civil Engineers, New York, 2007.
4. ASCE/SEI -07, ASCE standard, Minimum Design Loads for buildings and other Structures, American Society of Civil Engineers, New York, 2005.
5. OpenSees (2011), Open system for earthquake engineering simulation. Pacific Earthquake Engineering Research Center,http://peer.berkeley.edu/
6. Vamvatsikos D., Cornell C.A., Incremental dynamic analysis, *Earthquake Engineering and Structural Dynamics*, 31:3. 491–514, 2002.
7. Estekanchi, H. E. and Basim, M. Ch., Optimal damper placement in steel frames by the Endurance Time method, *The Structural Design of Tall and Special Buildings*, 20:5, 612-630, 2011.
8. FEMA P695, Quantification of Building Seismic Performance Factors, Federal Emergency Management Agency. Washington DC, 2009.
9. Hancock J, Watson-Lamprey J, Abrahamson NA, Bommer JJ, Markatis A, McCoy E, Mendis R., An improved method of matching response spectra of recorded earthquake ground motion using wavelets, *Journal of Earthquake Engineering*; 10, 67–89, 2006.
10. http://myweb.csuchico.edu/
11. Riahi, H. T. and Estekanchi, H. E., Seismic Assessment of Steel Frames with Endurance Time Method, *Journal of Constructional Steel Research*, 66:6, 780-792, 2010.

Cyclic nonlinear analysis of reinforced concrete slit walls with shear connections

Sergiu Andrei Baetu[1], Ioan Petru Ciongradi[1]
[1]*Department of structural mechanics,* "Gheorghe Asachi" Technical University, Jassy, *Romania*

Summary

An economical design of buildings based on performance criteria takes into account the dissipation of the seismic energy accumulated in the structure. In a tall structural wall, plastic hinges appear only at the base of the wall and the rest of the wall has not ductility resources and remains undamaged. A solution to increase the seismic performance of a reinforced concrete structural wall is to create a slit zone with short connections. Yielding of this shear connections increases the energy dissipation. The objective of these solutions is to create an improved structure for tall multi-storey buildings that has a rigid behavior at low seismic action and turns into a ductile one in the case of a high intensity earthquake. In this article, a comparative nonlinear cyclic analysis between slit walls and a solid wall is performed in the finite element software ANSYS and our main objective is to evaluate the nonlinear behaviour of the proposed walls.

KEYWORDS: reinforced concrete slit walls, short connections, cyclic nonlinear analysis, ductile behavior, energy dissipation capacity.

1. INTRODUCTION

Reinforced concrete walls are structural elements used in multi-story buildings in earthquake prone countries like Romania, Turkey, Chile, Mexico, China, Japan, USA, Peru etc., because they have a high capacity of resisting lateral loads. Nevertheless, such walls also require sufficient ductility to avoid brittle failure under the action of strong seismic loads. When a structure is subjected to strong earthquakes, it is necessary to assure, for economical design reasons, inelastic deformations without the failure of the building; this is because the design of buildings based on performance criteria takes into account the dissipation of seismic energy accumulated in the structure. The fact is that, in a tall structural wall, plastic hinges appear only at the base of the wall and the rest of the wall remains undamaged. There is an alternative solution which overcomes this

ISSN 2285-2735, Pages 25 - 42

drawback, consisting of creating a slit zone with short connections introduced into the wall structure. The solution proposed in this paper –structural reinforced concrete slit walls– changes the behavior of a the solid wall and provides to the structure more ductility, energy dissipation and adequate crack patterns (Figure 1).

The first precast slit panel was patented by Professor K. Muto, in Japan, in 1973 (Figure 1a) [1]. This is the first energy dissipation system used in Japan. This solution consisted of precast RC vertical strips introduced in the steel frames. Other solutions of slit walls have been proposed by Chinese, Korean, Iranian and Russian researchers. The Korean researchers proposed a slit panel used for reinforced concrete framed buildings in which strips are anchored into the beams (Figure 1b) [2]; in China was proposed a cast-in situ structural slit wall with a slit zone with short connections or inserted rubber belts (figures 1d and 1e) [3 – 5]; in Iran was proposed a cast-in situ reinforced concrete slit walls with a variable number of slits on the height (Figure 1f) [6, 7]; and in Russia it has been patented a precast panel with concrete strips assembled by post-stressing (Figure 1c) [8]. These solutions have been used to construct high-rises buildings up to 38 floors in Japan [9] and China [5], buildings that behaved very well during recent seismic events. The slab in these types of buildings can be cast-in situ or precast, and the structural walls are positioned at the border of the building or into the core, in order to reduce the influence of the slab stiffness.

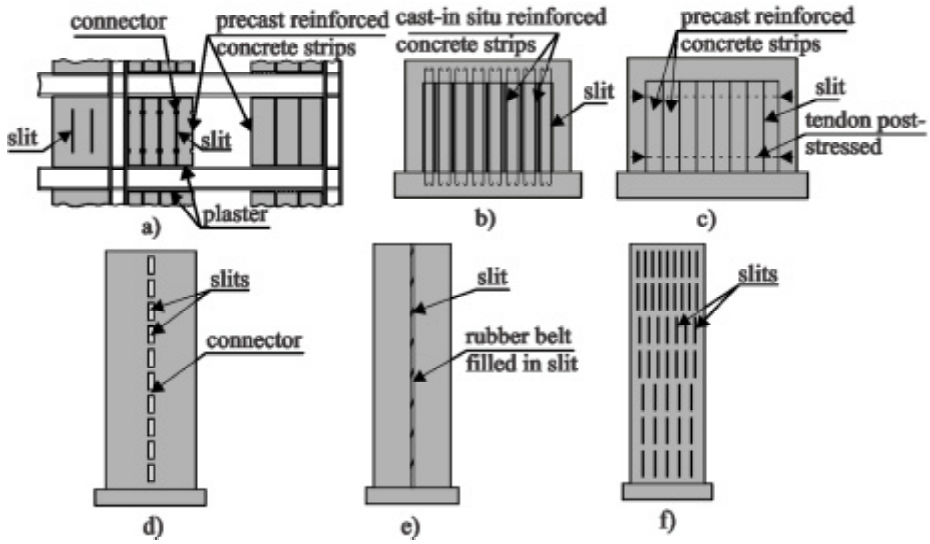

Figure 1. Slit panels and walls: a) precast slit panel with strips introduced in steel frames [1], b) slit panel with strips anchored in beams [2], c) precast panel with strips assembled by post-stressing [8], d) cast-in situ slit wall with a slit zone with short connections [3], e) cast-in situ slit wall with rubber belts inserted in slit zone [4] and f) cast-in situ reinforced concrete slit walls with a variable number of slits on height [6]

The reasons for introducing these solutions are related to the effects of soft soil – stiff structure interaction and the reduction of seismic design forces. In the case of a soft soil and a stiff building, the soil will absorb the seismic energy through deformations that can cause the overturning of the building [10]. By reducing the lateral stiffness, the fundamental natural period of vibrations is increased and resonance can be avoided. With this solution, the seismic demands can be significantly reduced and an economical design can be reached.

A case study corresponding to a 20 levels building designed for a seismic area with a dual reinforcement is analysed and discussed. A structural wall is extracted from this building and its detailed nonlinear structural analysis is performed. The same wall is then modified into a slit wall with short connections, in order to study the improvement if its behaviour when compared with that of the original wall. We performed the cyclic nonlinear analyses of RC structural walls studied in this article by using the finite element software ANSYS 12. This software allows calculating the behaviour of short connections with a realistic finite element model able to handle complex geometries and to describe precisely the complex stress state and the cracking pattern.

2. STRUCTURE DESCRIPTION

The case study considers a multi-storey building in a seismic area from which a reinforced concrete structural wall is isolated. The building is located in the city of Iasi, Romania, which has the following site characteristics: design ground acceleration a_g =0.2g, control period T_c=0.7s, ductility class H, importance factor ?$_I$=1 [11]. The building has dual reinforced concrete structure and regular form in plan and elevation. The seismic lateral loads applied upon the building are absorbed by the concrete core and, in the short direction, by the border walls. It has 20 levels with a height of 3m each. In plan, the building has 31 m in length and 21 m in width (Figure 2). The concrete used in the analysis is C32/40. The fundamental period of the structure is T_1=1.077s. The study is focused on a lateral wall with a length of 10m (Figure 3). The design analysis was performed with the computer program SAP2000 with which a thickness of the wall of 40 cm was obtained; the wall is reinforced with vertical bars ø14/15 and horizontal bars ø10/15 and, at the boundary it has 8ø28 bars [12, 13]. The number of short connections is varied along the wall height. The height of each connection is 0.40m and the thickness of the slit is 5cm. Comparative analyses were conducted on the slit walls and on a solid wall.

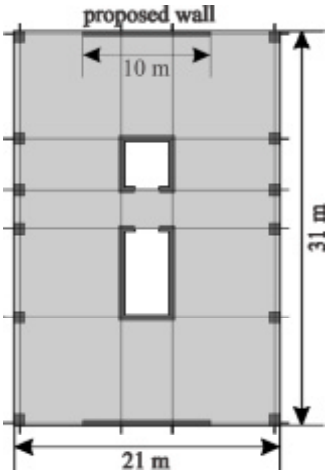

Figure 2. Dimensions of the studied building

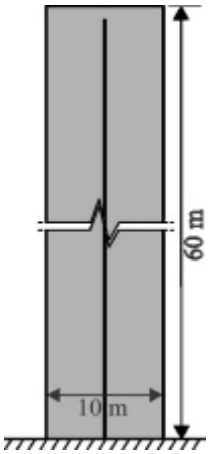

Figure 3. Dimensions of the studied slit wall

3. FINITE ELEMENT ANALYSIS BY ANSYS 12 SOFTWARE

The concrete used in the analysis is C32/40. In the analysis of the short connection performed with the ANSYS 12 computer program, the finite element used for concrete is Solid 65 with cubic shape and the dimension of 50 mm (Figure 4a). Solid 65 elements are capable of plastic deformation, cracking in three orthogonal directions, and crushing. The loading is applied in the y direction through a steel plate in order to prevent stress concentrations. The steel plate is meshed with finite element Solid 45 (Figure 4b) with the same dimensions as concrete. The rebars were modeled by using the smeared model (Figure 4a) [14 – 20].

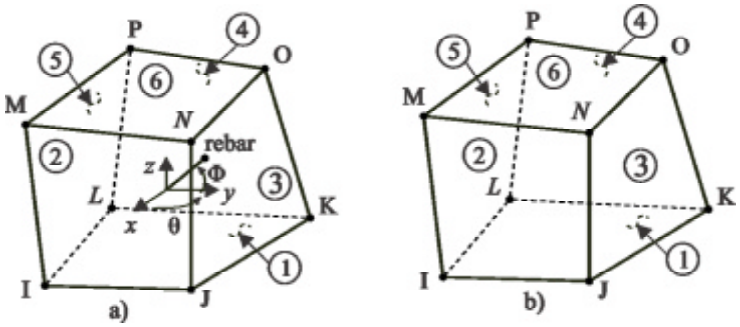

Figure 4. Finite elements used in analysis: a) Solid 65 for concrete and c) Solid 45 for steel plate [18]

The multilinear isotropic material uses von Mises failure criterion along with the Willam and Warnke (1974) model to define the failure of the concrete. For the boundary elements a confined concrete was set. The compressive uniaxial stress-strain curve for the unconfined and confined concrete is shown in the Figure 5 [15, 16, 18]. The multilinear isotropic stress-strain curve for unconfined concrete is computed with equations proposed by Desayi and Krishnan in 1964 [21], and for confined concrete can be used the curve used for unconfined concrete with increased strength and deformations according to SR EN 1992-1-1:2004 [22].

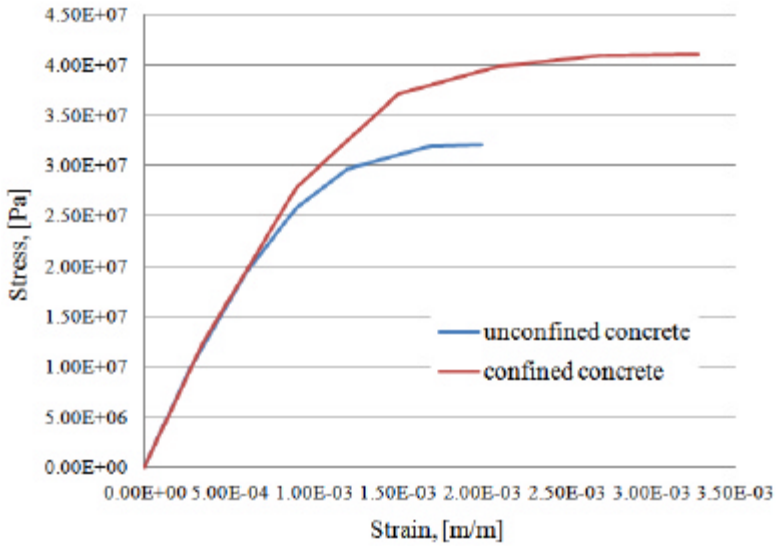

Figure 5. Uniaxial stress-strain curve for the unconfined and confined concrete

Implementation of the Willam and Warnke material model in ANSYS requires different constants be defined (Table 1) [17].

Table 1. Concrete Properties

1	Shear transfer coefficients for an open crack (b_t)		0.4
2	Shear transfer coefficients for an closed crack (b_c)		0.8
3	Uniaxial tensile cracking stress (f_r)		2.2E+006 Pa
4	Uniaxial crushing stress (f_c)	unconfined concrete	3.2E+007 Pa
		confined concrete	4.1E+007 Pa

For the reinforcement definition, parameters to be considered are material number, volume ratio and orientation angle (? and F) in X and Y directions respectively (Table 2). Volume ratio refers to the ratio of steel to concrete in element.

Table 2. Real constants for concrete

Particulars	Constants		
	Real constant for rebar 1 (vertical rebar)	Real constant for rebar 2 (horizontal rebar)	Real constant for rebar 3 (vertical rebar-boundary element)
Material number	2	2	2
Volume ratio	0.00513	0.00377	0.0308
Orientation angle ?	90	0	90
Orientation angle F	0	90	0

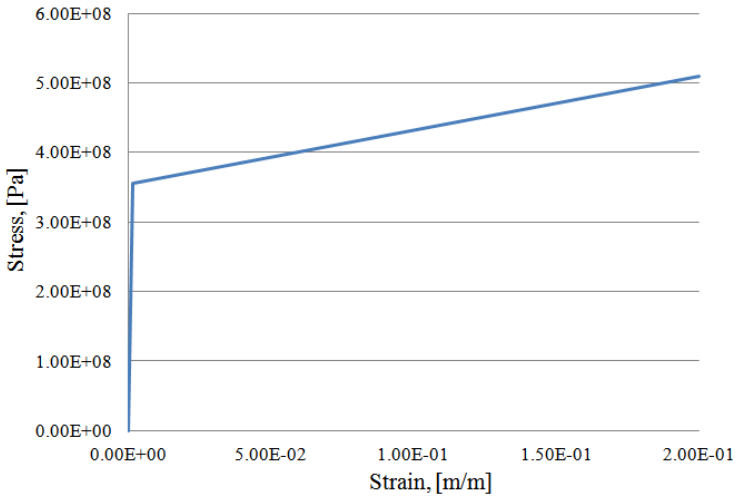

Figure 6. Stress-strain curve for reinforcement

In Figure 6 is shown the stress-strain curve of reinforcement used in this study. The bilinear kinematic hardening model (BKIN) was used [18, 21]. The bilinear model requires the yield stress (f_y =3.55E+008 Pa) and the hardening modulus of the steel ($E_s^{'}$ =2.1E+009 Pa).

4. CYCLIC ANALYSIS

4.1 Loading and boundary conditions

The structural wall is fully restrained at the base (Figure 8). Cyclic analysis is done with forces that are disposed uniform along the height of wall. In Figure 7 are presented the load patterns for each studied wall.

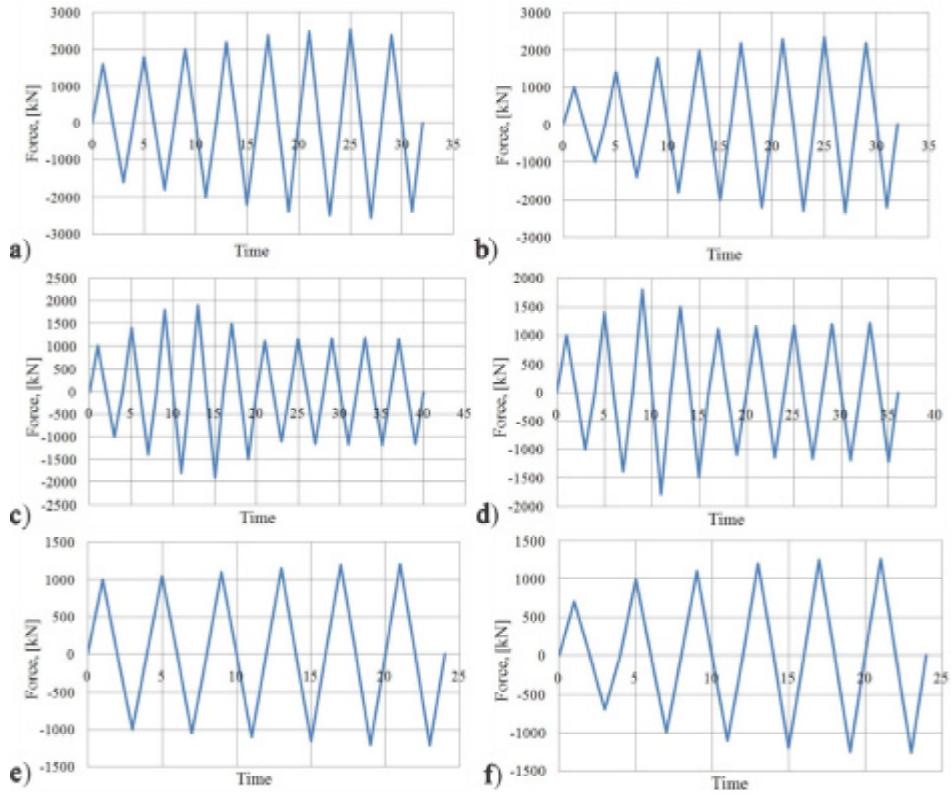

Figure 7. Load pattern for the studied walls: a) solid wall and slit wall with 20 connections, b) slit wall with 10 connections, c) slit wall with 5 connections, d) slit wall with 4 connections, e) slit wall with 3 connections and f) slit wall with 2 connections

Concentrated forces are applied at each level through steel plates to avoid the stress concentrations. The gravity loads include structural wall weight which is taken by the program and loads from floor connected to the wall 47.3 kN divided on each node of the slab zone.

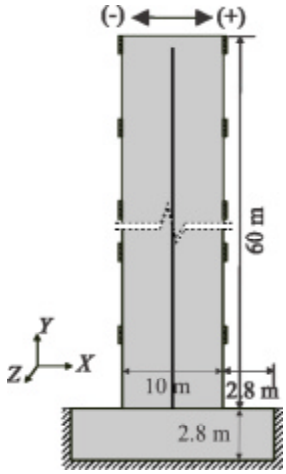

Figure 8. Boundary conditions

4.2 Comparative analysis of the slit and solid walls

In this part of the article, comparative analyses were conducted on the slit walls and on a solid wall. The number of short connections is varied along the wall height and the height of the connections is kept 40 cm. Figure 9 shows the lateral load vs. displacement hysteresis diagrams of the studied walls: solid wall (Figure 9a), slit wall with 20 connections (Figure 9b), slit wall with 10 connections (Figure 9c), slit wall with five connections (Figure 9d), slit wall with four connections (Figure 9e), slit wall with three connections (Figure 9f) and slit wall with two connections (Figure 9g). From these hysteretic loops we can observe that by introducing a slit zone into the structural wall the behavior of the element is changed, a greater displacement being obtained by a sudden degradation of strength following the failure of the shear connections. The solid wall and the slit wall with 20 connections have almost the same behavior, both fails at a low displacement due to large crushing of the concrete at the base. Cracks due to bending are extended on less of the half of the solid wall (Figure 11). Before the ultimate load many shear cracks at 45^{o} develop at the base of the wall. The slit wall with 10 connections fails as well due to large crushing of the concrete at the base and due to failing of five connections from the bottom zone that split the structural wall in two walls only to the middle. This mean that this slit wall has an undesired behavior because weakens the bottom zone and the slip doesn't appear on all height of the wall how should occur. As we can see from hysteresis loop for the reinforced concrete structural slit wall with five connections after the maximum load was reached and the short connections have crushed, the stiffness of the wall is drastically decreased and the slipping along the connections zone has appeared. After this point the hysteresis behavior of the slit wall became stable and a lot of hysteretic energy is dissipated.

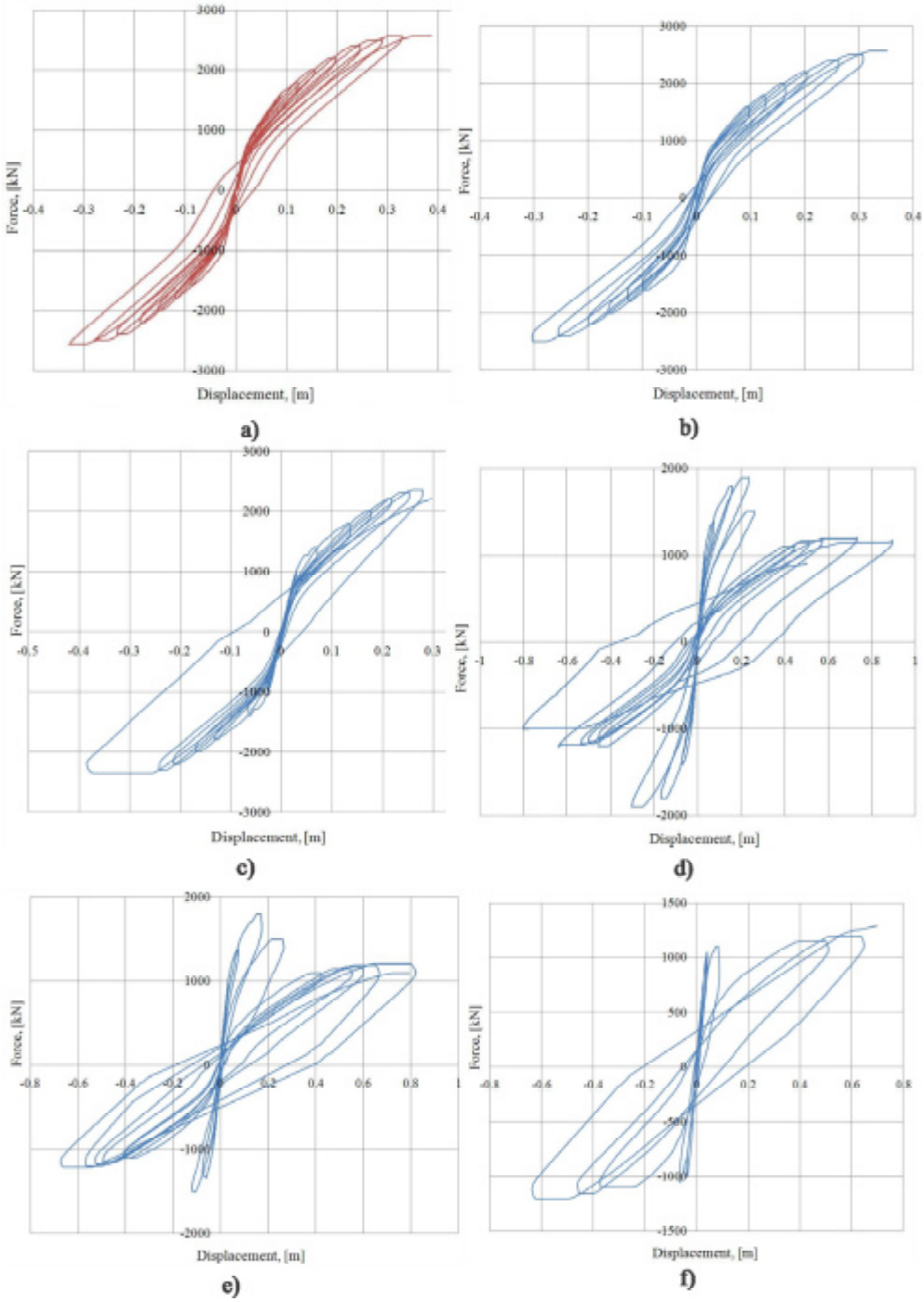
Force, [kN]
Displacement, [m]
a)
b)
c)
d)
e)
f)

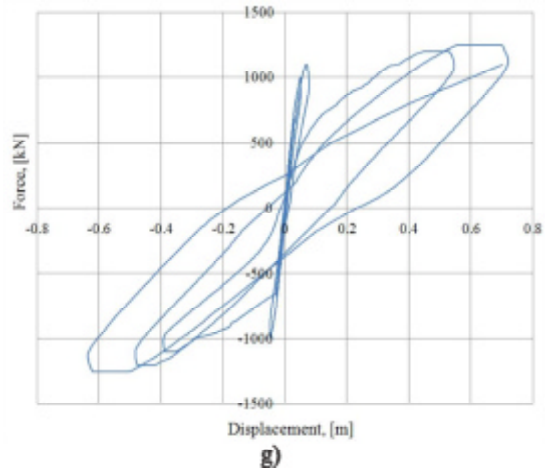

Figure 9. Cyclic behavior of the studied walls: a) solid wall, b) slit wall with 20 connections, c) slit wall with 10 connections, d) slit wall with 5 connections, e) slit wall with 4 connections, f) slit wall with 3 connections and g) slit wall with 2 connections

The behavior of the slit wall with four connections is almost identical with that of the slit wall with five connections having a lower maximum load and better hysteresis behavior with large loops after the short connections break. For slit walls with three and two connections the initial high stiffness decreases at a low lateral force and at a small displacement. These slit walls fails at a low number of cycles because each wall split in two slender walls very fast, and the plastic hinges appear concentrated at the base exactly as in the case of solid wall with a worst crack pattern. Figure 10 shows the comparison between strength envelopes of the studied walls.

Analyzing Figure 11 we can observe that the slit wall with five connections have a better crack pattern than solid wall before failure. In both walls the concrete is crushed on a length of 1.2…1.6 m on all border zones and on all height of first floor. To compare the behavior of the studied walls the ductility factor (μ) based on cyclic response and the hysteretic energy are calculated. Ductility is defined as the capacity of an element to undergo inelastic deformations with acceptable stiffness and strength reduction. Brittle elements fail after reaching their strength limit at very low inelastic deformations and ductile elements fail at large inelastic deformations. Most structures and elements are designed to behave inelastically under strong earthquakes for reasons of economy. The response amplitudes of earthquake-induced vibrations are dependent on the level of energy dissipation of structures, which is a function of their ability to absorb and dissipate energy by ductile deformations. For low energy dissipation, the structures may develop stresses that correspond to relatively large loads. These structures should be designed to withstand lateral forces of the same proportion of their weight to

remain in the elastic range. This is uneconomical in all practical applications with the exception of nuclear power plants, offshore platforms, water-retaining structures and other safety-critical structures [23].

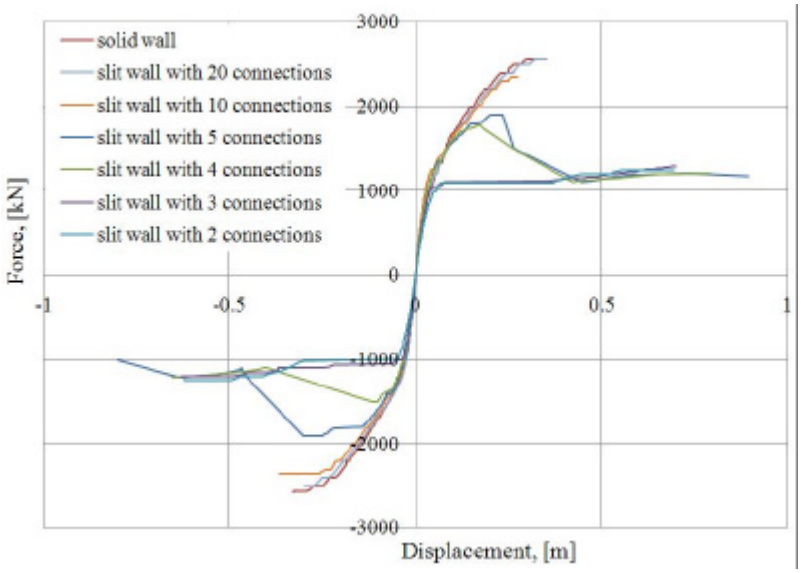

Figure 10. Comparison between strength envelopes of the studied walls

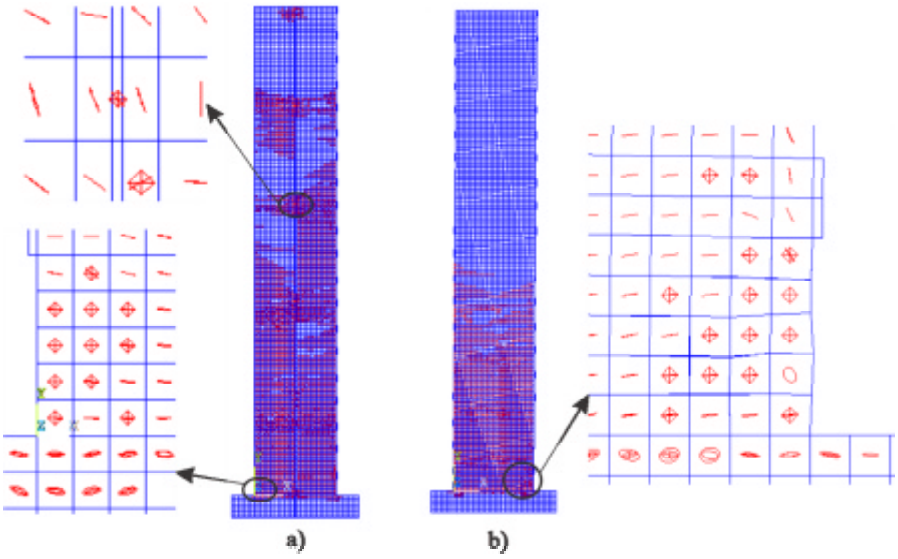

Figure 11. Crack pattern before collapse for: a) slit wall with 5 connections and b) solid wall

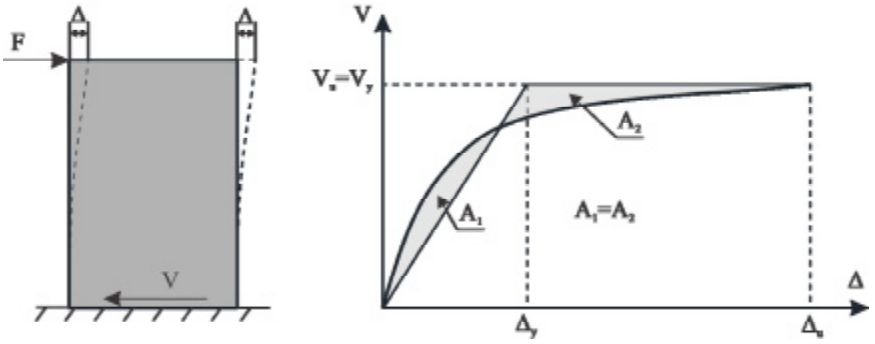

Figure 12. Yield point determination method

Definition of ductility factor based on cyclic response is given below and is related to the cyclic deformations:

$$m = \frac{\left|\Delta^{+}_{\max}\right| + \left|\Delta^{-}_{\max}\right|}{\left|\Delta^{+}_{y}\right| + \left|\Delta^{-}_{y}\right|} \tag{1}$$

Where: $\Delta^{+}_{\max}$, $\Delta^{-}_{\max}$ - are the positive and negative ultimate displacements,

Δ^{+}_{y}, Δ^{-}_{y} - are the positive and negative yielding displacements.

In seismic design, high ductility is essential to ensure plastic redistribution of actions among components of lateral resisting systems and to allow for large absorption and dissipation of earthquake input energy. Ductile structures may withstand extensive structural damage without collapsing or endangering life safety. The evaluation of the yield displacement from strength envelopes is not always straightforward.

Yield points are often wrong defined because of non-linearities and formations of plastic hinges in component elements. Response curves of reinforced concrete frequently do not present well-defined yield points because of cracking of concrete and sequential yielding of reinforcement bars. There are various definitions for yield displacements and in this paper we chose displacement corresponding to the yield point of an equivalent elasto-plastic system with the same energy absorption as the real system (Figure 12), [24]. Strength envelopes (Figure 13) are used to extract the yielding force and the ultimate displacement by replacing each strength envelope with the idealized curve. The case of slit walls with four and five short connections is a special one because the strength envelope has strength degradation and the idealized curve has to be tri-linear and, therefore, it was developed according to FEMA 440 [25]. The sum of the areas enclosed between the curve and the idealized curve must be zero. In the case of the slit walls with three and two

short connections is not necessary to replace the strength envelope with an idealized curve because the strength envelope has an idealized elasto-plastic shape (Figure 13f and g), and the yield point can be easily chosen. For these two walls the yield points are considered to appear when the short connections suddenly break and the stiffness drops close to zero.

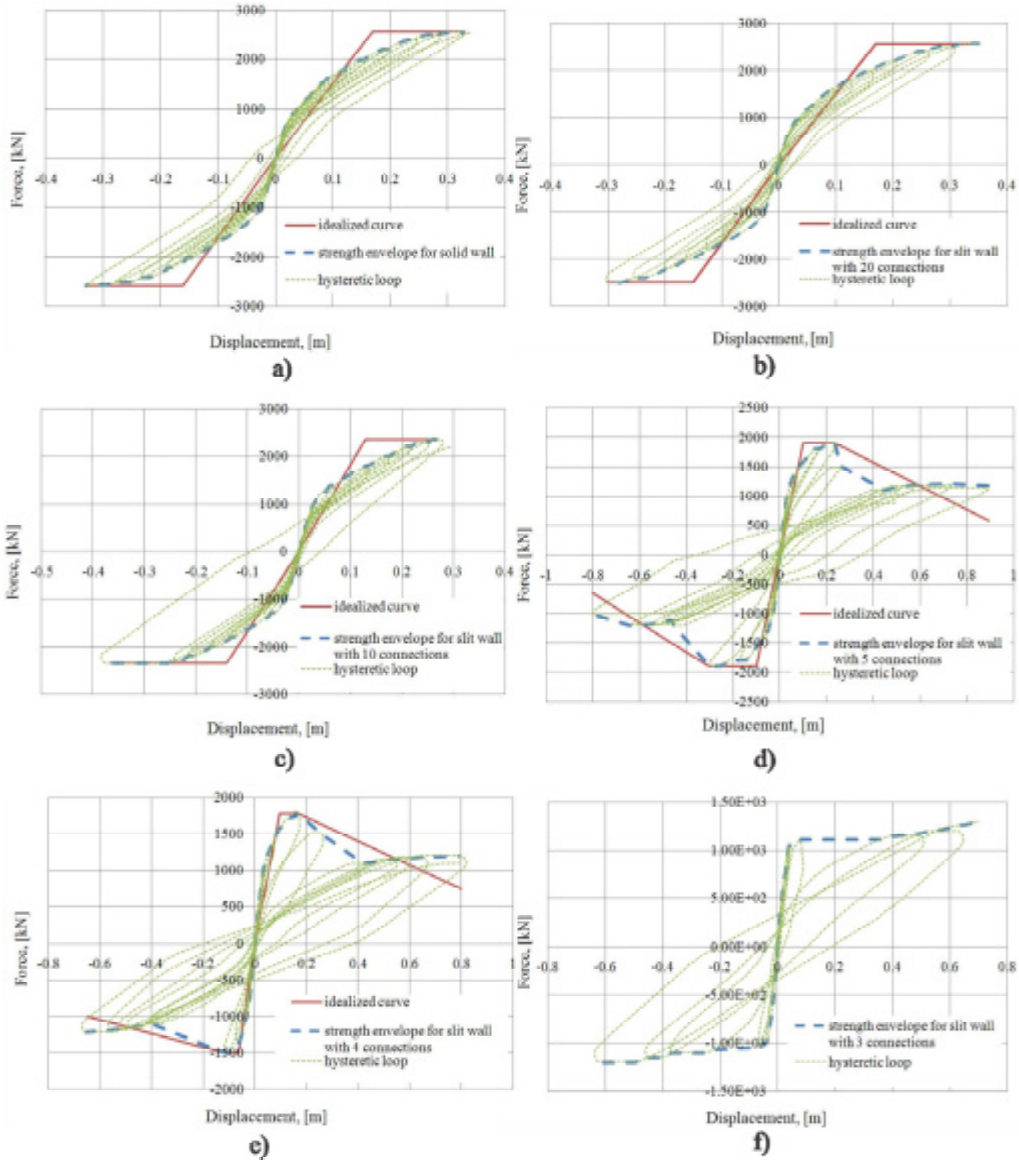

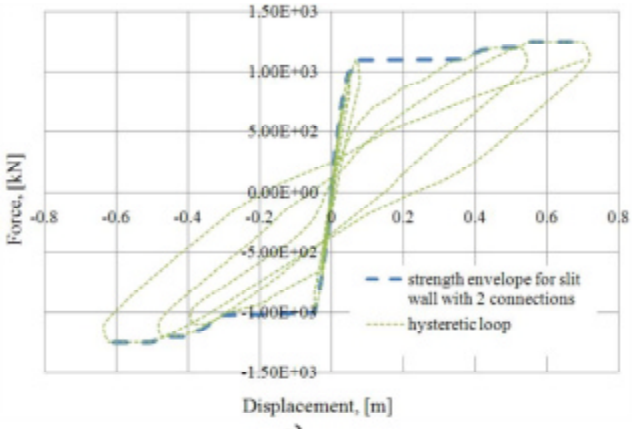

Figure 13. Idealized curves for the studied walls: a) solid wall, b) slit wall with 20 connections, c) slit wall with 10 connections, d) slit wall with 5 connections, e) slit wall with 4 connections, f) slit wall with 3 connections and g) slit wall with 2 connections

Table 3. The parameters required to calculate the ductility factor

Studied walls	Δ^{+}_{max}	Δ^{-}_{max}	Δ^{+}_{y}	Δ^{-}_{y}	μ
Solid wall	0.328	0.33	0.17	0.16	1.994
Slit wall with 20 connections	0.35	0.30	0.17	0.15	2.03
Slit wall with 10 connections	0.27	0.366	0.13	0.14	2.355
Slit wall with 5 connections	0.894	0.80	0.10	0.10	8.47
Slit wall with 4 connections	0.80	0.65	0.095	0.065	9.063
Slit wall with 3 connections	0.60	0.62	0.072	0.06	9.24
Slit wall with 2 connections	0.68	0.62	0.067	0.06	10.23

Figure 14. Ductility variation with the number of short connections

In Table 3 are introduced all the parameters required to calculate the ductility factor, these being extracted from idealized curves for the studied walls presented in Figure 13. Then, a graphic variation of ductility factor with the number of short connections disposed on the wall height is done (Figure 14). From this graphic we can see that the slit walls with 20 and 10 connections have a small ductility that is very close to the solid wall ductility, resulting that these structural elements are brittle. As we can see the ductility factor increases with the decrease of the number of short connections. For the slit walls with five, four, three and two short connections disposed on the wall height the ductility factor reaches high values.

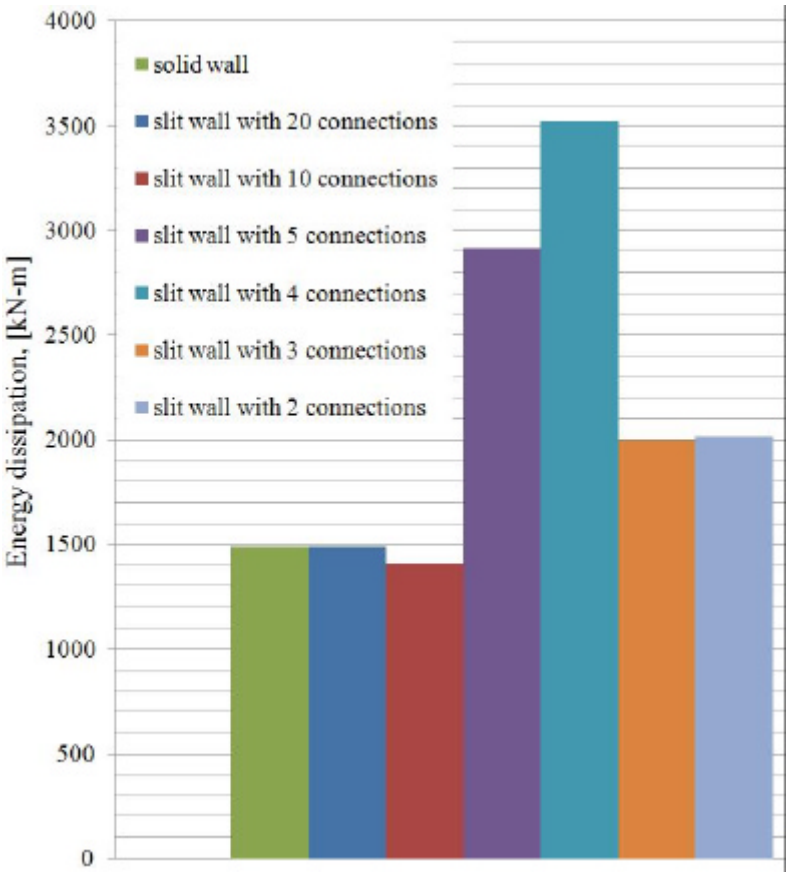

Figure 15. Comparison between cumulative hysteretic energy dissipated by slit walls and solid wall

Figure 15 shows the total energy dissipated of studied walls proposed in this analysis. The area enclosed by a hysteretic loop at a given cycle represents the energy dissipated by the wall during that cycle. It is found that the slit wall with four and five short connections have the highest energy dissipation capacity

resulted from the ability to withstand many cycles of loading. This is also due to energy dissipation mechanism that is different for these slit walls and other walls from this study. These slit walls dissipates seismic energy by cracks extended on all the surface of the wall and by crushing of the shear connections while the other slit walls and the solid wall dissipates seismic energy only by cracks at the base of the wall.

5. RESULTS INTERPRETATION

These analyses demonstrate that introducing a slit zone with short connections in a structural wall, with a rational disposal and a correct number of the short connections can significantly increase the dissipated hysteretic energy of this element. The seismic performance can be controlled by setting the short connections to satisfy different design criteria under different earthquake levels. Comparisons between the studied structural walls reveal that they have a different behavior. The solid wall is very stiff and the plastic zone is concentrated at the base, from this reason fails at a low displacement due to huge crushing of concrete. The slit walls with 20 and 10 short connections have a behavior close to the solid walls, because having a great number of connections disposed on the wall height no slipping appear in the slit zone and only a few connections from the base break, resulting that these slit walls fail as well at the base. On the other hand, the slit walls with four and five short connections have an initial stiffness compared with the solid wall but when the shear connections break, the strength starts to decrease, in this way the base of the walls being protected. The final displacement of these slit walls is much bigger than that of the solid wall. These slit walls have also a higher value of ductility factor than the solid wall. Reducing the number of short connections to three or two, the short connections break very fast at a small lateral displacement, resulting that the base of the walls remain in the elastic range, without cracks. In the calculation of the ductility factor for these walls it was considered that the yield displacement is the lateral displacement when the connection break and the stiffness is reduced. From this reason extremely high values for ductility factors emerge from these calculations. However, these two slit walls have a lower energy dissipation capacity because after the connections break the plastic hinges form quickly at the base and doesn’t resist at many cycles of loading.

6. CONCLUSIONS

An economical design of buildings based on performance takes into account the dissipation of seismic energy accumulated in the structure. Reinforced concrete walls are frequently used as strength elements for structures designed in areas with high seismic risk. If ductility is a major concern, structural walls are not considered an efficient structural component. The main problems of these structural elements - low ductility and reduced energy dissipation capacity - are removed through the solutions presented in this article. The short connections disposed on the wall height in the slit zone prevent collapse of the structural element under extreme seismic excitations by dissipating hysteretic energy through an improved crack pattern. From these analyses we can conclude that the slit walls with four and five short connections have the best behavior, the highest ductility and the highest energy dissipation capacity. Also, it can be concluded that the number of short connections disposed on the wall height have a great influence on the ductility and on the energy dissipation capacity of the slit walls, that's why this number must be chosen wisely if we want to reach to the best behavior.

References

1. Muto, K., Ohmori, N., Itoh, T., *Composite building structure and walls therefor*, United States Patent 3736712, 1973.
2. Liou Y.W., Sheu S. M., *Prediction of lateral stiffness for fully slitted RC shear wall*, Journal of the Chinese Institute of Engineers, vol. 21, 1998, pp. 221-232.
3. Kwan, A.K.H., Dai, H., Cheung, Y.K., *Non-linear seismic responce of reinforced concrete slit shear walls*, Journal of Sound and Vibration, vol. 226, 1999.
4. Lu X., Wu X., *Study on a new shear wall system with shaking table test and finite element analysis*, Earthquake Engineering and Structural Dynamics, vol. 29, 2000, pp. 1425-1440.
5. Lu X., Huanjun J., *Nonlinear earthquake response analysis and energy calculation for seismic slit shear wall structures*, Earthquake Engineering and Engineering Vibration, vol.1, no. 2 (2002), pp. 227-237.
6. Sabouri J., Ziyaeifar M., *Shear walls with dispersed input energy dissipation potential*, Asian Journal of Civil Engineering (Building and Housing), vol. 10, no. 5 (2009), pp. 593-609.
7. Labafzadeh M.S.R., Ziyaeifar M., *Seismic behaviour of RC dual ductility mode shear walls*, The 14th World Conference on Earthquake Engineering, Beijing, China, October 12-17, 2008.
8. Pavlik, V.S., Vasionkin, A.N., *Earthquake resistant building*, Patent nr.512279, URSS, 1976.
9. Aoyama H., *Dr. Kiyoshi Muto (1903-1989)*, Structural Engineering International, vol. 1, 2005, pp. 50-52.
10. Marin M., Roman O., *Hazardul seismic al Timisoarei*, Buletinul AGIR, no. 2-3 (2010), pp. 36-42.(in Romanian)
11. Code for seismic design of buildings P100-1/2006. (in Romanian)
12. Code for the design of buildings with reinforced concrete stuctural walls CR 2-1-1.1-2005. (in Romanian)
13. Sergiu Andrei Baetu, Ioan Petru Ciongradi, Georgeta Vasies, *Static nonlinear analysis of structural reinforced concrete walls energy dissipators with shear connections*, "Computational Civil Engineering 2010", International Symposium, Iasi, Romania, May 28, 2010.

14. Greeshma S., Jaya K.P., Annilet S.L., *Analysis of flanged Shear Wall Using ANSYS Concrete Model*, International Journal for Civil and Structural Engineering, vol. 2, no. 2 (2011), pp. 454-465.
15. Kheyroddin A., Naderpour H., *Nonlinear Finite Element Analysis of Composite RC Shear Walls*, Iranian Journal of Science & Technology, vol. 32, no. B2 (2008), pp. 79-89.
16. Raongjant W., Jing M., *Finite Element Analysis on Lightweight Reinforced Concrete Shear Walls with Different Web Reinforcement*, The Sixth PSU Engineering Conference, May 8-9, 2008, 61-67.
17. Terec L., Bugnariu T., Pastrav M., *Analiza Neliniara a Cadrelor din Beton Armat cu Pereti Turnati în Situ*, Romanian Journal of Materials, vol. 40, 2010, pp. 214-221.
18. Wolanski J.A., *Flexural Behavior of Reinforced and Prestressed Concrete Beams Using Finite Element Analysis*, Master Thesis, Marquette University, Milwaukee, Wisconsin, 2004.
19. Kazaz I., Yakut A., Gulkan P., *Numerical simulation of dynamic shear wall tests: A benchmark study*, Computers & Structures, vol. 84, 2006, pp. 546-562.
20. ANSYS 12 Structural Analysis Guide, 2009.
21. Kachlakev D., Miller T., Yim S., *Finite Element Modeling of Reinforced Concrete Structures Strengthened with frp Laminates*, Oregon Dept. of Transp., USA, Res. Group, Final Report SPR 316, May 2001.
22. Proiectarea structurilor din beton, SR EN 1992-1-1:2004.
23. Elnashai A.S., Di Sarno L., *Fundamentals of earthquake engineering*, John Wiley & Sons, 2008.
24. Sittipunt C., Wood L.S., *Finite element analysis of reinforced concrete shear walls*, Research Grant BC 589-12992, University of Illinois, 1993.
25. FEMA 440 – Improvements of nonlinear static seismic analysis procedures 2005.

Probabilistic assessment of the seismic damage in reinforced concrete buildings

Alex H. Barbat[1], Yeudy F. Vargas[1] Lluis G. Pujades [1] and Jorge E. Hurtado[2]
[1] *Universidad Politécnica de Cataluña, Barcelona, Spain*
[2] *Universidad Nacional de Colombia, Manizales, Colombia*

Summary

The main objective of this article is to assess the expected seismic damage in reinforced concrete buildings from a probabilistic point of view by using Monte Carlo simulation. To do that, the seismic behavior of the building is studied by using random capacity obtained by considering the mechanical properties of the materials as random variables. Starting from the capacity curves, one can obtain the damage states and the fragility curves as well as to develop curves describing the expected seismic damage of the structures as a function of a seismic hazard characteristic. The latter can be calculated using the capacity spectrum and the demand spectrum according to the methodology proposed by the RISK-UE project. For defining the seismic demand as a random variable, a set of real accelerograms are obtained from the European and Spanish databases in such a way that the mean of their elastic response spectra is similar to an elastic response spectrum selected from Eurocode 8. In order to combine the uncertainties associated with the seismic action and the mechanical properties of materials, two procedures are considered for obtaining functions which relates the PGA to the maximum spectral displacements. The first one is based on a series of nonlinear dynamic analyses. The second one is based on the well known procedure named equal displacement approximation exposed in ATC 40. After applying both procedures, the probability density functions of the maximum displacement at the roof of the building are obtained and compared. The expected structural damage is finally obtained by replacing the spectral displacement obtained by using the ATC 40 and the incremental dynamic procedure. In the damage functions the results obtained from incremental static and dynamic analyses are finally compared and discussed from a probabilistic point of view.

KEYWORDS: Probabilistic seismic assessment, capacity curves, vulnerability, fragility curves, expected damage.

1. INTRODUCTION

The vulnerability of structures subjected to earthquakes can be evaluated numerically either by using incremental static analysis or pushover analysis or by means of nonlinear dynamic analysis performed in an incremental way. All the variables involved in such structural analyses, mainly the mechanical properties and the seismic actions, should be considered as random. The reason is that the randomness of the implied variables combined with the uncertainties in the seismic hazard, may lead to an underestimation or an overestimation of the actual vulnerability of the structure, but they are not always treated in this way. Due to the current capacity of the computers, a great number of structural analyses can be performed in order to study the behavior of buildings from a probabilistic standpoint within the framework of Monte Carlo simulation.

This study focuses on the nonlinear seismic response of reinforced concrete buildings and on their damage analysis considering the involved uncertainties (Fragiadakis & Vamvatsikos 2009). In the pushover analysis, previous studies already considered uncertainties (Bommer & Crowley 2006; Borzi et al. 2007; Fragiadakis & Vamvatsikos 2010) and evaluated the nonlinear behavior of structures considering uncertainties in the mechanical properties of materials and in the nonlinear static analysis (pushover) by means of the Monte Carlo method. Dolsek (2010) considered in this type of studies the seismic action as a random signal using real accelerograms roughly compatible with design spectra, but did not take into account the uncertainties associated to the structural characteristics. The present paper aims to assess the seismic vulnerability of the structure considering both the mechanical properties of the materials as random variables and the seismic actions as random signals. The seismic demand for the area is obtained in probabilistic terms starting from the response spectrum chosen from Eurocode 8. Afterwards, a procedure for selecting accelerograms whose response spectra are compatible, in a mean sense, with the mentioned response spectrum, is applied. In this study, we compare the results carried out by using the above mentioned analyses: 1) Incremental static analysis or pushover analysis (PA). 2) Nonlinear dynamic analysis (NLDA) in an incremental way, that is, an incremental dynamic analysis (IDA) (Vamvatsikos and Cornell 2002). PA and NLDA have been compared in previous studies (Mwafy & Elnashai 2001; Poursha et al. 2007; Kim & Kuruma 2008). The PA is used to determine the capacity curves of the structure and to obtain the expected displacement at the roof of the building for a given seismic area (Borzi et al. 2008; Barbat et al. 2008; Lantada et al. 2009; Pujades et al. 2011). The roof displacement obtained with this procedure will be considered as a random variable and will be compared with the displacement calculated via IDA. Finally, the results are discussed and compared from a probabilistic point of view.

2. DESCRIPTION OF THE STUDIED BUILDING

The reinforced concrete building selected for this study is shown in Figure 1. The building is located in Spain and, therefore, some of the selected accelerograms are taken from the Spanish database. However, due to the low seismicity of the area, we use additional accelerograms taken from the European database. The building is regular in plan, allowing the use of a 2D model. Nevertheless, this building has not a framed structure but a structure with columns and slabs which, in this case, are waffled slabs. In Spain, this type of building is frequently used for family housing and for offices and has been previously studied (Vielma et al. 2009; Vielma et al. 2010). For the purpose of this study, we use a simplified equivalent framed model. The main geometric characteristics of the building can be seen in Figure 1.

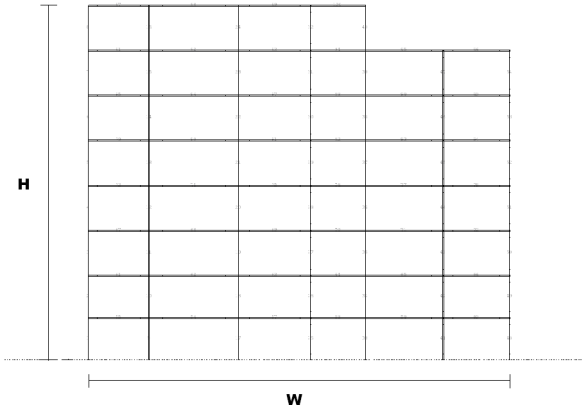

Figure 1. Equivalent frame of the reinforced concrete structure used in the probabilistic simulation

The constitutive law of the structural elements is elastoplastic without hardening or softening. In order to define the yield surfaces for the material of the columns and beams, it is necessary to create an interaction diagrams between the bending moment and the axial force, and between the bending moment and the angular deformation, respectively. Programs have been developed in MATLAB in order to calculate the yielding points which are necessary when defining the behavior of the structural elements used in the nonlinear static and in the dynamic analyses of the structures which, in this article, are performed by means of the RUAUMOKO computer software (Carr 2000).

3. MONTECARLO SIMULATION

3.1. Nonlinear static analysis

As mentioned before, the mechanical properties of the materials, such as the concrete compressive strength, *fc*, and the reinforced yield strength, *fy*, are random variables. The distribution assumed for these variables is Gaussian; the parameters that define these distributions, the mean value μ and the standard deviation σ, as well as the coefficient of variation r, are shown in Table 1. These parameters correspond to the values given in the original blueprints of the structure.

Table 1. Characteristics of the probability distribution of the mechanical properties of the structural elements

	Col 1	Col 2	Col ..
fc	30000	1000	3.33%
fy	411510	22093	5.36%

It is important to note that, in each pushover analysis, the strength of the structural elements is not constant because, for each of them, a new stochastic data is generated. On the other hand, in the PA the results change depending on the variation of the load pattern with the height. Besides, it is very difficult to establish how much to increase the load; moreover, a load maintaining the pattern corresponding to the first mode of vibration of the elastic structure cannot capture the effect of higher-modes (Poursha et al. 2008). To overcome these difficulties, we use the so-called adaptive pushover method in its version proposed by Satyarno (1999) and it is this one which will be referred in the following as PA. The advantage of the PA is the independency of the results on the loading pattern, because this is calculated as a function of the mass, the equivalent frequency and the deformed shape of the structure; furthermore, the horizontal load limit is controlled by the current stiffness of the structure. Figure 2 shows a comparison among different capacity curves calculated for different load patterns.

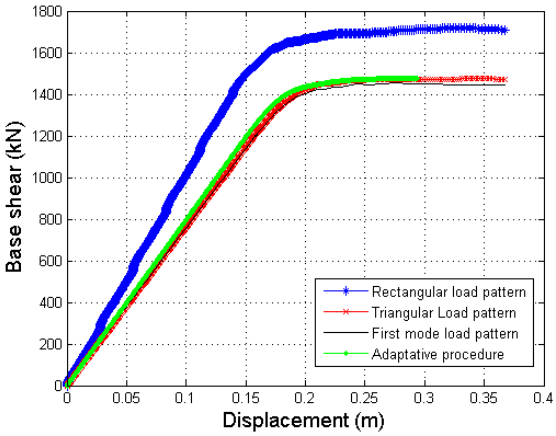

Figure 2. Capacity curves obtained with different load patterns

After generating 1000 samples of mechanical properties *fc* and *fy* by using the latin hypecube method, 1000 capacity curves are obtained and plotted in Figure 3 in which the uncertainties in the results can be seen.

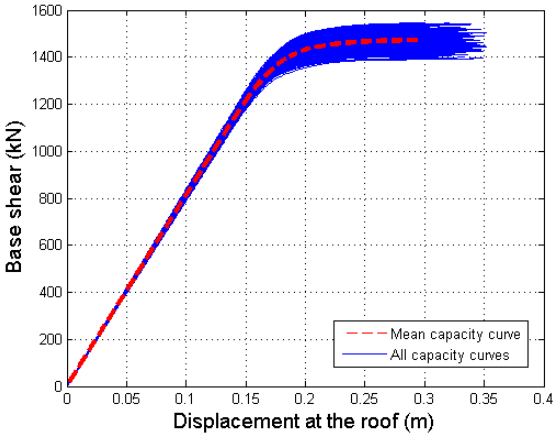

Figure 3. Capacity curves obtained via Monte Carlo simulation

3.1. Nonlinear static analysis

In order to consider the randomness of the seismic action, the response spectrum corresponding to EUROCODE 8 of type 1 and for soil type D is taken as target. Although we performed several tests using the type 2 spectra, we eventually used

in this article the type 1 spectrum for soil D, in order to achieve the nonlinear inelastic behavior of the structure, because for type 2 spectra the accelerograms require to be scaled for peak ground accelerations (PGA) higher than those expected in Spain; in the following, we will refer to this spectrum as the code spectrum. 20 acceleration records are selected whose mean 5% damped elastic response spectrum is in the range of +/- 5% of the code spectrum. There are several methods for selecting the accelerograms which describe the seismic hazard of an area (Hancock et al. 2008). In this paper we use a procedure based on least squares which consists in selecting a group of accelerograms whose mean spectrum minimize the error respecting the target spectrum (Vargas et al. 2012). In Figure 4, the code spectrum and the mean spectrum corresponding to the 20 selected accelerograms are shown.

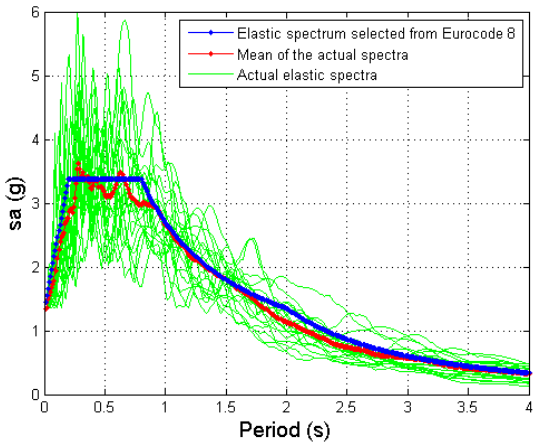

Figure 4. Comparison between the spectrum of EUROCODE 8 and the mean of the spectra of the earthquakes selected from the Spanish and European databases

The selected accelerograms are scaled to different levels of the peak ground acceleration and are then used to perform a series of NLDA within the framework of the incremental dynamic analysis, IDA. The scaling method used in this article consists of incrementing the acceleration ordinates by a scalar allowing to define the desired PGA levels. Even if in this way we maintain the initial frequency content of the seismic action, this scaling method is adequate for the purpose of this article, which is the comparison in a probabilistic way of the results obtained with static and dynamic nonlinear analysis methods considering uncertainties. Nevertheless, in the Monte Carlo simulation we considered 20 accelerograms scaled in this way, having their frequency content certain variability. The role of IDA in this article is to combine the uncertainties in the mechanical properties of the building with those involved in the seismic action. The objective is to obtain the evolution of a dynamic response variable, for instance the displacement at the

roof of the building, as a function of a variable describing the seismic action; we considered that this last variable is the PGA, which, in this case, is increased up to 0.25 g which is the maximum PGA value in the Spanish seismic design code. In the IDA, the variable which is related to the PGA is the expected spectral displacement (ESD). Obviously, as the seismic demand is obtained as a random variable, the ESD will also be random and, therefore, the values shown in Figure 5 are the mean values. This figure shows the variation of ESD, when PGA increases, together with the +/-1.65 standard deviation intervals that is, a confidence level of 95%. Figure 6 shows the evolution of the standard deviation of the ESD.

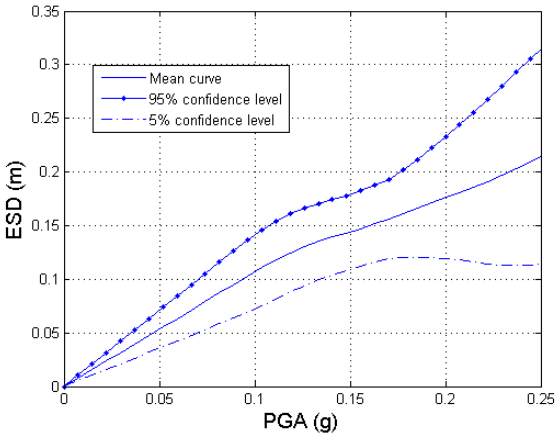

Figure 5. Relation between PGA and mean expected spectral displacement

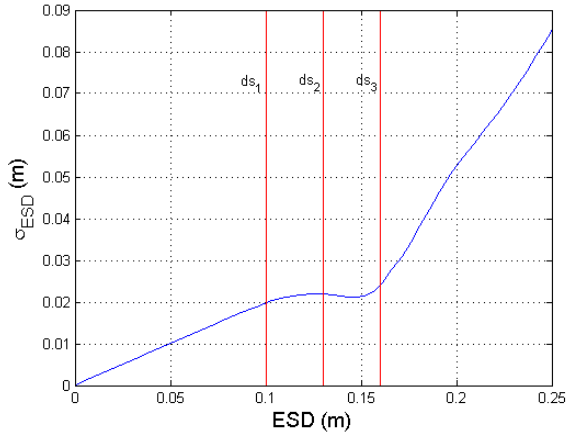

Figure 6. Relation between the mean expected spectral displacement and the standard deviation

In Figure 5, a major change in the slope of the curve approximately for 0.16 g can be seen, but other significant changes in the behavior of the structure can be not appreciated in this graph. However, Figure 6 shows three points related to significant changes in the slope of the curve; these points can be also seen in Table 2, where the first is related to the first change of the slope of the curve. The second point corresponds to the first maximum and the third one is related to the beginning of a straight line with maximum slope. Later on, we will use these points to discuss the damage states of the structure and, thus, its seismic behavior.

Table 2. Coordinates of the particular points which are identified in Figure 5

Point	X coordinates (m)	Y coordinates (m)
1	0.1	0.02
2	0.13	0.0294
3	0.16	0.0298

4. CAPACITY SPECTRUM, DAMAGE STATES AND FRAGILITY CURVES

4.1. Capacity spectrum and bilinear representation

Once calculated the capacity curve of the structure, it is useful transforming it in the capacity spectrum by means of the procedure proposed in the ATC-40 (1996). The capacity spectrum is represented in spectral acceleration-spectral displacement coordinates (*sa*-*sd*) and is often used in its simplified bilinear form, defined by the yielding point (*Dy*, *Ay*) and the ultimate capacity point (*Du*, *Au*), as it can be seen in Figure 7.

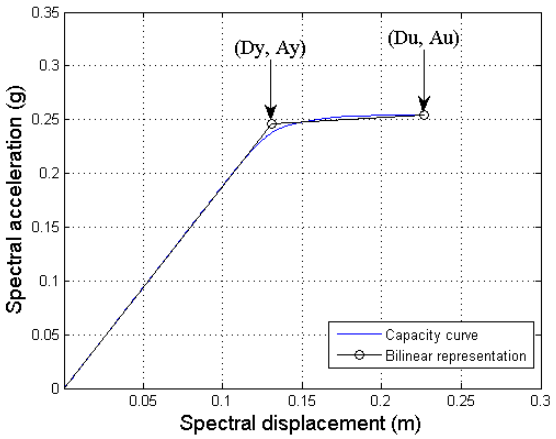

Figure 7. One of the capacity spectra of the studied building and its bilinear representation

4.2. Damage states

In order to analyze the expected damage we use simplified methods allowing to obtain the damage states thresholds *ds* and the corresponding fragility curves. Four non-null damage states are considered: (1) *slight*, (2) *moderate*, (3) *severe* and (4) *extensive-to-collapse*. For a given damage state, according to the hypothesis considered in the RISK-UE project (Milutinovic & Trendafiloski 2003), the damage state threshold is defined by the 50% probability of occurrence. This damage state threshold can be defined in the following simplified way from the bilinear capacity spectrum (Lantada et al 2008; Barbat et al 2010; Barbat et al 2011):

$$\begin{aligned} ds_1 &= 0.7 * Dy \\ ds_2 &= Dy \\ ds_3 &= Ds_2 + 0.25 * (Ds_4 - Ds_2) \\ ds_4 &= Du \end{aligned} \tag{1}$$

The damage states thresholds have been established for all the capacity spectra calculated for the studied structure. Thus, considering the damage states thresholds as random variables, Figure 8 shows the results obtained and the mean values for each damage state. This figure also shows how the dispersion increases when the damage states increase. This fact indicates that, when the structure enters into nonlinear behavior, the uncertainties in the damage level increase. The mean and standard deviation of *sa* and *sd* of each damage state are shown in Table 3. It is important noting the agreement of these values with those of Table 2. The points 1, 2 and 3 of Table 2 correspond to the mean values of the damage state thresholds ds_1, ds_2 and ds_3; the changes in the slope of the standard deviation calculated via IDA correspond to the damage state thresholds indicated in Figure 6.

Table 3. Mean and standard deviation of damage states.

ds	m_{sd} (m)	s_{sd} (m)	m_{sa} (g)	s_{sa} (g)
1	0.0985	0.0013	0.1878	0.0038
2	0.1314	0.0017	0.2504	0.0050
3	0.1583	0.0049	0.1878	0.0051
4	0.2212	0.0148	0.2504	0.0054

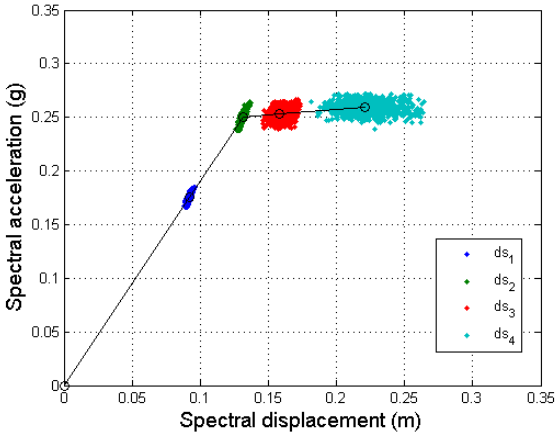

Figure 8. Damage states as random variables

For each damage state threshold, the corresponding fragility curve is defined by the probability of being exceeded the corresponding threshold as a function, in our case, of the spectral displacement. It is assumed that the fragility curves follow a standard lognormal cumulative distribution function.

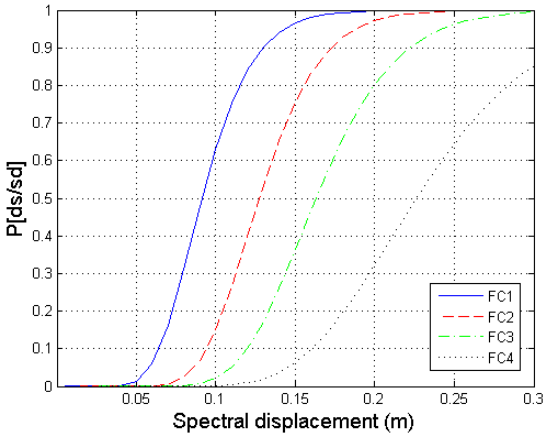

Figure 9. Example of one fragility curves for the building

Each fragility curve is then obtained by using the following equation:

$$P[i/sd] = f\left[\frac{1}{b_{ds_i}} Ln\left(\frac{sd}{\overline{sd}_{ds_i}}\right)\right] \tag{2}$$

where *sd* is the spectral displacement and $\overline{sd_{ds_i}}$ is the mean value of the lognormal distribution which is the corresponding damage state threshold as defined above. b_{ds} is the standard deviation of the natural logarithm of the spectral displacement of ds. In equation 2, the mean values, $\overline{sd_{ds_i}}$, can be determined from the capacity spectrum and b_{ds} can be estimated by assuming that the damage follows a binomial distributions and, finally, by using a mean square procedure to fit the fragility curves (see Lantada et al. 2008). Notwithstanding, there is a correlation between the ductility of the building and the variables b_{ds} of each fragility curve, which has been found by relating the results obtained with the Monte Carlo Method. This correlation is very useful because one can obtain the fragility curves applying directly this method, avoiding the mean square procedure described in Lantada et al. 2008, being thus the calculation time considerably reduced. Figure 10 shows graphically this correlation.

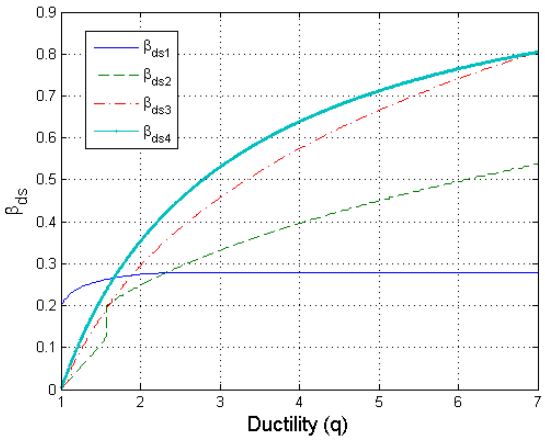

Figure 10. Correlation between ductility and the variables b_{ds}

Figure 11 shows 1000 fragility curves obtained for all the calculated capacity spectra applying the simplified method exposed above. Obviously, according to Figure 8, as the considered damage state increases, the uncertainties involved in the corresponding fragility curve also increase. As an example, the fragility curves corresponding to the damage sates *slight* and *collapse* can be seen in Figure 11. Figure 12 shows the results of a sensitivity test on the influence of the mechanical properties of the materials and the damage state thresholds; the stiffness is used as an independent variable in this test.

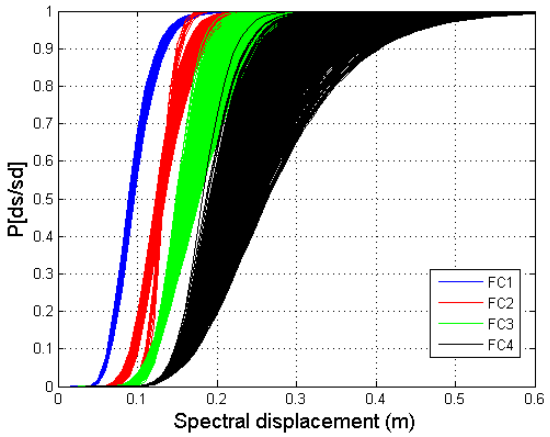

Figure 11. Fragility curves as random variables

ds_1 and ds_2 damage states are practically independent on stiffness, while for ds_3 and ds_4 the spectral displacement decreases with increasing stiffness, indicating that the probability of the corresponding damage states increases with stiffness. Figure 13 shows the mean fragility curves and Figure 14 shows the corresponding standard deviations as a function of *sd*.

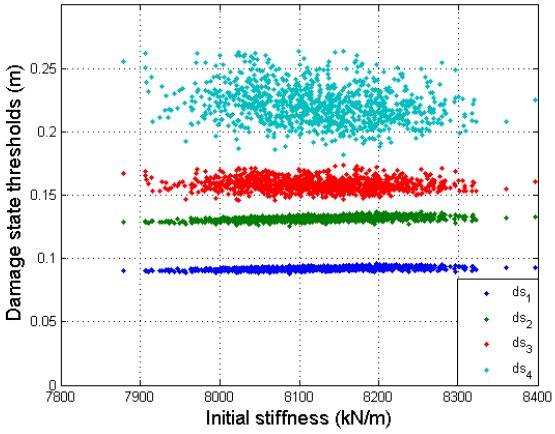

Figure 12. Sensitivity test for *ds* and the initial stiffness

Figure 13 clearly depicts the dependence of the uncertainties on the damage grades. For instance, the coefficient of variation of the damage state *ds4* may be greater than 10%, which means that, for a confidence level of 95%, the increase in the

probability of failure will be greater than 16.5%. This increase reaffirms the importance of analyzing the problem from a probabilistic viewpoint.

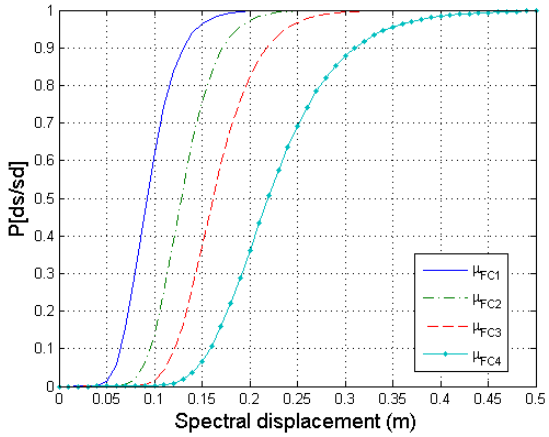

Figure 13. Mean fragility curves obtained via Monte Carlo simulation

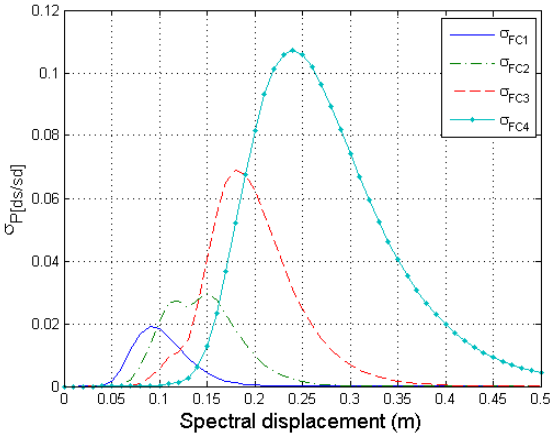

Figure 14. Standard deviation of the fragility curves

5. EXPECTED SPECTRAL DISPLACEMENT AND DAMAGE INDEX

The maximum expected spectral displacement in a building due to the seismic hazard of the area is obtained in section 4 using NLDA and the results were presented in figures 5 and 6. Different studies have searched for simplified procedures to estimate the expected spectral displacement (Kim et al 2008). A much more simplified procedure is the so-called equal displacement approximation, EDA, which is described in ATC-40 (1996) (see also Mahaney 1993). The EDA is performed by using the spectra corresponding to the selected accelerograms in order to perform a better comparison with the results obtained from the NLDA. Due to the fact that the EDA is a linear procedure, the results will be linear; for this reason, it is enough to scale the spectra for a single PGA. In order to express the expected spectral displacement as a function of the PGA, the spectra are scaled to 0.25 g obtaining the mean and standard deviation. Figure 15 shows graphically the EDA procedure considering the uncertainties associated to the seismic action and to the mechanical properties of the materials.

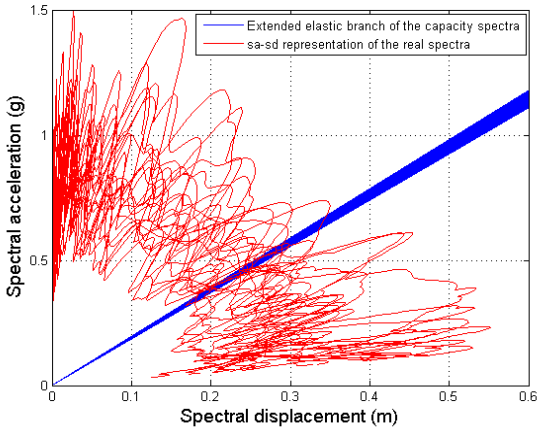

Figure 15. Equal displacement approximation considering the uncertainties associated to the seismic action and to the mechanical properties of the materials

These results are shown in figures 16 and 17, respectively, where the NLDA results are also given. The main conclusion of this analysis is that the EDA methodology provides an adequate approximation for the expected spectral displacement of the building, because it does not underestimate the expected displacement.

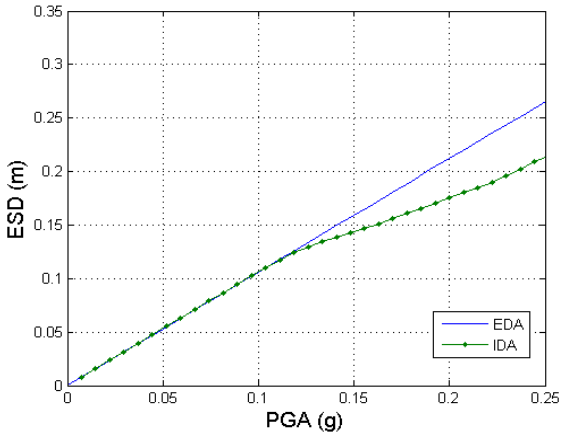

Figure 16. Comparison between the relation of the PGA to the expected spectral displacement obtained by using EDA and NLDA

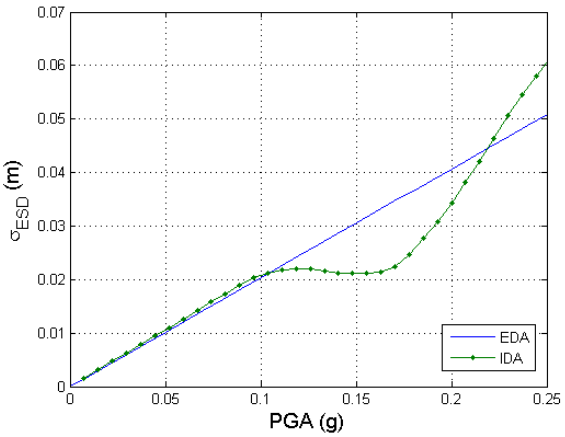

Figure 17. Comparison between the relations of the PGA to the standard deviation of the expected spectral displacement obtained by means of EDA and NLDA

Moreover, from a probabilistic viewpoint, this method is also conservative because, in the nonlinear range, the standard deviation obtained with EDA is higher than that obtained with NLDA. On the other hand, we can calculate a damage index, *DI*, which is defined by the following equation:

$$DI = \frac{1}{n}\sum_{i=0}^{n} iP(ds_i) \tag{3}$$

where n is the number of non-null damage states (n=4 in this case) and $P(dsi)$ is the probability of the damage state i which can be easily calculated from the fragility curves (see Figure 18). DI is the normalized mean damage grade which is a measure of the overall damage in the structure (Barbat et al. 2008). The authors proposed equation (3) for calculating the overall damage taking into account that the higher damage states ds_i have more influence on the global damage state DI of the structure and, also, because this equation provides the main parameter of the binomial distribution which allows obtaining the fragility curves in a simpler manner. Obviously, the values of the coefficients of the four probabilities of the damage states (0.25, 0.5, 0.75, 1.0) could be calibrated in order to improve DI if observed damage values would be available.

DI can be also plotted as a function of the expected spectral displacement. Thus, DI can be calculated for any spectral displacement but, in order to include the randomness associated to the seismic action, the comparison between DI obtained with EDA and with NLDA requires computing the PGA corresponding to each spectral displacement by using the relation shown in Figure 16. Figure 19 shows the obtained results, namely the mean values and the 95% confidence level curves. Again, our results confirm that the EDA is conservative respect to NLDA, even when considering a confidence level of 95% for random variables. But, if the variables were not treated by using a probabilistic approach, this would result in an underestimation of the actual damage that may occur in the building. In the case of the building analyzed in this article, the damage index estimated by using a deterministic approach is 0.25 lesser than that computed from a probabilistic viewpoint.

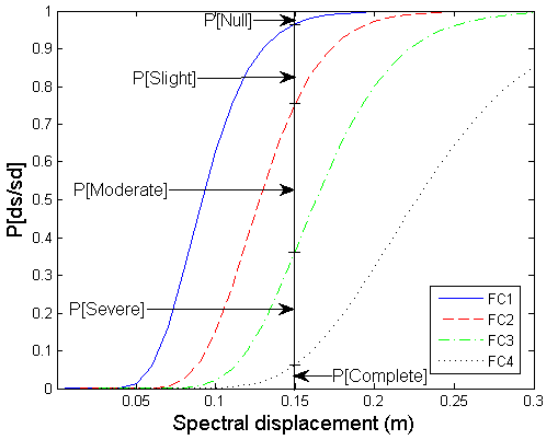

Figure 18. Probability of each damage state depending on the expected spectral displacement

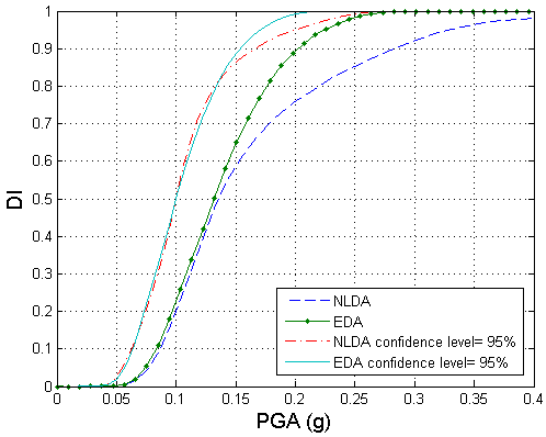

Figure 19. Damage index obtained with NLDA, EDA, and a confidence level of 95%

6. DISCUSION AND CONCLUSION

The assessment of the vulnerability, fragility and expected damage in a reinforced concrete building is performed in this article. However, the results obtained herein go further and they compare, in a probabilistic way, nonlinear static and dynamic analysis procedures. We face the problem from a probabilistic point of view, since we consider the uncertainties in the parameters related to the mechanical properties of the materials and the seismic demands. A first hint is that, notwithstanding that incremental dynamic analysis is a powerful tool in the assessment of the structural behavior of buildings when submitted to seismic actions, this procedure has little sense if the seismic demand is not carefully and properly selected. We put special care in the selection of the accelerograms used in this study. We have selected accelerograms corresponding to seismic events from the Spanish and European strong motion records databases. In order to reach a wide range of spectral displacements, the Eurocode type 1 design spectrum for soil type D has been taken as target demand. The accelerograms have been selected according to this criterion and have been scales to cover PGA values until 0.25 g. We used standard pushover analysis to obtain probabilistic capacity curves. A modified adaptive technique has been used to define the horizontal incremental load limit in order to stop automatically the pushover analysis during the run of high number of structures, 1000 in this case. Starting from the capacity spectra, simplified methods allow obtaining damage states thresholds and probabilistic fragility curves. An interesting conclusion of this exercise is that uncertainties increase in the nonlinear range. For the *collapse* damage state, the uncertainties in the fragility curves may be greater

than 10%. EDA and NLDA are used to obtain the expected spectral displacement and its standard deviation as a function of the PGA. Again, uncertainties increase with increasing PGA. This fact can be attributed to the increase of the inelastic behavior of the building. EDA is a successful approach because it does not underestimate the actual displacement, but it can be too conservative in structures with higher ductility. Furthermore, the fact that both the expected spectral displacement and the standard deviation are greater when calculated with EDA than when calculated with NLDA, confirms that EDA is conservative. In the NLDA, the seismic action is the main responsible for uncertainties in the spectral response, being less significant the influence of the uncertainties in the mechanical properties of the building. However, as the damage state increases, a sensitivity test shows a correlation between stiffness and spectral displacement. For the damage states ds_3 and ds_4, the spectral displacement decreases when stiffness increases, indicating that the probability of the corresponding damage state increases with the stiffness. This result is important since the damage states ds_3 and ds_4 have a high influence upon the calculation of the damage index. Finally, the comparison of the damage index as a function of PGA and the corresponding uncertainties shows that, for damage states from *severe* to *collapse* and for a confidence level of 95%, the uncertainties in the damage index may be higher than 0.25 units or 42% of the damage index. Thus, perhaps, the most important conclusion is that both static and dynamic structural analyses should be faced by using probabilistic approaches.

Acknowlodgements

This work was partially funded by the Geological Institute of Catalonia (IGC), by the Spanish Goverment and by the European Commission with FEDER funds, through the research projects: CGL2008-00869/BTE, CGL2011-23621, CGL2011-29063, INTERREG POCTEFA 2007-2013/73/08, MOVE—FT7-ENV-2007-1-211590 and DESURBS-FP7-2011-261652.

References

1. ATC-40. 1996. *Seismic evaluation and retrofit of concrete buildings.* Applied Technology Council, Redwood City, California.
2. Barbat, A.H. Pujades, L.G. Lantada, N. and Moreno R., 2008. Seismic damage evaluation in urban areas using the capacity spectrum method: application to Barcelona. *Soil Dynamics and Earthquake Engineering*, 28, 851–865.
3. Barbat, A.H. Carreño, M.L. Pujades, L.G. Lantada, N. Cardona, O.D. and Marulanda, M.C., 2010. Seismic vulnerability and risk evaluation methods for urban areas. A review with application to a pilot area. *Structure and Infrastructure Engineering*, 6, 1–2, 17–38.
4. Barbat, A.H. Carreño, M.L. Cardona, O.D. y Marulanda, M.C., 2011. Evaluación holística del riesgo sísmico en zonas urbanas. *Revista internacional de métodos numéricos para cálculo y diseño en ingeniería*, 27(1), 3-27.
5. Bommer, J.J. & H. Crowley (2006). The influence of ground motion variability in earthquake loss modelling. *Bulletin of Earthquake Engineering* 4 (3), 231-248.

6. Borzi, B. Phino, R and Crowley H., 2008. Simplified Pushover analysis for large-scale assessment of RC buildings. *Engineering Structures*, 30, 804-820.
7. Carr, A.J., 2000. Ruaumoko-Inelastic Dynamic Analisys Program. Dept. of Civil Engineering. Univ. of Canterbury, Christchurch, New Zealand.
8. Eurocode 8. 2004. Design of structures for earthquake resistance. Part 1: General rules, seismic actions and rules for building.
9. Fragiadakis, M. and Vamvatsikos, D., 2009. Estimation of Uncertain Parameters using Static Pushover Methods. *The 10th International Conference on Structural Safety and Reliability, ICOSSAR 2009, Osaka, Japan.*
10. Hancock, J., J.J. Bommer & P.J. Stafford (2008). Numbers of scaled and matched accelerograms required for inelastic dynamic analyses. Earthquake Engineering & Structural Engineering 37 (14), 1585-1607.
11. Kim, S.P and Kuruma Y.C., 2008. An alternative pushover analysis procedure to estimate seismic displacement demands. *Engineering structures*, 30, 3793-3807.
12. Lantada, N. Irizarry, J. Barbat, A.H. Goula, X. Roca, A. Susagna, T and Pujades L.G., 2008. Seismic Hazard and risk scenarios for Barcelona, Spain, using the Risk-UE vulnerability index method. *Bulletin of Earthquake Engineering*, 8, 201-229.
13. Lantada, N. Pujades, L.G. and Barbat A.H., 2009. Vulnerability index and capacity spectrum based methods for urban seismic risk evaluation. A comparison. *Natural Hazards*, 51, 501-524.
14. MATLAB. The mathworks inc.
15. Mahaney, J.A. Paret, T.F. Kehoe, B.E. and Freeman, S.A., 1993. The capacity spectrum method for evaluating structural response during the Loma Prieta earthquake. *National earthquakes conference*, Memphis.
16. Mwafy, A.M. and Elnashai, A.S., 2001. Static pushover versus dynamic collapse analysis of RC buildings. *Engineering Structures*, 23, 407–424.
17. Milutinovic Z.V. and Trendafiloski G.S., 2003. *WP04 Vulnerability of current buildings.* RISK-UE project of the EC: an advanced approach to earthquake risk scenarios with applications to different European towns
18. Poursha, M. Khoshnoudian, F. & Moghadam, A.S., 2009. A consecutive modal pushover procedure for estimating the seismic demands of tall buildings. *Engineering Structures*, 31, 591-599.
19. Pujades, L.G. Barbat, A.H. González-Drigo, R. Avila, J. and Lagomarsino S., 2011. Seismic performance of a block of buildings representative of the typical construction in the Eixample district in Barcelona (Spain). *Bulletin of Earthquake Engineering.* (in press)
20. Satyarno I., 1999. Pushover analysis for the seismic assessment of reinforced concrete buildings. Thesis (PhD). University of Canterbury.
21. Vamvatsikos, D and Cornell, C.A., 2002. Incremental Dynamic Analysis. *Earthquake Engineering and Structural Dynamics*, 31(3), 491-514.
22. Vargas, Y. F., Pujades, L. G., Barbat A. H. and Hurtado, J. E., 2012, Evaluación probabilista de la capacidad, fragilidad y daño sísmico en edificios de hormigón armado. *Revista Internacional de Métodos Numéricos en Ingeniería*, 28(4) (in press).
23. Vielma, J.C. Barbat, A.H. and Oller, S., 2009. Seismic performance of waffled-slabs floor buildings. *Structures and Buildings (Proceedings of the Institution of Civil Engineering)*, 162(SB3), 169-18.
24. Vielma, J.C. Barbat, A.H. and Oller S., 2010. Seismic safety of limited ductility buildings. *Bulletin of Earthquake Engineering*, 8(1), 135-155.

Modelling of the line construction of building by the method network analysis

Renáta Bašková
Institute of Civil Engineering Technology and Management
Faculty of Civil Engineering, Technical University of Kosice, Slovakia
e-mail: renata.baskova@tuke.sk

Summary

The line method of work scheduling in construction of objects is characterized by smoothness and uniformity of work carried out simultaneously in time but by shift in space. Technological and organizational conditionality of processes, in the schedule processing by a computer, are entered by bonds in the network graph. The paper deals with mathematic apparatus of various methods of network analysis and its conformity with the requirements for planning, debugging, tracking and automatic update of the scheduling line construction.

KEYWORDS: line construction, scheduling, networks analysis methods

1. INTRODUCTION

For every computer software for scheduling of construction there is a specific method of the network analysis. From its mathematical program depends ability to meet the needs of its user, which arise in the creation, debugging, monitoring and automated updates of the schedule in pre-production, production and implementation phase of the construction.

2. METHODS OF BUILDING CONSTRUCTION

In the construction of multi-zones buildings construction works can be arranged on the principle of parallel, line, or a gradual method (Figure 1).

The line method of construction of the linear buildings or larger buildings of civil engineering is characterized by parallelism of many activities that take place at the same time at different zones of the building. Most of the work overlaps with a time lag depending on the size of the minimum work queue.

ISSN 2285-2735, Pages 62 - 71

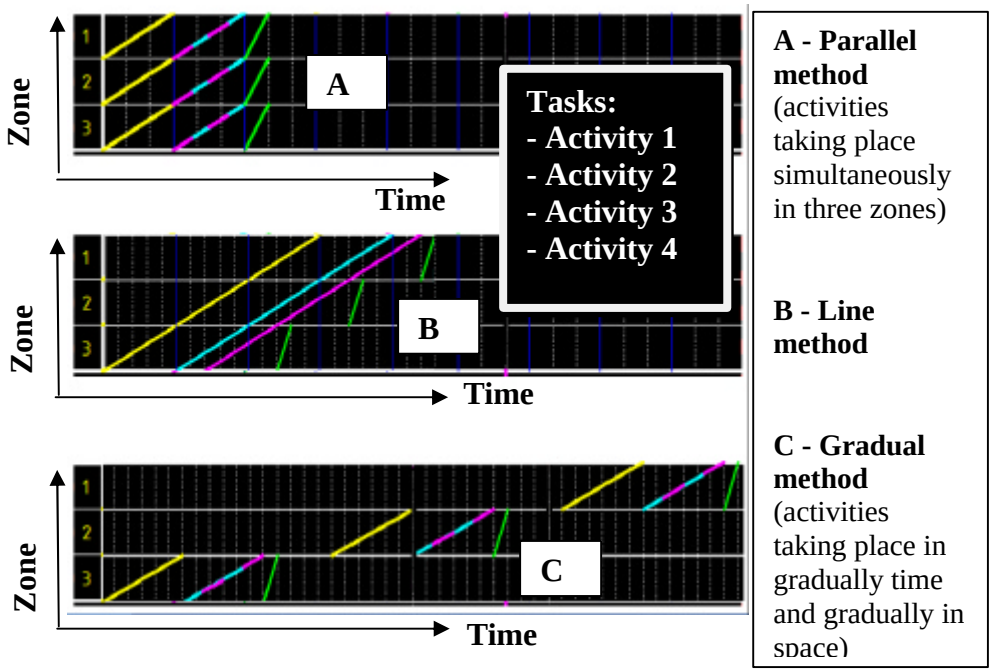

Figure 1: Time-space graph: a display of (A) parallel method, (B) line method and (C) gradual method construction of building

The line method is characterized by three principles in the scheduling of construction:

- ***Continuity*** - working parties should not interrupt their work in the transition between zones of the building.
- ***Uniformity*** - working parties should be uniformly labour loaded during the entire work. Building zones, through which the line passes, should have a comparable labour intensity so that working parties could work in a fixed composition throughout their deployment.
- ***Rhythm*** - working parties should stay at each construction zone the same length of time, technologically conditioned immediately consecutive activities should work with the same production rate.

3. BONDS IN THE METHODS OF NETWORK ANALYSIS

The base for automated modelling of time project course is always particular network analyses method. During the modelling of building time course by computer it is possible to define in the network topology technological or

organization activities relativities only by these mathematical bonds, which are defined in the particular network analyses method and its mathematical mechanism. [1] [2]

The mathematical bonds between activities/milestones are divided into:

- ***Simple bonds*** – these bonds express the connection between one event of previous activity and one event of next activity. There are connections: finish-start (FS), start-start (SS), finish-finish (FF) and the bonds, which are derived from them, such partial start-start and partial finish-finish. Each type of connections is characteristic also way of definition and time assessment of distance (for example e_{ZZ} =3 days means that the subsequent activity begins 3 days after initiation of the predecessor). The definition of necessary the earliest date belongs among simple bonds too.

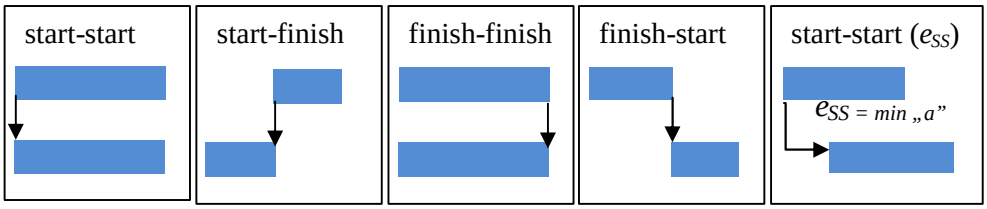

Figure 2: Simple bonds

- ***Double bonds*** – allow by one mathematical mechanism to express the connection between two events (also one) of previous activity and between two events (or one) of next activity. They are the mathematical connections of two simple bonds (SS+FF). Their elementary representative is critical approach bond. The construction-technological bond and line bond reflect activity development date and activity reduction date, as well as spatial parameters of structure, entered by value of the coefficient of the work queue.

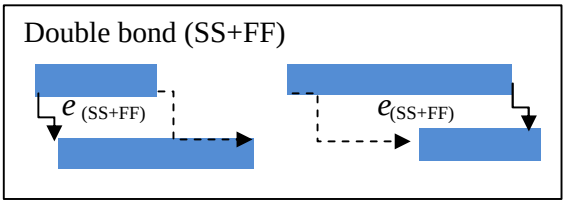

Figure 3: Double bond

- ***Multiple bonds*** – interconnects activities with defined number of events, such as a subdivision activity at part of the going in the area through various working zones. It can be bulk specified for the activity "in a line" (linking

parts of the same activity between zones) or between two activities, where is specified interconnection of activities parts in the individual zones.

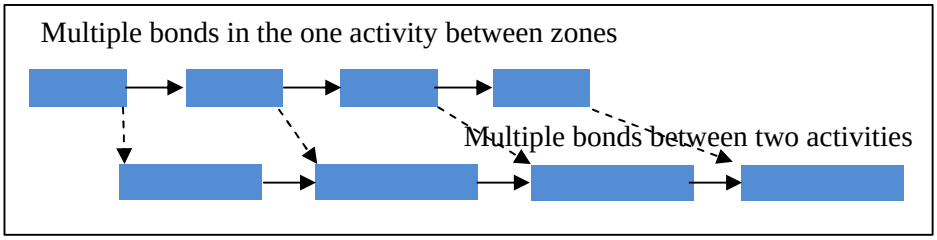

Figure 4: Multiple bonds

- ***Cyclic bonds*** – these bonds express a feedback between event of next activity/milestone and event of previous activity/milestone. That is the bond, which has a given particular maximal possible value of time distance „b“ (where b ? 8). Eventually, it can be a double bond between events of two activities, where first bond has given a maximal possible time distance and second bond has a maximal accepted time distance. The elementary representative of cyclic bond is a definition of the latest or stable necessary date. There belongs a stable activity connection without the interruption possibility of working teams (or with given maximal possible interruption) between two activities - finish work of one activity and start work of another activity.

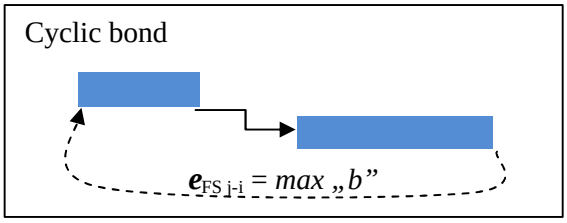

Figure 5: Cyclic bond

Specific bond types in a network diagram have the mathematical relationship to determine the latest date of activities in the earliest possible dates activity "forward calculation" and latest acceptable dates by "back calculation". Based on the "forward calculation" and "back calculation" to determine the activities lying on the critical path and are calculating a float time for non-critical activities.

Critical path in the nodes-defined network diagrams is sequence activities going from the beginning of the chart up to its end, the greatest sum of bonds specified intervals lying to her beginnings.

4. SCHEDULING OF CONSTRUCTION BY METHODS OF NETWORK ANALYSIS

In the construction of larger buildings parallel, gradual or line methods of work scheduling may be applied. The parallel method, as well as for the gradual methods of work scheduling, you can enter the sequence of work in scheduling in computer environment only through simple bonds. For planning of line organization of work scheduling double or multiple bonds are required, because single bonds using their mathematical formulas, do not allow to specify clearly the division of space structures on zones.

Software and their mathematical methods of network analysis that are used for scheduling construction can be divided into three groups:

1. group – in this method only single bonds are used for interconnection of activities in network graph [3];

2. group – method of network analyses allows to specify a single or double bonds between the processes, progress of work in space is specified by the coefficient work queue [8];

3. group – single bonds and multiple bonds are used for scheduling processes, they enable you to add and connect activities, carried out at construction at multiple zones, and shots can be given size, volume or location within the building [7] [9] [10].

The second and third group of software in terms of scheduling of construction allows in the network graph to enter not only parallel and gradual, but especially a line activities execution. On the other hand, construction practice very often uses software for scheduling of construction, can use belonging to the first group, which creates the risk of non-conformity of schedules for automatic updates of the plan in time of the construction [5].

Produce a schedule with line organization of work is possible using only single bonds. Problematic, time consuming and technically demanding is but the subsequent debugging. During the implementation of construction projects, often occur to errors and irregularities in the auto-update schedule of work.

4.1 Network critical path and the line method of construction

By using simple bonds for planning of line method of construction may arise uncertainties in computer-generated during the activities on the critical path. Given the type of bonds and specified forced deadlines may be not duration of critical path directly dependent on the duration of critical activities. Extension or shortening their duration does not affect the proportion calculated the shortest duration of construction.

In terms of debugging schedule of work, critical activities may be threefold type:

- ***Normal critical activities*** – connect on critical path by bonds FS, critical path influence values $e_{FS\ i-j}$ a $e_{FS\ j-k}$ - change the duration of action varies the duration of the project;
- ***Neutral critical activities*** – connect on critical path by bonds ZZ, critical path influence value $e_{SS\ i-j}$ and $e_{SS\ j-k}$ -change their duration (of course, in the interval) does not change the duration of the project (Fig.6 - activity D and E);
- ***Negative critical activities*** - connect on critical path by bonds FF with previous activity and SS bond with the next activity, the critical path affects the value $e_{FF\ i-j}$ and $e_{SS\ j-k}$ - shortening their duration of the project is certainly not reduced, but their extension could lead to a reduction of the project (Fig. 6 - activity C).

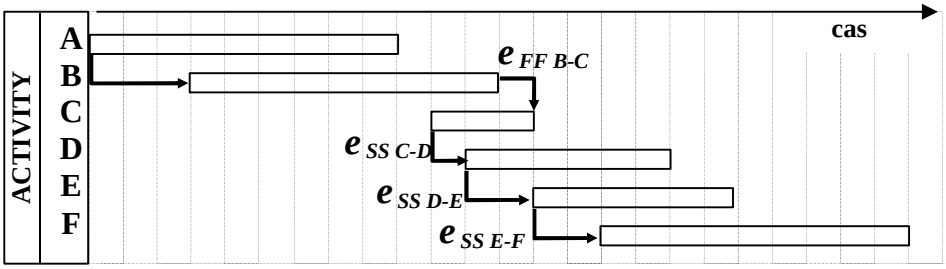

Figure 6: Activity interconnect by single bonds

It is clear that discernment of these three types of critical activities is not theoretical significance only, but their understanding, together with mastering of inputting the appropriate type and the time value of bonds, may have practical applications especially in the planning activities with the application of the principles of line methods of construction.

4.2 Scheduling of construction line method by software MS Project

SW MS Project has given simple bonds only. One way how to express by simple bond interval, less than the duration of the previous activity, is enter the time value of specific bond (Fig. 7-A), number or % of time predecessor. To change the duration of activity must always be reviewed and the time value of bond.

The second way assignments line implementation of activities is that work certain kind formally divided into more activities, going through individual zones of building, organization are linking activities by bond FS. Their linkage with following by especially dividing activities of another kind, allow to capture the real continuity with overlapping of work. FS bond connect at each zone the end of the previous frame with the start of the next activity (Fig. 7-B).

Concurrence of activities in the time but at price a considerable increase in the number of planning activities sometimes and even stronger growth in the number of bonds to their technological and organizational links. The downside is that so the divided work is not possible to specify the requirement for continuous work working parties.

In both cases shown in the figure (Fig. 6 and Fig. 7-A,B), it is possible to partially eliminate some disadvantages to balance periods of work working parties in the zones, in the line method is in a zone desirable comparable to the duration of subsequent works. If works on the building were planned with the same production rate, in the first case (Fig. 7-C) the reduced total time of implementation of works and in the second case (Fig. 7-D) would reduce the risk of interruption of work working parties in the transition between zones.

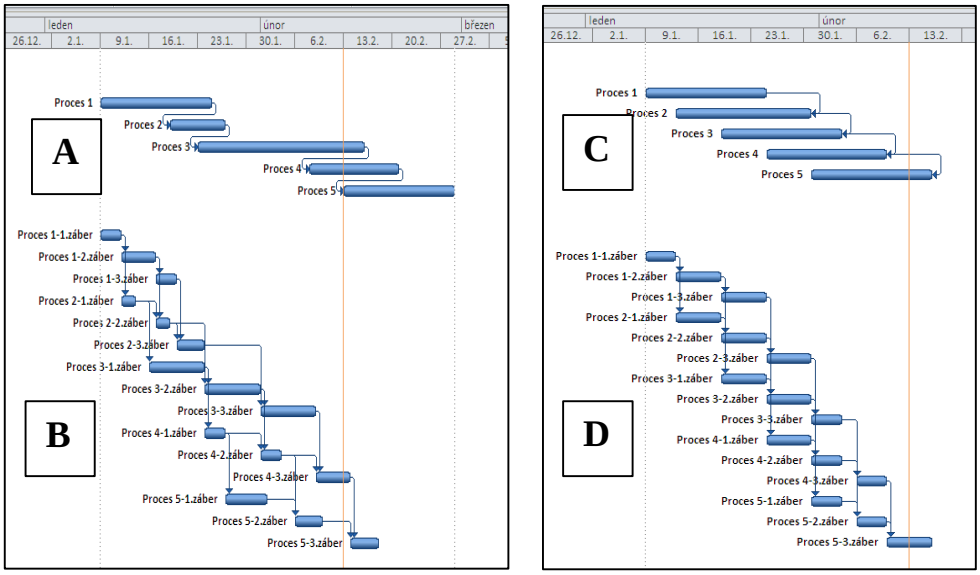

Figure 7: Specifying of the time course of the work on the three zones by single bonds only

In the figures (Fig. 8, 9) are samples of the errors in schedule after the automatic rescheduling of the project to the current date. Errors are due to a lack of conformity of network analysis methods, with the requirements for entering the technological conditionality of activities, running through multiple zones of structure. The duration of an unbalanced activities (Fig. 8 - A1), to enter the technological conditionality with one single bond only with a time interval, after the automatic update is not guaranteed that the predecessor created and released the workspace for successor. For example, at the figure (Fig. 8 - B1) activity no.2 after the rescheduling ends even earlier than his predecessor.

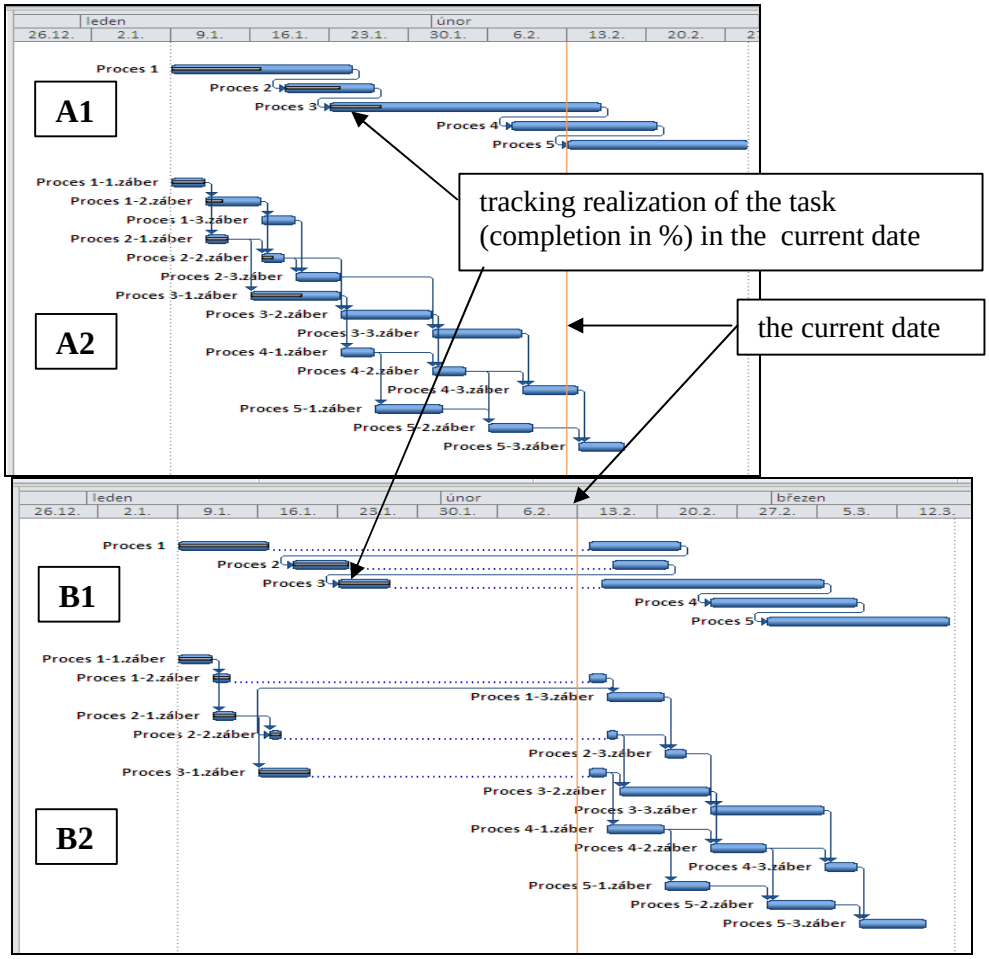

Figure 8: Automatic rescheduling activities with unbalancing duration to the current date

Neither the balancing of the duration of activities (Fig. 9 - C) does not guarantee a smooth upgrade schedule. Instead of the originally line organization of work can be scheduled after the update the implementation of several activity simultaneously at the same time and in the same area, what is from the organizational and technological site unacceptable (Fig. 9 - D1, D2). Conformity provides a FF bond only (Fig. 9 - D3), is less suitable for debugging of the schedule, as by percent specified the time value does not compute, at difference from other software, from duration of successor, but from duration of the predecessor.

Distribution of labor working parties to zones is not a suitable solution for high frequency of planned activities and labor intensive to compile a network diagram (Fig. 8 - A2; Fig. 9 - E).

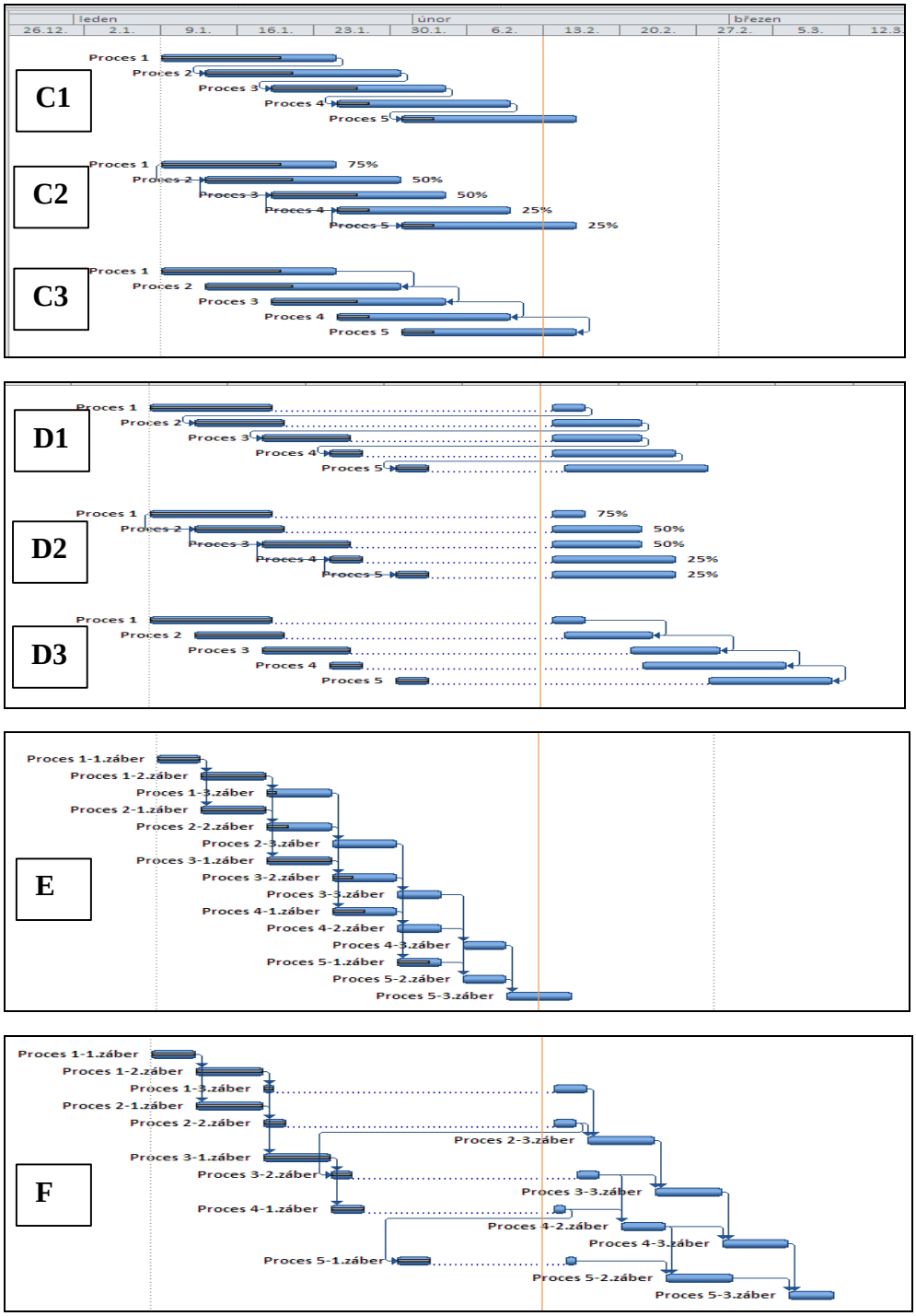

Figure 9: Rescheduling to the current date (work on zones with duration balanced)

There is a risk that in preparing the network diagram will not be given all the technological and organizational bonds (for 5 activities and 3 zones of the building is necessary to enter the 15 activities, 10-times organizational and 12-times technological bonds). Balancing of the duration of activities is no guarantee that crews will not interrupt a work between zones (Fig. 9- F) after the rescheduling.

CONCLUSION

When using a network diagram as a model of construction, where is technological conditionality of activities specified by single bonds only, use the automatic update of the project requires follow control of schedule of work and in most cases, treatment to eliminate errors and debugging of the updated schedule also.

Acknowledgements

Contribution was written within the implementation of the project VEGA 1/0840/11 Multi-dimensional approaches to support integrated design and management of construction projects.

References

1. Bašková, R.: Automation of building process time structure models. In: "INTERSECTIONS" International Journal. Vol.5, No.4, 2008, “Systemic Analysis”. Iasi, Romania: Societatea Academica “Matei-Teiu Botez”. p. 19-28, ISSN 1582-3024
2. Bašková, R.: Computational modeling of building process time behavior. In: "INTERSECTIONS" International Journal. Vol.3, No.6, 2006, ”Construction Management”. Iasi, Romania: Societatea Academica “Matei-Teiu Botez”. p. 13-24, ISSN 1582-3024
3. Bašková, R.: Casové plánovanie výstavby v programe MS Project. Košice: TUKE, 2011. 64 strán
4. Makýš, P.: Optimization of Time Management Schedules for Construction Works. In: Geotechnical Engineering/Construction Technology & Management: Proceedings of the 8th International Congress on Advances in Civil Engineering, ACE 2008, Volume 2, North Cyprus, Famagusta, 09. 2008. - Famagusta: Eastern Mediterranean University Press, 2008. - S. 563-570
5. Kozlovská, M.: Space-time analysis of building process safety risks. In: Proceedings of Inter. Scientific Conference –Quality, environment, health protection and safety management development trends, NEUM (Bosna and Herzegovina). Brno: Tribun EU, 2008. p. 154-159
6. Makýš, P.: The Automation of Construction Scheduling Considering Variability of Working Environment. In: The 27th international symposium on automation and robotics in construction. Brno: Tribun EU, 06. 2010. Str. 534-543.
7. Kozlovská, M. –Sabol, L.: Using of the newest CAD/BIM tools in construction project. In: Design, technology, Refurbishment and Management of Buildings. Proceedings of 37th. IAHS World Congress on Housing Science, Santander (Spain), October 26 – 29, 2010. Florida (USA): International Association for Housing Science. pp 281 (CD-ROM, p. 1-6.)
8. http://www.contec.cz/
9. http://www.astadev.com/software/
10. http://www.vicosoftware.com

Composite materials in bridge consolidation

Gheorghita Boaca[1], Cristian-Claudiu Comisu[2]
[1]*Department of Transportation Infrastructure and Foundation, "Gh. Asachi"Technical University of Iasi, Romania, boaca_gheorghita@yahoo.com*
[2]*Department of Transportation Infrastructure and Foundation, "Gh. Asachi"Technical University of Iasi, Romania, comisucristian@yahoo.com*

Summary

This article presents the technical solution for the rehabilitation of an arches bridge on an national road in Romania. The bridge is 61 years old and is in satisfactory condition and requires execution of building works.

The consolidation solution of bridge for taking current and future loads will be made with composite materials based on carbon fibers arranged to take over sectional efforts.

To determine the amount of material was made static calculation for the entire bridge structure. The values for sectional efforts have determined the carbon fiber amount necessary for taking requests.

Consolidation works will be done without being interrupted road traffic and pedestrian on bridge.

Finally, the bridge will have to take loads of traffic and to ensure appropriate gauge crossing national roads in Romania.

KEYWORDS: bridge, consolidation, composite materials.

1. INTRODUCTION

Since its appearance, composite materials have attracted special attention in the construction field due to its efficient behavior under tensile loading, their great resistance against external agents and the simplicity of their application, among other advantageous characteristics. These properties have allowed these materials to be considered for the repair and strengthening of concrete structures [1,2].

ISSN 2285-2735, Pages 72 - 79

Since these products are new in the construction field, there is little available research on its behavior. On the other hand, the technical specifications given by the manufacturers are limited to its field of application.

The behavior of composite materials has been studied and characterization tests have been carried out in many international laboratories and to the Technical University of Iasi, at Faculty of Civil Engineering and Building Services, where have been prepared several PhD theses and reports. Studies have focused on the composite material independently analyzed and the elements and structures strengthened with composite material.

Figure 1. View of bridge on national road at Bicaz

2. BRIDGE ON DN 15 KM 287+062 AT BICAZ, OVER BICAZ RIVER

The bridge has a static undetermined structure made up of two double reinforced elastic arches recessed way up in collaboration with a concrete deck on the frame elastic continuous beams and two longitudinal beams solidarity transversely with beams at 5,00 m and plate concrete on top.

Concrete arches have a rectangular section of constant width 0,60 m and variable height, 1,40 m to 1,00 m at birth and key. Arches were length of 40.00 m measured on the birth line, providing a report f / l = 1/5, and were born in Piatra Neamt abutment 0,40m above in relation to the birth of the abutment Bicaz. In cross

section arcs are located at 5,00 m inter-axle symmetrically in relation to the longitudinal axis of the bridge directly.

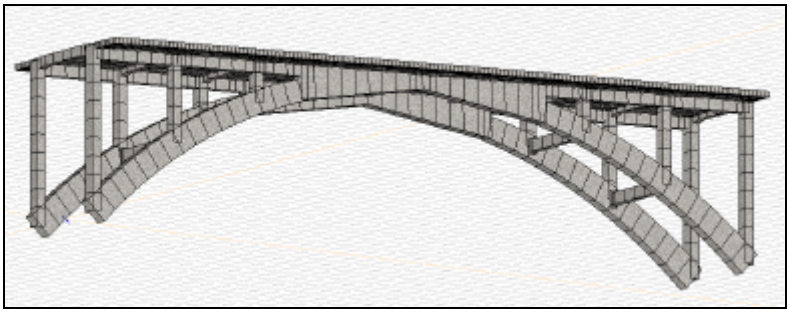

Figure 2. The model of bridge

The arches are solidarity together with reinforced concrete diaphragms with rectangular section 0,60 x 0,30 m in field and 1,00 x 0,30 m in recess, the front arches. The link between arcs is provided with four apertures located at 5,00 m from one another, along the bridge.

The key area for a length of 15.00 m arcs cast firmly attached to the deck beams, solidarity between the arches being covered deck spacers, and top plate of the deck concrete.

The resistance structure of deck consists of reinforced concrete frames with reinforced concrete columns keep the rectangular section 0,50 x 0,60 m and longitudinal beams of rectangular section 0,35 x 0,75 m, with reinforced concrete slab variable height on top. Working between the main beams is provided by beams of rectangular section 0,35 x 0,75 m bridge located along the inter-axle distance 5,00 m.

On top of beams network is secured by a reinforced concrete slab with fixed edges in the network of beams with variable thickness, 0,20 m in the longitudinal axis of the bridge and at least 0,16 m in the inner beams.

The road bridge is composed of the 7,0 m wide carriageway and two bumpy sidewalks each 1.5 m wide.

The bridge parapet covering a total length of 87.60 m. The connection the abutment embankments is provided by reinforced concrete frame type, the 10,50 m long, buried in embankments, foundations arcs with common foundations. Items collected are teaching the same elements as staff liaison between arches and deck.

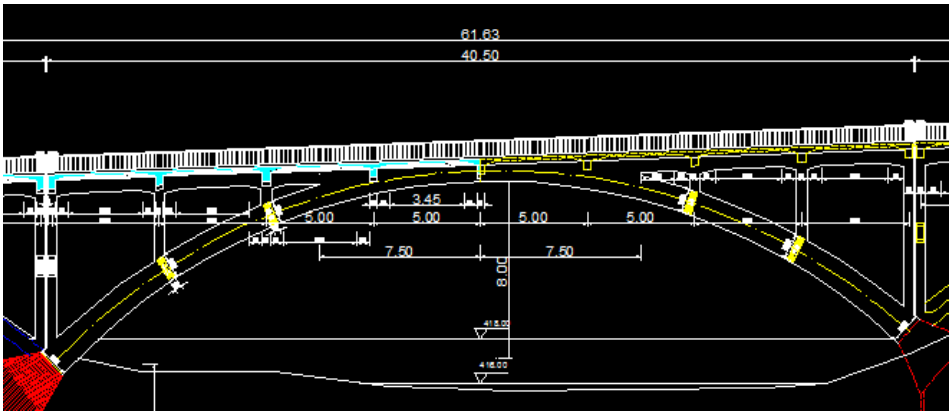

Figure 3. Bridge longitudinal section of bridge

The abutments are of reinforced concrete frame, frames with openings of 5,00 m with columns embedded in the foundation arches, common foundation, buried in embankments. This type of abutment embankments provides connection with a length of 10,50 m with slope 2/3.

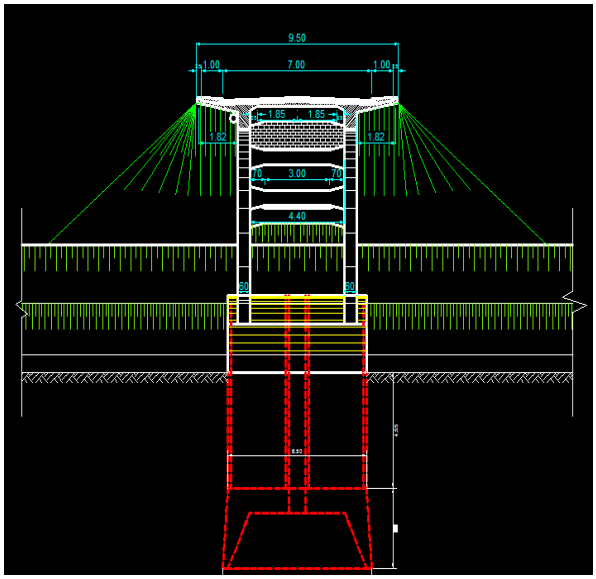

Figure 4. Cross section of the bridge

The foundations are such foundations directly taken to share with compressed air. Foundation block dimensions are 8,82 x 6,50 and the foundations were lowered 9,20 m at elevation 406,90 m Bicaz abutment and abutment 407,70 share Piatra

Neamt. To share the path, the sole foundation is 18,55 m to 19,35 m concerned, providing low-water line to about 9,50 m

The connection is done to the bridge embankments with quarter's cone of pears. Upstream quarters cone are in operation, and the embankment under the bridge embankments have collapsed. Left bank downstream quarter cone is in operation while the downstream quarter cone as completely destroyed. Due disposals embankment slope area covered the bridge was destroyed in the upper walls and embankments support was achieved with a dry underpinning of stone blocks with direct bearing on the existing embankments.

On the left bank upstream of bridge length of 50,0 m were provided of bank that is in operation, and a defense on the right bank downstream of the bridge was destroyed in floods.

3. CONSOLIDATION SOLUTIONS

The elements that need strengthening are:

- Reinforced concrete slab geometry of the deck and deck restoration.
- Consolidation and completion of structural reinforcement sections.
- Strengthening of the main beams and arches to increase the class's loading - truck convoy A30, and special vehicle on wheels V80.
- Strengthen and add structural elements to extend the life of the structure and bring it within the parameters imposed on the carrying capacity without affecting the existing aesthetic valences.
- Repair damaged areas of concrete infrastructure

3.1. Classical method - the bearing shirt

This solution takes into account to increase the bearing capacity of structure, using a well-known and common technology to strengthen the bearing. Since the bridge will have to take current and future traffic loads, the calculated arc section has insufficient carrying capacity. Taking over the efforts to ensure sectional efforts section is increased by the addition of concrete and reinforced all around the elements making a shirt section.

The calculations require a shirt sections on: arches, longitudinal beams and transversal beams. The shirt should have a thickness of 15 cm and two planes of reinforcement.

Strengthening the shirt structure leads to a significant additional load from the weight of the structure.

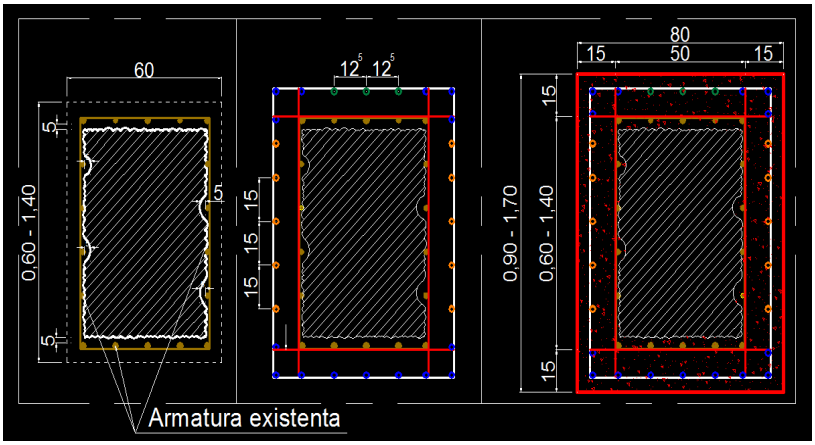

Figure 5. Consolidation of section with shirt

3.2. Modern method - Consolidation with composite materials

The solution of consolidation with composite materials has been studied to reduce the main disadvantage of traditional method, to reduce effort’s from permanent loads.

Considered composite materials are based on carbon fiber with high resistance, low weight, corrosion resistance, durability.

Consolidation of resistance structure with carbon fiber associated with special high resistance mortars retain structural dimensions, reducing the completion time of work and perhaps most important contribution is their minimum weight.

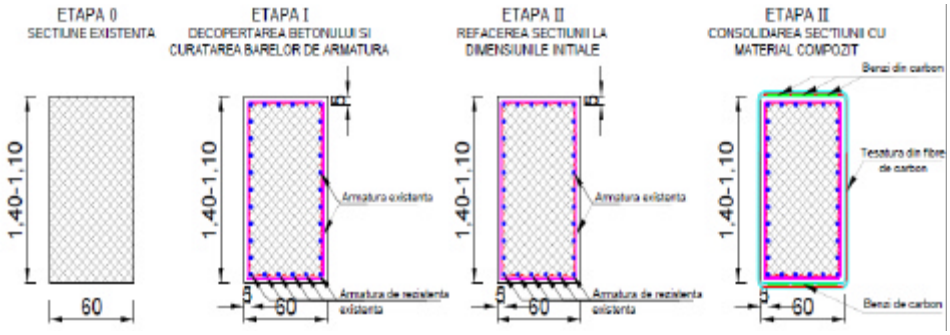

Figure 6. Section consolidation with carbon fiber

4. STRUCTURE CALCULATION

For exact quantity of composite material was necessary a structural modeling in a computer program. The structure was modeled in AxisVM 10 program, which resulted sectional efforts.

The calculation was done in several situations:

1. The first hypothesis was to determine the sectional efforts to bridge requested by its own weight, no route, no sidewalks and no parapets.
2. In the second hypothesis were calculated sectional efforts with self-weight produced by all consolidated bridge, sidewalks and fences.
3. A third case was the traffic loads, convoy of special vehicles V80 being the worst.

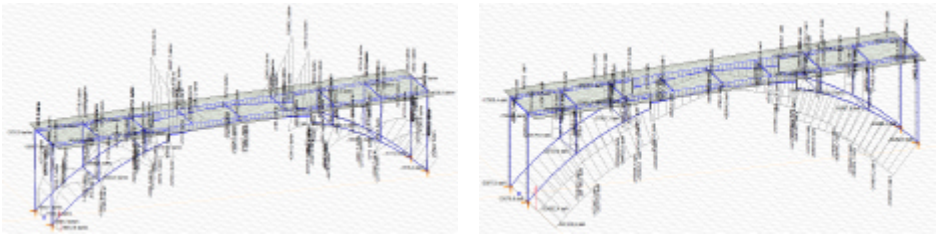

Figure 7 – Bending and axial force diagram from permanent loads

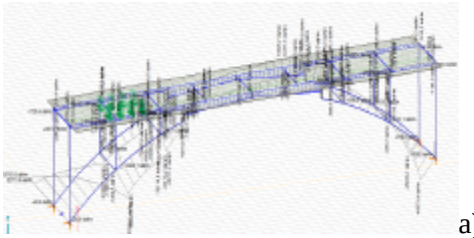

a)

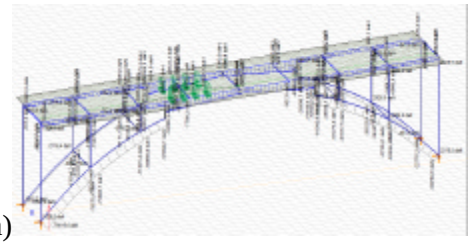

b)

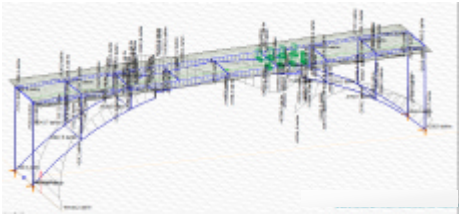

c)

Figure 8 – Bending and axial force diagram from convoy V80 loads. a) Bending of superior fiber; c) Bending of inferior fiber

Knowing the sectional efforts can be dimensioned the necessary quantity of carbon strips for taking over the bending moment and the amount of carbon fiber for taking over the axial and shear force.

5. CONCLUSIONS

The composite materials for consolidation of bridges can often be legally viable technical and economical solution. The cost of new materials is greater than the classical ones, but by reducing the time and the necessary equipment can be saved, so that total costs are comparable.

The adoption of composite materials would not have done that support the concrete case; it would have been in an advanced state of decay.

Using composite materials not solve all solutions to consolidation of bridges, but can be taken into account when analyzing building solutions.

References

1. G. Ramos, J.R. Casas, A. Alarcon - Repair and strengthening of segmental bridges using carbon fibers – *Engineering Structures* 26 (2004), ISSN 609-618
2. Technical project „Rehabilitation of bridge on DN 15 km 287+062, at Bicaz ” – S.C: POD-PROIECT S.R.L., Aprilie 2012
3. *Tehnologii moderne de reabilitare a podurilor cu materiale compozite* – Workshop, Facultatea de Construc? ii ? i Instala? ii din Ia? i, Ia? i, 7 Martie 2000
4. Comisu, C. C., Boaca, G., „Design and Development of System Identification and Nondestructive Inspection of Bridges Network in Romania”, *Proceedings, PANNDT2011 5th Pan American Conference for NDT*, 2-6 October 2011, Cancun, 9 pg. , ISBN 978-968-9288-10-
5. Boaca, G., Comisu, C. C., „Rehabilitation of the bridge over the Danube river Iron Gate I – Romania”, *Proceedings, 11th International Scientific Conference VSU’ 2011*, 2-3 June 2011, Sofia, Bulgaria, Vol II, pg. VI-60-65, ISSN 1314-071X

Experimental study regarding the induced ductility at the steel column base by the baseplate's flexibility

Budescu Mihai [1] Melenciuc Silviu Cristian [2] and ? tefancu Andrei-Ionu? [1]

[1]*Department of Structural Mechanics, Gheorghe Asachi" Technical University of Iasi*
Faculty of Civil Engineering and Building Services, Iasi, 700050, Romania
[2]*Department of Civil and Industrial Buildings, "Gheorghe Asachi" Technical University of Iasi*
Faculty of Civil Engineering and Building Services, Iasi, 700050, Romania

Abstract.
The present design regulations postulate that the structural strength requirements should not prevail to the ductile ones in a design process. In case of steel columns, brittle failure of the bases (bolt's failure, concrete crushing) should be avoided. In this context, the ductility or the rotational capacity should be determined mainly by the flexibility of baseplates. Experimental studies may reveal specific local phenomena otherwise "invisible" (by numerical simulations, failure theories or other analysis methods). The main objective of this paper is to describe the overall structural behavior and evaluate the parameters involved in the connection design of two exposed rigid baseplates. The connections have been analyzed by means of full-scale tests that lead to failure modes validated by finite element models.

KEYWORDS: base column joint; base plate, ductility

1. INTRODUCTION

The column base represents one of the most important parts of a steel structure. It haves the role of load transfer from the superstructure to the foundation system. When laterally loaded, exposed baseplate solutions for steel columns deform - under bending moments and (associated) shear forces – mainly by rotations. Behavior of connections in these regions is of major importance in the overall structural behavior under lateral loading conditions. Previous research studies, (Grauvilardell et al, 2005; Hamizi and Hamachi, 2007; Stamatopoulos and Ermopoulos, 2011), showed that connections between columns and foundation elements behave in a semi-rigid manner and, in most of the cases, heavily influence the overall structural system.

As stated above, experimental research studies may reveal specific local phenomena otherwise “invisible”. In this order, an experimental program involving full-scaled models of columns with exposed baseplates seconded a numerical analysis. The experimental tests evaluated the behavior of exposed baseplate steel columns connections under cyclic loading conditions with the aim of validating the numerically obtained results. Evaluation of parameters not possible to quantify by the numerical simulations was also of interest.

Nonlinear numerical analyses of the tested models were performed by the Finite Elements Method based ANSYS Workbench 12 software package (Ansys, 2009; Melenciuc, 2011).

2. EXPERIMENTAL PROGRAM AND TEST SET-UP SECOND CHAPTER

The experimental tests were performed in the dynamic and seismic test laboratory of the Structural Mechanics Department of the Faculty of Civil Engineering and Building Services of Iasi.

A specially designed stand completing the ANCO shaking table was used to test the column base ends connections (Fig. 1). The test set-up consisted in: stiff concrete slab supporting the shaking table, foundation system simulating foundation block - anchored to the laboratory ground slab using four M80 bolts. The acting member was equipped with a 200kN load cell.

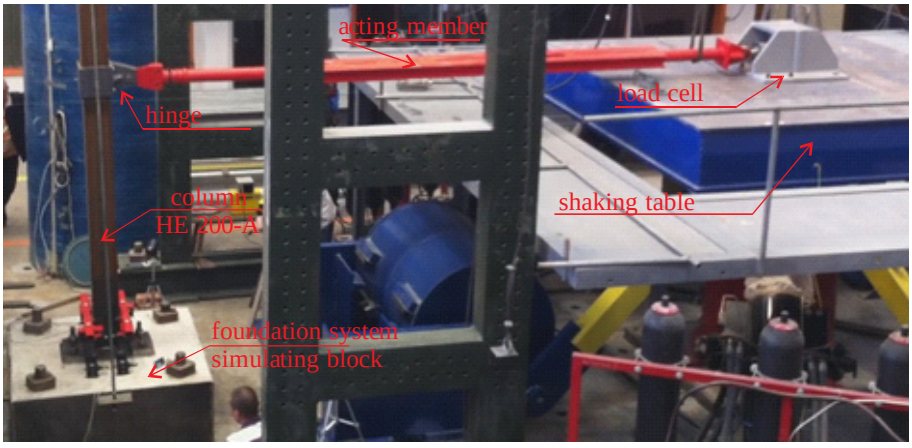

Figure 1. Experimental stand; load transmission system

The tests performed involved only lateral horizontal loading, without any axial components (excepting the column dead load). In this manner, the column' base behavior under extreme conditions was observed. It may be stated that this reflects the rather common situation of real structures, especially in case of perimetral columns in slender steel structures under seismic actions, when the axial components may be neglected. The horizontal action transmitted by the shaking table was applied at a 2.10m height with respect to the column base.
A "sinus beat" type action was applied under displacement control, with maximum amplitudes (?) of 10, 20, 40, 60, 80 and 100 mm, (Fig. 2).

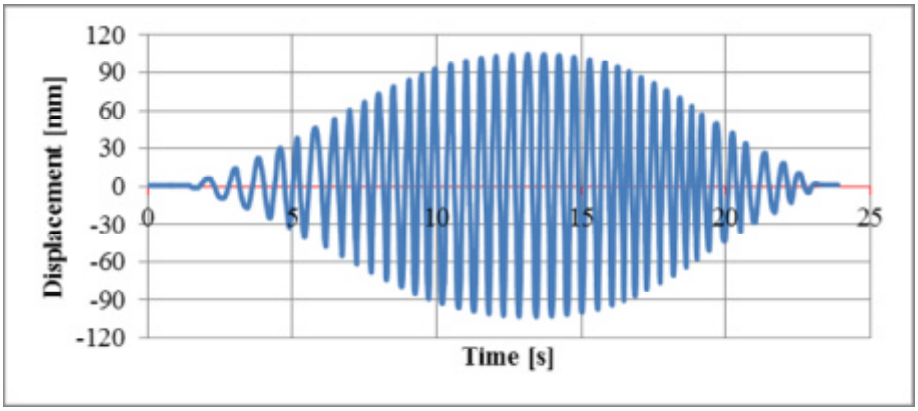

Figure 2. Imposed displacements, maximum amplitudes (?) 100mm

The action was indirectly applied by imposing successive displacements. The load applied to the steel column was monitored using a load cell placed at the end of the acting member, connected on the platform.

300mV/V/inch sensitivity, CELESCO thread type displacement transducers (T) were used in order to determine the structural response of the column models. The load-displacement curve at the level of load application (acting member level) was obtained using the readings of the T0, (Fig. 3).

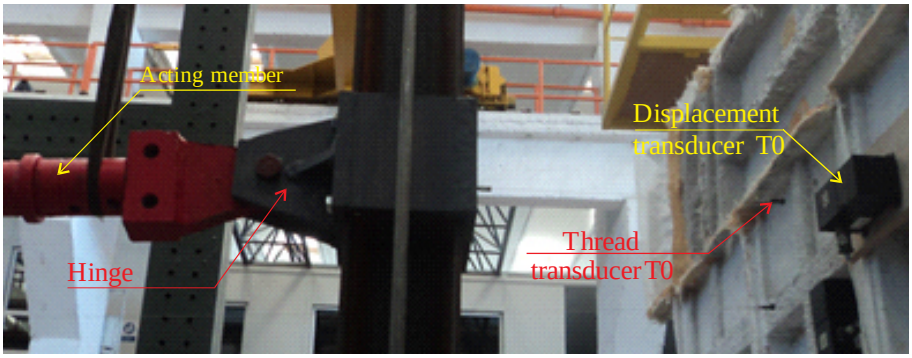

Figure 3. Horizontally placed displacement transducer (T0)

The other transducers were placed at the base level by connecting them to the steel column and measuring the relative displacements between the baseplate elements and the foundation system. The transducers were fixed on the column, at a 250mm span from the bottom face of the baseplate, in order to monitor the potential plastic hinge formation region, (Stamatopoulos and Ermopoulos, 2011).

Relative column base - foundation system displacements, in case of baseplated models, were monitored using T1 to T4 transducers; displacements of the baseplates were accounted using the T5 to T8 transducers, (Fig. 4), (Stamatopoulos and Ermopoulos, 2011).

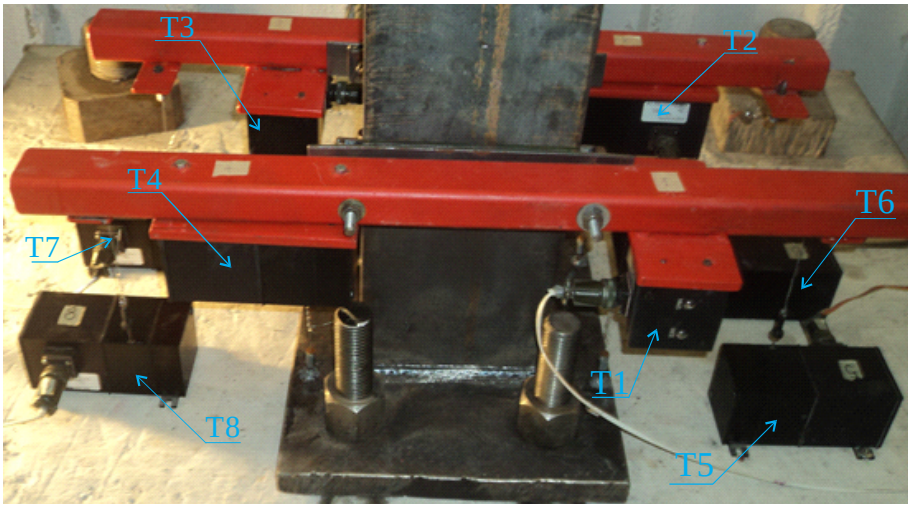

Figure 4. Baseplate tranducers location

2.1. Test specimen

The experiments analyzed and compared the structural behavior of two specimens.

The first tested specimen is composed of a 2.10m high, HE 200-A cross-sectioned steel column and the baseplate, having the dimensions of 350x33-490, anchored in the reinforced concrete foundation block using four M36 bolts, (Fig. 5).

The second tested assembly used the same steel column and the baseplate having the dimensions 350x33-690.

The anchoring bolts were fixed in the foundation block with a clear deformation span of 360mm. The column and the baseplate were made of S355 steel while the concrete used for the foundation was of C20/25 class.

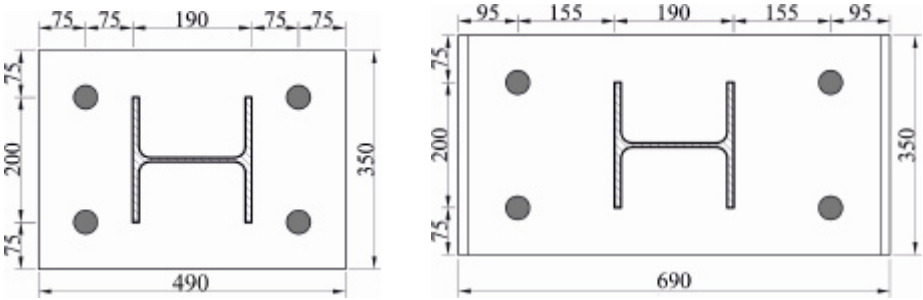

Figure 5. 350x490 mm steel column base `plate

The connection' rotations were determined based on the vertical displacements of the baseplate at the column section flanges level and used the following relation, (Hamizi and Hamachi, 2007):

$$q = (a - b) / x \tag{1}$$

where:

q - rotation of the column baseplate;
a, b - vertical displacements of the column baseplate;
x - span between the displacement measuring points.

2.2.1. Test results

For each of the loading cycles, graphs using the load readings of the load cell and the displacements given by the T0 transducer were plotted.

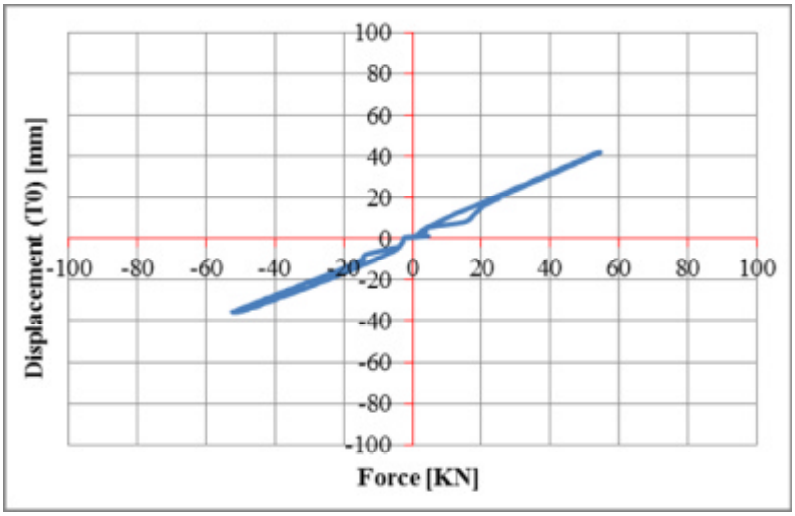

Figure 6. Load-displacement curve during the maximum amplitude cycle of 40mm

The specimen behaved in a linear elastic manner up to loading cycle of maximum amplitude of displacement of 40mm, (Fig. 6). The base plate presented a rigid behavior and presented no plastic deformations.

Starting with the load cycle of maximum displacement amplitude of 60mm, the behavior of the model became elastic-plastic, due to occurrence of plastic hinges at the column base level, (Fig. 7).

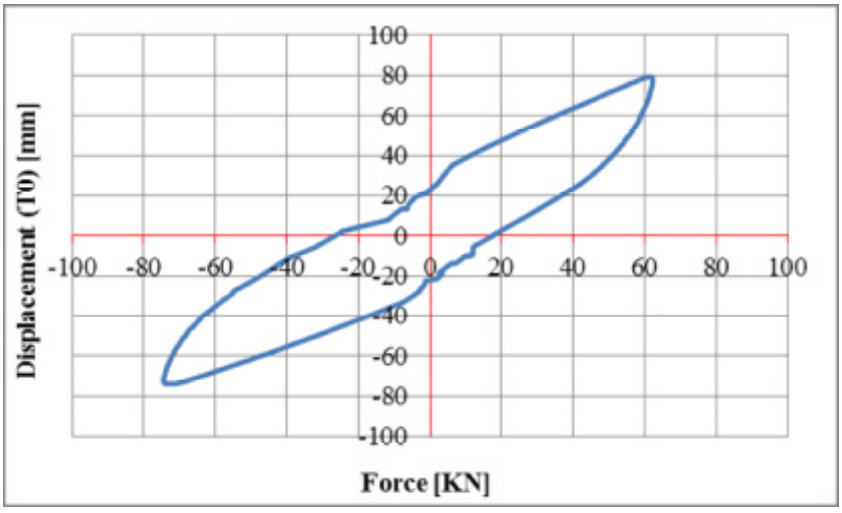

Figure 7. Load – displacement curve for the connection, ? =80 mm

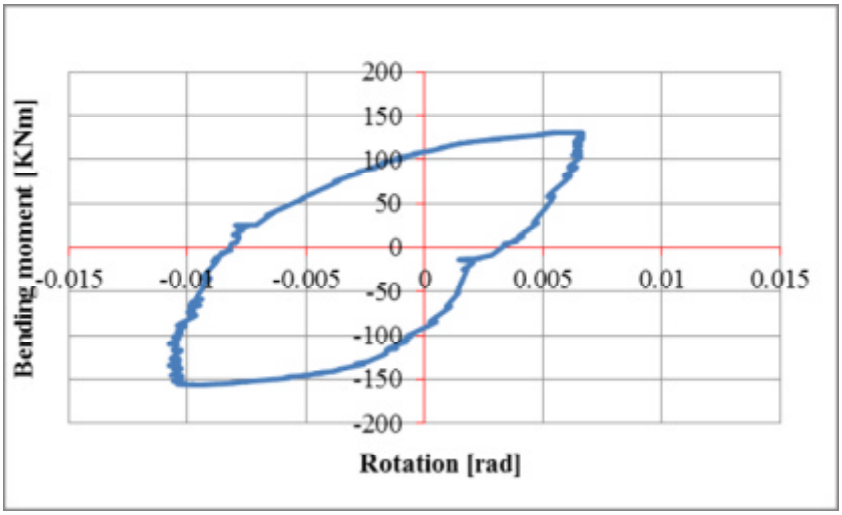

Figure 8. Bending moment – rotation curve for the connection, ? =80 mm

The bending moment-rotation curve of the connection is depicted in Fig. 8. The shape of the graph is not uniform; fact attributed to the loosening of nuts. The bending moment capacity of the connection was evaluated at 156.6 KNm, corresponding to a maximum baseplate rotation of 0.011 rad. The vertical displacements of the column baseplate were determined as arithmetic mean values given by the displacement transducers, when the amplitude of the action was of ? = 80 mm.

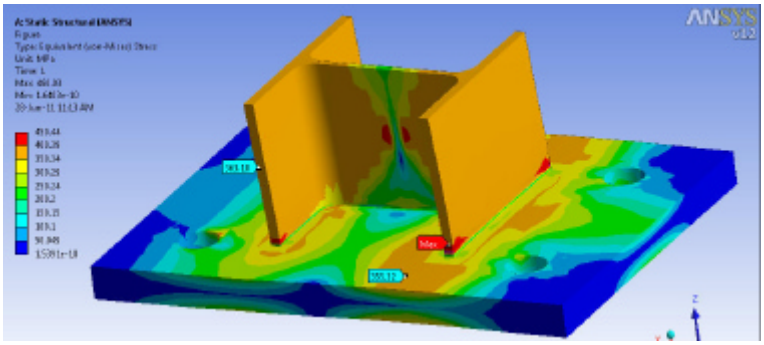

Figure 9. Von-Mises equivalent stresses distributions, ? =100 mm

The connection failed by the plastic hinge formation in the column due to the loss of the local stability of compressed flanges, (Fig. 10). The failure occurred at a load level corresponding to the maximum displacement of 80mm. The failure manner was also described by the numerical simulations, as the maximum Von-Mises equivalent stresses show in Figure 9, (Melenciuc, 2011).

Figure 10. Plastic hinge formation in the column

The second test specimen had the dimensions of the baseplate - 350x33-690 mm.

During the load cycle of maximum amplitude of displacement of 60mm, the behavior of the model became elastic-plastic without the degradation of the connection bearing capacity. When the displacements reach 60mm the plastic deformations appear in the baseplate.

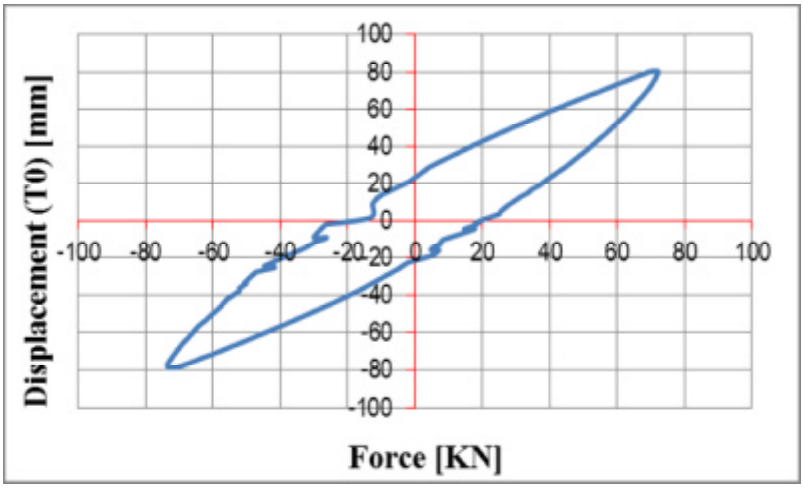

Figure 11. Load-displacement curve EXP 350x690x33, maximum amplitude ? =80 mm

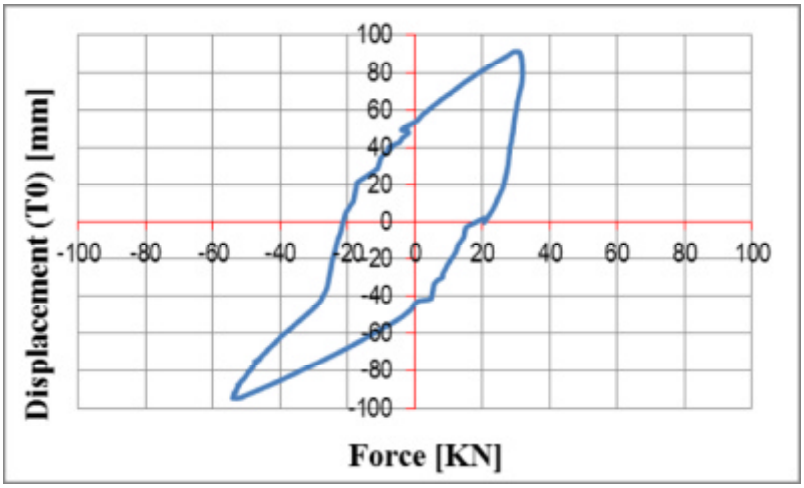

Figura 12. Load-displacement curve EXP 350x690x33,
maximum amplitude ? =100 mm

A strong nonlinear behavior of the connection occurs during the load cycle with the maximum amplitude of the displacement of 80mm.The capable moment of the connection is 154.5KNm, with a 0.025 rad baseplate rotation.

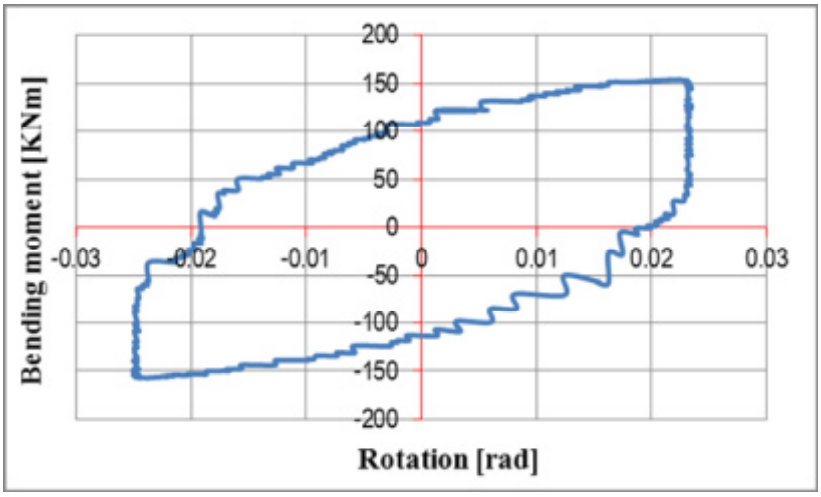

Figure 13. The bending moment-rotation curve EXP 350x690x33, maximum amplitude
? = 80 mm

As the applied displacement increases the plastic deformations of the baseplate improves and the bearing capacity of the connection decreases. Thus, when the displacement is 100mm, the moment overtaken by the connection reaches the value 114.0 KNm

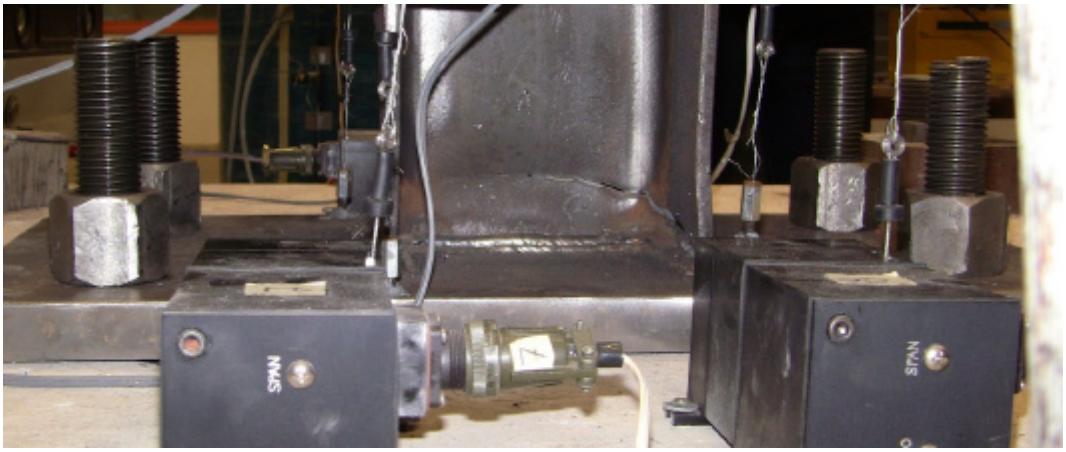

Figure 14. Model EXP 350x690x33 – web failure, ? = 100 mm

After 12 load cycles with the displacement of 100mm, a crack appears at the column pad subjected to extension in the thermal affected area. The crack is spreading suddenly, sectioning the column above the baseplate.

3. CONCLUSIONS

The behavior of exposed baseplate steel columns connections is highly influenced by the thickness of the baseplate. When using rigid baseplates, design parameters characteristic to full capacity connections may be obtained.

As a direct consequence of the baseplate increased stiffness – given by the large thickness and short outstands – the joint rotation was significantly influenced by the anchoring bolts deformation. This aspect should be avoided in case of structures likely to experience seismic actions during lifetime.

The experimental tests results for connections with the exposed, rigid baseplates, due to the large width and the reduced cantilever length, confirmed the numerical analysis results. The models had total resistance and a rigid behavior. The rotation was determined in the first place by the column’s deformations and anchoring bolts’ elongation and less by the baseplate bending.

The yielding occurred during 90's load cycles after the appearance of the plastic deformations.

The plastic hinge occurred after 15 full cycles having the imposed displacement magnitude of 80mm. The experimental tests confirmed the results obtained numerically and in the case of the connection with the large baseplate, but flexible because of large cantilever length. Thus, the connection presented total resistance and necessary rigidity in accomplishing the imposed ductility for structures located in seismic areas.

The baseplate flexibility had an important significance in the connection's rotation, a favorable aspect from the ductility point of view.

The connection yielding manner could not be numerical observed. After 130 load cycles and the plastic deformations appearance, a crack occurred at the tensioned column flange in the thermal affected area that spreaded suddenly in the column web.

References

1. ANSYS Inc., ANSYS Workbench 2.0 Framework Version: 12.0.1 (2009).
2. Grauvilardell, J. E., Lee D., Hajjar, J. F., Dexter, R. J., Synthesis of Design, Testing and Analysis Research on Steel Column Base Plate Connections in High-Seismic Zones. Structural Engineering Report No. ST-04-02, Department of Civil Engineering, University of Minnesota, October 1 (2005).
3. Hamizi M. si Hannachi N. E., Evaluation by a Finite Element Method of The Flexibility Factor and Fixity Degree for the Base Plate Connections Commonly Used. Strength of Materials, Vol. 39, No. 6 (2007).
4. Melenciuc S.C., Determinarea caracteristicilor de calcul a îmbinarilor stâlpilor metalici cu funda? iile de beton armat utilizând metoda elementelor finite. Volumul conferintei Creatii universitare 2011, Al IV-lea Simpozion National, Iasi, ISSN: 2247-4161, pag. 65-74 (2011).
5. Melenciuc S.C., Contributii privind imbunatatirea comportarii imbinarilor structurilor metalice amplasate in zone seismice. Politehnium, Iasi 2011, ISBN: 978-973-621-365-6 (2011).
6. Stamatopoulos G.N.,* , Ermopoulos J.Ch., Experimental and analytical investigation of steel column bases. Journal of Constructional Steel Research, Volume 67, Issue 9, september 2011, pp 1341-1357 (2011).

Probabilistic Seismic Risk Assessment of Barcelona, Spain

Omar D. Cardona[1], Mabel C. Marulanda[2], Martha L. Carreño[2], and Alex H. Barbat[2]

[1]*National University of Colombia, Manizales, Colombia*
[2]*International Center for Numerical Methods – CIMNE, Technical University of Catalonia, 08034, Spain*

Summary

Understanding disaster risk due to hazard events, such as earthquakes, creates powerful incentives for countries to develop planning options and tools to reduce potential damages. The results of the seismic risk assessment of the city of Barcelona using CAPRA (Comprehensive Approach for Probabilistic Risk Assessment) presented in this paper involve the evaluation of probabilistic losses of the exposed elements using probabilistic metrics, such as the exceedance probability curve, the expected annual loss and the probable maximum loss, which are useful for multi-hazard/risk analyses. The outcomes obtained with techno-scientific methodologies like CAPRA are oriented to facilitate decision-making. Using CAPRA, it is possible to design risk transfer instruments; evaluation of probabilistic cost-benefit ratio, to consider the net benefits of risk mitigation strategies; land use planning, loss scenarios for emergency response, early warning, on-line loss assessment mechanisms and holistic evaluation of disaster risk based on indicators. These applications facilitate the integrated risk management by the different stakeholders involved in risk reduction decision-making.

KEYWORDS: probabilistic seismic risk assessment, average annual loss, pure premium, loss exceedance curve.

1. INTRODUCTION

A disaster is the materialization of existent risk conditions. The risk level of a society is related to its development achievements and its capacity to intervene the existing risk. Hence, urban planning and efficient strategies are necessary to reduce risk and improve sustainable development. Risk management is a fundamental development strategy that considers four principal policies: risk identification, risk reduction, disaster management and risk transfer.

ISSN 2285-2735, Pages 91 - 108

From the financial point of view, it is essential to estimate and quantify potential losses in a given exposure time given that the budget for both emergency response and recovery and reconstruction could mean a fiscal exposure and a non explicit contingent liability for governments at city and country levels (Pollner 2001; Andersen 2002). Estimation of contingent losses provides information and permits to set out strategies *ex ante* for reducing or financing them (Marulanda et al 2008a, 2010a; Cardona 2010a; Cardona 2010b). Assessment of potential losses allows budget allocation for structural retrofitting to reduce damages and implementation of effective financial protection strategy to provide loss coverage of public infrastructure and private buildings to protect government resources and safeguard socioeconomic development; in summary, to achieve the greater awareness, security culture and economic prosperity, the financial protection must be a permanent and long term policy (Freeman et al. 2003).

Thus, one of the key strategic activities of disaster risk management is the assessment of the risk of disaster or of extreme events, which requires the use of reliable methodologies that allow an adequate calculation of probabilistic losses in exposed elements. The use of catastrophic risk models and the results obtained from risk analysis make feasible determining the potential deficit existing in case of the occurrence of an extreme event. Catastrophe risk models –based on metrics such as the Probabilistic Maximum Loss or the Average Annual Loss– are used to estimate, building by building, the probabilistic losses of different portfolios of exposed elements.

This paper performs a seismic risk assessment of the city of Barcelona, Spain. The probabilistic methodology Comprehensive Approach for Probabilistic Risk Assessment, CAPRA (Cardona et al. 2010a), is considered to be the most robust for this type of modeling and identifies the most important aspects of catastrophe risk from the financial protection perspective according to the fiscal responsibility of the states.

Vulnerability and risk analysis for Barcelona were developed starting from the seismic hazard information available for the city and the detailed cadastral information provided by the city administration in order to obtain the probable maximum losses (loss exceedance curve) and the pure risk premiums (average annual loss) of each building of the city. These risk metrics help to the knowledge of the contingency liabilities of the public sector and of the economic impact of the private sector, facilitating thus the consideration of risk transfer strategies for financial protection. Additionally, potential scenarios of damage can be obtained with the model, that can be used to develop emergency response plans and to implement risk reduction measures from physical, social and organizational point of view.

2. THE MODEL

The frequency of catastrophic seismic events is particularly low and this is the reason why very limited historical data are available. Considering the possibility of future highly destructive events, risk estimation has to focus on probabilistic models that can use the limited available information to best predict future scenarios and consider the high uncertainty involved in the analysis. Therefore, risk assessments need to be prospective, anticipating scientifically credible events that might happen in the future. The earthquake prediction models use the seismological and engineering bases for its development, allowing the assessment of the risk of loss given a catastrophic event. Since large uncertainties related to the severity and frequency characteristics of the events are inherent in models, the earthquake risk models have to use probabilistic formulations that incorporate this uncertainty into the risk assessment. The probabilistic risk model built upon a sequence of modules (Woo 1999, Grossi and Kunreuther 2005; Cardona et al 2008a/b/c/d), quantifies potential losses arising from earthquake events as shown in the Fig. 1.

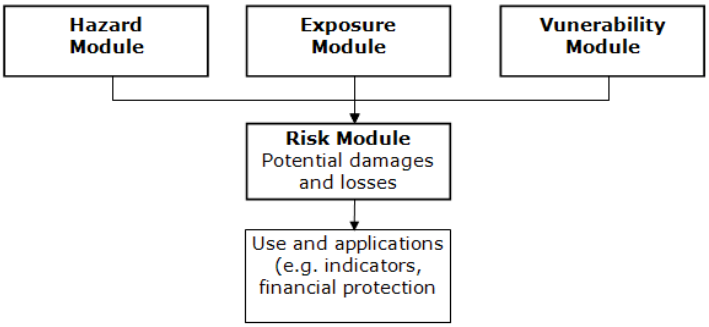

Figure 1.Probabilistic risk model

3. SEISMIC HAZARD MODULE

The hazard module of the probabilistic risk modeldefines the frequency and the severity of a hazard at a specific location. This is completed by analyzing the historical event frequencies and reviewing scientific studies performed on the severity and frequencies in the region of interest. Once the hazard parameters are established, stochastic event sets are generated which define the frequency and severity of thousands of stochastic events. This module can analyze the intensity at a location, once an event of the stochastic set has occurred, by modelling the attenuation of the event between its location and the site under consideration, and

evaluates the propensity of the local site conditions to either amplify or reduce the impact. The seismic hazard is quantified in terms of return periods (or exceedance rates) and the module provides the relevant seismic intensities necessary to evaluate the behavior of the structures. Its calculation includes the contribution of the effects of all seismic sources located in a certain influence area.

The application to the city of Barcelona takes into account the seismic sources for the Catalonia region of Spain identified by Secanell et al. (2004). Additionally, it considers the effects of the attenuation of the seismic waves by means of probabilistic spectral attenuation laws that include different source types Ambraseys (1996), as well as the local amplification effects based on microzonation studies. The site effects, considering the amplification of seismic hazard parameters according to the geological characterization of Barcelona, were established by Cid et al (2001) where a transfer function and an amplification factor for the acceleration level at the rock level characterized each zone (see Figure 2).

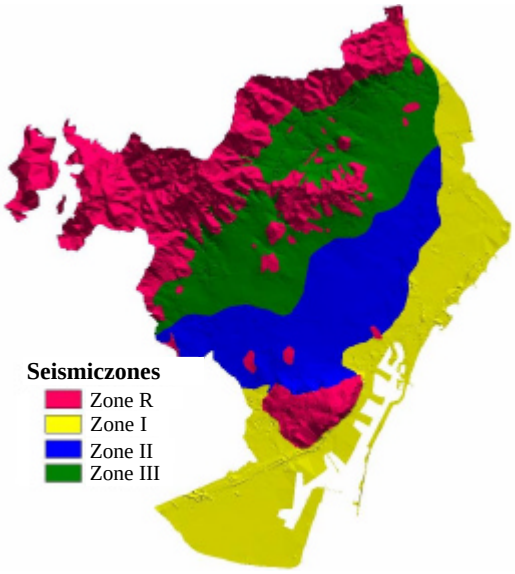

Soil zone	Vs (m/s)	Eurocode subsoil class
R	225	C
I	384	B
II	405	B
III	800	A

Figure 2. Seismic zonation based on local effects (Cid et al. 2001)

The seismic hazard was simulated by using the CRISIS 2007 code. The code allows estimating the hazard associated to all possible events that can occur, or to a group of selected events, or even to a single relevant event. Using the hazard module, it is possible to calculate the probable maximum value of the intensity, characterized for different exceedance rates or return periods. An .ame file type is created in this module (.ame comes from amenaza –hazard- in Spanish) which

includes multiple grids on the area of study, of the different parameters of intensity of the considered phenomena. Each grid is a scenario of the intensity level obtained from historical or stochastic generated events, with their frequency of occurrence. For this case, the parameter of seismic intensity selected is the spectral acceleration.

Further, the desired risk parameters such as percentages of damage, economic losses, effects on people and other effects are evaluated, in a probabilistic framework, for each of the hazard scenarios and then these results are probabilistically integrated by using the occurrence frequencies of each earthquake scenario. For Barcelona, 2058 seismic hazard scenarios were generated.

4. EXPOSURE MODULE

The *exposure* is mainly related to the infrastructure components or to the exposed population that can be affected by a particular event. The exposure module is based on files in *shape* format corresponding to the exposed infrastructure included in the risk analysis. To characterize the exposure, it is necessary to identify the individual components, including their location, their main physical, geometric and engineering characteristics, their vulnerability to hazardous events, their economic value and the level of human occupation that can have in a given analysis scenario. The exposure value of assets at risk is usually estimated from secondary sources such as available databases. The degree of precision of the results depends on the level of resolution and detail of exposure information.

The information used was compiled by Lantada (2007); the economic value of the exposed elements was supplied by the Cadastral Office of Barcelona, and 70655 buildings were considered (Figure 3). They are distributed in 10 municipal districts (Figure 4), 73 neighborhoods, 233 Basic Statistical Areas (in Spanish AEB– Áreas Estadísticas Básicas) and 1061 census sections. For each one of the buildings, the geographic location, economic value, year of construction, number of levels, structural type and human occupation, were defined. In order to proceed with the risk calculations, the results were calculated building by buildings, but they can be presented by considering any geographical level according to the required resolution.

In order to calculate the social impact, the general information related to building occupation is also estimated. Maximum occupancy and occupancy percentage at different hours of the day are also defined, allowing establishing different time scenarios of the event’s occurrence. When no specific occupation information was available, an approximate occupation density by construction class was used to complete the information.

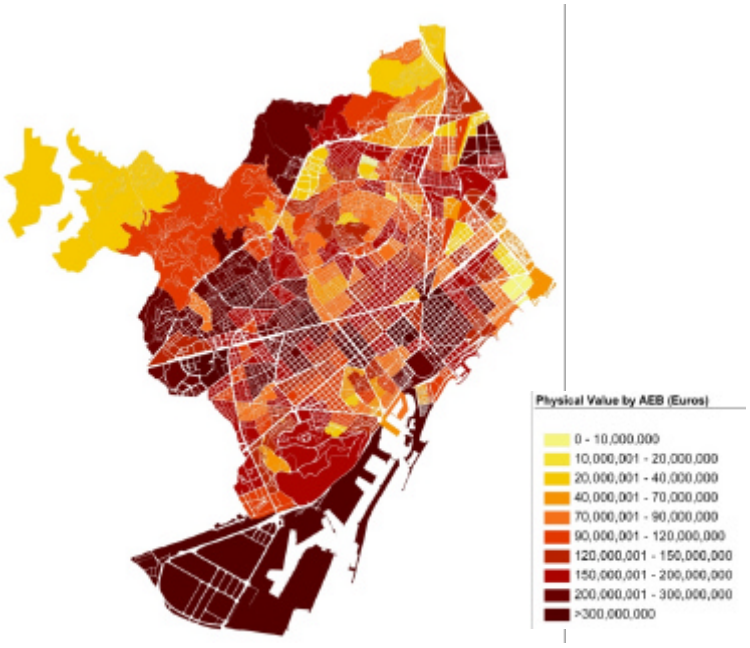

Figure 3. Exposed value of Barcelona by AEBs

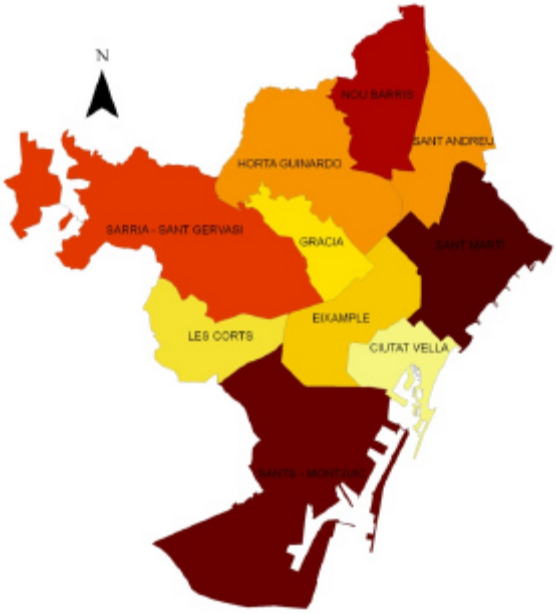

Figure 4. Administrative division of Barcelona

5. VULNERABILITY MODULE

The vulnerability module quantifies the damage caused to each asset class by the intensity of a given event at a site (Miranda, 1999). The classification of the assets is based on a combination of construction material, construction type (i.e. wall & roof combination), building use, number of levels and age. Estimation of damage is performed in terms of the mean damage ratio, MDR, which is defined as the ratio of the expected repair cost to the replacement cost of the structure. A vulnerability curve is defined relating the MDR to the earthquake intensity that can be expressed in terms of maximum acceleration (e.g. useful for 1-2 story buildings), spectral acceleration, velocity, drift or displacement (e.g. useful for multi-story buildings) at each location.

Most part of the building stock of Barcelona was constructed when no seismic-resistant construction codes existed. The combination of very old buildings constructed without seismic code with a highly populated and active produced a high vulnerability which can generate a significant risk even under the effects of a moderate earthquake. The vulnerability module of the ERN-CAPRA platform defines the vulnerability of the buildings in the city by using vulnerability functions. The assignment of the vulnerability function to each exposed element is carried out in the exposure module by means of a shape format file. There is a vulnerability function corresponding to each building typology; the most common structural system used in Barcelona is the unreinforced masonry, followed by the reinforced concrete, whose construction has increased rapidly in recent decades. Steel structures are less used and they are not usually used for residential buildings but for industrial buildings, markets, sports areas, among others. The used typologies were defined in RISK-UE (2004) and are shown in Table 1.

Each structural type is subdivided into 3 classes according to the height:

- *Low, L.* 1 to 2 floors for masonry and wood structures; and 1 to 3 floors for reinforced concrete and steel buildings.
- *Medium, M.* 3 to 5 floors for masonry and wood structures; and 4 to 7 floors for reinforced concrete and steel buildings.
- *High, H.* 6 or more floors for masonry and wood structures; and 8 or more floors for reinforced concrete and steel buildings.

Table 1. Building typology matrix for Barcelona (RISK-UE 2004)

UNREINFORCED MASONRY	M3.1	Unreinforced masonry bearing walls with wooden slabs
	M3.2	Unreinforced masonry bearing walls with masonry vaults
	M3.3	Unreinforced masonry bearing walls with composite steel and masonry slabs
	M3.4	Reinforced concrete slabs
REINFORCED CONCRETE	RC3.1	Concrete frames with unreinforced masonry infill walls with regularly infill frames
	RC3.2	Concrete frames with unreinforced masonry infill walls with irregularly frames (i.e., irregular structural system, irregular infill, soft/weak storey)
STEEL MOMENT FRAMES	S1	A frame of steel columns and beams
STEEL BRACED FRAMES	S2	Vertical components of the lateral-force-resisting system are braced frames rather than moment frames.
STEEL FRAMES WITH UNREINFORCED MASONRY INFILL WALLS	S3	The infill walls usually are offset from the exterior frame members, wrap around them, and present a smooth masonry exterior with no indication of the frame.
STEEL AND RC COMPOSITE SYSTEMS	S5	Moment resisting frame of composite steel and concrete columns and beams. Usually the structure is concealed on the outside by exterior non-structural walls.
WOOD STRUCTURES	W	Repetitive framing by wood rafters or joists on wood stud walls. Loads are light and spans are small.

Figure 5 shows the vulnerability functions used for unreinforced masonry buildings and Figure 6 shows the functions for other building typologies, for low (L), medium (M) and high (H) buildings. These functions relate the severity of the event, represented by the spectral acceleration with the average damage in the building.

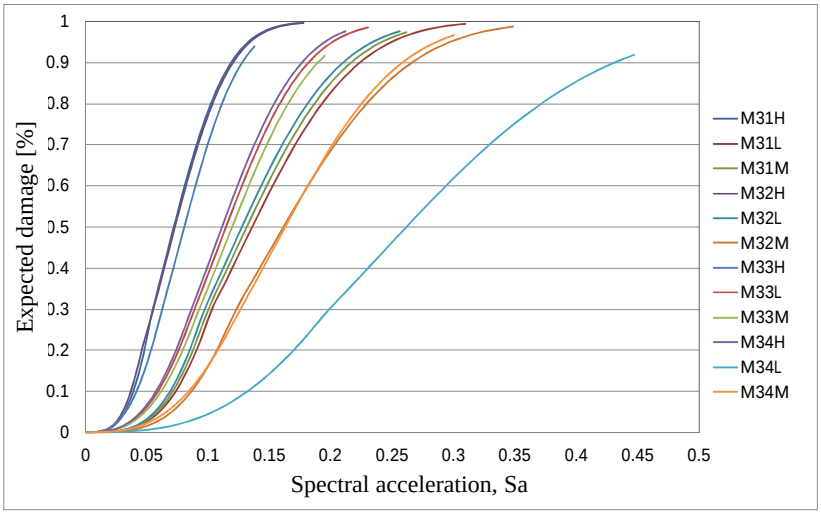

Figure 5. Vulnerability functions for unreinforced masonry buildings

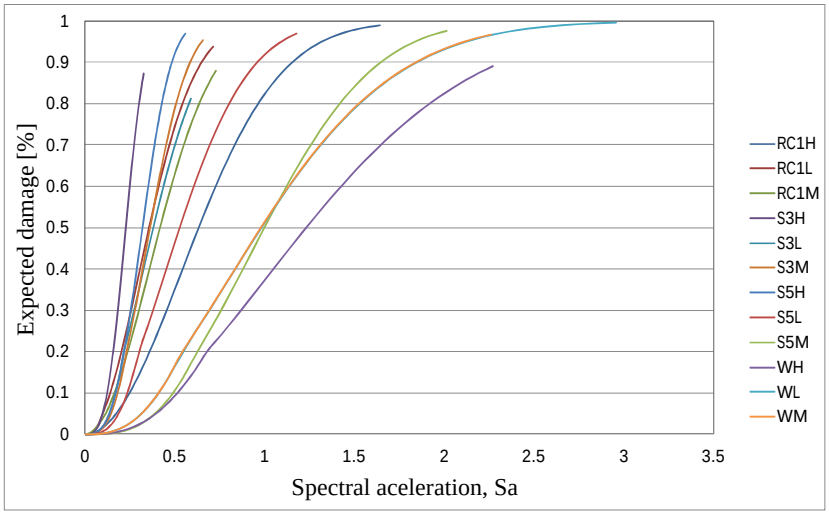

Figure 6. Vulnerability functions for reinforce concrete, steel and wood buildings

6. RISK MODULE

The physical seismic risk is evaluated by means of the convolution of the hazard with the vulnerability of the exposed elements; the results are the potential

consequences. Risk can be expressed in terms of damage or physical effects, absolute or relative economic loss and/or effects on the population.

Once the expected physical damage is estimated (average value and its dispersion) as a percentage for each of the assets or infrastructure components included in the analysis, one can make estimates of various parameters useful for the proposed analysis. Risk metrics calculated by using the model provide risk managers and decision makers with essential information required to manage future risks. One measure is the Average Annual Loss and the other is the Loss Exceedance Curve. Other measures, such as the Pure Risk Premium and the Probable Maximum Loss, can be computed based on the former.

- *Average Annual Loss.* AAL is the expected loss per year. Computationally, AAL is the sum of products of event expected losses and event annual occurrence probabilities for all the stochastic events considered in the loss model. In probabilistic terms, AAL is the mathematical expectation of the annual loss.
- *Pure Risk Premium.* PRP is the AAL divided by the replacement value of the asset, usually expressed as a rate per mill of monetary value.
- *Loss Exceedance Curve.* LEC represents the annual frequency with which a loss of any specified monetary amount will be exceeded. This is the most important catastrophe risk metric for risk managers, since it estimates the amount of funds required to meet risk management objectives. The LEC can be calculated for the largest event in one year or for all (cumulative) events in one year. For risk management purposes, the latter estimate is preferred, since it includes the possibility of one or more severe events resulting from earthquakes.
- *Probable Maximum Loss.* PML represents the loss amount for a given annual exceedance frequency, or its inverse, the return period. Depending on the stakeholder's risk tolerance, the risk manager may decide to manage for losses up to a certain return period (e.g. 1 event in 300 years). For that stakeholders (e.g. a public or private agency), the PML is the 300-year loss. For others, it may be 150 years or 500 years. It is noteworthy that it is frequent that certain stakeholders set the insolvency criterion at return periods between 150 years and 200 years. However, other involved stakeholders (e.g. governments or regulation agencies) have chosen much longer return periods, such as the Mexican Insurance Commission, which uses a return period of 1500 years to fix solvency margins of insurance companies in Mexico.

As previously said, the probabilistic risk analysis is done based on a series of hazard scenarios that adequately represent the effects of any event of feasible magnitude that can occur in the area of influence. Each of these scenarios has an associated specific frequency or probability of occurrence. The probabilistic

calculation procedure comprises the assessment using appropriate metrics, in this case the economic loss, for each exposed asset considering each of the hazard scenarios with its frequency of occurrence, and the probabilistic integration of the obtained results.

The Average Annual Loss for physical assets, fatalities and injuries are calculated for each building of the city. The probabilistic results for of Barcelona are shown in tables 2, 3 and 4. Figure 7 shows the PML curve obtained for Barcelona. Figure 8 shows the expected annual loss for each AEB of Barcelona. As it was previously mentioned, the expected annual economic loss was calculated building by building and Figure 9 shows the obtained results at this resolution. Figure 10 and Figure 11 show the expected annual loss for injured and deaths by AEB in Barcelona.

Table 2. Physical exposure

PHYSICAL EXPOSURE		
Exposed value	€ x10^6	31,522.80
Average Annual	€ x10^6	72.14
Loss	‰	2.29‰
PML		
Return period	Loss	
(Years)	€ x10^6	%
50	729.35	2.31%
100	1,770.16	5.62%
250	3,699.35	11.74%
500	5,172.26	16.41%
1,000	6,510.67	20.65%
1,500	7,021.14	22.27%

Table 3 Dead people

DEAD PEOPLE		
Exposed value	Inhab.	1,639,880.00
Average Annual	Inhab.	28.27
Loss	‰	0.017‰
PML		
Return period	Loss	
(Years)	Inhab.	%
50	101.41	0.01%
100	654.30	0.04%
250	2,069.97	0.13%
500	3,380.29	0.21%
1,000	4,898.39	0.30%
1,500	5,799.44	0.35%

Table 4. Injured people

INJURED PEOPLE		
Exposed value	Inhab.	1,639,880.00
Average Annual	Inhab.	113.55
Loss	‰	0.07‰
PML		
Return period	Loss	
(Years)	Inhab.	%
50	101.41	0.01%
100	654.30	0.04%
250	2,069.97	0.13%
500	3,380.29	0.21%
1,000	4,898.39	0.30%
1,500	5,799.44	0.35%

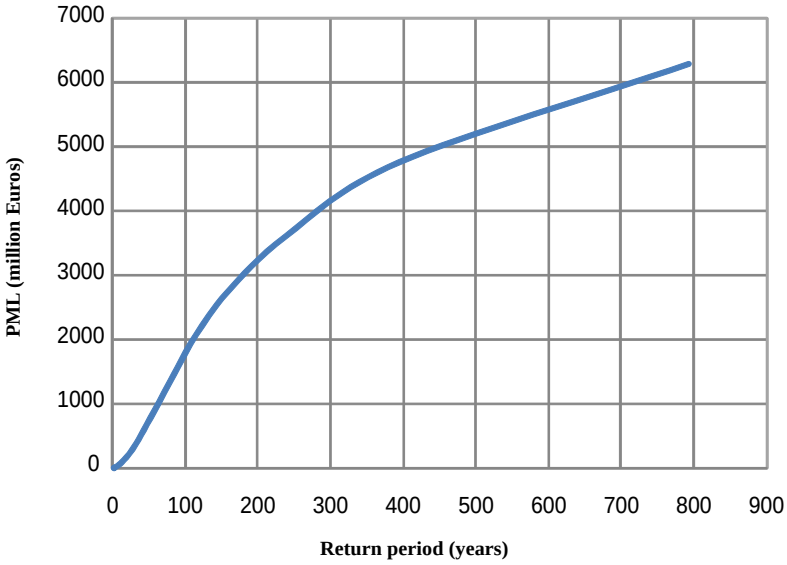

Figure 7. PML curve for Barcelona

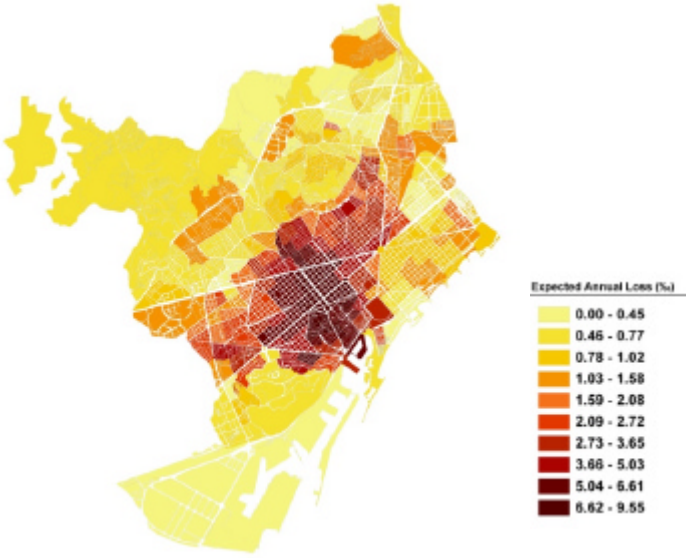

Figure 8. Expected annual loss for the AEBs of Barcelona

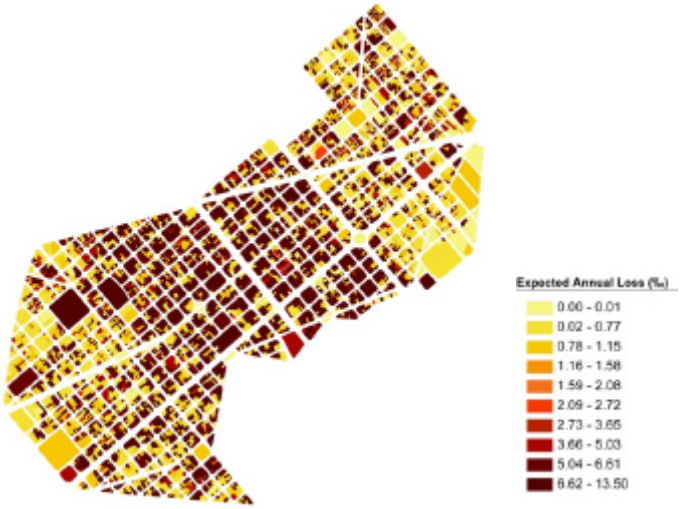

Figure 9. Expected annual loss for each building in the Eixample District of Barcelona

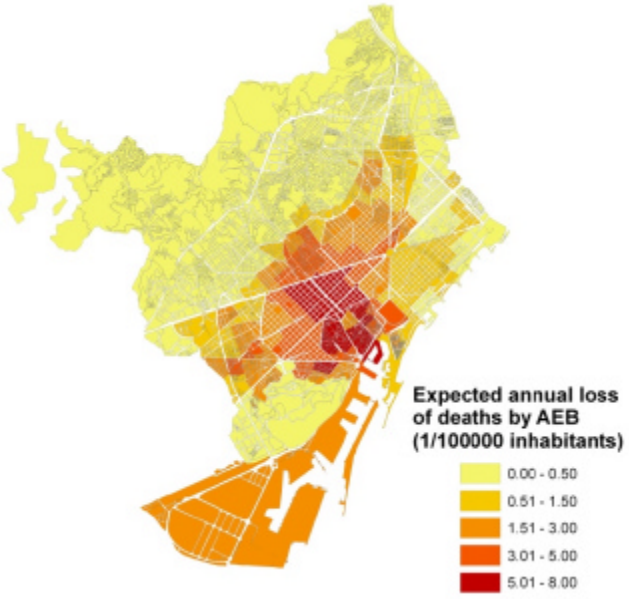

Figure 10. Expected annual loss for deaths by AEB in Barcelona

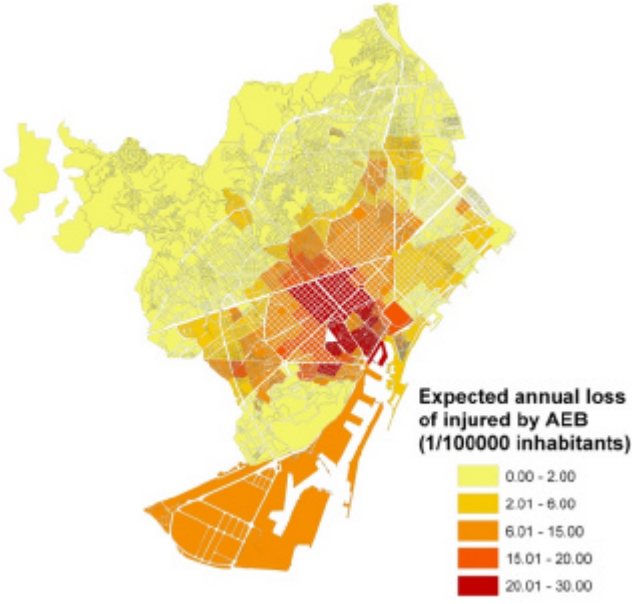

Figure 11. Expected annual loss for injured by AEB in Barcelona

In addition to the probabilistic economic figures, it is also relevant for the emergency response plans of the city to count with critical earthquake loss scenarios. In the case of Barcelona, a critical scenario for a loss with a return period of approximately 1000 years was chosen, to estimate the people that could lose their job or their houses. Assessments of these figures are based on the percentage of damage of each structure (greater than or equal to 20%). Table 6 presents the information of the critical scenario for Barcelona.

Table 6. Information of the critical scenario for Barcelona

Nº	Scenario		Loss	
	Source	Magnitude	€ x10^6	%
600	Zona 4_SF2	6.56	6.78E+03	21

The Figure 12and Figure 13 show the scenarios of homeless and jobless by AEB in Barcelona.

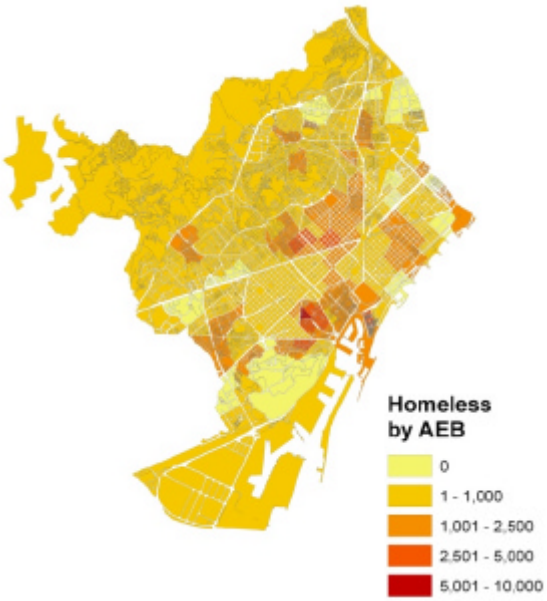

Figure 12. Homeless by AEB in Barcelona.

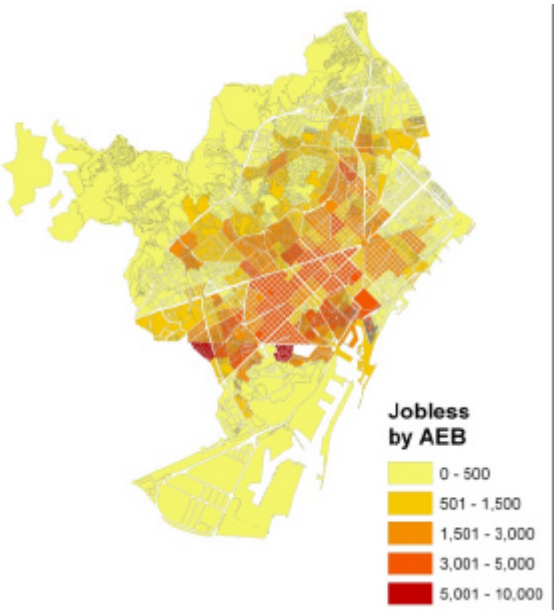

Figure 13. Jobless by AEB in Barcelona.

7. CONCLUSIONS

Catastrophic risks such as earthquake risk impose a dreadful threat not only for private insurers and reinsurers, but also for governments whom, in turn, are risk-takers for most of the uninsured and uninsurable risk. Therefore, seismic risk models become powerful tools for government officials in economic and financial planning institutions. The retention and transfer of risk should be a planned and somewhat controlled process, given that the magnitude of the catastrophic problem could represent a great governmental response and financial liabilities. For management purposes, the risk assessment should improve the decision-making process in order to contribute to the effectiveness of risk management, identifying the weaknesses of the exposed elements and their evolution over time. It is

expected that the application in Barcelona will be useful for the risk reduction and emergency preparedness plans in the city.

This study focuses on the risk assessment at urban level (by geographic units) due to the earthquake hazards, using as risk measure the Probable Maximum Loss (PML) for different return periods and the Average Annual Loss (AAL) or technical risk premium. The values of PML and AAL are the main results of this application. These measures are of particular importance for the future design of risk retention (financing) or risk transfer instruments, and therefore they will be a particularly valuable contribution to further studies to define a strategy for financial protection to cover the fiscal liability of the State.

References

1. Ambraseys, N.N., Simpson, K.A. and Bommer, J.J. (1996): "Prediction of horizontal response espectra in Europe". Earthquake Engineering and Structural Dynamics 25: 375-400.
2. Andersen, T. (2002). *Innovative Financial Instruments for Natural Disaster Risk Management*. Inter-American Development Bank. Sustainable Development Department. Technical Papers
3. Barbat, A.H.; Carreño, M.L.; Pujades, L.G.; Lantada, N.; Cardona, O.D. and Marulanda, M.C. (2010).“*Seismic vulnerability and risk evaluation methods for urban areas. A review with application to a pilot area*”. Structure and Infrastructure Engineering. Vol. 6, Nos. 1-2, Taylor & Francis.
4. Cardona O.D., Ordaz, M.G., Reinoso, E., Yamín, L.E., Barbat, A.H. (2010a). *Comprehensive Approach for Probabilistic Risk Assessment (CAPRA): International Initiative for Disaster Risk Management Effectiveness.* in Proceedings of 14th European Conference on Earthquake Engineering, August 2010, Ohrid, Macedonia.
5. Cardona O.D., Marulanda, M.C. (2010b). *Mecanismos Financieros, Seguro y Reaseguro contra Desastres Naturales en América Latina y el Caribe: Experiencias Recientes.* Secretaría Permanente del Sistema Económico Latinoamericano y del Caribe, SELA, SP/SR-IPMFSRCDALC/DT Nº 2-10, Caracas. Available at: http://www.sela.org/attach/258/EDOCS/SRed/2010/11/T023600004489-0-TDR_Estudio_Seguro_contra_Desastres_ALC_2010_REV-ODC.pdf
6. Cardona, O.D., Ordaz, M.G., Marulanda, M.C., & Barbat, A.H. (2008a). Estimation of Probabilistic Seismic Losses and the Public Economic Resilience—An Approach for a Macroeconomic Impact Evaluation, *Journal of Earthquake Engineering*, 12 (S2) 60-70, ISSN: 1363-2469 print / 1559-808X online, DOI: 10.1080/13632460802013511, Taylor & Francis, Philadelphia, PA.
7. Cardona, O.D., Ordaz, M.G., Yamín, L.E., Marulanda, M.C., & Barbat, A.H. (2008b). Earthquake Loss Assessment for Integrated Disaster Risk Management, *Journal of Earthquake Engineering*, 12 (S2) January 48-59, ISSN: 1363-2469 print / 1559-808X online, DOI: 10.1080/13632460802013495, Taylor & Francis, Philadelphia, PA.
8. Cardona, O.D., Ordaz, M.G., Marulanda, M.C., Barbat, A.H. (2008c). Fiscal Impact of future earthquakes and country’s economic resilience evaluation using the disaster deficit index, *Innovation Practice Safety: Proceedings 14th World Conference on Earthquake Engineering, Beijing*, China.
9. Cardona, O.D., Ordaz, M.G., Yamin, L.E., Arámbula, S., Marulanda, M.C., Barbat, A.H. (2008d). Probabilistic seismic risk assessment for comprehensive risk management: modeling for

innovative risk transfer and loss financing mechanisms, *Innovation Practice Safety: Proceedings 14th World Conference on Earthquake Engineering*, Beijing, China.
10. Cid J., Susagna T., Goula X., Chavarria L., Figueras S., Fleta J., Casas, A. y Roca, A. (2001): "Seismic Zonation of Barcelona Based on Numerical Simulation of Site Effects." Pure Applied Geophysics 158: 2559-2577.
11. Cid J. (1998). Zonación sísmica de la ciudad de Barcelona basada en métodos de simulación numérica de efectos locales. Tesis doctoral. Dpto. Ingeniería del Terreno, Cartográfica y Geofísica. Universidad Politécnica de Cataluña, Barcelona. 215 pp.
12. Freeman, P., Keen, M and Muthukumara, M. (2003). Dealing with Increased Risk of Natural Disasters: Challenges and Options. IMF – International Monetary Fund. Working Paper 03/197.
13. Grossi P. & Kunreuther H. (2005). Catastrophe modeling: A new approach to managing risk, Springer Science.
14. RISK-UE (2004). An advanced approach to earthquake risk scenarios with applications to different European towns. Project of the European Commission, Contract number: EVK4-CT-2000-00014.
15. Lantada N. (2007): Evaluación del riesgo sísmico mediante métodos avanzados y técnicas gis. Aplicación a la ciudad de Barcelona. Doctoral dissertation. Universidad Politécnica de Cataluña, Barcelona, Spain.
16. Marulanda, M.C., Cardona, O.D., Barbat, A.H. (2010) Revealing the socio-economic impact of small disasters in Colombia using DesInventardatabase, *Disasters*, December 11/2009; 34(2): 552- 570, Overseas Development Institute, Blackwell Publishing, Oxford.
17. Marulanda, M.C., Cardona, O.D., Ordaz, M.G., Barbat, A.H. (2008). La gestión financiera del riesgo desde la perspectiva de los desastres: Evaluación de la exposición fiscal de los Estados y alternativas de instrumentos financieros de retención y transferencia del riesgo. Monografía CIMNE IS-61, Universidad Politécnica de Cataluña, Barcelona.
18. Miranda, E. (1999) Approximate seismic lateral deformation demands on multistory buildings, *Journal of Structural Engineering* 125:4, 417-425.
19. Pollner, J. (2001). Managing Catastrophic Disaster Risks Using Alternative Risk Financing and Pooled Insurance Structures. World Bank Technical Paper, No. 495.
20. Secanell, R., Goula, X., Susagna, T., Fleta, J. y Roca, A. (2004): "Seismic hazard zonation of Catalonia, Spain integrating uncertainties". Journal of Seismology 8 (1): 24-40.
21. Woo, G. (1999): *The Mathematics of Natural Catastrophes*, Imperial College Press.Yamin, L.E., Gallego, M., Cardona, O.D., Phillips, C.A. (2004). “Recent Advances in Seismic Microzonation Studies, The Manizales-Colombia Case”, 13th World Conference on Earthquake Engineering, Vancouver.

Integration of web-enhanced teaching tools in undergraduate construction and civil engineering higher education

Cristina Cosma
Department of Construction Management, Wentworth Institute of Technology, Boston, MA, 02115, USA

Summary

For the past several years web-based instructional technology has been constantly developed and used at Wentworth Institute of Technology to assist the face-to-face interaction. A first step was to use the Blackboard learning system to post syllabus, lecture handouts and laboratory assignments. A second step was to facilitate student assignment submission via Blackboard and use web-based assessments of student learning outcomes which offered just-in-time feedback both for instructor and students. In 2010 a third step towards on-line anytime anywhere learning was taken by developing a full set of video tutorials for laboratories.

The paper will describe and analyze the development of a complete set of on-line laboratories for CCEV 406 – Construction Project Scheduling which is offered every fall semester to the junior construction management students. The advantages and disadvantages of using these novel instructional methods will be assessed based on students' evaluations and comments and also on instructor's experience. The paper particularly outlines the technical challenges encountered in building the on-line course content, class assignments and student learning assessment tools.

KEYWORDS: Wentworth Institute of Technology, Web-enhanced learning, Blackboard, On-line laboratories, Video tutorials

1. INTRODUCTION

Located in Boston, MA, Wentworth Institute of Technology (WIT) is a private, coeducational college founded in 1904. Wentworth offers bachelor's degrees with majors in the fields of applied mathematics, architecture, computer science, construction management, design, engineering, engineering technology, and management. Wentworth provides a comprehensive interdisciplinary, project-based education that integrates classroom, laboratory, studio, cooperative and experiential learning resulting in a career-ready, skilled professionals and engaged citizens. Wentworth has a student body of more than 3,200 full time students from 33 US states and approximately 46 countries [1].

For the past ten years the teaching and learning landscape at Wentworth has been continuously changing in a sustained effort to satisfy the increasing demand for a more diversified and flexible type of higher education. Among the strategies used at Wentworth can be mentioned the integration of learning technology complemented by the changing face of instructional design, implementation of novel teaching strategies and the determination of meaningful learning objectives.

The Wentworth Laptop Program which started as a pilot in 2004 was one of the first initiatives aiming to accommodate the specific needs of students in terms of time and place of study. The program provides all full-time students and faculty members with a laptop computer (MacBook Pro for students in Architecture or Design and Facilities departments and Lenovo for all other departments). The computers are capable of running the high-end software that is customized to meet both the academic requirements and current industry demands for each specific major. To ensure that the students have the most updated hardware and software, each laptop is refreshed during the junior year. At the end of their senior year, once a student graduates, they take their computer with them. The cost of the laptop program is part of student tuition [1].

The laptop program is a fundamental tool highly needed to support the shift from a teacher-centric lecture model of instruction to a learner-centric, technology-enhanced learning model. The program was concurrently a key driving force towards the adoption of new teaching and learning methods and the effect of the dramatic growth of the internet and web-based applications for educators.

The Division of Technology Services (DTS) and the Division of Academic Affairs/Office of the Provost at Wentworth are the two main departments in charge to build on the educational innovations and also to inspire and offer support to faculty members to get involved and develop sound teaching strategies for the effective and stimulating utilization of technology in educational environments.

Figure 1 below shows a snapshot of the main website window with on-line resources available to faculty.

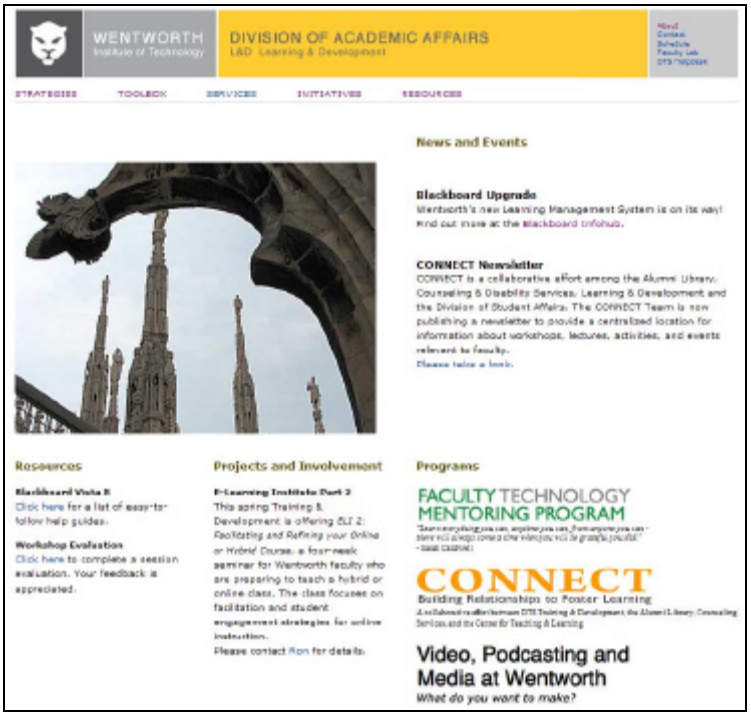

Figure 1. Learning and Development webpage

2. TRADITIONAL TEACHING FRAMEWORK

2.1. Existing situation

CCEV 406 “Construction Project Scheduling” (2-2-3) is offered once a year during the fall semester to junior CM students.

The learning goals of CCEV 406 are:

- Goal #1: to understand how schedules can be used to help plan, direct and control the construction process
- Goal #2: to manually develop a construction project schedule using the Critical Path Method (CPM)

- Goal #3: to use the computer as a tool to create and maintain a construction schedule
- Goal #4: to strengthen team building and communication skills.

The course consists of 2 hours traditional lecture time and 2 hours of laboratory-based instruction. In fall 2010 there were a total of 98 students registered for this course. The course is offered in 3 lecture sections having a maximum of 40 students each and 6 laboratory sections (2 laboratory sections for each lecture section) with a maximum of 20 students each.

In the past years during the laboratory hours the students were exposed to hands-on instruction on various planning and scheduling tools and software (Excel, Microsoft Visio, Microsoft Project, Primavera P6). The scheduling skills achieved by students in the first half of the semester were mastered through a class project assigned to teams of two students.

The laboratory hours were customary conducted on campus in a traditional manner. In most laboratory classes in the first part of the laboratory the instructor was offering a short review of the subjects presented during the lecture and was giving one or two additional examples of practical applications of the lecture subjects.

In the second part of the 2 hour laboratory the students were practicing on using various scheduling techniques, tools and software under the close supervision of the laboratory instructor.

In order to perform the assigned tasks the students were provided a Laboratory Manual which contained step by step instructions for each laboratory assignment. Also the instructor was performing the laboratory steps in the same time with the students and was projecting the output on the screen making it easier to follow. This instructional approach necessitated the laboratory instructor have an excellent knowledge of the tools and software presented and used. One of the implications of this particular skill requirement was the difficulty in finding adjuncts to teach the laboratory for CCEV 406.

The difficulty of the instructional approach used in the past was that the faster students were losing interest while waiting for the instructor (and the rest of the class) to reach a certain laboratory phase or step and sometimes were disturbing the class. Meanwhile the slower students ended up being left well behind and having to finish the laboratory on their own, outside the laboratory time.

The class project was introduced to the students in week 5 of classes and was due by the end of the semester. By this time students have been already introduced to the main notions and methods of scheduling and in the lab they have already practiced on using various scheduling software.

For the class project the students created teams of 2 students/each. All teams were given construction drawings for the same construction project. The main tasks of

the teams were to analyze the project, produce a Scope of Work (SOW), plan the construction of the building and the main construction packages, produce a Work Breakdown Structure (WBS), establish the logic sequence of construction the building, and finalizing the project by producing the construction schedule and various scheduling reports.

Due to the fact that most of the laboratory time was allocated to introducing and training the students on using scheduling tools and software, there was little time left for discussing class project and phases. Most of the feedback or answers to students' questions on class project were given during the office hours.

2.2. New training approach

In summer 2010 a Bistline Grant was awarded to research and extend the use of innovative distance learning techniques in order to create a hybrid laboratory for the fall 2010 semester. The course (CCEV 406 - "Construction Project Scheduling") is offered to the junior Construction Management (CM) students. There were a total of 98 students registered for this course. The course is offered in 3 lecture sections having a maximum of 40 students each and 6 laboratory sections with a maximum of 20 students each.

The outcome of this research was a complete set of on-line laboratory classes for CCEV 406 "Construction Project Scheduling" (2-2-3). Ten on-line laboratories have been created. For each laboratory a set of video tutorials was developed. The videos are between 3 min to 18 min long.

One main objective of this project was to contribute to creating a student-centered learning environment where students are challenged to think critically, to be effective team players, and to be self-directed learners. This objective was achieved through the usage of video tutorials for the laboratory assignments. Students were given the opportunity to work on lab assignments anytime anywhere, perform the requested tasks at their own pace and also engage with peers in sharing, organizing and discovering the learning content.

Another objective of the research was to appeal to diverse learning styles by developing instructional materials based on a hybrid of Problem-Base Learning (PBL) and Active/Cooperative Learning (ACL) techniques that incorporate both visual, interactive teaching methods and extensive use of modern computational approaches. This objective was achieved by changing the focus of the laboratory class from training the students on the usage of various scheduling software to developing a team based and real-world project based learning environment.

3. DEVELOPMENT OF WEB-ENHANCED TEACHING

The research project had as a main goal to create a complete set of on-line laboratory classes for CCEV 406 “Construction Project Scheduling”. This goal was achieved in three main phases:

- Phase 1: Assessment of on-line laboratory delivery methods and strategies
- Phase 2: Training and practicing on on-line delivery tools
- Phase 3: Develop on-line laboratory tutorials
- Phase 4: Development of contingency plans in case of technical problems

3.1. Assessment of on-line laboratory delivery methods and strategies

The first step in developing the on-line laboratories was to analyze the existing laboratory subjects and plan the on-line delivery methods and strategies to be used. During this assessment phase the first step to be performed was to determine how much information from each laboratory should be uploaded to the online classroom.

With the support of the instructional designers from DTS a Course Map has been developed correlating the lecture subjects with the homework assignments, subject assessments (quizzes), laboratory assignments and project phases.

The second step was to determine what proportion of classroom interaction should occur online in the hybrid course. It was decided to offer on-line part of the class project and all laboratory assignments. The class project was divided into 3 phases. Each phase is concluded by an in-class team presentation. This organization resulted in 5 in-class scheduled meetings during the semester.

The third step was to determine how to evaluate levels of class participation. After discussing with the instructional designers it was decided that a scoring system based on three performance indicators (Need Improvement, Meet Expectations & Exceptional) will be used.

Next step was to establish what technological features of online courseware enhance the quality of online laboratory. With the support of DTS instructional designers the following software and technical equipment were identified to be useful for the laboratory:

- Camtasia Studio for producing video tutorials of laboratory assignments
- Blackbord discussion boards for facilitating group communication

- Blackboard learning modules for structuring the hybrid laboratory, class project particularly
- Flip cameras for video recording team presentations for the class project
- Digitizing Tablet for providing feedback for on-line assignments

Finally in conjunction with creating the Course Map the existing laboratory content had to be analyzed and alterations were performed in order to match the new approach to the existing lecture content. Additional materials were created for online delivery but also for the in-class parts of the laboratory and for assignments.

3.2. Training and practicing on on-line delivery

Three main tasks were performed during this phase: (1) Meetings with DTS instructional designers; (2) Participating to the Annual Sloan Consortium Emerging Technologies for Online Learning Symposium and (3) Practicing on producing pilot recordings and on-line laboratory tutorials.

3.2.1. Training meetings with DTS instructional designers

During the training phase the instructor interacted with DTS instructional designers during several meetings discussing the available resources and support for on-line teaching. Other subjects discussed were related to the technical aspects of video sharing on Blackboard and methods of student on-line engagement and interaction.

One potential problem that was identified was the fact that the available depositing space for files on Blackboard is limited. It was estimated that a number of almost 25 video files for the ten on-line laboratories (about 3 video recordings for each lab) can be recorded/produced. The pilot video recordings produced during this phase were quite large (20 MB/each or more). The estimated storage space needed for all the files was close to 1 GB (1,000 MB = 1 GB). The solution suggested by the instructional designers was to use the 2 GB storage space provided for free by TechSmith for Jing and Camtasia users on screencast.com.

3.2.2. Practicing on producing pilot recordings and on-line laboratory tutorials

At the end of this phase pilot recordings and on-line laboratory tutorials were produced. Blackbord digital tools for on-line communication (i.e. discussion boards) were used and a couple of short video tutorials using screen capture software (Jing and Camtasia Studio) were created.

After practicing both with Jing and Camtasia Studio it was decided to use Camtasia Studio for producing the laboratory video tutorials because this software offers a much wider variety of video effects than Jing.

Some of the video effects that can be used in Camtasia Studio and which definitely contribute to an increased quality of the laboratory video tutorials facilitating student learning are:

- Import images, recording files and video clips
- Apply SmartFocus and zoom-in keyframes on the recordings to draw viewers'
- attention to specific action in the video
- Make basic edits on the timeline like cut and splip clips, move clips, add markers, etc.
- Record camera video or add a video clip as a Picture-in Picture on the timeline
- Add title clips and transitions
- Add callouts, captioning, mouse highlight, flash quizzes or surveys
- Edit the audio by removing noises, m-ms, etc.

Most of the above video effects have been used in the laboratory tutorials developed.

3.3. Development of on-line laboratory tutorials

During Phase 3 a full set of on-line laboratories was developed based on the laboratory course map created in Phase 1 by using the on-line tools and software (Camtasia Studio) learned in Phase 2.

Table 1 below shows the screen casts and sets of video tutorials that were created for each lab.

Table 1. Laboratory Video Tutorials

Laboratory	**Video Tutorial**
Lab Assignment 1 Build a Gantt/Bar Chart Schedule using Excel & Microsoft Project	1. PART A video (6 min) - Introduction to general scheduling concepts and Bar Charts. 2. PART B video (30 min) - shows students how to use Excel to build a Bar Chart 3. PART C video (12 min) - instructions on how to create a Gantt Chart schedule in Microsoft Project
Lab Assignment 2 Build a Gantt/Bar Chart Schedule using Primavera Project Manager (P6)	4.PART A video (13 min) - brief Introduction to the portfolio, OBS & EPS concepts and shows the steps students need to take to create these structures in P6 5. PART B video (16 min) - shows students how

Laboratory	Video Tutorial
	to use P6 to build a Bar Chart 6. PART C video (8 min) - instructions on how to create a Scheduling Report in P6
Lab Assignment 3 Build a Gantt/Bar Chart Schedule for a Renovation Project (32 activities) using Primavera Project Manager (P6)	7. PART A video (5 min) - brief Introduction to Lab Assignment 3 and project data. 8. PART B video (3 min) - reviews the steps on how to assign predecessors to activities in P6. 9. PART C video (6 min) - instructions on how to assign the holidays/non-work days to the schedule calendar and create the final schedule & the 2 lab submittals
Lab Assignment 4 Organizing & Sorting the Renovation Project Schedule in P6	10. PART A video (11 min) - brief Introduction to Lab Assignment 4 and instructions on how to create and assign activity/project codes. 11. PART B video (13 min) - steps on how to generate Submittals 1, 3 & 4.. 12. PART C video (7 min) - instructions on how to produce Submittal #2.
Lab Assignment 5 Customize the Renovation Project Schedule using Filters & Sorts in Primavera Project Manager (P6)	14. PART B video (10 min) - steps on how to generate Submittals 2, 3 & 4. 15. PART C video (5 min) - instructions on how to produce Submittal #5.
Lab Assignment 6 Review the use of P6 Create a WBS & OBS Structure	16. PART A video (14 min) - brief Introduction to Lab Assignment 5 and instructions on how to create Submittals 1 & 2. 17. PART B video (20 min) - instructions on how to create the new project and prepare for the Submittals 2 to 6. 18. PART C video (5 min) - instructions on how to produce Submittal #6.
Lab Assignment 7 Perform a Schedule Update on the Industrial Building Project	19. PART A video (8 min) - a brief Introduction to Lab Assignment 7 and on the importance and methods of updating a schedule 20. PART B video (18 min) - instructions on how to update the project and prepare for the Submittals 2 & 3. 21. PART C video (7 min) - instructions on how to produce Submittals 4 & 5.
Lab Assignment 8 Cost Load the Renovation Project	22. PART A video (3 min) - brief Introduction to Lab Assignment 8. 23. PART B video (17 min) - instructions on how to create cost accounts, resource codes, cost load a schedule and prepare for Submittals 1 through 4.

Laboratory	Video Tutorial
	24. PART C video (7 min) - instructions on how to produce Submittals 1 through 4..
Lab Assignment 9 Create Graphical Reports on Resource & Cost Usage for the Renovation Project	25. Video tutorial (8 min) – instructions on how to produce the required submittals
Lab Assignment 10 Create a short video training tutorial	No video tutorials were developed for this laboratory

3.4. Development of contingency plans in case of technical problems

During the last phase of this project potential pitfalls and troubleshooting associated with each laboratory were identified. Based on previous in-class experience with the lab assignments the instructor created several very short video tutorials (less than 5 min) showing how to redress from certain issues that students can encounter while using various scheduling software, Primavera Project Management (P6) particularly.

One main part of the contingency plan was to create and provide a Laboratory Manual for the lab assignments. The Manual contents are similar to the videos and offer step by step instructions on how to fulfill each assignment. Most of the written instructions in the Manual are also supported by pictures showing how to use the scheduling software and how the final submittals should look. The Manual is intended to overcome any problems related to internet connections and students access to the video tutorials.

4. TECHNICAL FINDINGS

4.1. Capturing team presentations using Flip camcorders

By offering the laboratory assignments on-line more lab time was opened to hands-on real-world project based learning and teamwork. Students were assigned in teams mimicking real organizational structure for project management. A team would have 3 to 4 students each of them being assigned a specific role in the team: project manager, estimator, scheduler and superintendent (for the teams of 4 students). Each team was assigned a real project that is being built in Massachusetts. The team has to study and analyze the project documents, drawings and specs and produce a complete schedule for it.

The first phase of the class project was finalized with a team presentation of the work, findings and submittals. The presentations were captured on camera and were available on you-tube for feedback and corrective actions. Two Flip camcorders were used to record the team presentations. One was a Flip MinoHD with a recording capacity of 60 min and the other was a Flip UltraHD with a recoding capacity of 120 min. The focus was on recording the presentations of the teams in the hybrid laboratory (3 teams which presented 15 min/each). Due to the remaining recording capacity the presentations in two other in-class laboratory sections were also recorded.

One of the limitations of using the camcorders was related to their recording capacity and to the large number of presentations taking place in the very same week. The lab sections are scheduled on Tuesday, Wednesday and Thursday. There was no time to download the videos to create space in the cameras in order to capture all presentations. Also the time to recharge a battery for a Flip camera can vary between 2 to 5 hours if a Flip charger is being used or up to 10 hours if charging is done through the computer. Some student teams expressed their disappointment of not being able to receive feedback related to their presentations.

4.2. Bandwidth usage

The video tutorials were made accessible to all the students registered for CCEV 406 and not only to the hybrid laboratory section. The videos were stored on screencast.com and they were made accessible to the students through a link created on Blackboard.

The tutorials were received very well by students. An indicator of student level of comfort with this new educational system is the large number of students that submitted the laboratory assignments well ahead of the required deadline.

Table 2 below shows student access of the video tutorials for the first three laboratories.

Table 2. Bandwidth usage

Laboratory	**# Views**	**Bandwidth usage (GB)**
Lab 1A	201	2,75
Lab 1 B	208	5.16
Lab 1 C	164	2.10
Lab 2 A	246	2.92
Lab 2 B	235	3.93
Lab 2 C	146	1.37
Lab 3 A	148	1.98
Lab 3 B	198	1.20
Lab 3 C	103	2.35

To be noticed that as students got more comfortable with the video tutorials and also with the scheduling software used, their access of the videos (measured by the # of views) started to drop. There were 98 students registered for CCEV 406. It can be noticed that the number of views per video varies between 1.05 to 2.5 views per student. Anecdotal evidence from several students showed that the opportunity to play back and listen again to the laboratory instructions was highly appreciated and welcomed.

An analysis of the bandwidth usage column shows that for each laboratory the range was between 5.53 GB to 10 GB total usage. This created an unexpected problem during the very first week of classes. TechSmith's provides a free video storage web space (screencast.com) of max 2 GB and also a max bandwidth allowance of 2 GB. For the first lab the 2 GB bandwidth was used in 48 hours. The solution was to buy additional bandwidth from TechSmith.

4.3. Using Wacom Cintiq 12WX digitizing tablet

A Cintiq 12WX was rented from DTS in order to grade and provide feedback to the students for some of the (homework) assignments. The usage of the digitizing tablet was quite easy and user-friendly but the installation time for the system took more than 30 min which suggests that renting this system for a limited period of time is not recommended.

The digitizing tablet facilitated the usage of a digital pen for writing comments on student assignments. Students were asked to save their assignment in Adobe/Pdf format and submit it on Blackboard. Once assignments were submitted the instructor opened and saved them her computer and after correcting and grading the assignments was sent back to the student(s) (also on Blackboard). The system worked quite efficiently despite the fact that due to opening of many Adobe files instructor's computer crushed a couple of times.

5. CONCLUSIONS AND RECOMMENDATIONS

The development of an on-line, hybrid or blended course requires a thorough advanced planning and training for the faculty involved in this type of teaching. There is the misconception that an on-line class can follow the traditional class format. Faculty interested in getting involved in developing an on-line class should be aware of the lack of flexibility of this particular type of class and the need to create a thoroughly structured course. It is difficult to improvise for on-line course delivery.

For a high quality well-structured on-line course planning should start two semesters in advance leaving a full semester for producing, editing and improving the on-line lectures/labs. Close co-operation and communication with the instructional designers during the planning, development and further while offering the on-line classes is the key to the success of such a class.

An on-line course should be the result of teamwork. The team members should be the faculty teaching that class and an assigned instructional designer for (that particular) course development. The support and involvement of the instructional designers in planning, development and delivery of on-line courses should go well above and beyond training and (technical) problem solving.

Both the planning and development phases require an extensive technical knowledge and skills which, if required from the faculty, can have either positive or negative effects. The positive effects would be extending faculty knowledge in high tech areas which can result in the reduced involvement of the instructional designer and an increased feeling of self-actualization for the faculty. One negative effect can be the reduced motivation of faculty feeling uncomfortable with high tech tasks. Another negative effect can be faculty losing interest in on-line education due to the altering of teaching tasks and skills and because faculty development initiatives might focus only on on-line technology skills.

Planning for on-line courses goes well beyond faculty involvement. There are many (technical) resources available for free but also at more or less affordable prices. Online education has to be looked at like an investment in the future. It needs a substantial "down payment" in order to bring profit on long term. The electronic resources available or to be used in on-line class development and implementation need more than anything storage space. An assessment should be made in order to decide the dimensions of this space (in GB or TB of course) and what are the financial implications of borrowing, leasing or owing it.

Another technical aspect to be considered when offering on-line classes is the rhythm of (electronic) resource usage. A particularity of these resources is that their usage comes at a price (the same way as electricity, water or gas). Strategies of lowering the usage can be developed. Reaching upstream into training the students not to waste these resources should be seriously considered maybe in combination with including the price of usage in the tuition fee.

Considerations should be made related to offering (technical) support to faculty delivering on-line classes in all locations where engagement in collaborative activities is necessary. The delivery of on-line classes requires both student and faculty access to the internet. Solutions should be considered for individuals with poor or occasional connectivity which limits the access to rich content and the engagement in collaborative activities.

Students can also be reluctant to taking on-line classes. If students are exposed to this particular learning environment without a preliminary preparation their engagement and involvement will be poor or missing totally.

Last but not least more training and faculty development is necessary in order to expand faculty “buy-in” and “stay-in” into the on-line/hybrid/blended educational systems. Teaching on-line requires a different pedagogy than face-to-face instruction and interactivity is very different in the on-line environment

References

1. Academic Support Services, Wentworth Institute of Technology, Office of Academic Affairs, http://wit.edu/academic-affairs/index.html
2. Cosma, C., *Development of on-line video tutorials*, Bistline Research Grant, Final Report, Boston, 2010.

Analytical method for axial– flexural interaction diagram in case of reinforced concrete columns confined with fibre reinforced polymers

Ciprian Cozmanciuc[1], Ruxandra Oltean[2]
[1]*Department of Concrete Structures, Building Materials, Technology and Management, "Gh. Asachi" Technical University, Iasi, Romania*
[2]*Department of Civil and Industrial Engineering, "Gh. Asachi" Technical University, Iasi, Romania*

Summary

Reinforced concrete (RC) columns in buildings framing systems are structural members subjected to combinations of axial compression and bending moment, rather than pure axial loading. This type of action can be induced by several factors, such as vertical misalignments, unbalanced moments at connecting beams, or lateral forces resulting from wind or seismic actions.

Externally application of FRP jackets to RC columns can be used to increase strength and ductility of members, when subjected to inadvertent load eccentricities or combined axial–flexural (N–M) loading.

To design an axial load – bending moment diagram for an unconfined RC column, one needs the geometric properties of the cross – section, the internal reinforcement properties, quantity and placement in section and the concrete strength, this being described in all textbooks on RC design. For an FRP-confined RC column the design of N-M interaction diagram is not a common matter and limited experimental studies have been carried out. Because experimental tests on FRP-strengthened columns are difficult to perform, researches done so far do not comprise detailed interaction curves.

This paper presents a procedure that allows the development of a simplified N-M interaction diagram for FRP-confined RC columns for practical design applications. In the proposed method, the analysis of FRP-wrapped columns is carried out based on principles of equilibrium and strain compatibility equivalent to that of unconfined RC columns, the main difference being given by the use of stress-strain model developed by Lam and Teng for FRP-confined concrete.

KEYWORDS: concrete; fibre reinforced polymers, bond, finite element analysis, strengthening.

1. INTRODUCTION

Confining RC columns with FRP membranes is a frequently used technique, when it is desired to improve the load carrying capacity and/or ductility of such compression members. The necessity of enhanced strength is given especially by higher load capacity demands required by more restraining codes and changes in the structures use. The need of ductility enhancement is given by the energy dissipation reasons, which allows the plastic behaviour of the element and, finally, of the entire structure [1].

There has been a continuously increasing interest in the use of FRP materials over the past decade in the repairing, retrofitting, rebuilding, strengthening and new construction of columns in engineering structures. An important aspect for FRP membranes is that opposed from steel which applies a constant confining pressure after yield, FRP composites have an elastic behaviour up to failure and therefore exerts a (passive) confining action on concrete specimens under axial load [2,3].

Most columns, in practice, are eccentrically loaded, thus their sections are subjected to combined axial compression and bending moments. The FRP confining systems have proven their efficiency not only in case of axially loaded columns but also for eccentrically loaded columns [4, 5].

In literature there can be found several experimental studies analyzing the behaviour of FRP confined concrete cylinders, prisms and columns subjected to eccentric compression or combined axial and bending loads. It can be concluded that the load bearing capacity of the element improves when the number of confinement layers are increased, but is decreasing with the increasing of the eccentricity. The efficiency of the confining system is proportional to the stiffness of the FRP membrane, which controls the dilation of the concrete cross section and leads to a larger axial deformation capacity [6, 7].

The studies carried out so far on the behaviour of FRP strengthened RC columns eccentrically loaded have conducted to theoretical axial – flexural (N-M) interaction diagrams [8-11]. In this paper is presented an analytical method, based on ACI design guide lines, for realising the simplified N-M diagram in case of noncircular cross-section columns following the principles of equilibrium and strain compatibility, being limited to the compression-controlled region of the interaction diagram. An extensive experimental program carried out and some results referring to the performance of eccentrically loaded columns externally strengthened with FRP membranes are presented in the paper. Further on, there are described the N-M interaction diagrams for the tested columns according to the proposed analytical method [12].

2. DESIGN METHOD FOR THE N-M INTERACTION DIAGRAM

The interaction diagram for a RC element section is a graphic representation of all possible combinations between the axial forces (N_u) and the bending moments (M_u) which produces failure, as it can be observed from Figure 1. In order to design the interaction diagram it is necessary to know the dimensions of the cross-section and mechanical properties of the internal steel reinforcement and of the external confinement system [13].

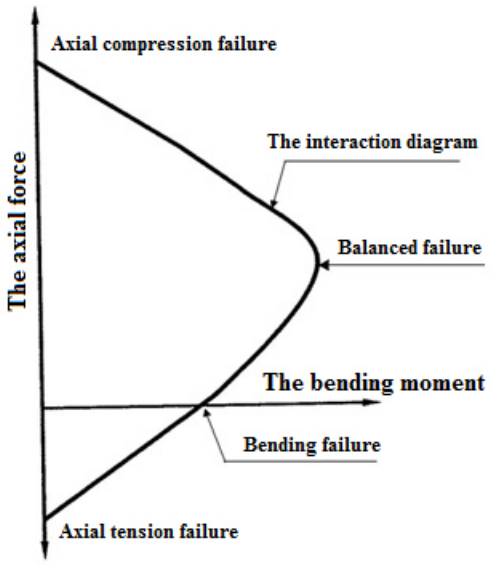

Figure 1. The interaction diagram for a RC element cross-section

The procedure for realising the interaction diagram in case of FRP confined elements is similar to the one for RC columns, except that the stress – strain model for FRP confined concrete is adopted in the compression region. For simplified computation, instead of a continuous curve, the N-M diagram can be obtained as a number of segment lines which are joining the axial force and bending moment values, resulting five characteristic points, as it can be seen in Figure 2.

In the interaction diagram, point A represents the pure compression case (with zero bending moment), while point E represents the pure bending moment case (with zero axial force), where position of the neutral axis is obtained by following the conventional RC beam theory. In case of points B, C and D, the neutral axis position (c) is determined by similar triangles in strain distribution corresponding to each case [10, 12].

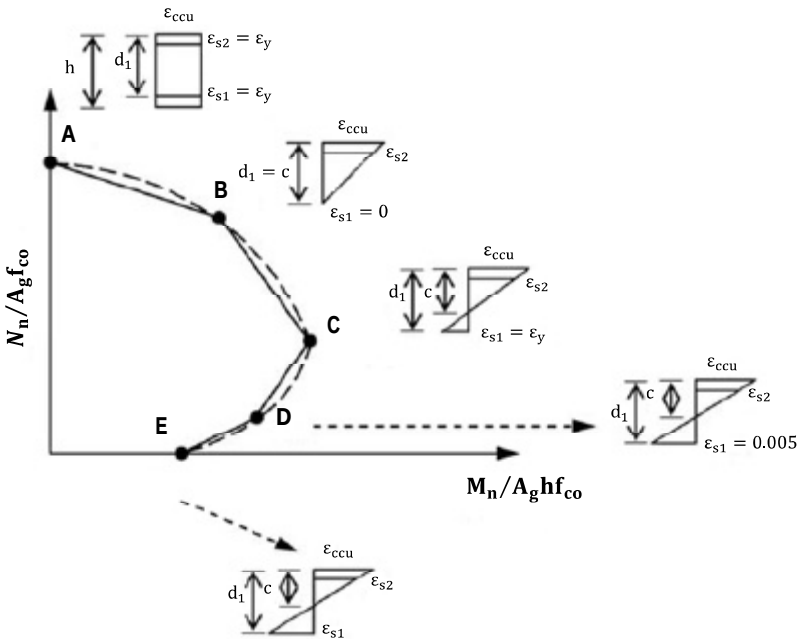

Figure 2. The interaction diagram for elements with circular and noncircular cross-sections

The nominal axial force (N_n) corresponding to point A can be determined by applying the following relation:

$$N_{n(A)} = [0.85 f_{cc} (A_g - A_s) + f_y A_s] \quad (1)$$

Where f_{cc} represents the compressive strength of confined concrete, f_y is the yield strength of longitudinal steel reinforcement, A_g is the total cross-sectional area and A_s is the area of internal steel reinforcement.

The nominal axial force (N_n) and the nominal bending moment (M_n) for points B, C and D are evaluated by integrating the stresses over the noncircular cross-section of concrete, according to the following relations:

$$N_{n(B,C,D)} = \int_0^c (b) f_{co} (y) dy + \sum A_{si} f_{si} \quad (2)$$

$$M_{n(B,C,D)} = \int_0^c (b) \left(\frac{h}{2} - c + y \right) f_{co} (y) dy + \sum A_{si} f_{si} d_{si} \quad (3)$$

Where *b* and *h* are the dimensions of the noncircular cross-section, *c* is the distance from the extreme compression fibre to the neutral axis position of the cross-section, *y* is the variable of integration within the compression zone, d_{si} is the distance from the position of the "*i*th" layer of longitudinal steel reinforcement to the geometric centre of the cross-section, f_{co} is the unconfined concrete compressive strength, f_{si} is the stress in "*i*th" layer of longitudinal steel reinforcement and A_{si} is the cross-sectional area of the "*i*th" layer of longitudinal steel reinforcement.

Starting from ACI 440.2R-08, in order to simplify the applications, Rocca et al. proposed a model which allows the development of a simplified axial – flexural interaction diagram for RC columns confined with FRP membranes [8, 10]. In the proposed model the analysis of FRP confined RC columns starts from the principles of equilibrium and strain compatibility taking into consideration the stress – strain model for FRP-confined concrete proposed by Lam and Teng [14, 15].

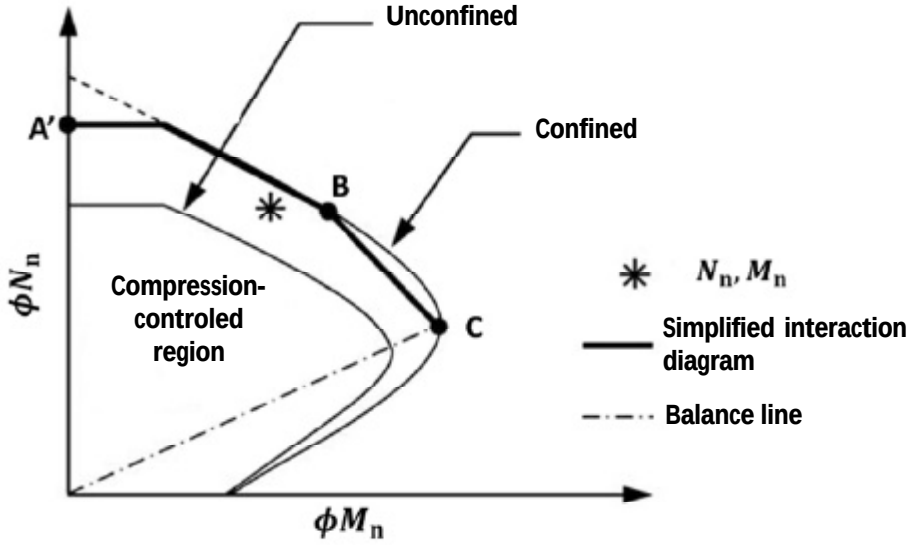

Figure 3. The simplified interaction diagram

The increase in strength can be considered only when the position of the point with the coordinates given by the applied ultimate axial force (N_n) and bending moment (M_n) is above the line connecting the origin and the balanced points of the interaction diagram for the unconfined member, or in the so called compression-controlled region. This limitation is given by the fact that strength enhancement can be significant for the elements only in case of a compression failure.

To simplify the design methodology, the interaction diagram can be reduced to two bilinear curves passing through the points A, B and C, for covering the compression-controlled failure region, as it is presented in Figure 3.

The coordinates of point A can be determined by applying equation (1), resulting the nominal axial force (N_n), while the nominal bending moment (M_n) is zero. For points B and C are applied the equation (2) and (3). By taking into consideration that elements have a rectangular cross-section, substituting Lam and Teng's stress-strain relationship in equation (3) and expressing the axial compressive strain at any point in the compression region in terms of the integrating variable *y* according to similar triangles principle, equation (2) and (3) will become as it follows:

$$N_{n(B,C)} = \int_0^{y_t}\left[E_c\left(\frac{e_{ccu}}{c}y\right) - \frac{(E_c - E_2)^2}{4f_{co}}\left(\frac{e_{ccu}}{c}y\right)^2\right]bdy + \int_{y_t}^{c}\left[f_{co} + E_2\left(\frac{e_{ccu}}{c}y\right)\right]bdy + \sum A_{si}\, f_{si} \tag{4}$$

$$M_{n(B,C)} = \int_0^{y_t}\left[E_c\left(\frac{e_{ccu}}{c}y\right) - \frac{(E_c - E_2)^2}{4f_{co}}\left(\frac{e_{ccu}}{c}y\right)^2\right]b\left(\frac{h}{2} - c + y\right)dy + \int_{y_t}^{c}\left[f_{co} + E_2\left(\frac{e_{ccu}}{c}y\right)\right]b\left(\frac{h}{2} - c + y\right)dy + \sum A_{si}\, f_{si} d_{si} \tag{5}$$

Where y_t represents the vertical coordinate within the compression region measured from the neutral axis and it corresponds to the transition strain ($e_t^{'}$); E_c is the initial modulus of elasticity of concrete; E_2 is the slope of linear portion of stress-strain curve for the confined concrete and e_{ccu} is the ultimate axial compressive strain of confined concrete. With the following equation there can be determined *c* and y_t.

$$c = \begin{cases} d & \text{for point B} \\ d\dfrac{e_{ccu}}{e_{sy} + e_{ccu}} & \text{for point C} \end{cases} \tag{6}$$

$$y_t = c\frac{e_t^{'}}{e_{ccu}} \tag{7}$$

By integrating, equations (4) and (5) can be expressed as in equations (8) and (9), where the coefficients A, B, C, D, E, F, G, H and I are determined with relations (10).

$$N_{n(B,C)} = [A(y_t)^3 + B(y_t)^2 + C(y_t) + D] + \sum A_{si}\, f_{si} \tag{8}$$

$$M_{n(B,C)} = [E(y_t)^4 + F(y_t)^3 + G(y_t)^2 + H(y_t) + I] + \sum A_{si}\, f_{si} d_{si} \tag{9}$$

$$A = \frac{-b(E_c - E_2)^2}{12 f_c}\left(\frac{e_{ccu}}{c}\right)^2 \tag{10a}$$

$$B = \frac{b(E_c - E_2)}{12}\left(\frac{e_{ccu}}{c}\right) \tag{10b}$$

$$C = -bf_c \tag{10c}$$

$$D = bcf_c + \frac{bcE_2}{2}(e_{ccu}) \tag{10d}$$

$$E = \frac{-b(E_c - E_2)^2}{16 f_c}\left(\frac{e_{ccu}}{c}\right)^2 \tag{10e}$$

$$F = b\left(c - \frac{h}{2}\right)\frac{(E_c - E_2)^2}{12 f_c}\left(\frac{e_{ccu}}{c}\right)^2 + \frac{b(E_c - E_2)}{3}\left(\frac{e_{ccu}}{c}\right) \tag{10f}$$

$$G = -\left(\frac{b}{2} f_c + b\left(c - \frac{h}{2}\right)\frac{(E_c - E_2)}{2}\left(\frac{e_{ccu}}{c}\right)\right) \tag{10g}$$

$$H = bf_c\left(c - \frac{h}{2}\right) \tag{10h}$$

$$I = \frac{bc^2}{h} f_c - bcf_c\left(c - \frac{h}{2}\right) + \frac{bc^2 E_2}{3} e_{ccu} - \frac{bcE_2}{2}\left(c - \frac{h}{2}\right) e_{ccu} \tag{10i}$$

To prevent the possible accidental eccentricity, in the ACI design procedure, the nominal axial load capacity in case of RC columns with transverse reinforcement subjected to pure compression, represented by point A on the interaction diagram, is reduced with 20%. In Figure 3 this point is denoted as A' and equation (1) will become as it follows:

$$N_{n(A')} = 0.8[0.85 f_{cc}\,(A_g - A_s) + f_y\, A_s] \tag{1}$$

3. DESIGN OF THE N-M INTERACTION DIAGRAM BASED ON EXPERIMENTAL TESTS

At the Faculty of Civil Engineering and Building Services of Iasi there was carried out an experimental program which studied the behavior of CFRP confined RC rectangular columns under eccentric compression loads [6, 12]. All columns were designed alike, with the height of 1000 mm and with an identical distribution of the internal reinforcement. The longitudinal steel reinforcement consisted of four deformed rebars 12 mm diameter. For transversal reinforcement, were provided steel stirrups of 6 mm diameter plain bars spaced at 200 mm in the middle region of the specimen and at 84 mm to the ends of the column.

The specimens were grouped in two series of three identical columns: a first group having the side of the cross-section of 250 mm, noted C2, and the second group with the cross-sectional dimension of 300 mm, noted C3. In each group, one specimen was unconfined and the other two specimens were confined with one, respectively two, layers of CFRP. All specimens were tested under eccentric compression, for the first group of columns the eccentricity was of 50 mm, while for the second group the eccentricity was of 75 mm.

A summary of column specimens' configuration and the resulted experimental maximum load are given in Table 1.

Table 1. Configuration of column specimens and the experimental maximum load

Group (cross-section) (mm)	Specimen	Confinement condition	Load eccentricity (mm)	Maximum Load (mm)
C2 (250 x 250)	C2-0	No wrapping	50	1391.1
	C2-1	1 layer CFRP	50	2133.8
	C2-2	2 layers CFRP	50	2004.9
C3 (300 x 300)	C3-0	No wrapping	75	2121.1
	C3-1	1 layer CFRP	75	2295.5
	C3-2	2 layers CFRP	75	2480.7

The comparative graphic for N-M interaction diagrams, based on the model proposed by ACI 440.2R-08 and discussed in this paper, for group C2 of columns is presented in Figure 4. In Figure 5 are represented the comparative N-M interaction diagrams graphic for group C3 of columns which had been tested during the experimental program.

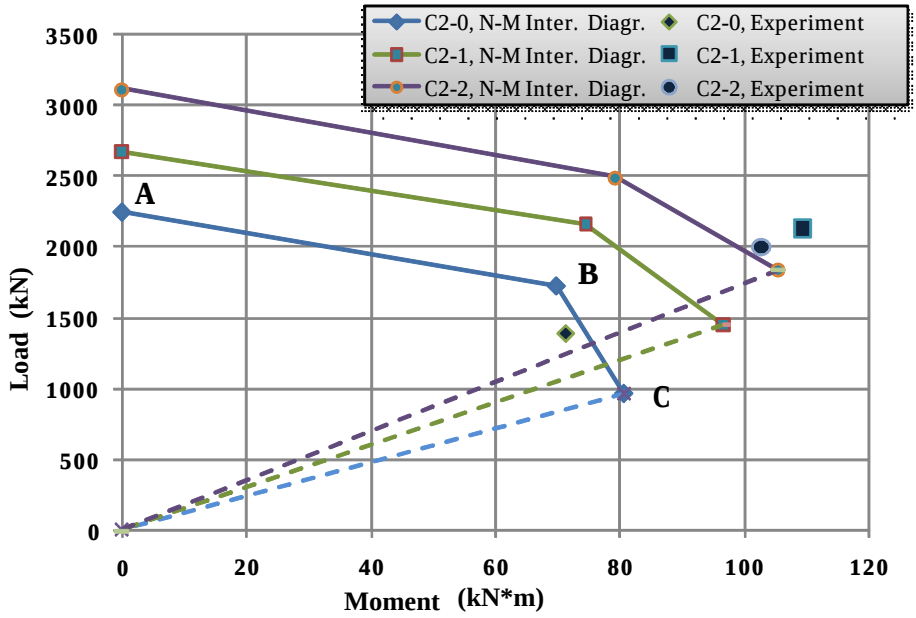

Figure 4. The N-M interaction diagrams for group C2 of columns

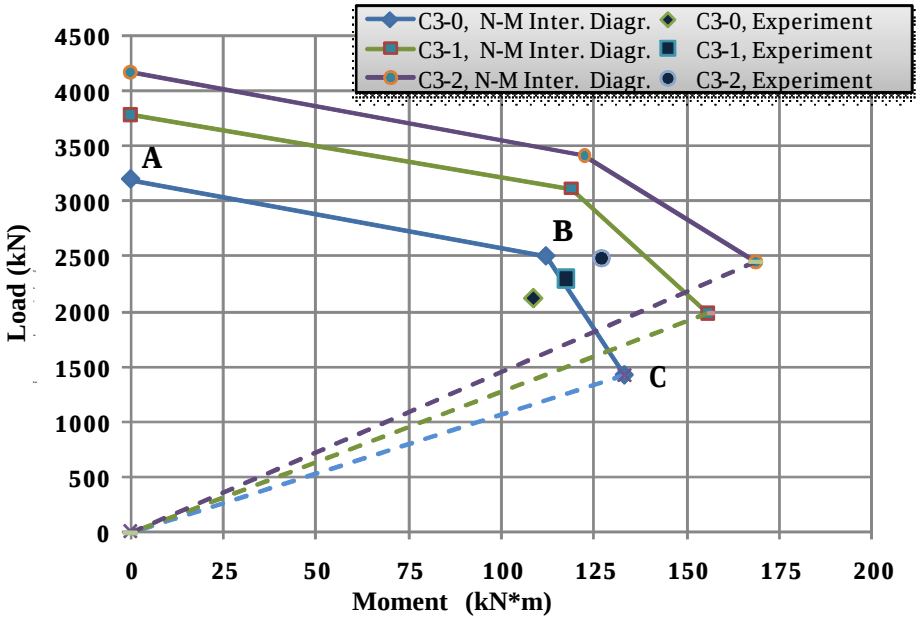

Figure 5. The N-M interaction diagrams for group C3 of columns

4. CONCLUSIONS

The proposed design approach for FRP-confined RC columns subjected to combined axial force and bending moment is responding to the need of a rational and simple method, by respecting the ACI requirements.

The design of the interaction diagram starts from principles of equilibrium and strain compatibility, equivalent to that of conventional RC columns but taking into consideration the Lam and Teng's stress strain model for FRP-wrapped concrete. For the compression-controlled region the N-M diagram is simplified to a series of straight segments which are joining only the characteristic points.

According to the experimental results the strength of rectangular FRP-confined RC columns under eccentric axial loads is improved as compared with identical unconfined columns.

In buildings many columns are subjected to eccentric loads and are influenced by slenderness effect. From this reasons it is important for design guidelines to establish slenderness limits and to outline procedures to deal with these loading types for RC columns strengthened with FRP materials.

References

1. Rocca, S., Experimental and analytical evaluation of FRP-confined large size reinforced concrete columns, Disertation, University of Missouri-Rolla, 2007.
2. Cozmanciuc, C., Oltean, R., Taranu, N., Analytical models for confinement systems of reinforced concrete columns with circular and noncircular cross sections utilizing composite materials, *Proceedings of the 8th Intenational Symposium Computational Civil Engineering 2010, „New Computational Concepts in Civil Engineering"*, Iasi, Romania, 2010.
3. Cozmanciuc, C., Oltean, R., Munteanu, V., Strengthening Techniques of RC Columns using Fibre Reinforced Polymeric Materials, *Buletinul IPI*, Tomul LV (LIX), Fasc. 3, 2009.
4. Teng, J.G., Chen, J.F., Smith, S.T., Lam, L., *FRP-strengthened RC Structures*, John Wiley & Sons, Ltd, England, 2002.
5. Cozmanciuc, C., Comportarea stâlpilor din beton armat confinati cu membrane compozite solicitati la compresiune excentrica, *Creatii Universitare, Al IV-lea Simpozion National*, Iasi, 2011. (in Romanian)
6. Cozmanciuc, C., Oprisan, G., Taranu, N., Munteanu, V., Oltean, R., Budescu, M., Structural behaviour of eccentrically loaded reinforced concrete columns confined with carbon fibre reinforced membranes, *The 11th International Scientific Conference VSU'*, Sofia, Bulgaria, 2011.
7. Quiertant, M., Clement, J.L., Behavior of RC columns strengthened with different CFRP systems under eccentric loading, *Construction and Building Materials*, 2011.
8. ACI Committee 440 Report, Guide for the Design and Construction of Externally Bonded FRP Systems for Strengthening Concrete Structures, *ACI Committee 440, Technical Committee Document 440.2R-08*, 2008.
9. El-Fattah, A., Rasheed, H., Esmaeily, A., A New Eccentricity-Based Simulation to Generate Ultimate Confined Interaction Diagrams for Circular Concrete Columns, *Journal of the Franklin Institute*, 2009.
10. Rocca, S., Galati, N., Nanni, A., Interaction diagram methodology for design of FRP-confined reinforced concrete columns, *Construction and Building Materials*, vol. 23, 2009.

11. Bisby, L., Ranger, M., Axial-flexural interaction in circular FRP-confined reinforced concrete columns, *Construction and Building Materials*, 24, 2010.
12. Cozmanciuc, C., *Consolidarea Stâlpilor din Beton Armat cu Sectiune Necirculara prin Confinare cu Materiale Compozite*, Editura Politehnium, Iasi, România, 2011.
13. Ghoneim, M., El-Mihilmy, M., *Design of Reinforced Concrete Structures, Second Edition, Volume 2*, 2008.
14. Lam, L., Teng, J.G., Design-oriented Stress-Strain Model for FRP-confined Concrete in Rectangular Columns, *Journal of Reinforced Plastics and Composites*, Vol. 22, No. 13, 2003.
15. Lam, L., Teng, J.G., Design-oriented Stress-strain Models for FRP-confined Concrete, *Construction and Building Materials*, 17, 2003.

Finite element analysis of square reinforced concrete columns confined with composite membranes subjected to eccentric compression

Ciprian Cozmanciuc[1], Ruxandra Oltean[2]
[1]*Department of Concrete Structures, Building Materials, Technology and Management, "Gh. Asachi" Technical University, Iasi, 700050, Romania*
[2]*Department of Civil and Industrial Engineering, "Gh. Asachi" Technical University, Iasi, 700050, Romania*

Summary

Finite element method (FEM) is an accurate numerical technique utilized in simulating the structural response of a genuine application and is found to be an efficient method for studying a wide range of engineering and research problems.

Strengthening of reinforced concrete (RC) elements and structures with externally bonded fiber reinforced polymers (FRP) is becoming increasingly popular and widespread technique in civil engineering community.

Over the past three decades numerous studies have been developed in order to analyze the confining effect on concentrically loaded RC columns. In this matter, utilizing FEM satisfactory results were obtained, when analyzing the effect given by thickness of composite membranes, increase of load bearing capacity and ductility of the elements which resulted in a large energy absorption capacity.

Studies on eccentrically loaded FRP confined concrete columns are relatively new and limited in number making clear the need of investigating the behavior of columns under eccentric loads. However, the FEM analysis indicates a good behavior of RC columns subjected to eccentric loads when they are strengthened with externally bonded FRP materials. To evaluate the behavior of RC elements wrapped with carbon fiber polymeric (CFRP) sheets and to predict the behavior of such strengthened columns, a finite element analysis was performed using Ansys package software. There were modeled one meter height square concrete columns, with longitudinal and transversal internal steel reinforcement. The eccentricity of the compressive load was of 50 mm and it was applied at both ends. In this paper are presented the simulated results using the finite element analysis in case of RC column before and after confining it with one layer of CFRP.

KEYWORDS: fiber reinforced polymers, reinforced concrete columns; finite element analysis, confinement.

1. INTRODUCTION

In recent years the behavior of small concrete elements confined with composite materials was analyzed through FEM in several studies [1-9]. Also, few studies evaluated the influence of internal, longitudinal and transversal, reinforcement in concrete columns strengthened with CFRP membranes [10-13].

The behavior of columns with rectangular cross-section confined with CFRP materials was studied, by applying the FEM, by Parvin and Schroeder [14]. Their purpose was to check the effect given by the thickness of the confining system and the increase in load bearing capacity and ductility when subjected to axial compression. They realized a stress distribution over the element cross-section and concluded that by increasing the layers of composite membrane the confining system will be more efficient.

In the studies developed by Taranu et al. [15-17], a FEM was realized using LUSAS software to investigate the behavior of axial compressed noncircular RC columns confined with CFRP materials. They observed that the confined concrete and the unconfined one have a similar behavior until the compressive strength of unconfined concrete is reached. This is because the confining system has a passive behavior and it becomes active when concrete has a high level of lateral deformations. The wrapping layers are producing an increase of stresses and strains.

As far as the literature on eccentric compressed RC columns confined with FRP materials is concerned, there are many fewer studies. Parvin si Wang (2001) [4] studied using non-linear FEM the behavior of RC square section columns confined with FRP composites and subjected to eccentric loads. The column was modeled in MARC software program (*MARC Users Guide* 1994). When meshing the specimen 240 tri-dimensional solid elements (bricks) for the concrete column and 168 membrane elements (shell) for the composite strip were used. Between the composite system and the concrete member perfect bonding was defined, even if at the interface separation between materials was possible. They have concluded that in case of centric compression, the effective concrete area, influenced by the confinement system is situated in the central zone and in the corners, while for eccentric compressed columns the confining system influence is increased mostly in the compressed area of the element.

The behavior of elliptical columns confined with FRP membranes subjected to axial loads was analyzed in a study conducted by Parvin and Schroeder [18]. The finite element analysis was performed using MSC Marc 2005 software program and the results obtained by FEM were compared with the experimental model developed by Teng and Lam (2002). Thus, they noticed that increasing the bending moment leads to an increase in normal and circumferential deformations on the opposite side of the eccentric load.

2. FINITE ELEMENT MODELING

In order to analyze through FEM the behavior of concrete columns strengthened with composite membranes, in ANSYS v'12 software were defined two identical RC columns, one unconfined and the second one confined with CFRP materials. The geometrical and mechanical characteristics of columns were alike with the experimental program that was carried out at the Faculty of Civil Engineering and Building Services of Iasi, Romania [19, 20].

From geometrical point of view, the columns were 1000 mm in height with a rectangular cross-section (250 x 250 mm), corner radius of 35mm and an identical distribution of the internal reinforcement. The longitudinal steel reinforcement was made of four deformed rebars of 12 mm diameter, whereas the transversal reinforcement consists of steel stirrups of 6 mm diameter plain bars spaced at 200 mm in the middle region of the specimen and at 84 mm to the ends of the column. The concrete cover up to the surface of the longitudinal steel bars was 25 mm. Since in the experimental program there were fixed six linear variable differential transducers (LVDTs) at the mid-height of the specimen, the obtained results were expressed for that region of the columns. To compare the experimental results with the FEM ones, the model was divided into three slices. For eccentric loading application special steel plates were designed and positioned on both ends of the columns (Figure 1), the load eccentricity being of 50 mm. The mechanical characteristics of concrete, internal reinforcement and CFRP membrane are given in Table 1. Nevertheless, for the concrete it was adopted the simplified bilinear stress –strain curve (Figure 2).

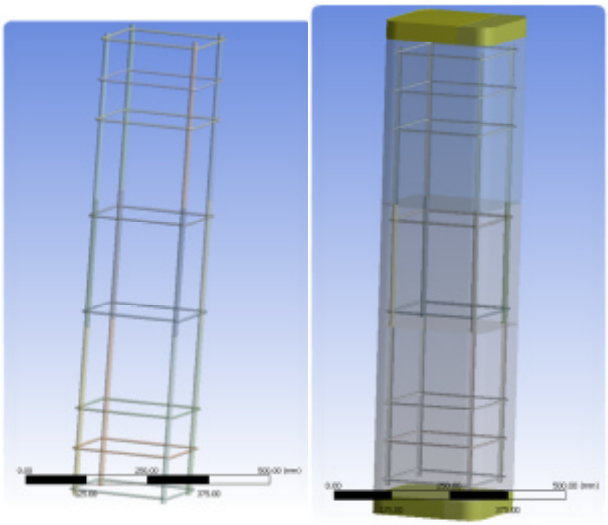

Figure 1. Column geometry defined with ANSYS software

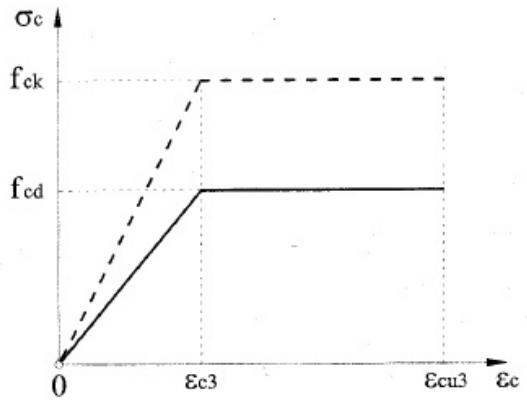

Figure 2. Simplified stress – strain curve for concrete

Table 1. Mechanical characteristics of materials defined in the model

	Unit of measure	Concrete	Longitudinal reinforcing bars	Transversal reinforcing bars	CFRP
Density	kg/m^3	2,300	7,850	7,850	-
Compressive strength	N/mm^2	32.34	-	-	750
Tensile strength	N/mm^2	3.05	355	255	800
Young modulus	N/mm^2	32,800	200,000	200,000	70,000
Poisson's ratio	-	0.2	-	-	0.25

The unconfined column was meshed using 248.043 nodes and 142.289 elements (Figure 3), while the confined column was meshed using 240.769 nodes and 134.468 elements. The eccentric loading of the elements was realized by assigning a linear uniformly distributed load at both ends of the column (Figure 4), equal with the maximum load obtained during the experimental tests. For the unconfined column the maximum experimental load was 5565 (N/mm), while for the confined column was 8467.5 (N/mm).

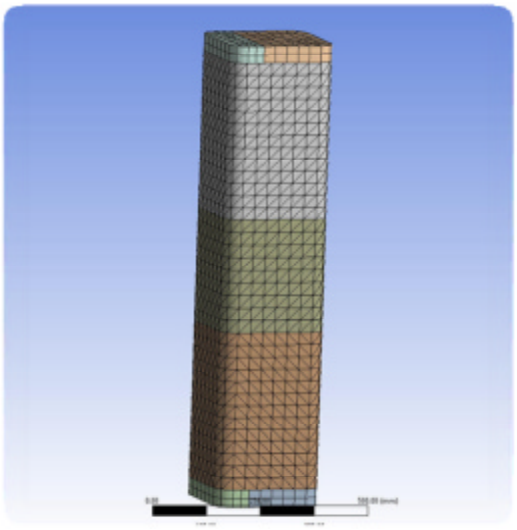

Figure 3. FE mesh

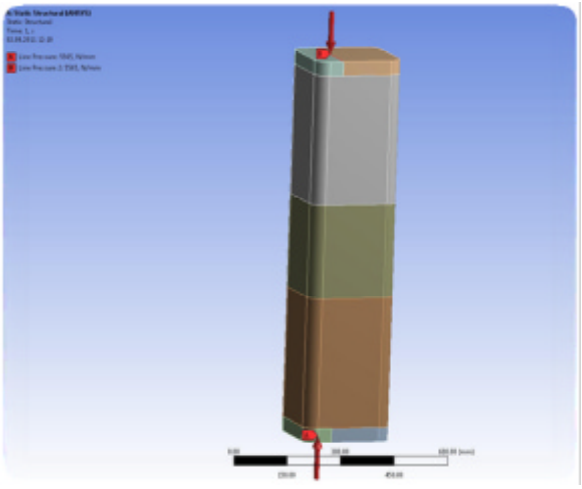

Figure 4. The eccentric loading of the elements

3. RESULTS AND DISCUSIONS

After simulating the behavior of an unconfined and a CFRP confined RC column subjected to eccentric compression, a set of results were obtained and presented in this paper. After the FE analysis, in Figure 5 and Figure 6 are presented the

longitudinal and transversal displacements registered at the mid-height slice of the element, for the unconfined and the CFRP confined RC column. It can be stated that by applying the externally bonded confinement system the displacement for the RC columns increases.

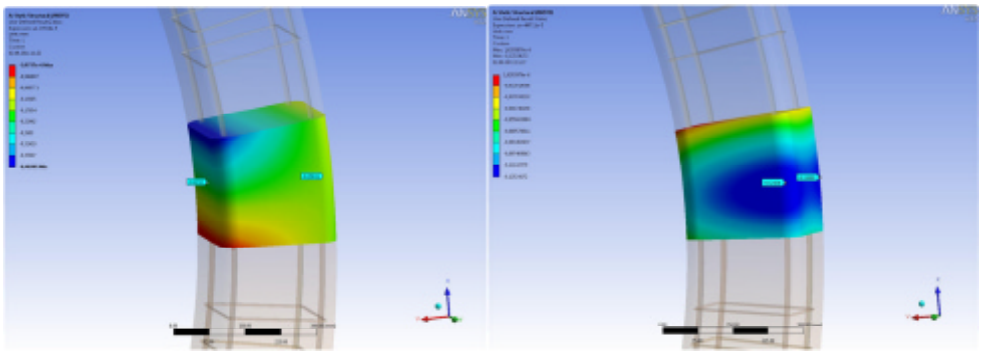

Figure 5. The longitudinal and transversal displacements for the unconfined element

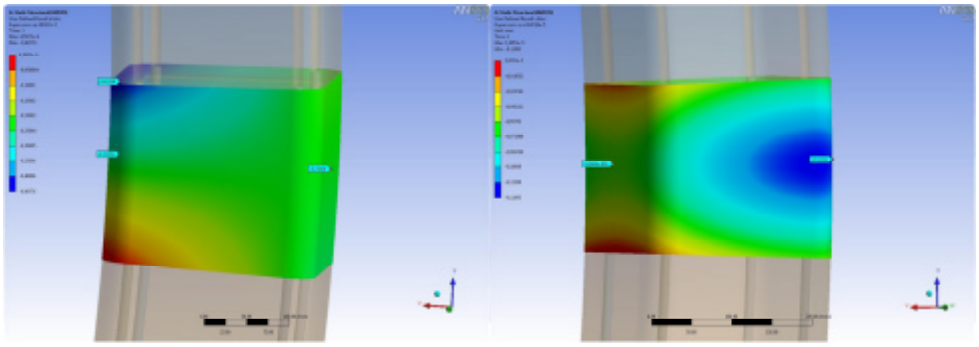

Figure 6. The longitudinal and transversal displacements for the CFRP confined element

In Figure 7 and Figure 8 are presented the axial stresses in a transversal cross-section, at the mid-height of the element, for the unconfined and the CFRP confined RC column. The FEM results are similar to the experimental ones. In the experimental program, the failure of the unconfined columns occurred in the compressed side due to concrete crushing. In the tensioned side, cracks developed in the transverse direction of the member, while in the compressed region it was observed the buckling of the longitudinal steel reinforcing bars. The externally strengthened columns failed by rupture of the CFRP jacket due to hoop tension and an important degree of concrete crushing was noticed, as well as, the buckled longitudinal steel bars. The CFRP jacket failure was initiated at a corner of the column at the most compressed side and occurred later on the tensile side [19]. It can be observed from Figure 7 and Figure 8 that the highest stress concentration is

at the compressed side of the elements and that by wrapping the RC column with one layer of CFRP membrane the elements can resist at higher loads and stresses.

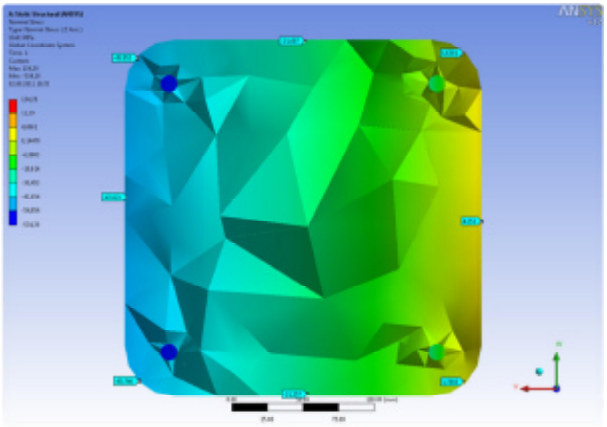

Figure 7. Axial stresses at the mid-height of the unconfined element, in the transversal cross-section

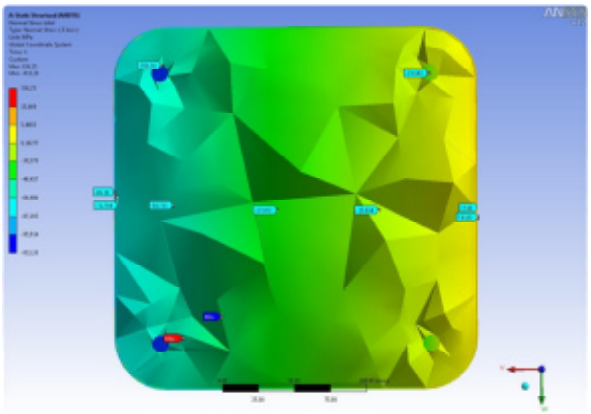

Figure 8. Axial stresses at the mid-height of the CFRP confined element, in the transversal cross-section

In Figure 9 are shown the comparative stresses for experimental and FEM for the unwrapped and wrapped RC columns with CFRP membranes.

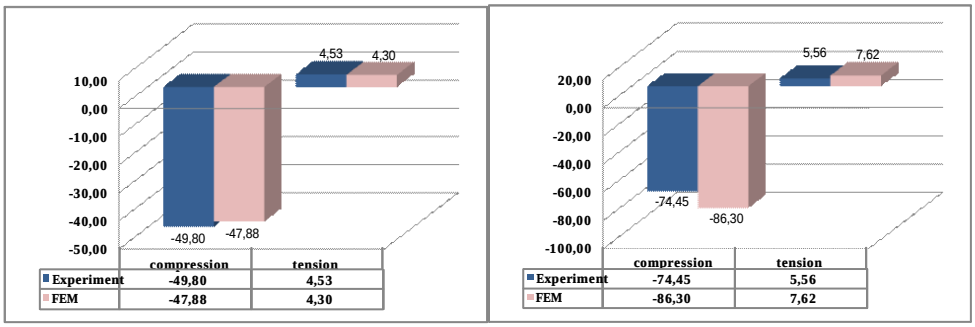

Figure 9. Axial stresses for the unconfined (left) and confined (right) RC columns

4. CONCLUSIONS

With FE analysis it is possible to model different elements with complex geometry, having various loading schemes and boundary, making it a very good alternative to the experimental programs and analytical approaches.

The evaluation of the structural response of rectangular RC columns confined with FRP composite membranes using FEM lead to satisfactory results, managing to describe in a satisfactory manner the confining effect of concrete using FRP systems. The simulations were performed using ANSYS v12 Workbench, finite element modeling program, in which the geometry configuration of the model closely approached to the experimental model, as well as the materials characteristics.

The confined column failed at a higher load level than the unconfined one. In case of elements subjected cu eccentric compression, by applying externally bonded CFRP membrane, the displacement and the stress level increased.

References

1. Rochette, P., Labossiere, P., A plasticity approach for concrete columns confined with composite materials, *Advanced Composite Materials in Bridges and Structures*, 1996.
2. Liu, J., Foster, S.J., Finite – Element Model for Confined Concrete Columns, *Journal of Structural Engineering*, Sept., 1998.
3. Mirmiran, A., Zagers, K., Yuan, W., Nonlinear finite element modeling of concrete confined by fiber composites, *Finite Elements in Analysis and Design*, 35, 2000.
4. Parvin, A., Wang, W., Behavior of FRP jacketed concrete columns under eccentric loading, *J. Compos. Constr*., 5(3), 2001.

5. Montoya, E., Vecchio, F.J., Sheikh, S.A., Numerical evaluation of the behaviour of steel- and FRP-confined concrete columns using compression field modelling, *Engineering Structures*, 26, 2004.
6. Karam, G., Tabbara, M., Confinement effectiveness in rectangular concrete columns with fiber reinforced polymer wraps, *J. Compos. Constr*., 9(5), 2005.
7. Chen, J.F., Pan, W.K., Three dimensional stress distribution in FRP-to-concrete bond test specimens, *Construction and Building Materials*, 20, 2007.
8. Banu, C., Taranu, N., Oltean, R., Cozmanciuc, C.I., Ionita, O.M, Finite Element Analysis of RC beams Reinforced with Fiber Reinforced Polymers Bars, *Proceedings of 7th International Symposium „Computational Civil Engineering 2009"*.
9. Koksal, H.O., Doran, B., Turgay, T., A practical approach for modelling FRP wrapped concrete columns, *Construction and Building Materials*, 23, 2009.
10. Nemecek, J., Padevet, P., Patzak, B., Bittnar, Z., Effect of transversal reinforcement in normal and high strength concrete columns, *Materials and Structures*, 38, Aug.-Sept., 2005.
11. Karabinis, A.I., Rousakis, T.C., Manolitsi, G.E., Three-Dimensional Finite Element Analysis of Reinforced Concrete Columns Strengthened by Fiber Reinforced Polymer Sheets, *FRPRCS-8*, University of Patras, Patras, Grecce, July 16-18, 2007.
12. Karabinis, A.I., Rousakis, T.C., Manolitsi, G.E., 3D Finite – Element Analysis of Substandard RC Columns Strengthened by Fiber – Reinforced Polymer Sheets, *Journal of Composites for Construction*, ASCE, Sept./Oct., 2008.
13. Majewski, T., Bobinski, J., Tejchman, J., FE analysis of failure behaviour of reinforced concrete columns under eccentric compression, *Eng. Str*., 30, 2008.
14. Parvin, A., Schroeder, J.M., FRP-confined rectangular concrete columns, *FRPRCS-8*, University of Patras, Patras, Grecce, July 16-18, 2007.
15. Taranu, N., Munteanu, V., Oprisan, G., Budescu, M., Performance of FRP confined square RC columns, *FRPRCS-9*, Sydney, Australia, 2009.
16. Oprisan, G., Taranu, N., Munteanu, V., Experimental and numerical analysis of compressed concrete elements confined with FRP composites, *Computational Civil Engineering - International Symposium Iasi*, 2007.
17. Oprisan, G., Munteanu, V., Cozmanciuc, C., Taranu, N., Entuc, I., Particularities of structural response of confined RC columns with composite membranes, *Proc. of the International Scientific Conference VSU*, Sofia, 2009.
18. Parvin, A., Schroeder, J.M., Investigation of Eccentrically Loaded CFRP-Confined Elliptical Concrete Columns, *J. of Comp. for Constr*., ASCE, 2008.
19. Cozmanciuc, C., Oprisan, G., Taranu, N., Munteanu, V., Oltean, R., Budescu, M., Structural behaviour of eccentrically loaded reinforced concrete columns confined with carbon fibre reinforced membranes, *The 11th International Scientific Conference VSU'*, Sofia, Bulgaria, 2011.
20. Cozmanciuc, C., *Consolidarea Stâlpilor din Beton Armat cu Sectiune Necirculara prin Confinare cu Materiale Compozite*, Editura Politehnium, Iasi, România, 2011 (in Romanian).

Nonlinear analysis in finite element program Abaqus

Gabriela Dascalu
Department of Concrete Structures, Building Materials, Technology and Management, "Gh. Asachi" Technical University of Iasi, Faculty of Civil Engineering and Building Services, Iasi,700050, Romania,

Summary

Nonlinear analysis is a research activity which assumes to establish the inelastic behavior of two principal components (steel and concrete) from which reinforced concrete is made and consider it in performing the numerical simulations and analytical calculations. The principal aim of this activity is to understand the real elastic-plastic response of structural assemblies in order to ensure the comfort and safety request and imposed by norms and standards through the design process. Presently, in construction domain, exists many programs for analysis, using the "finite element" concept, which facilitates the work of researches and design engineers and the obtained results are closed, or even identical, with those from reality. The present paper aims to describe such type of program, called Abaqus/CAE and to present results obtained on physical models based on reinforced concrete elements with voids.

Keywords: reinforced concrete, structural response, numerical simulation, stress states

1. INTRODUCTION

The structural analysis of an assembly has as first objective to establish the distribution either of stresses, either of strain and displacement which are developed inside of all structure or only in certain type of component elements. [4]

In order to make resistance calculation, according with existing norms and standard, it is necessary, in a first step, to model the geometry of analyzed structure, and also to model the constitutive materials behavior.

It is known that the reinforced concrete is a composite material, having 2 principal components (concrete and steel), each with higher properties to different type of loads. Thus, the concrete presents a higher resistance to compression and a small one to tension, while the steel has the capability to take the strong forces due to

ISSN 2285-2735, Pages 143 - 149

tension efforts. To model the behavior of this material, it is absolute necessary to model separately his 2 components, so that to be respected the condition imposed through norms, according which the models created to be conformed to reality and to the problems analyzed.

Modeling the constitutive materials behavior is a process through which is schematic by characteristics curves using some simple deformed models. At the end of this processes result 3 principal categories of materials: with linear behavior, with plastic behavior and with nonlinear behavior.

The final objective of numerical simulations is to obtain the necessary information which can be used in order to determine the sectional efforts developed inside the structural elements. These simulations are often made with programs special designed, based on theoretical aspects, this use being justify by the advantages obtained: the possibility to create models with different shape and dimensions, possibility to modify the type and/or value of loads applied so that can be performed analysis in a short time and reduce work and also with economical efforts relatively low than in experiments and the conclusions and results in both situations being closely.

At international level, exist a variety of such programs, from which are mentioned few like: DIANA, ANSYS, ABAQUS/CAE, ROBOT, SAP etc.

2. GENERAL DESCRIPTION OF NONLINEAR MODELS

Abaqus/CAE software provides the capability of simulating the damage using either of the two crack models for reinforced concrete elements: (1) Smeared crack concrete model and (2) Concrete damaged plasticity model. [5]

In Abaqus/CAE software, reinforcement in concrete structures is typically provided by means of rebars, which are one-dimensional rods that can be defined singly or embedded in oriented surfaces and used with metal plasticity models to describe the behavior of the rebar material and are superposed on a mesh of standard element types used to model the concrete. With this modeling approach, the concrete behavior is considered independently of the rebar. Effects associated with the rebar-concrete interface, such as bond slip and dowel action, are modeled approximately by introducing some “tension stiffening” into the concrete modeling to simulate load transfer across cracks through the rebar.

2.1 Model CSC – Concrete smeared cracking

The “concrete smeared cracking” model (CSC) is intended for modeling and analysis of all types of reinforced concrete structures, including beams, trusses,

shells, solids etc. and it was created for applications that are subjected to monotonic straining at low confining pressures. Uses oriented damaged elasticity concepts (smeared cracking) to describe the reversible part of the material's response after cracking failure. [5]

A particularity of this model is that assumes the cracking to be the most important aspect of the behavior, and because of this reason the representation of cracking and postcracking behavior dominates the modeling. Cracking is assumed to occur when the stress reaches a failure surface so called the “crack detection surface”, which represent a linear relationship between the equivalent pressure stress, p, and the Mises equivalent deviatoric stress, q. [5]

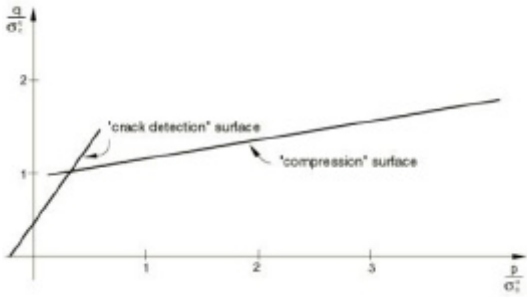

Figuge 1 – Failure surface in (p-q) plane [5]

Cracks are irrecoverable: they remain for the rest of the calculation, but may be open and close. No more than three cracks can occur at any point (two in a plane stress case, one in a uniaxial stress case). Following crack detection, the crack affects the calculations because a damaged elasticity model is used. The concrete model is a smeared crack model in the sense that it does not track individual “macro” cracks. Constitutive calculations are performed independently at each integration point of the finite element model. The presence of cracks enters into these calculations by the way in which the cracks affect the stress and material stiffness associated with the integration point. [5]

The postfailure behavior for direct straining across cracks is modeled with tension stiffening, which allows defining the strain-softening behavior for cracked concrete. This behavior also allows for the effects of the reinforcement interaction with concrete to be simulated in a simple manner. Tension stiffening is required in the concrete smeared cracking model and it can be specified by means of: [5]

- a postfailure stress-strain relation (fig. 2a) – a specification of strain softening behavior in reinforced concrete generally means specifying the postfailure stress as a function of strain across the crack. In cases with little or no reinforcement this specification often introduces mesh sensitivity in the analysis results in the sense that the finite element predictions do not converge

to a unique solution as the mesh is refined because mesh refinement leads to narrower crack bands. This problem typically occurs if only a few discrete cracks form in the structure, and mesh refinement does not result in formation of additional cracks. If cracks are evenly distributed (either due to the effect of rebar or due to the presence of stabilizing elastic material, as in the case of plate bending), mesh sensitivity is less of a concern.

- a fracture energy cracking criterion (fig. 2b) – Hillerborg (1976) defines the energy required to open a unit area of crack as a material parameter, using brittle fracture concepts. With this approach the concrete's brittle behavior is characterized by a stress-*displacement* response rather than a stress-*strain* response. Under tension a concrete specimen will crack across some section. After it has been pulled apart sufficiently for most of the stress to be removed (so that the elastic strain is small), its length will be determined primarily by the opening at the crack.

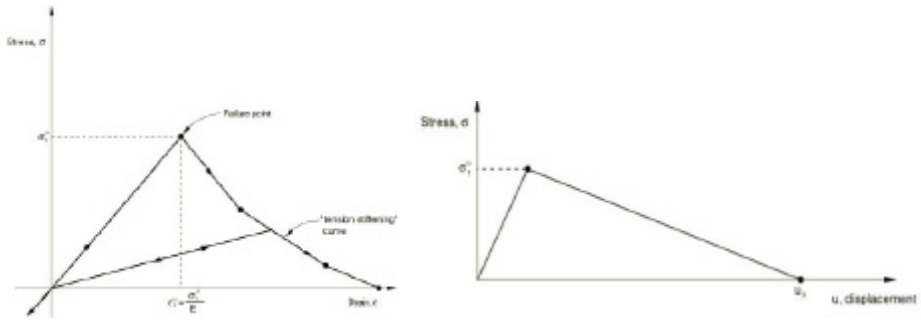

a) b)

Figure 2 – Tension stiffening: a)stress-strain relation;
b)fracture energy cracking criterion [3]

2.2 Model CDP – Concrete damage plasticity

The “concrete damage plasticity” model (CDP) it was design for modeling all types of structures from reinforced concrete and other quasi-brittle materials, which are subjected to monotonic, cyclic, and/or dynamic loading under low confining pressures. Uses concepts of isotropic damaged elasticity in combination with isotropic tensile and compressive plasticity to represent the inelastic behavior of concrete and consists of the combination of nonassociated multi-hardening plasticity and scalar (isotropic) damaged elasticity to describe the irreversible damage that occurs during the fracturing process. [5]

The model is a continuum, plasticity-based, damage model for concrete. It assumes that the main two failure mechanisms are tensile cracking and compressive crushing of the concrete material (fig. 3). The evolution of the yield (or failure)

surface is controlled by two hardening variables, and linked to failure mechanisms under tension and compression loading, respectively.

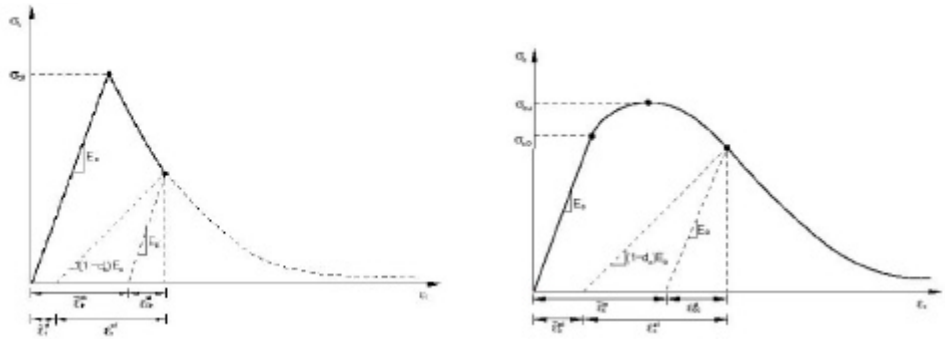

a) b)

Figure 3 – Illustration of: a) cracking strain;
b) crushing strain in CDP model [5]

The degradation of the elastic stiffness is characterized by two damage variables, d_t and d_c, which are assumed to be functions of the plastic strains, temperature, and field variables. The damage variables can take values from zero, representing the undamaged material, to one, which represents total loss of strength.

Same as the other nonlinear model, the CDP model requires defining the tension stiffening and it can be done using the same concepts of stress-strain relation and stress-displacement relation. In reinforced concrete the specification of postfailure behavior generally means giving the postfailure stress as a function of cracking strain, ε_t^{ck}, (fig. 3a) defined as the total strain minus the elastic strain corresponding to the undamaged material.

It can be defined the stress-strain behavior of plain concrete in uniaxial compression outside the elastic range. Compressive stress data are provided as a tabular function of inelastic (or crushing) strain, ε_c^{in} , (fig. 3b) and, if desired, strain rate, temperature, and field variables. [5]

The fracture energy cracking model can be invoked by specifying the postfailure stress as a tabular function of cracking displacement (fig. 4a) and alternatively, the fracture energy, G_f, can be specified directly as a material property; in which case, it has to be define the failure stress, σ_{t0}, as a tabular function of the associated fracture energy. This model assumes a linear loss of strength after cracking. (fig. 4b)

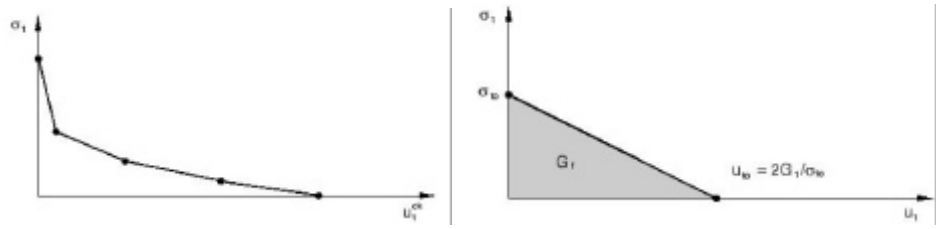

a) b)

Figure 4 – Postfailure curve for tension stiffening: a) stress-displacement; b) stress-fracture energy [5]

3. RESULTS OF ANALYSIS

The model analyzed in this study is represented by a strip, cut from the slab of an entire reinforced concrete structure, in order to simply the action of performing the nonlinear analysis and to reduced considerably the time that would be necessary to run the analysis. The length of this strip is L=11250 mm, the width is equal to 620 mm and the thickness of the voided slab is 230 mm, with 180 mm sphere diameter. The boundary conditions are placed in the zones which represent the contact area between the slab and the column.

Concrete used to design the strips in this study is C25/30 and the reinforcement is made from steel Pc52 with 18 mm diameter.

The physical model, together with the materials properties, was introduced in program and was run the nonlinear analysis, using both nonlinearity models consists in the program (CDP and CSC model). The results obtained in this two cases offers necessary information regarding the plastic deformations state (fig. 5) and load-displacement curve (fig. 6), information that is useful in the entire design process of these new constructive systems.

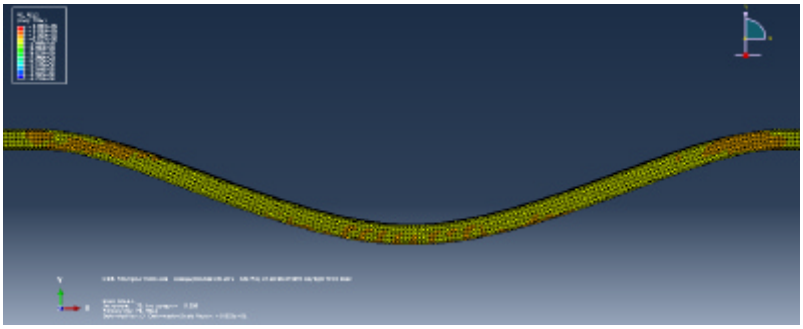

Fig. 5 – Plastic deformations state

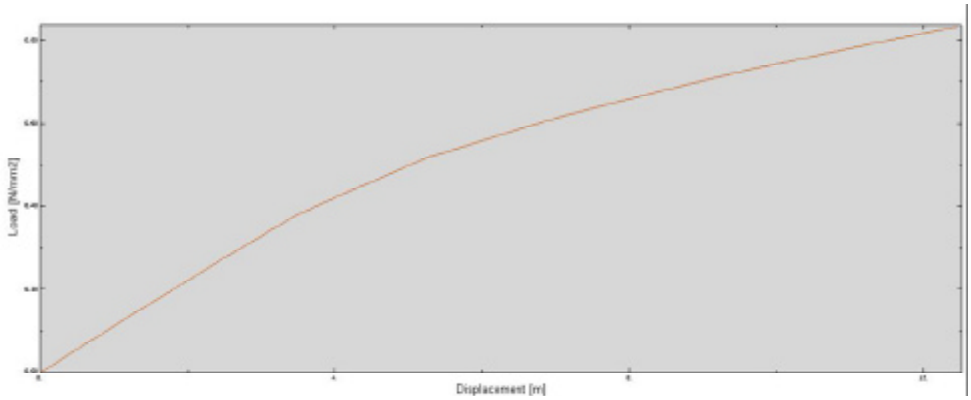

Fig. 6 – Load-displacement curve

3. FINAL CONCLUSIONS

Obtaining the deformation states in concrete elements is an important step in the design process because it provides essential information regarding assemblies' response to action of external loads. Based on the conclusions obtained, the designer defines the characteristics of the resistance structure and activities must be conducted so that the final products to ensure the comfort and safety wanted by the owners and imposed through the existing norms.

The nonlinear analysis performed using the finite element program Abaqus/CAE for the new voided slab system emphasizes the similarity with classical full slab system, so that the following research activities can be made using the theoretical aspects from the literature in domain, making, where is request, the necessary changes, in order to have accurate results, close to reality.

References

1. Pascu, R., *Comportarea si calculul elementelor din beton armat*, Ed. AGIR, Bucuresti, 2008.
2. Nilson, A.H., Darwin, D., Dolan, C., *Design of concrete structures*, Forth Edition, Mc Graw Hill, New York, 2010;
3. Ghali, A., Favre R., Elbadry, M., *Concrete structures-stresses and deformations*, Third Edition, Spon Press, New York, 2006;
4. ***Eurocod 2 – Proiectarea structurilor din beton armat
5. *** Manual de utilizare program Abaqus/CAE
6. www.simulia.com

Computer based assessment of building energy performance

Laura Dumitrescu, Dan Preda Stefanescu
Department of Civil and Industrial Engineering, "Gheorghe Asachi" Technical University of Iasi, Iasi, 700050, Romania

Summary

In the last decades, the tendency for energy-efficient construction became predominant in the building industry, because of the new regulations regarding resource conservation and environmental impact minimisation. The new standards refer both the construction of new buildings (passive houses, zero-energy buildings, etc.) and the rehabilitation of the existing ones with the target of energy savings.

The use of computer programs is a valuable aid in building energy calculations for two main purposes: (a) calculation of temperature distribution, heat streams and vapour diffusion streams within building elements, in two and three dimensional stationary and transient heat flow simulation, and (b) balance energy calculation for the entire building.

This paper presents a brief comparative study using two programs for thermal field simulation for a detailed thermal bridge calculation. A simplified method to include the thermal bridge effect into the assessment of the building energy performance is also proposed.

KEYWORDS: buildings, energy performance, thermal bridge, heat transfer.

1. INTRODUCTION

The energy conservation in buildings is the most important requirement for sustainable construction. It allows the reduction of the fossil fuel consumption and the correspondent pollutant emissions and opens the possibility of using locally produced clean renewable energy (solar, biogas, wind). This is a "sine qua non" condition for the new generation of low-energy houses and passive houses.

The building specialists from different countries made a significant effort to find global indicators to assess the energy performance of buildings and to unify national standards with European ones. Early performance indicators focused on thermal insulation of the building, and the most recent ones focus on primary energy needs - 'primary energy' means energy from renewable and non-renewable sources which has not undergone any conversion or transformation process [1].

Obviously, in this way reflects a multitude of factors: compactness of the building, composition of all elements of building envelope, heating, cooling, lighting, hot water, household equipment, solar collectors, photovoltaic devices, heat pumps, heat storage, urban networks for secondary energy transport (heat, electricity) and power plant where fuel is processed.

These indicators refer to the energy requirements in conventional conditions; the actual energy consumption also depends on the state of elements of construction and installation, climatic factors and the type of occupancy showing random variation.

2. NUMERICAL INDICATORS FOR ENERGY PERFORMANCE OF BUILDINGS

The main types of energy performance indicators that can be used to assess buildings are:

a) Indicators for assessing transmission heat losses through the building envelope, such as:

- *Transmission heat transfer coefficient*, H_T (W/K), which is the heat flow rate due to thermal transmission through the fabric of a building, divided by the difference between the environment temperatures on either side of the construction [2];

- *Mean adjusted coefficient of thermal transmission* U'_m and *mean adjusted specific thermal resistance* R'_m ($R'_m=1/U'_m$), used in the C107 series of Romanian norms [3] and calculated by the equation (1):

$$U'_m = \frac{\sum (A_i \cdot \tau_i \cdot U'_i)}{A}, \ [\mathrm{W/m^2K}] \tag{1}$$

where:

A_i is the area of the element *i* of the building envelope, and $A=\Sigma A_i$ (m^2);

U'_i is the adjusted coefficient of thermal transmission of element *i* of the building envelope (W/m^2K);

τ_i is the coefficient for the temperature correction (-).

b) Indicators for assessing the overall heat losses in buildings:

According to [4], these indicators are the *volume coefficient of heat loss* $F_V(W/m^3K)$ and the *surface coefficient of heat loss* $F_S(W/m^2K)$; the surface can be, optionally, the area of the building envelope, the heated area, etc. Such an indicator, used in Romania and defined by the C107 regulations is the *global coefficient of thermal insulation* G (for dwellings) and G1 (for buildings other than dwellings destination). The value of G is a building characteristic and represents the energy necessary to compensate the heat losses through transmission and ventilation corresponding to 1 m^3 of heated volume, caused by a temperature difference of 1K and is calculated by the equation (2):

$$G = \frac{\sum \frac{A_i}{R'_i} \cdot \tau_i}{V} + 0.34 \cdot n, \ [\mathrm{W/m^3K}] \tag{2}$$

where:

A_i is the area of the element *i* of the building envelope (m^2);

R'_i is the adjusted specific thermal resistance of element *i* of the building envelope (m^2K/W);

τ_i is the coefficient for the temperature correction (-);

V is the internal heated volume (m^3);

n is the natural ventilation rate of the building, i.e. the number of air changes per hour (h^{-1}).

c) Indicators for assessing the necessary of thermal energy

These indicators are based on the energy balance of building, and the most known method is the standard SR EN ISO 13790:2008 *Energy performance of buildings –*

calculation of energy use for space heating and cooling. There are also many buildings' thermal simulation programs which use a short-time step in calculations (typically one hour) and which calculate at the same time the heating and cooling energy needs and the interior temperature (e.g. EnergyPlus, Lesosai, EPIQR, CASAnova, etc.).

According to the C107 norms, the annually necessary of thermal energy for 1 m^3 of heated volume is estimated with the relation (3):

$$Q = \frac{24}{1000} C N_{12}^{\theta} G - (Q_i + Q_S), \text{ [kWh/m}^3\text{year]} \quad (3)$$

where:

C is the correction coefficient (-);

N_{12}^{θ} is the number of the degrees-days per year characteristic for the locality where the building is placed (Kdays);

G is the global coefficient of thermal insulation of the building (W/m^3K);

Q_i is the usable energy gains resulted from the building habitation (kWh/m^3year);

Q_S is the usable solar energy gains (kWh/m^3year).

Calculation of heat balance of buildings is difficult because of the three-dimensional domain, the complexity of geometry and composition of envelope elements, the effect of air movement, sunshine, time variation in temperature and humidity, etc. Therefore, most foreign and Romanian norms support the following simplifying assumptions:

-Steady-state conditions;

-Physical characteristics are independent of temperature and humidity;

-There are no heat sources inside the building elements.

d) Indicators for assessing the necessary of primary energy

Such indicators have started to be used in technical regulations published after 2000. The necessity of using a numeric indicator of primary energy use, based on primary energy factors per energy carrier, which may be based on national or regional annual weighted averages or a specific value for on-site production is stated in the EU legislation [1].

For a more relevant and comprehensive assessment of buildings impact on the environment in terms of energy consumption, the performance indicator should relate to *specific primary energy consumption over the lifetime of the building*, i.e. taking into account the embodied energy. This is particularly so since the report embodied energy/exploitation energy has changed considerably in recent years,

decreasing from values of 1:7 for older buildings to values around 1:3 for new low energy buildings [5].

Use of each indicator has advantages and disadvantages, the choice must be made depending on the purpose of the study, the life cycle stage of construction (construction, use, refurbishment), the available simulation programs, etc.

3. EVALUATION OF TRANSMISSION HEAT LOSSES

Not all European countries consider the influence of thermal bridges in their regulations for new buildings and even less for the renovation of the existing ones, because the correct calculation of linear thermal transmittance is quite laborious. However, buildings can contain significant thermal bridges, their total impact on the heating energy need is in general considerable and can be as high as 30% [6].

The direct heat transfer coefficient between the heated space and the exterior through the building envelope is defined by the equation (4):

$$H_D = \sum_i A_i U_i + \sum_j l_j \psi_j + \sum_k \chi_k, \text{ [W/K]} \tag{4}$$

where:

A_i is the area of element *i* of the building envelope (m^2);

U_i is the thermal transmittance of element *i* of the building envelope (W/m^2K);

l_j is the length of linear thermal bridge *j* (m);

ψ_j is the linear thermal transmittance of thermal bridge *j* (W/mK);

χ_k is the point thermal transmittance of point thermal bridge *k* (W/K).

To apply the calculation method, building-element dimensions are usually measured according to one of three systems (Figure 1): internal (in France), overall internal (in Romania), and external (optional Germany). Therefore, the term $\sum_i A_i U_i$ and the values of ψ_j are different, so they will be noted below with $\psi_{j,i}$, $\psi_{j,oi}$, $\psi_{j,e}$ and $A_{i,i}$, $A_{i,oi}$, $A_{i,e}$, respectively (index *i* for internal, *oi* for overall internal, and *e* for external dimension system).

In Figure 1, the numbers have the following meaning:

1- internal dimension (measured from wall to wall and floor to ceiling inside a room of a building);

2- overall internal dimension (measured on the interior of a building, ignoring internal partitions);

3- external dimension (measured on the exterior of a building).

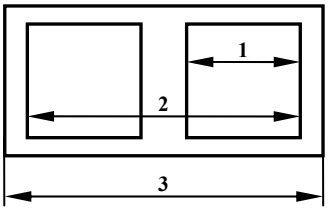

Figure 1. Dimensions systems

Using external dimensions may be preferred because it includes the total area of the envelope and is easier to calculate. It covers partly the additional losses due to thermal bridges. Consequently, the values of ψ_j are generally smaller for external dimensions, and can even be negative in some cases such as external corners. According to [2], when the main insulating layer (the layer with the highest thermal resistance in the elements flanking the potential thermal bridge) is continuous and of uniform thickness, with special attention to limit thermal bridge effect, the linear and point thermal transmittance may be neglected if external dimensions are used. This significantly simplifies the calculation, which is acceptable since a large number of parameters (thermal conductivity, thickness, climate regime, internal temperature, etc.) have random variation that deviate significantly from the conditions considered in the deterministic calculation. Corrections for other cases may be defined on a national basis. Traditionally, the alternatives available to designers for assessing thermal bridges have involved:

-to use thermal bridge atlases with ψ and χ values (for example, in C107 Romanian norms), but sometimes they are not a real help in solving specific problems;

-to perform detailed thermal bridge simulation, expensive and not at all part of the daily practice.

Other alternative could be the use of catalogs containing more flexible databases, such as the KOBRA software and EUROKOBRA database, offering a computerised thermal bridge atlas for 2-dimensional details. The main characteristics of this atlas is its user friendliness, the large flexibility of modifying the detail (layer thickness, materials, boundary conditions, etc.) and the way of presenting the results (e.g. color pictures showing the isothermal lines, the heat flux lines) [7].

4. COMPARATIVE STUDY REGARDING THE ENERGY PERFORMANCE OF A BUILDING

A typical dwelling building (Figure 2) was considered as a case study for the calculation of the thermal performance indicators.

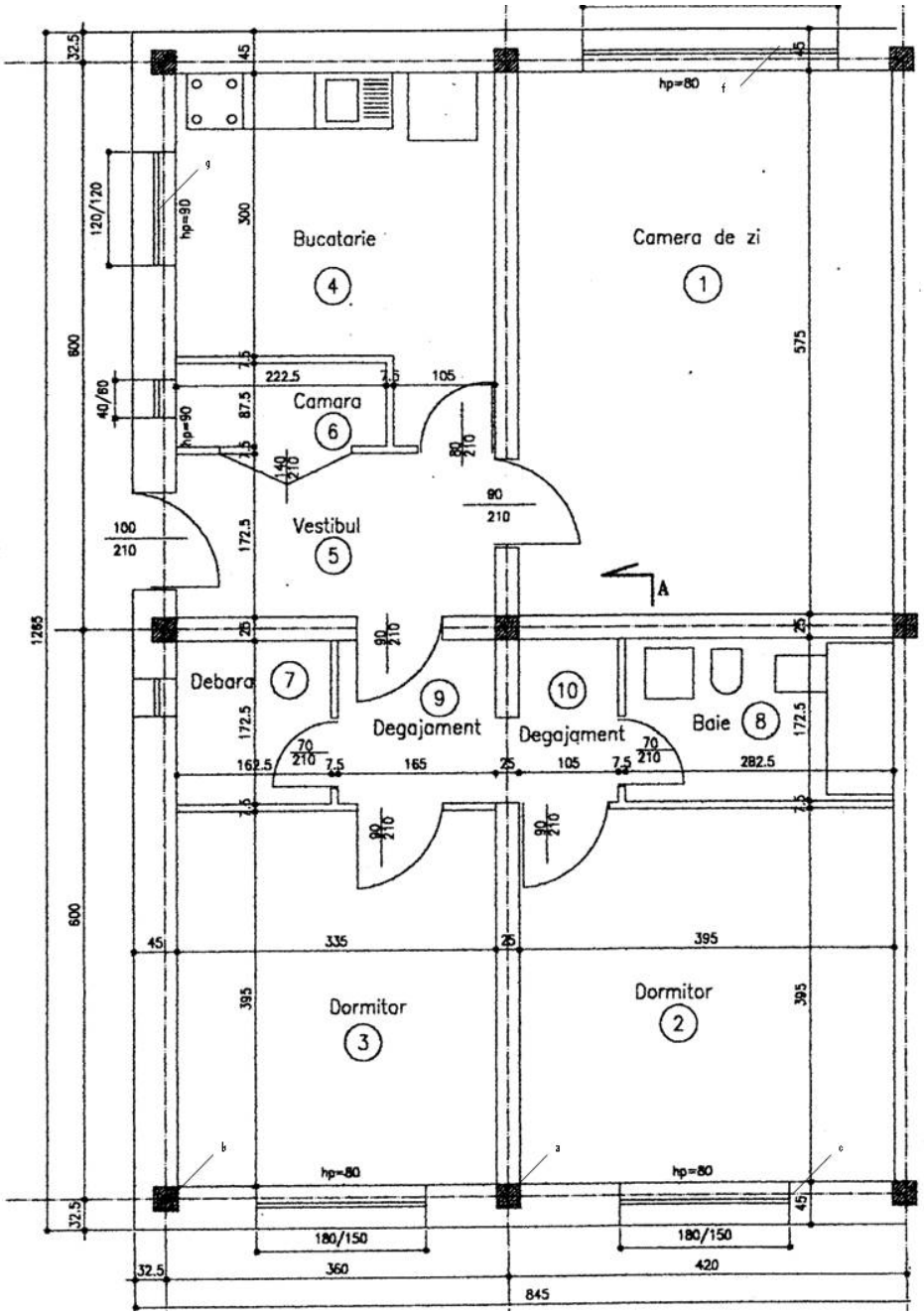

Figure 2. Ground floor plan

The building has two apartments of three rooms and it has ground floor, general basement and terrace roof. Bearing structure consists of bearing masonry of bricks and reinforced concrete cores of 25 cm thickness and reinforced concrete slabs of 15 cm thickness. Thermal insulation is from cellular polystyrene and it is protected by a half brick masonry. The quality of the constructive solutions is not covered by this analysis. The glazed areas have wooden frames and regular windows. The building is placed in the 2nd climatic zone (T_e= -15 °C) and the temperature in the basement is T_u=2.5°C. Given the symmetry of the building, all calculations are performed for an apartment. Building project has been drawn up in 1997. The thermal bridge details are presented in Figure 3.

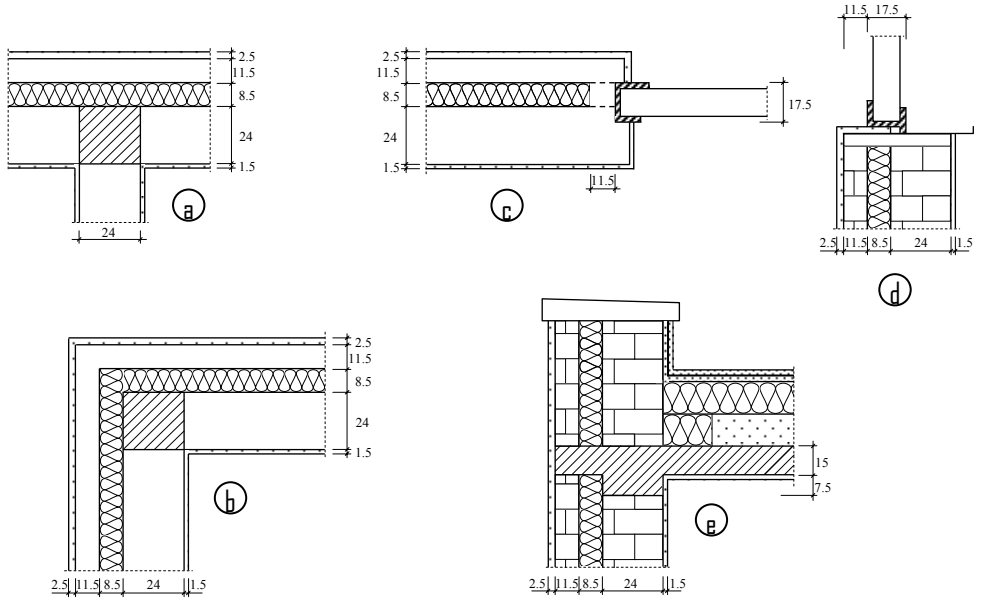

Figure 3. Thermal bridge details

The following energy efficiency indicators have been calculated:

-Mean adjusted coefficient of thermal transmission U'_m (W/m^2K);

-Global coefficient of thermal insulation G (W/m^3K);

-Annually specific energy demand for heating Q (kWh/m^2year).

The values of the linear thermal transmittance of thermal bridges have been determined both by numerical simulation and using EuroKOBRA program and the results are presented in Table 1, for the following methods of calculation:

- Case 1 – ψ_{oi} values according to the tables of normative C 107-2005;

- Case 2 – ψ_{oi} values obtained by numerical modeling;
- Case 3 – ψ_e values obtained by numerical modeling;
- Case 4 – ψ_i values according to EuroKOBRA thermal bridge catalog;
- Case 5 – ψ_e values according to EuroKOBRA thermal bridge catalog.

Table 1. Values of the linear thermal transmittance ψ (W/mK)

Thermal bridge	Scheme	ψ (W/mK)				
		Case 1	Case 2	Case 3	Case 4	Case 5
a –Wall „T" joint	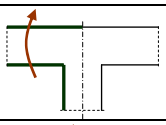	0.01	0.019	0.003	0.055	0.005
b – External corner	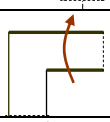	0.09	0.093	-0.086	0.090	-0.090
c –Window reveal	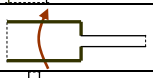	0.06	0.047	0.047	0.030	0.030
d – Windowsill	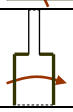	0.17	0.218	0.218	0.210	0.200
e – Attic	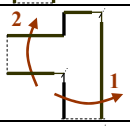	0.27 0.35	0.366 0.534	0.340 0.147	0.680	0.370
f - Lintel, h=50cm	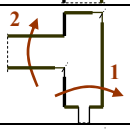	0.38 0.31	0.543 0.461	0.512 0.173	0.900	0.780
g - Lintel, h=70cm	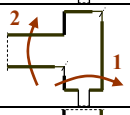	0.40 0.31	0.603 0.490	0.570 0.209	0.980	0.860
h – Vertical joint with inferior slab	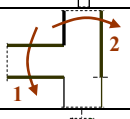	0.17 0.20	0.214 0.314	0.226 -0.130	-	-
i – Partition wall	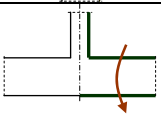	0.11	0.202	0.166	-	-
j – Internal wall	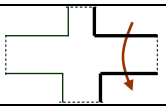	0.25	0.369	0.332	-	-

The differences between values of the same coefficient (ψ_{oi} - cases 1 and 2, respectively ψ_e – case 3 and 5), are due to working assumptions adopted in each

case. Because EuroKOBRA catalog does not provide details for all types of thermal bridges of the building, energy efficiency indicators were calculated only for the first three cases, using ψ values, lengths and areas according to the correspondent dimensions system (overall internal and external, respectively). The results are presented in Table 2.

Table 2. The values of the thermal performance indicators of the building

	U'_m (W/m^2K)	G (W/m^3K)	Q (kWh/m^2year)
Case 1	0.524	0.825	169.30
Case 2	0.579	0.883	183.66
Case 3	0.476	0.877	182.28

The results presented in Table 2 show relatively large differences between the values calculated using the same dimensional systems, depending on simulation software, work assumptions and simplifications adopted (cases 1 and 2) as follows: U'_m - 10.5%, G - 7 % and Q - 8.5%. Comparing the results obtained in cases 2 and 3, there is a big difference for U'_m indicator (21.6%), normal because the area varies greatly (overall internal dimensions, and external), but very similar values for G and Q indicators (difference of 0.7%).

To simplify calculations, it could be more convenient that all these indicators to be calculated using unidirectional thermal resistance values and applying an increase in U_m value. The calculation is made using external dimensions of the building and applying the following increases of the mean coefficient of thermal transmission U_m:

-For corrected thermal bridge: $\Delta U \leq 0.05$ W/m^2K;

-For common thermal bridges: $\Delta U = 0.10$ W/m^2K;

-For major thermal bridges: $\Delta U \geq 0.20$ W/m^2K.

The mean adjusted coefficient of thermal transmittance U'_m for the analyzed building will be calculated with the relation (5):

$$U'_m = \frac{\sum \frac{A_i \cdot \tau_i}{R_i}}{\sum A_i} + \Delta U, \ [W/m^2K] \tag{5}$$

where $\Delta U = 0.10$ W/m^2K, supplement of unidirectional heat transfer coefficient, which takes into account the influence of thermal bridges.

The relation for calculating the G indicator is obtained from equations (2) and (5) and it is given by (6):

$$G = \frac{\sum \frac{A_i \cdot \tau_i}{R_i} + \Delta U \cdot \sum A_i}{V} + 0.34 \cdot n, \ [\mathrm{W/m^3K}] \quad (6)$$

The values of the three energy performance indicators are U'_m=0.468 W/m^{2}K, G=0.867 W/m^{3}K, and Q=179.79 kWh/m^{2}year, very similar (differences 1.1-1.7%) of those obtained by calculation based on numerical modeling of thermal bridges (external dimensions).

5. CONCLUSIONS

The necessity of energy conservation in buildings is an important requirement for achieving sustainable development in construction. The ambition of the European Commission is for new European buildings to become "near zero energy buildings" in 2020.

The impact of thermal bridges in energy performance of buildings cannot be neglected and should be included in the calculation methods, although the correct calculation of linear thermal transmittance is quite laborious.

In conclusion, besides the development of thermal bridge catalogs as large as possible and including current technical solutions, a very useful solution is to adopt a simplified methodology, allowing calculation of transmission heat losses using unidirectional thermal resistance values (much easier to calculate) with default values for including the increased thermal losses due to thermal bridges, as proposed in this paper.

References

1. Directive 2010/31/EU of the European Parliament and of the Council of 19 May 2010 on the energy performance of buildings
2. SR EN ISO 13789:2008 Thermal performance o buildings – Transmission and ventilation heat transfer coefficients – Calculation method
3. C107-2005 Regulation regarding thermal calculation of the construction elements of buildings (in Romanian)
4. SR EN ISO 7345:1995 Thermal insulation – Physical quantities and definitions
5. Tywoniak, J. – *Thermal performance of buildings and building components – Tool on the way to sustainable buildings*, First International Seminar on environmental compatibility of structures and structural materials, Prague, 4-5 May 2000
6. Erhorn-Kluttig, H., Erhorn, H. – *Impact of thermal bridges on the energy performance of buildings, Information Paper P148 of EPBD Buildings Platform*, 27.03.2009
7. Wouters, P., Schietecat, J., Standaert, P. – *Practical guide for the hygrothermal evaluation of thermal bridges, a SAVE-KOPRACTICE-project document*, 7.05.2003

Improvement proposal for URGENT1 - Software for planning and simulation of emergency evacuation using auto transport

Augustin-Ionut Gavrila[1], and Neculai Scîntei[2]
[1] *Computer Science Ph.D. Candidate, "Gh.Asachi" Technical University, Iasi, Romania*
[2] *Civil Engineering Ph.D. Candidate,"Gh.Asachi" Technical University, Iasi, Romania*

Summary

The software URGENT1 was applied in a case study that simulated and planned decisions regarding population evacuation in emergency situations in a particular area. This program resolved the following problems: transportation plan, the making of the convoys, displacement itineraries, diagrams of population evaluation, it generated maps with information's regarding places, convoys, road segments, being of real use in training personnel that is responsible of population evacuation in cases of emergency.

KEYWORDS: emergency situation, population evacuation, simulation, deployment itinerary, evacuation diagrams, transport plans.

1. INTRODUCTION

The software for simulation, planning and optimization of decisions in risk and uncertainty conditions, considering population evacuation with auto transport means, took into consideration areas with different degrees of urgency, the road transport system, the existing and supplementary auto transport base using heuristics for a better time schedule of evacuation and having a final purpose of mineralizing risk taking.

The software URGENT1 was applied at a given study case for simulating, planning and optimizing decision making regarding population evacuation in emergency situations from an area affected for one day and 17 hours with a positive result. This software resolved the following problems: transport plan, map generation with information's referring to areas, convoys, road segments – at 10 minutes interval having the possibility of being of real help for personnel training in evacuation techniques (extended – of material property also) in emergency situations.

ISSN 2285-2735, Pages 161 - 166

The purpose of this software is to be used at institutional level and also at the level of local administration for the preparation of personnel and population in case of disaster. Using this resource will lead to economy to budgets both financial and material and mainly it would save human life.

The program Urgent1 may be improved including new parameters and extending at regional and national level, eventually a distributed algorithmic approach can be used instead of the centralized-sequential existent solution. The software can contribute to the fulfillment of the imposed goal found in the National Strategy concerning prevention of emergency situations and national centralized evacuation of property and people. Also, it can be taken in consideration the dynamic adjustment of emergency degrees of different areas during running of the software. This will result in a rescheduling of the population evacuation concerning initially omitted information's that affect the current state of evacuation.

2. PROPOSED IMPROVEMENTS FOR STRATEGIES, METRICS AND EVACUATION ALGORITHM

2.1. Algorithm of evacuation example

It may be considered a meta-algorithm that must imply the automatic generation of possible strategies with the calculations made in parallel on a distributed calculus architecture (cluster/grid/cloud-computing).

Through the comparisons of the obtained results and retaining optimum values for the computed possible scenarios the following algorithm will appear:

```
bestStrategy=NULL;
MaximumUtility= - 8 ;

Foreach**(strategy ?  GeneratedPossibleStrategies)

//computed in parallel, on a cluster/grid/cloud/other distributed systems
//**: examples of strategies:
//MaximumProfit:
MaximalDistance/MaximalPopulation/MaximalEmergencyDegreeEvacuation...
//MinimumRegret: MinimalTime for evacuation of local population from selected area
```

```
{
        while(∃i=UnsafeLocality* so that ActualPopulation[i]>0)
        //*test UnsafeLocality: population*EmergencyDegreeEvacuation*(1-safety)>0
        {
          i=ChooseUnsafeLocality(strategy**, distance***, EstimateTime,
        ActualPopulation, VehicleCover);
        //***distance – may be considered aproximate, on the shortest route possible,
        //or taking into consideration degrees and
        //time intervals to cover area arcs
          if(∃CoveringVehicles[i])
           {
            j=EvacuationPlanning(i);
            //considering:
            //time for loading, transport and unloading
            //anterior planning, degrees and intervals of occupancy
            //of road arches from the road network involved in evacuation
            EvacuationStart(i, j, SelectedPath, ComputedTimeIntervals, NecessaryStops);
           }
          else {
                  j=ChooseSafeSource(AvailableVehicles,TimeIntervals,
                  NeededSmallBusses,NeededBusses,NeededCoachBusses);
                  SendHelp(j,i,way, TimeInterval, NeededSmallBusses,
        NeededBusses,NeededCoachBusses);
                  }
        }
        currentUtility=function(maximumTimeNeededForLastEvacuatedPerson,
                          exposedPeoplePeriodInAffectedAreas*
                                  fn2(EmergencyDegreeEvacuation,dangerType));
        Monitor.Enter(); //synchronized code for critical resources computed
        {
        if(currentUtility> MaximumUtility)
                  {
                  MaximumUtility= currentUtility;
                  bestStrategy=strategy;
                          save(EvacuationComputedPlans, convoysComponents,
                          selectedRoutesForEachConvoy, plotsForGraphicsOfEvacuation,
                          mapsInformations);
                  }
        }
        Monitor.Exit();
}
```

2.2. Dynamic adaptation

The dynamic adaptation of the different degrees of emergency, of the affected areas and the available road sectors would permit adjusting the program run to real conditions, initially ignored or unpredicted.

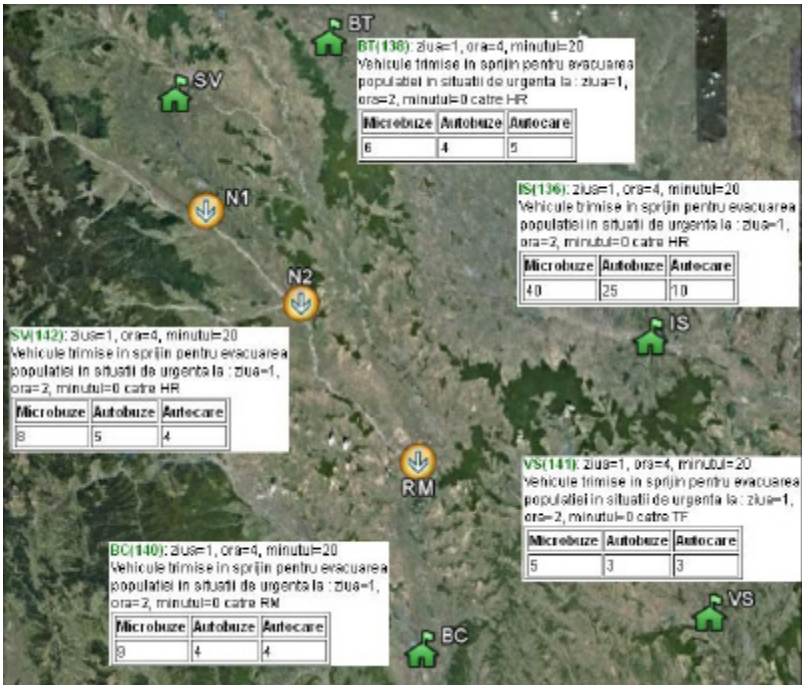

Figure 1. Transport vehicles requested and sent by the nearby support localities

2.3. Reducing of time divisions in the case of generated files containing information's regarding convoys, maps, road segments occupancy level

Having a better granularity, for example computations for each minute of program run, would permit a better follow-through of the simulation/planning of evacuation taking in consideration better decision making.

2.4. Continuous surveillance of the evacuation

Adding a software module for continuous surveillance of the obtained result, through 4-D visualization (space-time), allows good frame by frame run visualization on a desired area or road segment. Also this will permit a continuous monitoring of selectable characteristics for certain localities or road segments at any given time frame.

Figure 2. Convoys in motion at minute 1440 from evacuation start

Figure 3. Information’s concerning moving convoys at minute 1440 from evacuation start

2.5. Intermediary conclusion

Extending the follow-up of evacuation in simulated affected areas from a county level to a regional or national one through the partitioning of computations made for each area considering communication of data between simulated modules on different computation nodes (cluster, grid or cloud computing).

3. CONCLUSIONS

The software URGENT1 for simulation, planning and optimization of decisions in risk and uncertainty conditions, considering population evaluation with auto transport means, took into consideration areas with different degrees of urgency, the road transport system, the existing and supplementary auto transport base using heuristics for a better time schedule of evacuation and having a final purpose of mineralizing risk taking can be improved from the following perspectives: increase in number of scenarios through incorporation of variate evacuation strategies, independent parallel calculations, extension to regional and national level of emergency situations monitoring and evacuation from affected areas, inclusion of the human factor decision making and dynamic modification of different emergency degrees and available road segments.

References

1. Andrei Neculai: *Modele, programe de test si aplicatii de programare matematica*. Bucuresti: Ed. Tehnica, 2003. (in Romanian)
2. Buraga Sabin Corneliu: *Tehnologii Web*. Bucuresti: Ed. Matrix Rom, 2001. (in Romanian)
3. Cascaval Petru, Cascaval Doina: *Modelare si simulare*. Iasi: Ed. Gh. Asachi, 2002. (in Romanian)
4. Chitescu, S.: *Organizarea transporturilor auto.* Bucuresti: Ed. Tehnica, 1976. (in Romanian)
5. Craus Mitica: *Algoritmi pentru prelucrari paralele*. Iasi: Ed. Gh.Asachi, 2002. (in Romanian)
6. Croitoru Cornelius: *Tehnici de baza în optimizarea combinatorie*. Iasi: Ed. Univ. Al. I. Cuza, 1992. (in Romanian)
7. Ionescu Gh.Gh., Cazan Emil, Negruta Adina Letitia: *Modelarea si optimizarea deciziilor manageriale*. Cluj-Napoca : Ed. Dacia, 1999. (in Romanian)
8. Ionescu Tiberiu: *Grafuri-aplicatii*. Vol. I, Bucuresti: Ed. Didactica si Pedagogica, 1973. (in Romanian)
9. Ionescu Tiberiu: *Grafuri-aplicatii*. Vol. II, Bucuresti: Ed. Didactica si Pedagogica, 1974. (in Romanian)
10. Leon Florin, Zaharia Mihai Horia, Pal Cristea, Boronea Stefan Adrian, Didilescu Tudor: *Distributed Application for Traffic Control Using Intelligent Agents*, in Proceedings of the 9th WSEAS International Conference on Applied Informatics And Communications (AIC '09), WSEAS Press, 2009.

The effects of the seismic actions on bridge structures and structure control system

Adrian Haiducu, Elena Poida
Department of Structural Mechanics, Technical University of Civil Engineering, Bucharest, 020396, Romania

Summary

This work presents: the effects of the seismic actions on bridge structures and devices for limitation of the energy transfer namely seismic isolators, viscous dampers and a combination of the two systems.

A part same innovative systems for passive control through base isolation are presented, respectively oscillatory systems – laminated rubber bearings with or without lead core, non-oscillatory systems – systems type friction pendulum.

Advantages and disadvantages of different types of isolators applied to bridge structures are presented.

A numerical example is presented in the end of the work. Two bridge structures are analyses, a non-isolated structure and an isolated structure with two types of seismic isolators (oscillating systems - laminated rubber bearings with or without lead core).

KEYWORDS: Base isolation; Seismic action; Passive control devices; Stiffness; Bridge structure; Bearings

1. INTRODUCTION

The bridge is a work of art that supports a terrestrial communication way (road, railway, etc.) over a natural or artificial obstacle (river, channel, valley, etc.) ensuring continuity of the communication way and crossed obstacle.

The problem of bridges located in areas with severe seismic actions is that generally in piers there occur major seismic forces both on longitudinal and cross-section direction of the bridge. Therefore the problem is to find methods by which to reduce the influence of the deck mass on the bridge infrastructures (piers and abutments).

Chapter II presents the effects of earthquakes on bridge structures and the need for isolating them and Chapter III contains a brief overview of passive control devices

ISSN 2285-2735, Pages 167 - 177

by isolating the base, namely, laminated rubber devices with or without lead core and the system of type friction pendulum.

Chapter IV presents the case study of a bridge structure analyzed with or without seismic isolation system, each type of structure being analyzed by help of three generated acceleration diagrams (acc1, acc2, acc3) and the acceleration diagram registered by Incerc on March 4,1977 (acc77) and Chapter V presents the conclusions.

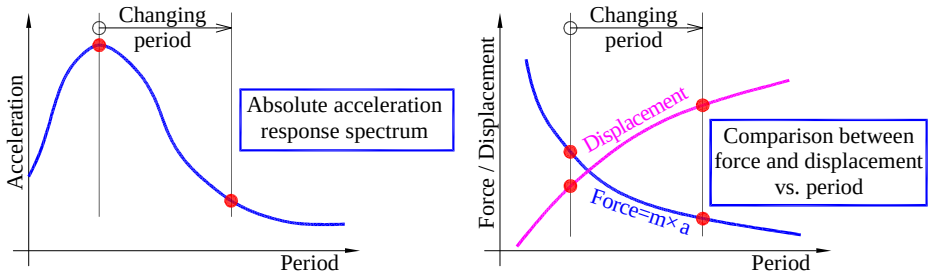

Figure1. Theoretic principle of base isolation

2. EFFECTS OF EARTHQUAKES ON BRIDGE STRUCTURES AND THE NEED FOR ISOLATING THEM

The images below present the effects of earthquakes on bridge structures. Effects depend on the intensity of the earthquake, depth where they can occur and the nature of the surface rocks.

Figure 2. Puente Viejo Pedestrian Bridge (the Veijo Bridge was restricted to pedestrian traffic two years before the earthquake) [4]; Figure 2. Bridges destroyed by the earthquake dated February 27, 2010 from Chile (8.8 degrees on the Richter scale, it lasted 9s, took place at a depth of 13km and was followed by 2 aftershocks bigger than 5 degrees) [5]

Figure. 3. Crash of bridge decks at the motorway intersection way, earthquake Northridge Earthquake, January 17, 1994, California, 6.8 degrees on the Richter scale [6]; Figure 4. Crash of a bridge pile because of the insufficient confinement reinforcements, earthquake Northridge Earthquake, January 17, 1994, California, 6.8 degrees on the Richter scale [6]

Figure 5. Seongsu bridge from Seoul (South Korea) having a total length of 1160m, crashed on October 21, 1994 [7]; Figure 6. “La Democracia” bridge erected in 1963 over Ulua river, crushed during an earthquake of 7.1 degrees on the Richter scale [8]

In case of conventional non-isolated structures, major seismic forces can cause degradation through permanent deformations, cracks and eventually cracks in the structural elements. Forces are much reduced at isolated structures with or without damping, many of the movements taking place across the isolation system, while the structure moves almost as a rigid body. The isolation system provided with damping has an additional advantage as compared to the isolation system without damping because, due to additional damping, the maximum movement of the isolator is less, the maximum movement of the isolated and damped system is less than the maximum movement of the isolated system.

In the case of seismic isolated bridges, base isolation of bridges means to separate the deck, which is the largest mass, from infrastructures, which transmit the lateral loads induced by seismic loads to foundations. If the seismic input energy is zero, the structure doesn’t need to be designed to support lateral loads.

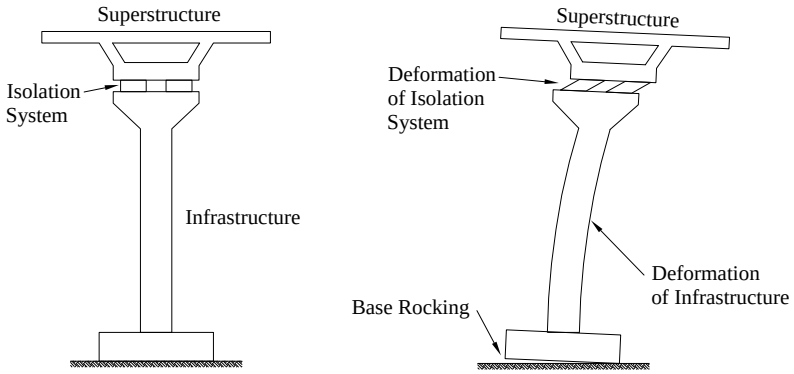

Figure 7. Actual lateral stiffness of the combined system, isolator-infrastructure

Generally, isolators are placed at the top of the infrastructures. This configuration reduces the overturning moment that would apply to the insulation devices. In addition, separating the superstructure from the infrastructure can be extremely beneficial because it eliminates the big moments that would otherwise be transmitted to piers from the superstructure, where it was fixed rigidly. Also, the design superstructure is simplified; it is reduced to a continuous, simply supported beam, or slab on elastic bearings both on longitudinal and cross-section direction of the bridge.

Seismic isolation systems combine two main component elements:

- an isolator, such as laminated rubber bearings with or without lead core or system type friction pendulum, mounted in the structure bearing area. Due to lateral stiffness much lower as compared to lateral stiffness of the structure, the isolator transfers the own lifetime of the structure beyond the most prevailing standard earthquakes.
- energy dissipation mechanism such as a damper, which dissipates the input energy and limits the forces transmitted to the structure through increased damping.

3. OVERVIEW OF PASSIVE CONTROL DEVICES BY ISOLATING THE BASE

This chapter presents a general study of various isolating devices that have been completed, successfully tested in laboratories and effectively implemented to bridge structures. This chapter highlights two main types of systems that have been

used extensively in the last twenty years, namely laminated rubber systems and systems type friction pendulum.

3.1. Laminated rubber bearing

Laminated rubber bearings, elastomeric bearings have been widely used in bridge superstructures to allow deformations and movements caused by temperature. In the last twenty years, the use of these bearings was extended to seismic isolation of buildings and bridge structures. Laminated rubber bearings can withstand high gravitational loads, providing only a fraction of the lateral stiffness of the superstructure that they support. As shown, a normal laminated rubber bearing is composed of alternating layers of elastomeric rubber and steel wheels joined tightly under pressure and at high temperature through a process of vulcanization.

Through alternation of steel and rubber layers, the capacity of laminated rubber bearing to resist gravity load is enhanced by reducing the thickness of individual layers of rubber. Although the lateral stiffness of the laminated rubber bearing depends only on the height and surface of the rubber in the unit, the vertical stiffness of the bearing is much enhanced by the presence of steel wheels. Steel wheels provide confinement and prevent rubber deformation during compression. Layers of steel wheels improve the stability of higher bearings during lateral load.

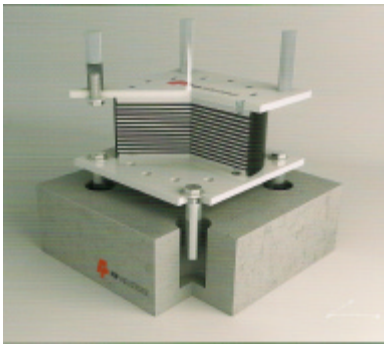

Figure 8. HDRB bearing [3];

Figure 9. HDRB bearing from Basarab passage

Key parameters in designing laminated rubber bearings are bearing capacity during gravity load, lateral stiffness and maximum relative movement that can be obtained between the top and bottom supports. Lateral stiffness of bearings influence directly the own lifetime of the isolated structure. Maximum relative acceptable movement is limited by admissible deformation of the rubber layers or by the general stability of the bearing during turnover.

A disadvantage of laminated rubber bearings is the relatively low damping provided by rubber. Lately rubbers with higher damping have been proposed for

laminated rubber bearings. It seems that layered rubber bearings with higher damping showed significantly higher energy dissipation than those made of rubbers with low damping. However, high damping rubber is sensitive to changes of properties related to heat produced during cyclic loading and wear effects that influence stiffness and energy dissipation capacity. This requires the provision of long and short term properties but also determination of appropriate limits of the bearing properties for the limited analyzes.

3.2. Laminated rubber bearing with lead core

One of the basic most developed isolation systems is the lead core laminated rubber. This system is composed of an elastomeric bearing incorporating a central core of lead. The lead core is inserted to enhance the damping through strong hysteretic shear deformation of the lead.

Main reason for choosing lead as the core material is that, at room temperature, lead is almost like an elastic-plastic solid and through shear it flows at a relatively low stress. Also, lead can be processed at hot, at room temperature. This means that lead properties are renewed continuously when subjected to an inelastic load cycle. Thus, lead has wear resistance properties. Another advantage of lead is high availability in high purity.

Key parameters in designing laminated rubber bearings with lead core are bearing capacity during gravity load, lateral stiffness, damping and maximum relative movement.

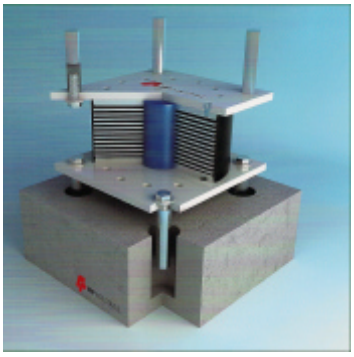

Figure 10. LRB bearing [3];

Figure 11. LRB bearing from Basarab passage

3.3. System type friction pendulum

The system type friction pendulum is a friction sliding bearing using gravity as a force for recovery. The system consists of an articulated friction slider moving on a consolidated concave spherical surface. The natural frequency of a structure isolated by help of friction system depends only on bearing radius. This advantage is significant since the period of isolation can be achieved no matter the superstructure weight.

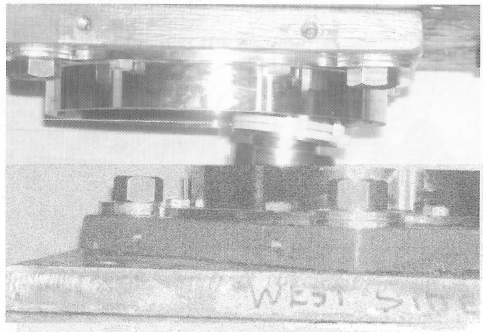

Figure 12.Seismic isolation with friction [2] Figure 13.System double friction pendulum [1]

Table 1. Types of isolators, advantages and disadvantages of these types

Types of base isolation systems	Advantages	Disadvantages
Natural rubber elastomeric isolators HDRB	- easy and inexpensive to manufacture; - easy to install; - not require replacement after a severe earthquake.	-should to be used in combination with systems that increase damping.
Natural rubber elastomeric isolators with lead core LRB	- easy and inexpensive to manufacture; - easy to install; - damping up to 30% of the fraction of critical damping; - takes over tensile forces.	-the system must be replaced after a severe earthquake.
Isolators type friction pendulum FPS	- re-centering provided by surface curvature; - properties depend less on the structure; - not require replacement after a severe earthquake; - small height of the device.	-stiffness variations induced sudden slip.

4. STRUCTURE MODELING. PERFORMED ANALYSES. RESULTS

The site is in Bucharest, where according to P100/2006 (National Annex) the peak acceleration of the designed soil is ag = 0.24g. Local soil conditions at the location are provided by corresponding spectra defined by the (peak) control period value Tc=1,6s. Seismic movement is described by response spectra in absolute normalized accelerations according to P100/2006, which have maximum coefficients of dynamic amplification β_0 =2,75 and β_{0v} =3,0.

Analysed structure consists of a reinforced concrete bridge, continuous beam on 5 spans of 50.00m each, having a total length L = 5 x 50.0m = 250.00m. In cross-section, the superstructure consists of a reinforced concrete box with sloping walls.

Variant I-1 considers the classic propping superstructure with mobile and fixed bearing devices, fixed bearing being located on the pier. Variant I-2 considers the superstructure propped with laminated rubber isolators of high damping and variant I-3 considers superstructure propped with laminated rubber isolators having lead core. The infrastructure elevations are considered to be embedded in the base. There are used three generated acceleration diagrams (acc1, acc2, acc3) and the acceleration diagram registered by Incerc on March 4, 1977 (acc77).

Isolators have diameter D=1200mm, height H=286mm and thickness of the neoprene te=120mm – I-2, diameter D = 900mm, height H=324mm and thickness of the neoprene te=144mm – I-3.

Analysed structure: elevation, joints of superstructure (5096 - abutment, 5092 - pier), joints of top infrastructure (3402 - abutment, 849 - pier) and joints of below infrastructure (3396 - abutment, 1 - pier).

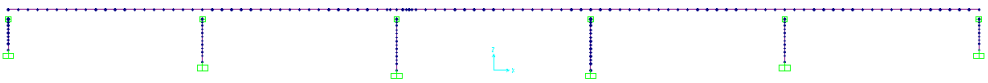

Figure 14. Structure analysed

Presentation of results: - vibration modules

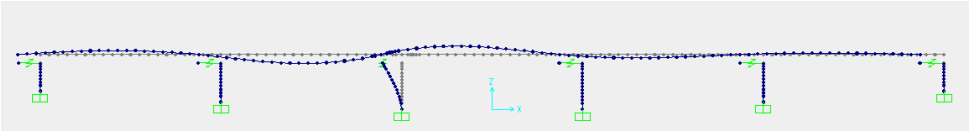

Figure 15. Structure I-1 – T=0.58s

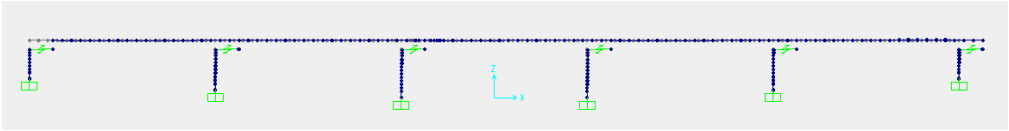

Figure 16. Structure I-2 – T=1.07s

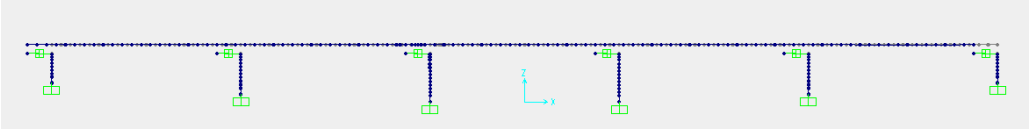

Figure 17. Structure I-3 – T=2.23s

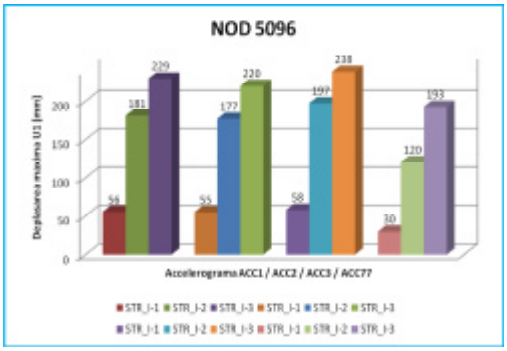

Figure 18. Maxim displacement - joints of superstructure (5096 / 5092)

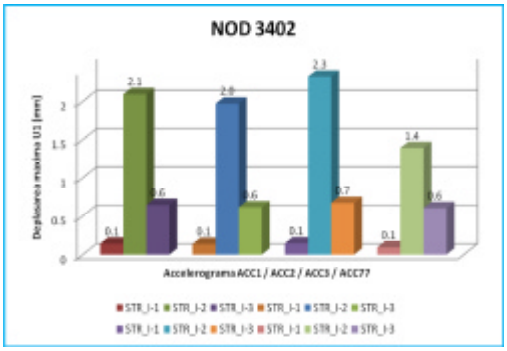

Figure 19. Maxim displacement - joints of top infrastructure (3402 / 849)

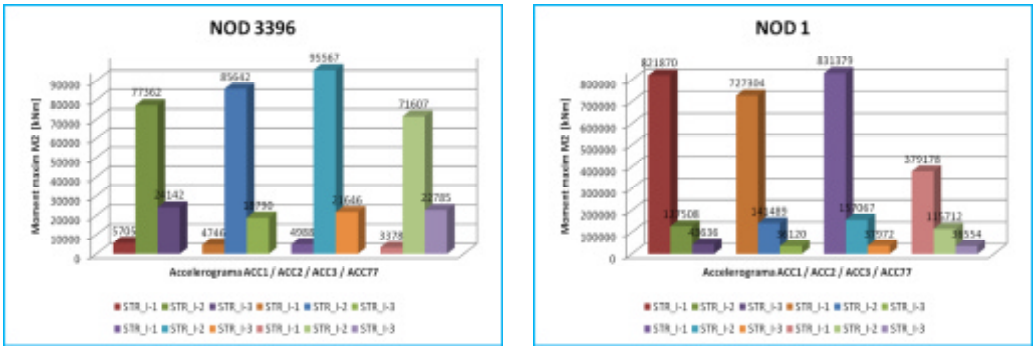

Figure 20. Maxim moment - joints of below infrastructure (3396 / 1)

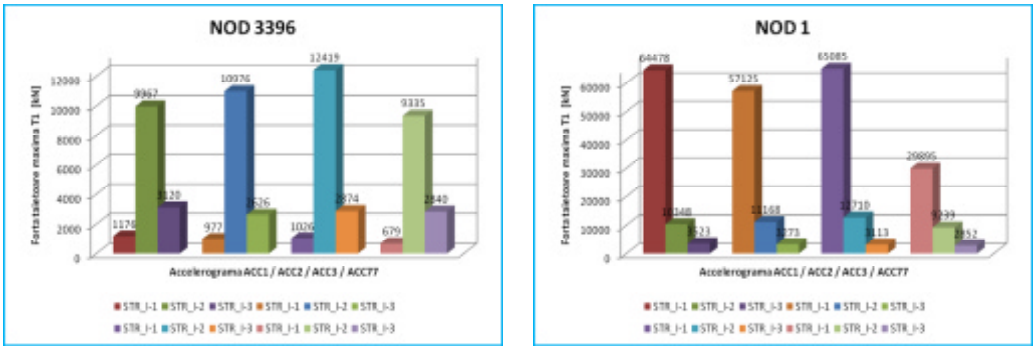

Figure 21. Maxim shear - joints of below infrastructure (3396 / 1)

5. CONCLUSIONS

In case the pier elevation is considered to be embedded in the base, when not taking into account the soil-structure interaction, the moments inside the piers can be much reduced via the seismic isolation and damping system, but the movements at the level of the superstructure increase.

As shown, at non-isolated structures (classic propping) is noticed that the movement at the level of the superstructure varies between 3 - 6 cm and at isolated structures the movement at the level of the superstructure varies between 12 - 24cm.

For the moments occurring at the elevation base, one can notice that at non-isolated structures (classic propping) the values vary between 379178 – 831379kNm for the

pier, and at isolated structures the values vary between 115712 – 157067kNm for the pier.

Insertion of isolators leads to reduction of the moments present at the base of piers and abutments but also increase of movements present at the ends of piers. This moment occurring at the base of piers is reduced up to 5 times and the deck movement increases up to 4 times.

With regard to the value of shearing force occurring at the base, also here one can notice a significant reduction in the case of isolated structures.

Table 2. Summarized table

References

1. [1] Christoponlos, C., Filiatrault, A., *Principles of Passive Supplemental Damping and Seismic Isolations*, Iuss Press, Pavis – Italy, 2006
2. Naeim, F., Kelly, J.M., *Design of seismic izolated structures*, John Wiley&Sous, New Yorg, 1995
3. [2] CONSTEL – Dispozitive telescopice si procedee tehnologice pentru consolidarea cladirilor prin controlul, linitarea si amortizarea oscilatiilor induse de activitatea seismica – Referat etapa I-a, 2008. Contract nr.32167/2008. beneficiarul Centrului National de Management Programe – programul: Parteneriate în domeniile prioritare; Director de proiect prof. dr. ing Dan Cretu.
4. [3] Catalog FIP INDUSTRIALE – Seismic Device – Elastomeric Isolators and Lead Rubber Bearings
5. Catalog ALGA – Seismic Devices – High Damping Rubber Bearings and Lead Rubber Bearings
6. [4] URL:< http://reidmiddleton.files.wordpress.com/2011/05/chili_4.jpg>
7. [5] URL:< http://minnesota.publicradio.org/display/web/2010/02/27/chile-quake/>
8. [6] URL:<http://whatiscivilengineering.csce.ca/structural_earthquakes.htm>
9. [7] URL:<http://populargusts.blogspot.com/2009/10/dark-side-of-miracle-on-han.html>
10. [8] URL:<http://www.telegraph.co.uk/news/picturegalleries/pictures-of-the-year/6872613/Pictures-of-the-year-2009-disasters-earthquake-flood-fire-tsunami-and-plane-crashes.html?image=5>

Aspects on building demolition waste and their impact on the environment

Vasile Iacob
[1] *Faculty of Civil Engineering and Building Services, "Gheorghe Asachi" Technical University, Iasi, 700050, Romania*

Summary

In the decade in which the cities face a chaotic urban development, by building residential houses and the demolition of the old buildings, the development of main streets, the construction and demolition waste are growing and must come up with a plan to reintegrate them.
Environment, built environment, natural environment are concepts that define the intervention to protect the environment on a global scale in construction and urban development.
Romanian and European concerns, on the recovery of demolition waste are summarized in this paper, with the declared intention to continue and deepen the problem.

KEYWORDS: concrete, air-placed concrete, durability, compacted, mixture, additive.

1. GENERAL ASPECTS

The wastes coming from buildings and demolitions are constituted from 2 individual components: wastes from buildings and wastes from demolitions. These wastes came from:

- materials resulting from buildings and buildings demolitions – cement, bricks, tiles, ceramic, stone, plaster, plastic, metal, cast iron, wood, glass, short ends, expired construction materials;
- materials resulting from the construction and the maintenance of roadways and afferent structures, tar, sand, rubble, bitumen, tarred substances, substances with bituminous or hydraulic bindings;
- excavated materials during the construction, decommissioning, spoil, decontamination activities: soil, gravel, clay, sand, rocks, vegetable remains.

ISSN 2285-2735, Pages 178 - 183

Also, the wastes resulting from natural disasters are considered wastes from buildings and demolitions. Objects / materials easy to remove from a structure (furniture, electric equipment and other equipments) are not considered wastes from demolitions and buildings.

Among the wastes resulted from constructions and demolitions we can mention those which are dangerous and very dangerous:

- dangerous materials: asbestos, tars and paints, heavy metals(chromium, lead, mercury), varnishes, paints, adhesives, polyvinyl chloride, solvents, polychlorinated biphenyl compounds, different types of resins used for conservation, fireproofing, waterproofing;
- risk-less materials which were contaminated by mixture with dangerous materials, for example construction materials mixed with dangerous substances, mixed materials resulted from the activity of unselective demolition;
- soil and gravel contaminated with dangerous substances.

The construction wastes represent the wastes resulted from the activities of construction and/or demolition specified at art. 2, line 1 in accordance with The European List of Wastes transposed by H.G. nr. 856/2002 about The Evidence of wastes management and for approving the list which contains wastes, including the dangerous wastes, which are founded at 17th code.

Wastes from constructions and demolitions, including excavated soil from contaminated land are constituted of three individual components: wastes from constructions, wastes from demolitions and excavated soil from contaminated lands. The classification is mentioned in The Regional Plan of Wastes Management.

The Ministry of Environment and Sustainable Development together with the Ministry of Development for Public Works and Houses have initiated in 2007 a proposal of legislation for the management of wastes. Due to this proposal, wastes was clasified in this way:

- wastes from demolitions;
- wastes from building new constructions;
- wastes from renovation of constructions;
- wastes from activities of roads reparation;
- wastes from activities of bridges reparation;
- wastes from natural disasters.

Wastes from constructions and demolitions represent about 25% , the majority of them coming from renovation or demolition of old buildings.

Nowadays, just a part of the wastes from constructions and demolitions is reported, especially that from the citizens who request Construction authorization for renovations/demolitions/new constructions.

The majority, consisting usually in rests of concrete, bricks or composite (brick with mortar) come from the building companies which usually do not declare it, because either they crush it and reuse it for roads in the yard or for filling the pits from the comunal roads, fact more or less legal, or they store it in places unauthorized by the Environmental Agency, but accepted by the local authorities.
Concerning other components such as the wood resulting from the replacement of door and window cases, doors, parquet or of floors, of roof repairs, this is recuperated in a proportion of 95 percent by poor people, who use it as fuel.
The metal consists in reinforcement bars made from reinforcing steel which appear especially after the crushing of reinforced concrete blocks and is valorified by the REMAT unities.
In this stage plastic materials do not represent a significant procent, but it's expected that in the following years (2010-2012) this component which will come especially from waste PVC industry (of whom lifetime isn't bigger than 10-12 years, if it was new and even less if it was second hand) to become a problem.
We have to take into account that in this moment 90% of new buildings' joinery is made of PVC and less from natural wood or laminated wood.
The glass is a component which, because is very brittle, most of the times is mixed up and is eliminated with the garbage, when it comes from people or with mixt wastes when it comes from building companies.
An explanation for the selective uncollecting of this fraction may be the lack of a recycler interested in the taking over of this waste in order to recycle it, as well as the lack of interest among some institutions for this problem, that's way it has come to the establishment of some nongovernmental organizations which fight for this problem.

Table 1. Types of demolition and constructions wastes which are the study object

Waste code	Waste type
170101	Concrete
170102	Bricks
170103	Tiles and ceramics
170106*	Mixture or fragments separated from concrete, bricks, tiles or ceramics with dangerous content
170107	Mixture or fragments separated from concrete, bricks, tiles or ceramics, other than those specified at 170106*
170201	Wood
170202	Glass
170203	Plastic materials
170204	Glass, plastic materials or wood with content of/ contaminated with dangerous substances
170401	Copper, bronze, brass.
170402	Aluminum
170403	Lead
170404	Zinc
170405	Iron and steel

170406	Tin
170407	Metal mixturies
170409*	Metal wastes contaminated with dangerous substances
170410*	Cables with content of oil, tar or other dangerous substances
170411	Cables, other than those specified at 170410*

According to statistic references, in 2006, all over the country there were collected cca. 475.000 tons of wastes from constructions and demolitions, quantity that was entirely eliminated through storage.

2. EUROPEAN PREOCCUPATIONS CONCERNING CONSTRUCTIONS' WASTES.

The wastes coming from constructions and demolitions represent in the European Union countries approximately 25 percent of wastes. They are done from different materials, a lot of them being able to be recycled, one way or another, like: (Surse, EIONET 2005):

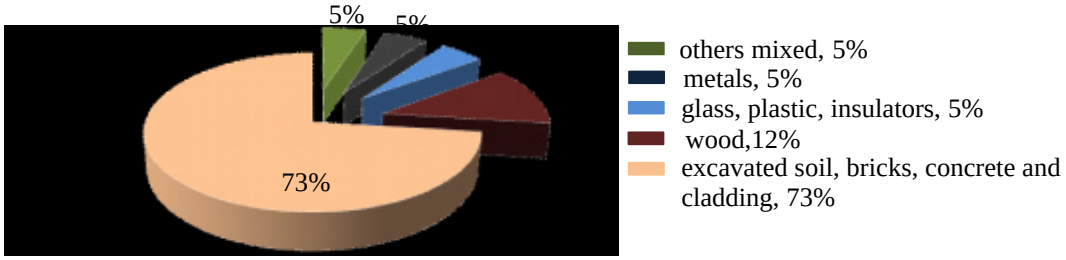

Figure 1. The structure of constructions and demolitions' wastes

A large number of the wastes coming from constructions and demolitions are recyclable and can be reused in producing materials for roads or reused in producing cement, if there are adequate facilities. The European Union reported a decrease in the storage of wastes coming from constructions and demolitions, since bigger depositing taxes were introduced, bigger than those cashed by the recycling companies. This thing was possible in Germany. It is suggested the onset of an European-level strategy because the wastes coming from constructions and demolitions can fill up spaces of 580.000 square km/year, supposing they are not totally recycled and recuperated.
This quantity may be significantly reduced by using a simple mincing and a sorting facility which can recuperate from 60 up to 70 per cent of the wastes coming from constructions and demolitions. Such facilities can cost between 3 and 4 million Euros for a structure that supports 500 tons of minced wastes per day. It is

suggested that this costs be smaller than the storage costs. This thing may be an initiative for the increase of recycling.
If Germany has made important steps concerning the urban ecology, integrating the problems of handling the wastes in a strategy of experimental ecological urban walling off, France is one of the first countries to have applied the European legislation of environment protection in the field of handling the yard wastes.
In France, ever since 1975, the law no. 75-633 of 15 July 1975, which constitutes in the application of directive no. 75/442/CEE concerning the wastes, has as objective the elimination of wastes and the recuperation of materials. This forbade the open air incineration of wastes and gave responsibility to the undertaking concerning the elimination of yard wastes, this demarche including the collecting, the transportation, the hoarding, the sorting, then the valorization through recycling or energetic capitalization.
Since 1992 – when law no. 92/646 of 13 July 1992 (Royal law), referring to the elimination of wastes and installations classified for the protection of the environment was adopted – until now, in France developed a system of planning the elimination of wastes through the regional plans (special industrial wastes) and departmental plans (municipal wastes).

3. ROMANIAN PREOCCUPATIONS CONCERNING CONSTRUCTIONS' WASTES

In Romania, the Ministry of Environment and Water Administration, through the Wastes and Hazardous Substances Management Division coordinates the elaboration, promotion, deploying and monitoring the deploying of the Wastes Management National Plan the National Strategy. These documents are the main instruments through which it is assured the deploying in Romania of European Union's politics concerning the wastes.
The Wastes Management National Strategy contains the national legislative frame and the stage of the deploying, the situation existent in the field of wastes management, general data concerning the wastes management, principles and strategic objectives. The strategic objectives are divided as following: general strategic objectives for wastes management, strategic objectives specific to certain flows of riskless wastes, general strategic objectives for hazardous wastes management and strategic objectives specific to certain flows of hazardous wastes.
The Wastes Management National Plan is made up from 3 parts: the first part – a general presentation, the second part – dedicated to municipal wastes and the third part – dedicated to production wastes, with a preponderant accent on hazardous wastes.
If the key elements of the National Strategy are the principles that stay at the basis of wastes management, as well as the general strategic objectives and those that are specific to certain flows of wastes, the National Plan attaches to the objectives

(which are provided in the Strategy) quantifiable targets where is the case and, in addition, it presents a number of alternatives of reaching the objectives and the afferent targets, respectively. The hierarchy of priorities in approaching wastes management in Romania is the one that stays at the basis of European politics and legislation, known internationally: the premonition and minimization of wastes generation, the material valorization through recycling, the energetic valorization, wastes' treatment in order to subtract the quantities and hazardous potential and at the end the storage. Among the general objective are to be mentioned: the development of organizational and institutional frame, the awareness of the implicated factors, the enhancement of preoccupations concerning the reducing of generated wastes' quantities, the exploitation of all technical and economical possibilities concerning the recuperation and recycling of wastes in order to reduce the quantity of eliminated wastes. A series of alternatives of reaching the strategic objectives is based, on short and medium term, on the usage of pilot-demonstrative installations. On their strength there will be made later evaluations and on the strength of the evaluations, the knowledge and the experience accumulated they will be able to extent for the implementation of a wastes management integrated system. Parallel with these there will develop population's informing and instruction campaigns in order to obtain the public acceptance necessary for later investments.

4. CONCLUSIONS

The wastes management problem is a complex problem. The correct understanding of the problems leads to the selection of their optimum resolving solutions and, in the end, to the rationally ecologic management and to the salvation of some natural resources, important for us, but mostly for next generations.

References

1. Maria Gheorghe, " *Turning waste and industrial by-products in building construction* ", Matrixrom, 2007;
2. Gabriel Stefan, " *Study on recovery of material from demolition and construction waste*", UTCB, Bucharest, 2003;
3. Ghecef I., " *Recovery technologies of concrete from demolition, an inevitable need for future* ", SINUC, Bucharest, 2005;
4. Queensland Government Environmental Protection Agency, Construction and Demolition Waste. *Waste management and resource use opportunities*, july 2002;
5. Departament of Environmental & Climate Change NSW, *Report into the Construction and Demolition Waste Stream Audit 2000-2005*;
6. EUROPEAN COMMISSION, *Management of Construction and Demolition Waste*;
7. Ministerul Mediului si Dezvoltarii Durabile din Romania, Ghid privind stocarea temporara a deseurilor periculoase din constructii si demolari (inclusiv soluri contaminate);

Improving mecanical and durability performances of air-placed concrete. Laboratory and situ researches.

Vasile Iacob
[1] *Faculty of Civil Engineering and Building Services, "Gheorghe Asachi" Technical University, Iasi, 700050, Romania*

Summary

This paper presents one modern and efficient method for the realization of concrete with low ration A/C, air-placing. In this paper we propose a modification for the traditional Romanian installation of dry mix air-placing, changes that lead to improved operation and reliability of the installation, increased quality and performances of air-placing concrete, reduced costs and material saved.
Throuch laboratory research mecanical and durabiliy performances are highlighted and the results are analyzed compared with provided normative values and with performances of standard concrete or with other aditives.

KEYWORDS: concrete, air-placed concrete, durability, compacted, mixture, additive.

1. INTRODUCTION

Cement concrete quality, expressed by its mechanical performance and homogeneity of the mixture composition is determined by the composition factors (quality and proportion of components) and execution technology (cooking, transportation, work release, treatment after concreting). Compared with the factors of composition, execution technology offers several possibilities for improving the mechanical performance and durability of concrete. The durability of concrete, expressed mainly by the impermeability to water and resistance to repeated freeze-thaw cycles, structural compactness is determined by the nature and distribution of pores in concrete. The structural compactness is directly influenced by the amount of water in concrete and the ratio w / c, whose values must be as close as possible to the value 0.361 for structural porosity is determined only occlusive volume occupied by air (a) without the contribution volume occupied by water evaporated or evaporated. For w/c = 0.361, Ae = 0, so the structural compactness is maximum. The nature and distribution of pores in concrete can be controlled by the type of additive used at preparation, the thermal regime of hardening, especially in

ISSN 2285-2735, Pages 184 - 189

the first period of curing and, especially, by concrete technological process used. In the present study were held technology superplasticizer concrete additives and concrete spraying, the technological processes that significantly influence the mechanical performance and durability of concrete.

2. SPRAYING OF CONCRETE

2.1. General issue.

Spraying is a special technological process of preparation and laying of concrete ratio w / c low pressure of compressed air and with a spraying installation. The process consists in the design pressure of the mixture moist microbeton or concrete, with a variable speed from 20 to 30 m / sec from 90 to 100 m / sec, through a nozzle, the support surface. The force of impact of jet material compacted in such a degree, that it remains alone, without sag or fall off the support surface, even if it is vertical or inclined .
Spraying is used to protect reinforcement tension around tubes, silos or prestressed tanks, the waterproofing works to repair damaged buildings or consolidation during the implementation or operation, the actual execution of construction and construction elements special, special shapes and pronounced slopes, which are difficult to execute with ordinary means laying and compaction. With this concrete are padded the tunnels, is achieved the wearing layers of floorings and roads, are executed construction elements. The gunite is applied in thin layers, the final thickness of concrete can reach 100 mm.

2.2. Micro concrete and shot concrete

Shot concrete must be waterproof, must have resistance to freeze-thaw and resistance to compression. Spraying process is giving high performance concrete in most cases. Micro concrete and gunite concrete composition is determined by class of concrete, gunite destination, type of cement and aggregates granularity; shot concrete composition design consist in to establish aggregates granularity and cement dosage.
For dry mixing process, the amount of water is added at dry mixture outlet from the nozzle, thus resulting in a homogeneous mixture, adherent and stable to the support surface.
Expected results depend to some extent and degree of training and specialization of person who work with the installation of spraying.

II/A-S32,5R cement dosage at the C18/22,5 gunite micro concrete class varies between 450 to 550 kg/m^3, as the maximum diameter of aggregate is 5 mm or 3 mm; w/c ratio varies between 0.45 and 0.36.
I42,5 cement dosage at the gunite micro concrete class C18/22,5 varies from 425 to 450 kg/m^3, as the maximum diameter of aggregate is 5 mm or 3 mm; w/c ratio varies between 0.47 and 0.44.
II/A-S32,5R cement dosage at the C18/22,5 gunite micro concrete class varies between 400 to 450 kg/m^3, as the maximum diameter of aggregate is 16 mm, 10 mm or 7 mm; w/c ratio varies between 0.40 and 0.36.
I42,5 cement dosage at the gunite micro concrete class C18/22,5 varies from 385 to 415 kg/m^3, as the maximum diameter of aggregate is 16 mm, 10 mm or 7 mm; w/c ratio varies between 0.41 and 0.38.

2.3. Spraying installation

There are two methods to making and implementation of shotcrete: dry mixing process and wet mixing process, each process uses specific spraying installations.
In Romania are used types of systems to spray dry mixture: drum installation spraying and cylinders and horizontal spraying installation with disc and alveoli.
The spraying installation with drum and cylinders has a flow rate of gunite by 3 m^3/ h at a pressure of (4-5)$\cdot 10^5$ Pa a required compressed air by 10 m^3/min.
Shotcrete concrete is not uniform in structure or in thickness, due to pressure suppression variables.
Gunite layer surface does not appear uniform and flat. Cement losses occur and compressed air. Therefore, this facility cannot be used as a characteristic process equipment widely used in practice for a concrete who has a low ratio w/c.

3. RESEARCH TO IMPROVE SHOTCRETE PERFORMANCE

The research aimed to improve the gunite machine, to improve mechanical performance and durability of concrete and gunite in situ and laboratory testing of the performance levels achieved by the concrete gunite.

3.1. Facility improvement of spraying

The installation with horizontal disk and alveoli was modified by changing attack angle of compressing air connecting pipes, for processing continuous mixing portions of the alveoli, reducing friction and eliminating pulsations during operation.
During the experiments has been replaced the air compressor which had the flow by 10 m^3/min (75 kW) with two compressors which had the flow by 1.5 m^3/min

(total 30 kW); so, has improved the operation of the facility and was made energy saving for production of compressed air.
Also, was used a mixing nozzle and some auxiliary devices for concrete flow adjustment, to eliminate the compressed air jet and for reducing losses by ricochet.

3.2. Shot concrete performance test

Were designed and tested standard waterproof concrete compositions and with superplasticizer additive FLUBET - concrete cast - and the concrete and gunite micro concrete who at the same dosage of cement, were differentiated by reports w/c and by granules diameter of aggregates used in prestressed tested.
To design concrete compositions who was cast, it was used the absolute volume method and it resulted the compositions presented in table 1.

Table 1. Experimental concrete compositions

Code	Concrete type	W (l/m^3)	W/C	C Kg/m^3	Fl. l/m^3	A_g Kg/m^3	?'$_b$ Kg/m^3
BS (standard)	C18/22,5/P_8^{10}-T_3/T_4-II/A-S32,5R/31	205	0,50	410	-	1740	2355
BAF FLUBET	C18/22,5/P_8^{10}-T_4/T_5-II/A-S32,5R/31 FLUBET	165	0,40	410	6,0	1725	2300
BT1 gunite	C18/22,5/P_8^{10}-T_3/T_4-II/A-S32,5R/16 gunite	180	0,44	410	-	1815	2405
BT2 gunite	C18/22,5/P_8^{10}-T_3/T_4-II/A-S32,5R/7 gunite	165	0,40	410	-	1855	2430

Mechanical performance and durability of concrete gunite were compared between them and with the performance of standard concrete and of concrete with superplasticizer additive Flubet cast and compacted by vibration. Have been compared the compressive strength test results determined at different time and different storage conditions of test piece, test results are presented in table 2.

Table 2. Evolution of compressive strength of experimental concrete

Mechanical resistance concrete type \ code	Standard BS	Additive BAF	Gunite BT1	Gunite BT2
R_{28}^N	36,0	36,0	36,5	36,7
R_{90}^N	42,0	43,6	44,0	45,0
R^N_{28+g}	42,8	44,3	45,0	45,5
R^{N+g}_{28+g}	38,7	41,1	42,2	43,1
R^N_{90+g}	44,0	46,1	47,5	48,5
R^{N+g}_{90+g}	41,0	44,2	46,3	47,4

The results of experimental concrete impermeability test were compared and this values are present in the table 3. Were tested concretes who were kept at normal

temperatures with concretes which have been subjected to repeated at freeze-thaw cycles, applied in terms of 28 days and 90 days.

Table 3. Evolution of experimental concrete permeability

Permeability concrete type \ code	Standard BS	Additive BAF	Gunite BT1	Gunite BT2
$P^{10}_{8\cdot28}$	4,03	2,96	2,03	1,83
$P^{10N+g}_{8\cdot28+g}$	5,30	3,72	2,76	2,10
$P^{10N+g}_{8\cdot90+g}$	4,72	2,25	2,10	1,98

4. CONCLUSIONS

The compression resistances at 28 days, respectively at 90 days are higher (with 12.5- 15%) than the minimal values imposed by standards. This is due to the imposition of impermeability condition in P_8 class, which limits the value of w/c ratio to maximum 0.5 for standard concrete (w/c = 0.53 for realizing the class condition) and 0.4 – 0.44 for concrete with additive or for gunite.

The compression resistances for concrete which were submitted to the G_{50} frost cleftness tests decrease with 7-10% at standard concrete, with 4 – 8% at concrete with superreducing water agent Flubet additive and with 3 – 7% at gunite, which has the best behavior at this test. What is important is that the compression resistances of all the concrete tried after G50 test are higher than the minimal resistances accepted by the normative NE 012/99.

The gunites micro concrete, as well as the concrete with superplastifiant Flubet additive behave very well at permeability – the value of permeability is approximately 5-6 times smaller than the maximum limit accepted. Even after the G50 frosting - defrosting test was performed – the value of permeability is approximately 4-5 times smaller than the maximum limit accepted.

The gunite micro concrete with 0-7 mm aggregate behaves the best at the permeability test. The permeability of the concrete submitted to the endurance test increases with 6% up to 20% , but it remains 4-5 smaller at the micro-gunite than the maximum limit accepted.

For the qualitative verification of the gunite adhesion and the stand surface was experimentally applied a layer of gunite on a stand surface made from carbonated concrete. After strengthening, on the attempt of breaking out, it was observed that the breaking was done through the layer of calcium carbonate and not at the gunite - stand surface contact. The modification of the gunite-gun provided a constant debit, an optimum dosed mixture and improved qualities of gunite. The power consumption decreased by 2.5 times. The ricochet losses decreased by 2 times. The gunite-jet has now a diameter of 10-20 cm at the contact with the stand surface, if

the application distance is 50-80 cm. The adhesion at the stand surface is now highly increased.
For the gunite's structural tightness improvement and for the costs' lowering, it is proposed the experimentation of some concrete compositions in which a 10-20 per cent of the cement's mix to be replaced with cementation additions such as micro-silica or steam power plant flier ash. For the production of ageing-proof gunites, the authors want to test as well gunite compositions made with dispersed reinforcement.
Also, the authors consider that the usage of the intense water reducing additives in composition of gunite may bring important improvements of the mechanical performances and of durability of gunite.

References

1. Ionescu, I., Ispas, T., *Proprietatile si tehnologia betoanelor*, Ed. Tehnica, Bucuresti, 1997;
2. Neville. A., M., *Proprietatile betonului*, Ed. Tehnica, Bucuresti, 1979;
3. Moldovan, V., *Aditivi în betoane*, Ed. Tehnica, Bucuresti, 1978;
4. Pamfil, E., s.a. *Influence de la température élevée durant la prise et la première période du durcissement sur la durabilité du béton*, Bul. IPIasi, 1995;
5. Chanvillard, G., D'Aloïa, L., *Prévision de la résistance en compression au jeune âge du béton; application de la méthode du temps équivalent*, Bull. De LLPC, Paris, 1994;
6. Pamfil, E., *Procedee tehnologice moderne de îmbunatatire a performantelor mecanice si de durabilitate ale betonului*, Conferinta Tehnologii moderne în constructii, vol. 1, Universitatea Tehnica a Moldovei, Chisinau, 2000;
7. Maidl, B., Stahlfaserbeton, Berlin, Ernst, Vrlag fur Architektur, 1991;

Nonlinear finite element analysis of masonry infill walls

Dorina Isopescu[1], Andrei-Ionut Stefancu[2] Silviu-Cristian Melenciuc[1]
[1]*Department of Civil and Industrial Buildings, "Gheorghe Asachi" Technical University of Iasi*
Faculty of Civil Engineering and Building Services, Iasi, 700050, Romania
[2]*Department of Structural Mechanics, Gheorghe Asachi" Technical University of Iasi*
Faculty of Civil Engineering and Building Services, Iasi, 700050, Romania

Summary

Masonry or masonry infill walls have been widely used in the past and are still a common design solution for low rise building nowadays. The infill walls are most of the times considered to be nonstructural elements. However, the seismic response of concrete structures is strongly influenced by their presence. The hereby papers analysis, using the finite element method, the behavior of masonry infill reinforced concrete frames. Three design scenarios have been considered as well as two types of infill. Homogeneous materials models have been used. The seismic force has been statically applied at the top of frames, mimicking the real case. The purpose of analysis was to highlight the influence of the design solution and the infill material on the overall behavior of a reinforced concrete frame.

KEYWORDS: masonry infill wall, nonlinear finite element analysis.

1. INTRODUCTION

In seismic regions the aspect of seismic hazard shall be taken into account in the early stages of the conceptual design of a masonry building, for enabling the achievement of a structural system which, within acceptable costs, satisfies the fundamental requirements. Additionally, the masonry buildings with a durable and economical structure provide thermal and sound insulation and an acceptable fire resistance. Masonry buildings, which are classified in unreinforced masonry, confined masonry and reinforced masonry, shall be composed of floors and walls, which are connected in two orthogonal horizontal directions and in the vertical direction.

The infill walls in masonry buildings are provided within the reinforced concrete structures without being analyzed as a combination of concrete and units elements, though in reality they act as a single unit during earthquakes.

According to the design codes, the structure of a masonry building shall be designed and constructed to withstand a seismic action having a larger probability

ISSN 2285-2735, Pages 190 - 202

of occurrence than the design seismic action, without the occurrence of damage and the associated limitations of use. The structure as a whole shall be checked to ensure that it is stable under the design seismic action. Both overturning and sliding stability shall be taken into account.

Masonry buildings are, usually, characterized by the existence of clear and direct paths for the transmission of the seismic forces, and the modeling, analysis, dimensioning, detailing and construction of these simple structures are subject to much less uncertainty and thus the prediction of its seismic behavior is much more reliable. In the design of masonry buildings the following norms are applied: P100/2006 [1], CR6/2006 [2], SR EN 1996 -1/2006 [3] and SR EN 1998 -1/2004 [4].

Masonry units should have sufficient robustness in order to avoid local brittle failure. Except in cases of low seismicity, the characteristic compressive strength of masonry modules, derived from normalized compressive strength of masonry units in accordance with SR EN 772-1 and mortar strength is:

$$f_k = K f_b^{0,70} f_m^{0,30} \quad (1)$$

where: f_k = the characteristic compressive strength of masonry modules;
f_b = the normalised compressive strength of masonry units;
f_m = the mortar strength;
k = constant that depends on the type of units used for masonry.

The characteristic compressive strength of masonry modules should be not less than the minimum values presented to table 8.1 from CR 6/2006. In Table 1 are presented the minimum requested values of the characteristic compressive strength of masonry modules f_k (N/mm^2) for simple masonry buildings (strength wall from ordinary buildings, not belonging in the other categories, or from buildings of minor importance for public safety, e.g. agricultural buildings, etc).

Table 1- The minimum characteristic compressive strength values of masonry modules

Building height	Design ground acceleration a_g		
	0.08g ÷ 0.16g	0.20g ÷ 0.25g	0.30g ÷ 0.40g
= GF+2F	2.00	2.50	3.25
= GF+3÷4F	2.50	3.00	4.00

* GF=ground floor, F=current floor

A minimum strength is required for mortar, $f_{m,min}$, which generally exceeds the minimum specified in CR 6/2006. The value ascribed to $f_{m,min}$ for use may be found in the National Annex. The recommended value is $f_{m,min}$ = 5 N/mm^2 for unreinforced or confined masonry and $f_{m,min}$ = 10 N/mm^2 for reinforced masonry.

A linear analysis presumes that: the structural response is directly proportional to the loading, large displacements do not occur, supports do not fail, the stress –

strain relationship is linear, the loads are constant etc. [5]. This type of behavior can accurately describe a limited number of real cases. For the rest of them, a nonlinear behavior can be expected. This arises from a number of causes [6], among which the next could be mentioned:

- parts may come in/out of contact, contact areas may vary with loading, frictional interaction between moving elements may exist;
- displacement and/or rotations may be significant enough to require the static equilibrium equations be written for the deformed shape of the structure;
- materials may exhibit non-linear stress-strain relations;
- thermal conductivity may vary with temperature.

Consequently a problem may evolve from a linear to a highly nonlinear one. In structural mechanics, a problem is nonlinear if the stiffness matrix or the load vector depends on the displacements.

Nonlinearity in structures may be classified as:

- geometric nonlinearity - when the nonlinear behavior of the problem is given by significant changes in the geometry of the structure. This case includes , beside others, large displacements/strains [7];
- material nonlinearity – is associated to the nonlinear behavior of materials and includes the case of plastic materials [8] or hyper-elastic materials [9];
- contact nonlinearity – occurs when the contact surface between two parts changes during the analysis.

Nonlinearity makes a problem more complicated because the equations that describe the solution must incorporate conditions not fully known until the solution is known – the actual configuration, loading condition, state of stress and support conditions. Nonlinear problems are describes using differential equations derived from continuum mechanics. Very often the solution of a set of differential equations may be hard to find. In this cases numerical method are used to provide an approximate solution to the given equations. Approximate methods include the finite element method (F.E.).

Over the last decades a large number of software packages that solve nonlinear problems using the F.E. have developed. One of these programs is ANSYS [10]. ANSYS is a comprehensive general-purpose finite element computer program capable of performing static, dynamic, heat transfer, and fluid flow and electromagnetism analyses [11].

The current problem includes material nonlinearities given by the behavior of the masonry as well as contact nonlinearities due to the interaction between the concrete frame and the infill wall.

2. CHARACTERISTICS OF THE ANALYSED MODELS

2.1. Description of the models

Three types of models, common to concrete frame structures, have been considered as design scenarios. The key geometric features, as well as the meshing, are presented in Figure 1, starting from the upper corner left hand side, as follows: frame with infill wall – upper part, frame with infill wall and door opening – medium part and frame with infill wall and window opening – lower part.

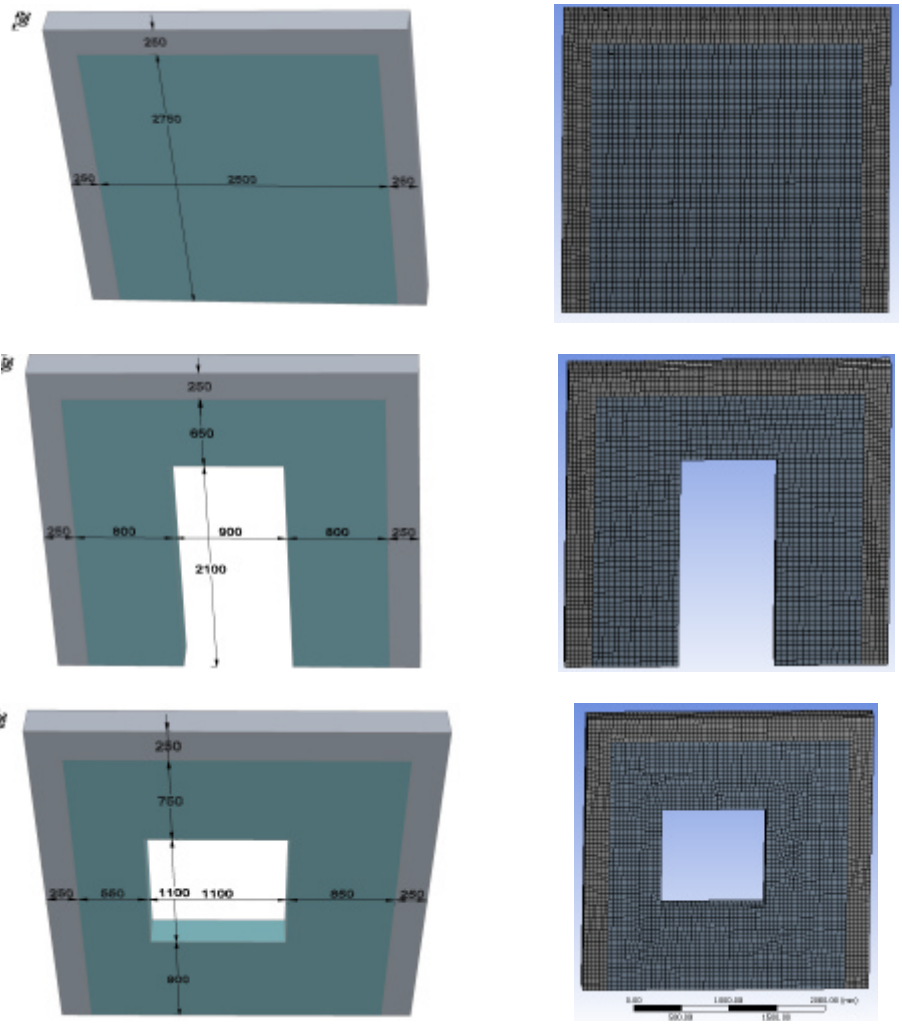

Figure 1. Layout of the analyzed configurations.

2.2. Materials used

The resistance and structural rigidity of masonry made of clay-bricks, are calculated using a parabolic – rectangular types of the stress – strain relationships "s -e" (constitutive laws) that show the real behavior of masonry (design, f_d, and characteristic values, f_k), Figure 2.

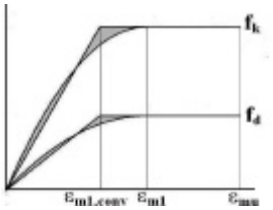

Figure 2. Parabolic - rectangular constitutive laws of clay-bricks.

The equation of constitutive law presented in Figure 2, is:

$$e = -\frac{1.1R}{E_0}\ln\left(1-\frac{s}{1.1R}\right) \tag{2}$$

where: R = ultimate compression strength of the masonry modules;
s = stress in the masonry modules;
? = strain of the masonry modules;
? $_{m1}$ = initial strain (at first crack) of the masonry modules;
? $_{mu}$ = ultimate strain of the masonry modules;
E_0 = initial elasticity modulus of the masonry modules.

The model of the stress – strain relationships "s -e" used for the autoclaved aerated concrete (AAC), also known as autoclaved cellular concrete (ACC) or autoclaved lightweight concrete (ALC) is presented in Figure 3.

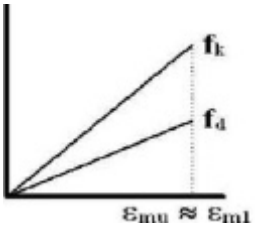

Figure 3. Linear - rectangular constitutive laws for AAC units.

The equation of constitutive law presented in Figure 3 is:

$$e = \frac{s}{E_0} \tag{3}$$

The materials are considered homogenous and isotropic and the values of their characteristics used in nonlinear finite elements analysis are presented in Table 2.

Table 2. The material characteristics used in nonlinear finite elements analysis.

Material characteristics	Clay-bricks	AAC	Reinforced concrete
Density [kg/m^3]	1600	700	2500
Young's Modulus [MPa]	10000	2420	25000
Poisson's Ratio	0.18	0.14	0.2

Besides the previous described design scenarios – geometry and materials, some additional information must be highlighted in what concerns the analysis, such as:

- the frame and the infill wall are fully restrained at the lower part;
- the interaction between the two structural components is realized using a frictionless contact (only compression stress between components are accounted for) ignoring thus the function of the mortar;
- two steps of analysis have been considered: during the first one the gravity is applied and during the second one a 100kN force is applied at the top part simulating thus transmitted by the flooring system to the frame in case of an seismic action.

The above are also presented in Figure 4.

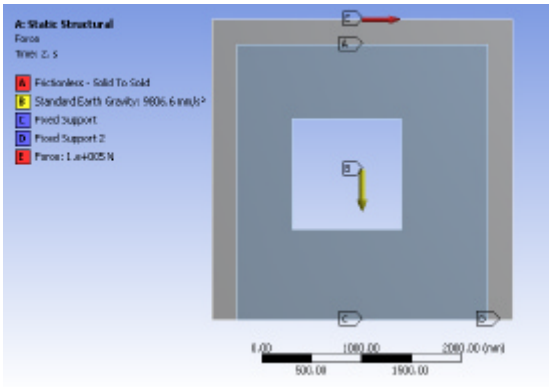

Figure 4. Boundary conditions and applied loads.

3. RESULTS OF THE ANALYSIS

The results of the analysis will be presented as contour plots. For each of the three geometries the stress distribution will be presented when using masonry (clay-bricks) and AAC as an infill material.

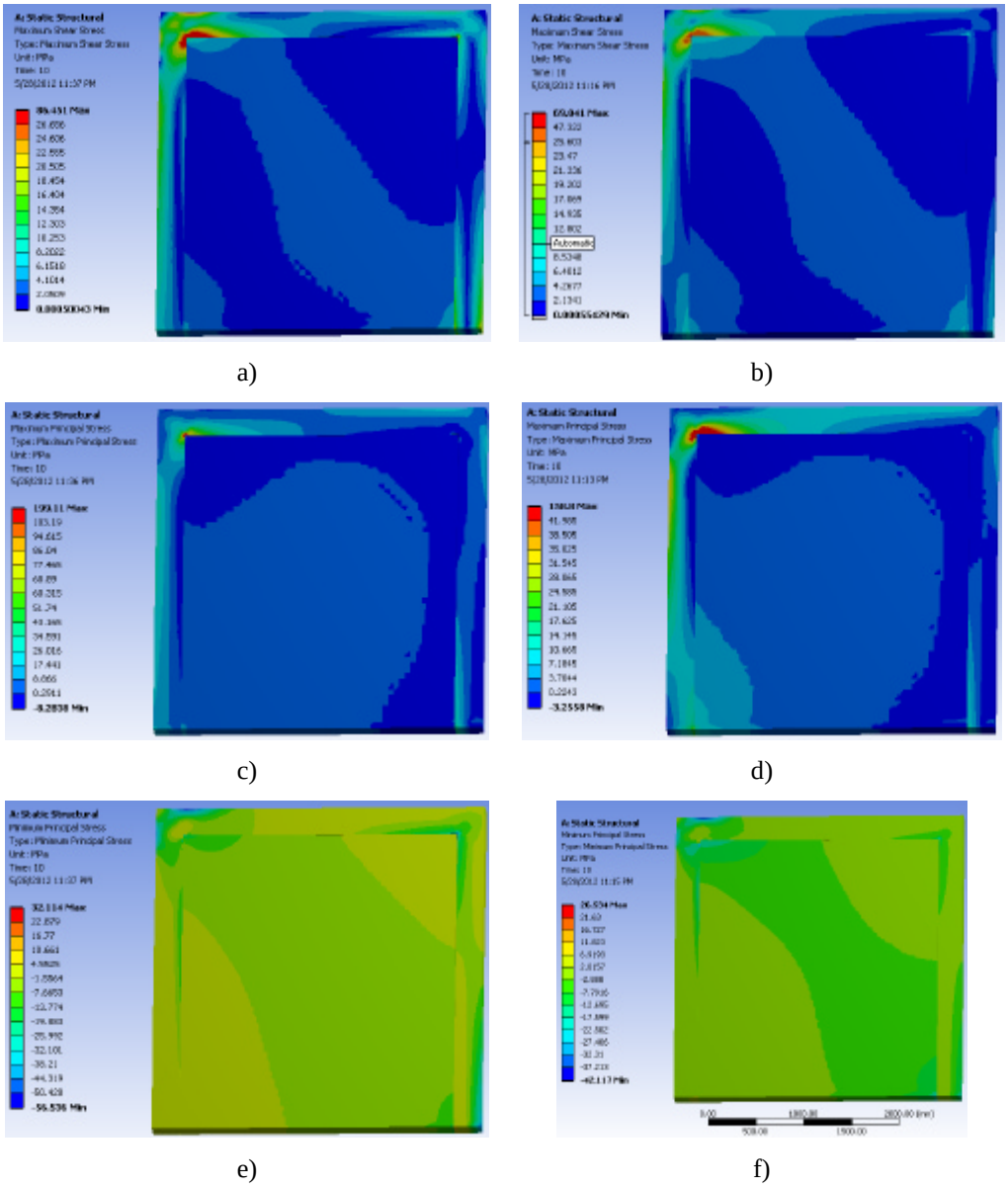

a) b)

c) d)

e) f)

Figure 5. Contour plots:
- maximum shear stress: a) AAC, b) masonry (clay-bricks);
- maximum principal stress: c) AAC, d) masonry (clay-bricks);
- maximum principal stress: e) AAC, f) masonry (clay-bricks).

The results will not be presented in a tabular manner given that their maximum values are influenced by stress singularities that occurs the interaction between the frame and the infill wall (the corner).

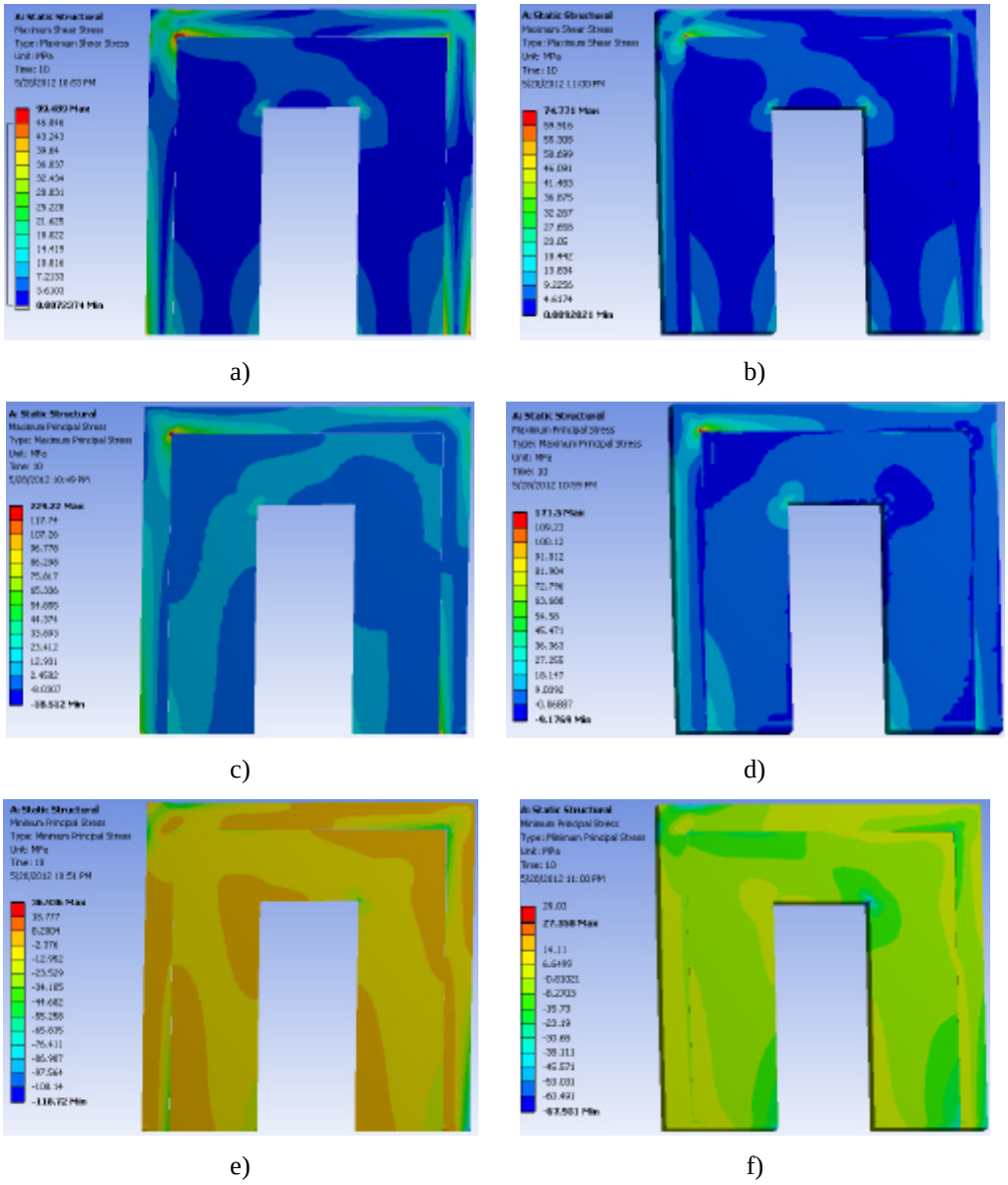

a) b)

c) d)

e) f)

Figure 6. Contour plots:
- maximum shear stress: a) AAC, b) masonry (clay-bricks);
- maximum principal stress: c) AAC, d) masonry (clay-bricks);
- maximum principal stress: e) AAC, f) masonry (clay-bricks).

As a general remark though, one could notice that the use of AAC (case that were and will be presented on the left hand side of Figures 5, 6 and 7) generally lead to higher value of stresses.

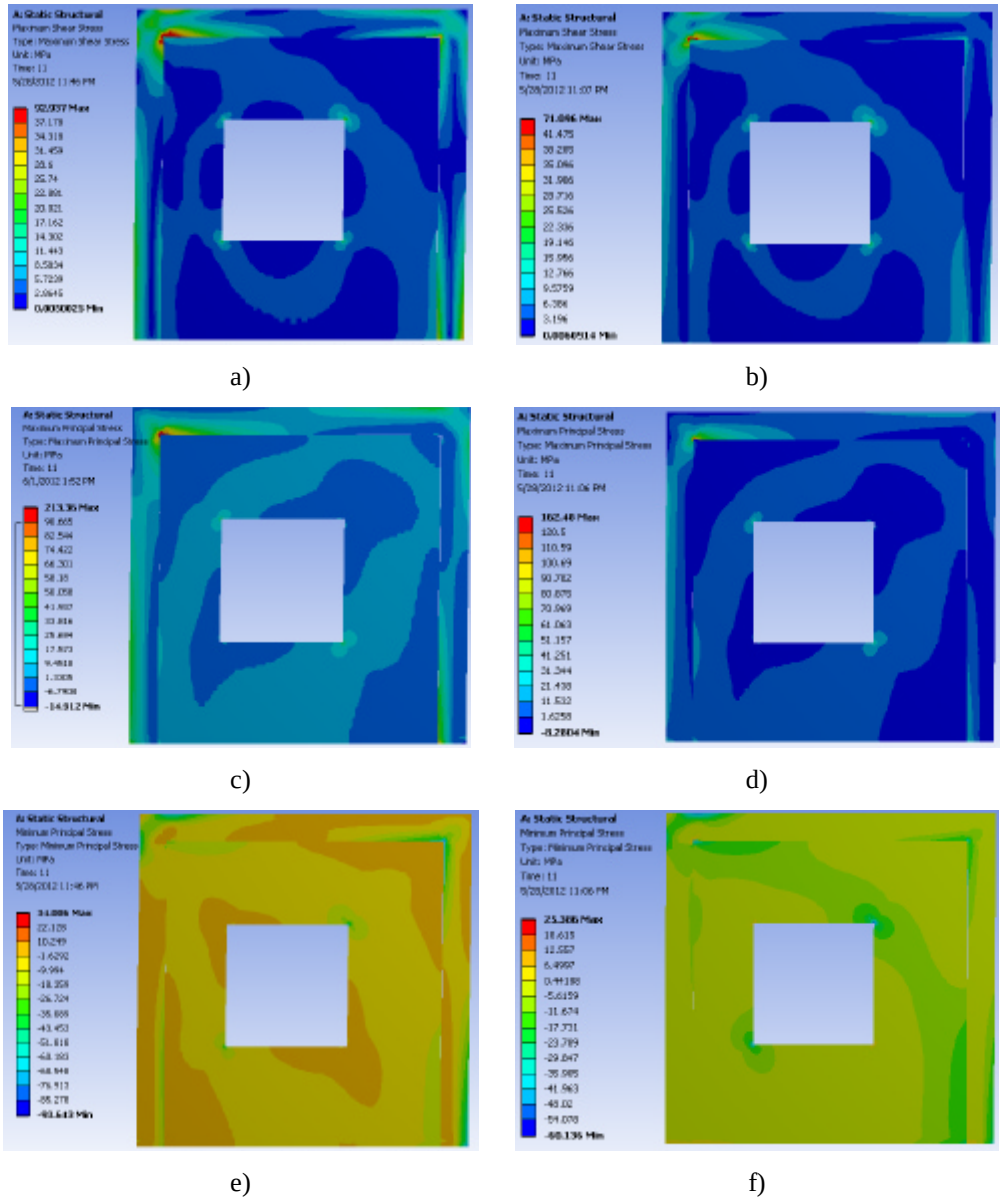

Figure 7. Contour plots:
- maximum shear stress: a) AAC, b) masonry (clay-bricks);
- maximum principal stress: c) AAC, d) masonry (clay-bricks);
- maximum principal stress: e) AAC, f) masonry (clay-bricks).

In terms of the overall behavior of the infill wall, as expected, it acts like a bracing system where a diagonal is tensed and the other one I compressed (as shown by the minimum and maximum principal stresses). High values of shear stresses occur along perpendicular planes (to the planes of principal stresses) with stress concentrations at corners (of door and window opening).

A more objective manner to evaluate the influence of geometry and infill material is given by the overall force reaction. In this way the influence of the stress concentration fade out and a more accurate evaluation of the phenomenon can be performed.

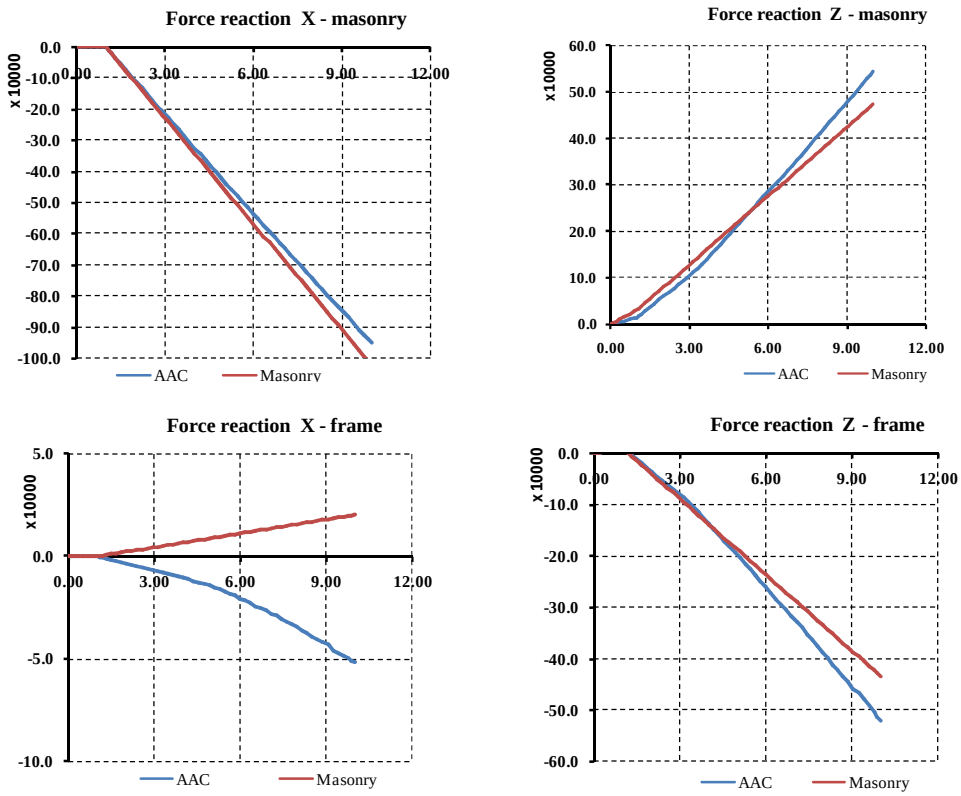

Figure 8. Force reactions at base for the frames without openings

As expected, given the material and geometric characteristics of the analyzed models (that lead to different lateral flexibilities of the two components – frame and infill) the biggest part of the exterior force is overtaken by the infill wall. Beside the X component, the applied action also leads to axial stress along Z. In this case the body forces acting upon the frame and the wall are equal but with opposite signs.

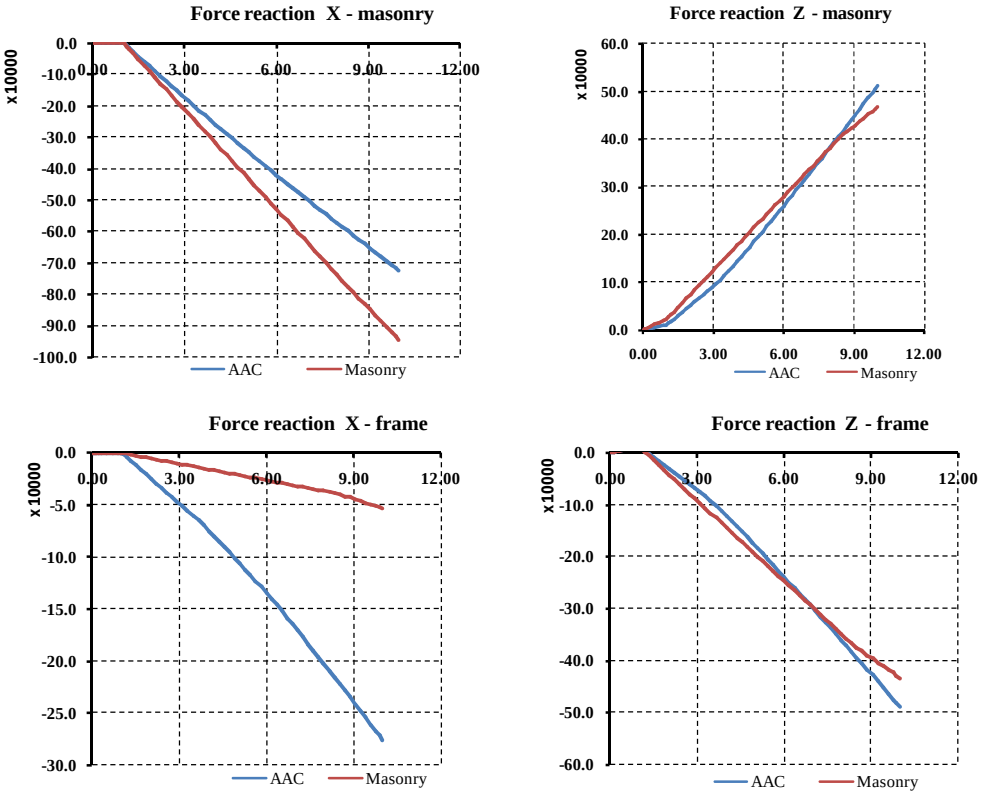

Figure 9. Force reactions at base for the frames with door opening

When comparing the effect of the infill materials one could notice that:

- the use of masonry as an infill material ensures that less horizontal forces are expected to be transmitted to the frame (in terms of reactions along X);
- considering that the amount of applied force is the same both cases, the previous statement implies that the infill material will be more stress out hence more prone to damage;
- since the AAC is lest capable of sustaining significant stress the infill wall will fail faster when using it;
- given that the models do not account for material damage, and no cyclic loading has been applied the results provided by this type of analysis can only be used as a preliminary stress evaluation

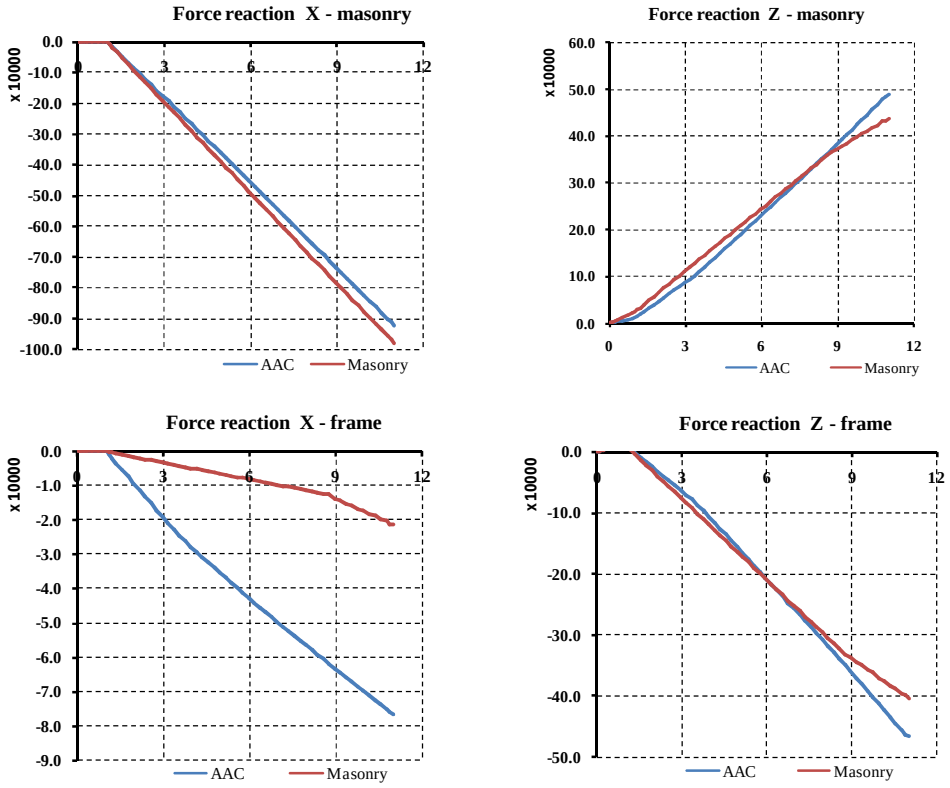

Figure 10. Force reactions at base for the frames with window opening

4. CONCLUSION

In light of the above one can conclude that using masonry as an infill material can improve the overall behavior of reinforced concrete structures if proper precautions are taken to limit the shear failure of the frames. The results show that the confining concrete frame increases the system ductility and the strength of the walls.

The structure behaves in different manner if openings are present in the wall. The force reactions in concrete frame (X direction) show considerable differences between wall without openings, wall with window opening and wall with door opening.

The use of AAC is likely to be efficient if appropriate measures are taken to limit local damages especially at the corners of the infill wall.

To overcome the limitations of the current study such as materials failure and stress concentrations due to contact between elements further studies must be performed to confirm the previously stated conclusions. Nevertheless, the step towards the development of reliable and accurate numerical models cannot be performed without a thorough material description and a proper validation by comparison with a significant number of experimental results.

5. References

1. **** - P100/2006, Romanian seismic code for design
2. **** - CR6/2006, Romanian codes for masonry design
3. **** - SR EN 1996 -1-1/2006, Romanian standards: Eurocode 6 – Design of masonry structures. General rules for masonry buildings.
4. **** - SR EN 1998 -1/2004, Romanian standard: Eurocode 8 – Building design in seismic area. General rules, seismic loads and rules for buildings.
5. Cook, R.D., Finite element modeling for stress analysis, John Wiley & Sons, 1995;
6. Cook, R. D., Malkus, D. S. and Plesha, M. E. (1989) *Concepts and applications of finite element analsys,Third Edition*, John Wiley & Sons.
7. Iu, C. K., Chan, S. L., A simulation-based large deflection and inelastic analysis of steel frames under fire, Journal of Constructional Steel Research, 2004;
8. Anandarajah, A., Computational Methods in Elasticity and Plasticity: Solids and Porous Media, Springer, 2010;
9. Bonet, J., Wood, R. D., *Nonlinear continuum mechanics for finite element analysis*, Cambridge University Press, 1997;
10. ANSYS Inc., ANSYS Workbench 2.0 Framework Version: 12.0.1, 2009/a;
11. Moaveni, S., Finite element analysis – Theory and application with ANSYS, Prentice Hall, 1999

Monitoring Steel Bearing Cables Using a Sound Scanning Technique

Ludovic Gheorghe Kopenetz[1], Dragos Florin Lisman[2]
[1]*Department of Structural Mechanics, Technical University of Cluj-Napoca, Cluj-Napoca, 400114, Romania*
[2] *Department of Structural Mechanics, Technical University of Cluj-Napoca, Cluj-Napoca, 400114, Romania*

Summary

The paper presents a monitoring technique for structures composed of steel cables. The main idea behind this technique is the fact that wires that compose wire strands emit certain sound frequencies when their rupture occurs. In the majority of cases, steel cables do not fail totally in a sudden manner. As a result the authors propose a method for detecting the initial rupture of one or several wire strands.

By being able to detect these initial degradations, the monitoring system based on this technique will be able to instruct the users of the structures about the mandatory steps that have to be followed in order to limit or prevent material losses and to prevent any human life loses.

The entire sound scanning system depends on a set of accurate sound acquisition devices. The data acquisition devices or the sensors are the most sensitive part of the entire system. Besides the sensors which are mounted in key points along the structure, such as for example the pillars of a cable car, the system is composed of filtering and amplifying devices, preprocessing hardware/software, communication devices and a hardware platform on top of which a software application is permanently running in order to perform real-time detection and send instructions to the end users.

The authors hope to prove by several tests that this is a feasible and cost-competitive method for cable structure monitoring. There are several issues to be dealt with during the system development including permanent energy supply for the data acquisition devices, secure transmission and if necessary retransmission of sensor data and an accurate scale for assessing the magnitude of the initial degradations.

KEYWORDS: sound scanning, monitoring, real-time detection.

1. INTRODUCTION

Structures built using bearing cables can be met in many civil, infrastructure, military or mining applications. These are flexible structures that sustain and transfer predominantly tensile forces. They make use of the strength of the materials through intermolecular cohesion.

In a large number of application steel cables are used. The cables are manufactured using high quality steel and their use is, in principle, unlimited taking into account that their profitability increases with the increase of the spanning distances.

Due to the fact that these cables are subject to considerable efforts and also withstand the diverse actions of natural elements, they have to be subject to careful monitoring and any degradation or defect must be identified as soon as it may develop or even predicted, if possible.

Monitoring structures composed of bearing cables should be a permanent operation that supplies accurate information about the structural health of the objective. Any change in the cable's behaviour or of its physical properties should be available to the owners and especially to the current users of the structure.

2. MONITORING TECHNIQUES

The confirmation of the safety of bearing cable structures is based on a static and dynamic structural analysis, using beside other properties, real geometry, which means that the current observations are insufficient [1]. Real geometry for bearing elements depends on a series of aspects such as: intensity of the load, material type, operating conditions, etc.

Throughout history, different construction materials have been used for cables such as: papyrus, camel hair, flax and hemp until the 19^{th} century, when the first steel wire cables were produced. Due to the particular properties of steel, such as high breaking strength compared to its sole weight, high flexibility and durability, steel wire cables became indispensable for a large number of structural engineering domains.

Cables used for bearing structures can have a classic or a special construction, using metallic insertion elements with three or five edges. Steel cables are produced from high quality carbon - steel with an average carbon content of 0.5% and a breaking strength of approximately 60daN/mm [2].

By wiredrawing, the circular section steel ingot is transformed into wire and the breaking strength increases up to 120 - 200daN/mm. After wiredrawing, the wires are subject to heat treating and thus the material regains its plastic properties. The

individual wires are twisted in a single or in multiple layers around a central wire forming a strand. In turn, strands are twisted around a central core forming the final cable rope [2].

The purpose of monitoring is to establish a relation between the values of the input quantity and the values of the output quantity. There are two possibilities for closed or open monitoring. The open monitoring system does not check or validate the relation between the input and output values. The closed monitoring system performs a validation of the relation between input and output values [3].

For in situ monitoring, the following methods are most frequently used: visual observation, electrochemical methods such as voltage method, magnetization method or mechanical sound method and non-electrochemical methods such as microscopic observation, gravimetry, infrared thermography, gammagraphy, radiography in the radar method [3].

In the context of the afore monitoring methods, the authors of this paper are developing a new monitoring technique based on sound scanning which they call SONCAB. The technique's test bench is pending patenting with national authorities.

3. SOUND SCANNING

This technique is based on capturing the acoustic signals emitted in the preceding moments and during the moments when elementary steel wires break. The breaking of composing wires of bearing cables can generate certain sounds and can represent an important signal of bearing strength degradation [4]. This sound signal propagates both through cable material and air. The intensity of the signal is proportional with the number of ruptured wires and thus appears the possibility of designing a efficient and strong structural control [5].

3.1. General architecture of the sound scanning system

The general architecture proposed for the SONCAB system under development has the main building blocks presented in Figure 1. These are:

- several sensing blocks;
- the trigger and signal identifier block;
- one or several data aggregation block;
- one or several data storage blocks;
- several data analysis and interpretation blocks.

The sensors that will be used in the test implementation of the system have to be robust, easy to mount and must have electromagnetic screening. The sensors are chosen in such a way that vibrations, environmental temperature and the effects of

electric or magnetic fields have a very small influence on their functioning. The main component of each sensing block is composed of at least one measurement microphone. A measurement microphone provides an analog output signal that is proportional to the variation in the acoustic pressure acting upon a flexible diaphragm.

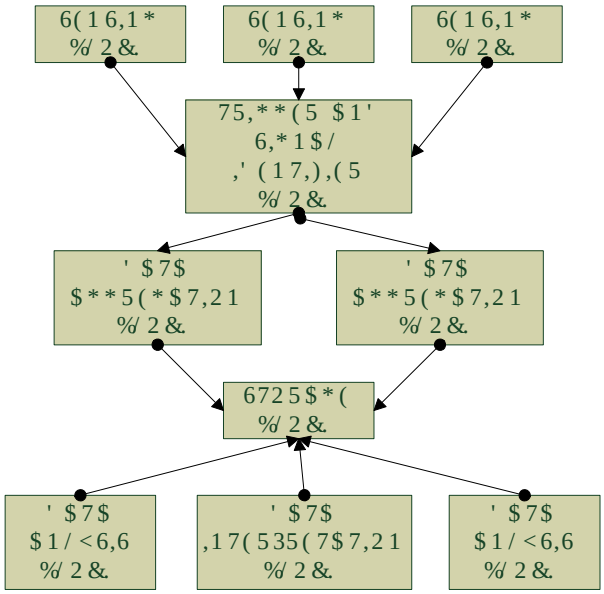

Figure 1. The building blocks of SONCAB system

3.1.1. Sensing blocks

As presented above, the measurement microphone is the most important component of the sensing block. These microphones are very different from those used in audio applications because their main feature is to accurately reproduce the sound waveform without distortion and with a linear relationship between the voltage and the pressure sensed by the microphone's diaphragm [6].

One of the most important properties of a good measurement microphone is sensitivity. Sensitivity is the ratio between its output voltage and the acoustic pressure sensed by the diaphragm. Sensitivity is measured in mV/Pa. For a microphone sound measuring system, the magnitude of the sensitivity is used to establish the minimum sound pressure that the microphone can measure accurately [7].

If there are variations of the sensitivity over the range of frequencies to be measured, these produce a distortion in the output signal compared to the acoustic

signal. The minimal requirements that a measurement microphone must comply to are:

- it has to exhibit a constant sensitivity over the range of frequencies to be measured; to have a flat frequency response;
- it has to have a nearly constant sensitivity over a wide range of temperatures and barometric pressures;
- the microphone sensitivity should exhibit the linearity property, namely, it should be nearly constant over a wide range of sound pressure levels. This produces a linear dependence between the microphone's output voltage and the sound pressure [6].

The composing elements of a sensing block are presented in Figure 2. These are the measurement microphone(s), cables, power supply and amplifiers.

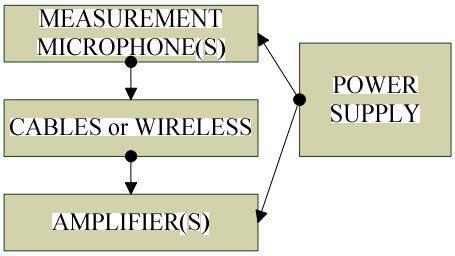

Figure 2. Sensing block

The most common measurement microphone types used in sound sensing applications are [8]:

- piezoelectric microphones;
- capacitive microphones;
- dynamic microphones.

Piezoelectric microphones are a good choice for a sound monitoring system like SONCAB due to the fact that they are often used in high pressure measurement situations. Still, there exists a disadvantage of using such a microphone: they have a low noise floor which limits their use in precision sound measurement applications [9].

Dynamic microphones are well suited for voice and audio applications but are not a good choice for sensing the sounds produced by the rupture of individual steel wire elements due to the following disadvantages: limited dynamic range, high sensitivity to vibrations and a frequency response that is not flat enough [6].

In the case of capacitive or condenser-based microphones, the movement of the diaphragm is relative to a fixed plate which produces a capacitance variation proportional to the sweep of the diaphragm. The capacitance variation is converted to a voltage variation. This type of microphone is the most appropriate choice for

the sound wave sensing component in the SONCAB monitoring system. The following characteristics make it the most appropriate choice: high stability, low internal noise, wide dynamic range, low distortion, high sensitivity and a flat frequency response.

In what concerns the connecting cables, usually these are the most error-prone component of the sensing block. Nevertheless, they should be able to support a wide temperature range and must accurately function under high humidity conditions. As an alternative to these cables, the sensing blocks can be equipped with wireless transmitters/receivers. This would imply that other blocks have to have the same wireless capabilities in order to be able to communicate with the sensing blocks.

The power supply must be temperature and time stable. It also has to resist to shocks and vibrations and have low susceptibility to magnetic and RF fields.

The amplifiers are responsible for providing gain, impedance matching, output drive current and for performing additional signal processing tasks. They also provide gain stability, linearity and they must have low residual noise and a zero temperature coefficient.

3.1.2. Trigger and signal identifier block

This block contains components responsible for sending the command signals to the sensing blocks. This is a complex process that takes as input the sound waves captured by a sensing device and decides based on their values to trigger the sound wave acquisition on other sensing devices.

This block is responsible for performing the function of an adaptive detection trigger which samples the signals received from a certain number of channels by comparing them to an adjustable reference voltage with the help of a set of voltage comparators.

3.1.3. Data aggregation blocks and the storage block

The data aggregation blocks are responsible for gathering the sensed and conditioned sound wave data from the sensing blocks. Several sensing blocks fan the data in an aggregation block. From the aggregation block data is routed to the storage block. An aggregation/storage block can be either a data acquisition system like the HBM MGCplus device available in the research team's experimental laboratory or it can be a PC or laptop equipped with proper extension boards and a storage interface to a memory capable of storing large amounts of data at high speeds, like for example a flash memory system [10], [11].

3.1.4 Data analysis and interpretation

The sound taken into account when performing data analysis and interpretation is the sound transmitted through the cable from the sound source (the breaking point of one or several elementary wires) to the sound sensors. For evaluation purposes, only the direct sound generated will be taken into account. For the directly transmitted sound, attenuation created by the cable mass has to be accounted for by using the mass laws specified in dB by Equation (1):

$$TL = k \log MS + r \tag{1}$$

The sound frequencies propagate through the cable material with a velocity of approximately 5000m/s towards the anchoring points of the cables [4]. The intensity of the sound signal is proportional to the number of broken wires or strands, thus having the possibility of developing an efficient structural control system.

A typical scenario of using the SONCAB steel cable monitoring system is presented in Figure 3.

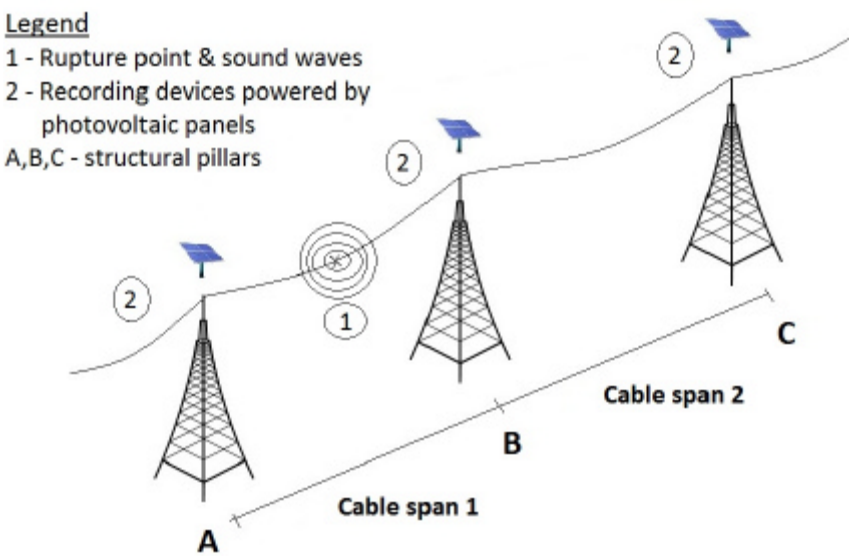

Figure 3. SONCAB scenario

This scenario presents a transport cable passing above a set of three structural pillars (A, B, C). On each pillar a sensing device along with a data recording device is mounted (2). The sensing devices have solar panels as energy supplies in order to be independent and in order to harvest the available luminosity. The calibration

tests for the sensor require intense work in order to obtain the required transfer function.

If a rupture event occurs at point (1) on the cable as suggested in Figure 3, the sound taken into account when measuring is the sound transmitted through the cable from the sound source, namely the breaking point of one or several elementary wires, to the sound sensors. For evaluation purposes, only the direct sound generated by the rupture, will be taken into account. The filtering of refractory components is assured through electronic screening.

The problems posed by the interpretation of data resulted from the sound monitoring of bearing cable structures are of great complexity, due to the multiple of random variables that intervene. As a result, the authors propose one interpretation method using fuzzy-logic based reasoning for interpretation and quantification of data resulted from monitoring [2].

4. CONCLUSIONS

With the increasing degree of complexity of constructions (high-rise and with large-spans) using bearing steel cables, an increase in the need of evaluating the associated risks appears.

Continuous, periodic or continuous-periodic monitoring helps analyze and mitigate these risks. The results of monitoring constitute a starting point when taking decisions concerning interventions to the structure in order to avoid local or chain collapse.

The authors hope to prove the feasibility of sound monitoring of steel bearing cables during the following months by testing a prototype of the SONCAB system out of the laboratory.

Up to now, several tests have been performed with different sensing devices in the faculty's experimental laboratory by sensing and recording the sound waves produced during the controlled rupture of different steel cables with diameters around 12mm.

References

1. Lazar-Mand, F. and Lisman, D.F., Practical aspects about linear dynamic analysis of cable structures, Proceedings of the 6th International Symposium "Computational Civil Engineering", Iassy, Romania, ISBN: 978-973-8955-41-7, 2008.
2. Kopenetz, L.G. and Gobesz, Zs., The Structural Expertise of Steel Cables, Transportation Infrastructure Engineering, edited by Intersections, Vol. 4, Iassy, Romania, pp. 49-62, 2007.

3. Kopenetz, L. and Lisman, D.F., Relatime Behavioral Monitoring of Cable Transport Structures, Journal of Applied Engineering Sciences, vol. 2(15), Issue 1/2012, Oradea, Romania, e-ISSN: 2284-7197.
4. Pellerin, G., Acoustique architecturale: Théories et pratiques, electronic version, 2006, http://assoacar.free.fr/archives/Cours/Ac%20des%20salles/Acoustique_Architecturale_CNAM.pdf, viewed at 07/03/2012 (in French).
5. Malet, T., Acoustique des salles - Le guide de référence du praticien, Publications Georges Ventillard, Neuilly sur Marne, France, 2005.
6. Townsend, C. and Arms, S., Test and Measurement Microphones, Chapter 18, pp. 481-501, from Sensor Technology Handbook, Elsevier Newnes, Oxford, UK, 2005.
7. Tashev, I.J., *Sound Capture and Processing: practical approaches*, John Wiley and Sons Ltd., West Sussex, UK, ISBN: 978-0-470-31983-3, 2009 .
8. Fraden, J., *Handbook of Modern Sensors, Physics, Designs and Applications*, 4th edition, Springer Science, New York, USA, ISBN: 978-1-4419-6465-6, 2010.
9. Brandstein, M. and Ward, D., *Microphone Arrays: Signal Processing Techniques and Applications*, Springer Verlag, Berlin, Germany, ISBN: 978-3-642-07547-6, 2010.
10. ***, Product web site, http://www.hbm.com/en/menu/products/measurement-electronics-software/laboratory-test-stand/mgcplus/, accessed on 05/03/2012.
11. ***, SD Association Homepage, https://www.sdcard.org/consumers/speed/, viewed on 03/03/2012